2(mix

FINAL REPORT

RESEARCH STUDY ON STABILIZATION AND CONTROL

– MODERN SAMPLED-DATA CONTROL THEORY

April, 1973

BY B.C.KUO
G.SINGH
R.A.YACKEL

PREPARED FOR GEORGE C. MARSHALL SPACE FLIGHT CENTER

HUNTSVILLE, ALABAMA

CONTRACT NAS8-28584 DCN 1-2-40-23018

SYSTEMS RESEARCH LABORATORY

P.O. BOX 2277, STATION A
CHAMPAIGN, ILLINOIS 61820

TABLE OF CONTENTS

1. DIGITAL APPROXIMATION BY POINT BY POINT STATE COMPARISON

1.1 Introduction

The problem is that of approximating a continuous-data system by a sampled-data model by comparison of the states of the two systems.

Consider that the continuous-data system as shown in Fig. 1-1 is described by the following time-invariant dynamic equations:

$$\dot{\underline{x}}_c(t) = A\underline{x}_c(t) + B\underline{u}(t) \tag{1-1}$$

$$\underline{u}(t) = E(0)\underline{r}(t) - G(0)\underline{x}_c(t) \tag{1-2}$$

where

$\underline{x}_c(t)$ = n x 1 state vector

$\underline{u}(t)$ = m x 1 control vector

$r(t)$ = m x 1 input vector

A = n x n coefficient matrix

B = n x m coefficient matrix

$E(0) = I$ = m x m identity matrix

$G(0)$ = m x n feedback matrix

The initial state is given by $\underline{x}_c(0) = \underline{x}_{c0}$

Substituting Eq. (1-2) into Eq. (1-1) yields

$$\dot{\underline{x}}_c(t) = [A - BG(0)]\underline{x}_c(t) + BE(0)\underline{r}(t) \tag{1-3}$$

The solution of Eq. (1-3) for $t \geq t_o$ is

$$\underline{x}_c(t) = e^{[A-BG(0)](t-t_0)}\underline{x}_c(t_0) + \int_{t_o}^{t} e^{[A-BG(0)](t-\tau)}BE(0)r(\tau)d\tau \tag{1-4}$$

where

$$e^{[A-BG(0)](t-t_0)} = \sum_{j=0}^{\infty} \frac{1}{j!} [A - BG(0)]^j (t - t_0)^j \qquad (1\text{-}5)$$

The block diagram of the sampled-data system which is to approximate the system of Fig. 1-1 is shown in Fig. 1-2. The outputs of the sample-and-hold devices are a series of step functions with amplitudes denoted by $\underline{u}_s(kT)$ for $kT \leq t < (k + 1)T$. The notation, $G(T)$ and $E(T)$, denote the feedback gain and the forward gain of the sampled-data system, respectively. The dynamic equations for the sampled-data model are:

$$\dot{\underline{x}}_s(t) = A\underline{x}_s(t) + B\underline{u}_s(kT) \qquad \underline{x}_s(0) = \underline{x}_{s0} \qquad (1\text{-}6)$$

$$\underline{u}_s(kT) = E(T)\underline{r}(kT) - G(T)\underline{x}_s(kT) \qquad (1\text{-}7)$$

for $kT \leq t \leq (k + 1)T$.

The A and B matrices in Eq. (1-6) are identical to those of Eq. (1-1). Substituting Eq. (1-7) into Eq. (1-6) yields

$$\dot{\underline{x}}_s(t) = A\underline{x}_s(t) + B[E(T)\underline{r}(kT) - G(T)\underline{x}_s(kT)] \qquad (1\text{-}8)$$

for $kT \leq t \leq (k + 1)T$.

The solution of Eq. (1-8) with $t = (k + 1)T$ and $t_o = kT$ is

$$\underline{x}_s[(k + 1)T] = \left(e^{AT} - \int_{kT}^{(k+1)T} e^{A(kT+T-\tau)} d\tau BG(T) \right) \underline{x}_s(kT)$$

$$+ \int_{kT}^{(k+1)T} e^{A(kT+T-\tau)} d\tau BE(T)\underline{r}(kT) \qquad (1\text{-}9)$$

The problem is to find E(T) and G(T) so that the states of the sampled-data model are as close as possible to that of the continuous-data system at the sampling instants, for a given input $\underline{r}(t)$. Furthermore, in order that the solution for E(T) is independent of $\underline{r}(t)$ it is necessary to assume that $\underline{r}(\tau) \cong \underline{r}(kT)$ for $kT \leq t < (k+1)T$. Therefore, effectively, the input of the continuous-data system of Fig. 1-1 is assumed to pass through a sample-and-hold device. The above assumption would not affect the solution if $\underline{r}(\tau)$ has step functions as its elements. However, if the inputs are other than step functions, the approximation is a good one for small sampling periods.

Now letting $t_o = kT$ and $t = (k+1)T$ in Eq. (1-4), and assuming $\underline{r}(\tau) \cong \underline{r}(kT)$ over one sampling period, we have

$$\underline{x}_c[(k+1)T] = e^{[A-BG(0)]T}\underline{x}_c(kT) + \int_{kT}^{(k+1)T} e^{[A-BG(0)](kT+T-\tau)}d\tau BE(0)\underline{r}(kT) \qquad (1\text{-}10)$$

$kT \leq t \leq (k+1)T$.

The responses of Eq. (1-9) and Eq. (1-10) will match at $t = (k+1)T$ for an arbitrary initial state $\underline{x}_c(kT)$ and an arbitrary input $\underline{r}(\tau)$, if and only if the following two equations are satisfied.

$$e^{[A-BG(0)]T} = e^{AT} - \int_{kT}^{(k+1)T} e^{A[kT+T-\tau]}\,d\tau BG(T) \qquad (1\text{-}11)$$

and

$$\int_{kT}^{(k+1)T} e^{A(kT+T-\tau)}\, d\tau BE(T)\underline{r}(kT) = \int_{kT}^{(k+1)T} e^{[A-BG(0)](kT+T-\tau)}\, BE(0)\underline{r}(\tau)\, d\tau \tag{1-12}$$

First working with Eq. (1-11), we let $\lambda = (k + 1)T - \tau$. Then, Eq. (1-11) becomes

$$e^{[A-BG(0)]T} = e^{AT} - \int_0^T e^{A\lambda}\, d\lambda BG(T) \tag{1-13}$$

In principle, the feedback matrix, G(T), of the sampled-data system can be determined from Eq. (1-13). However, it is subject to the limitations as discussed in the following section.

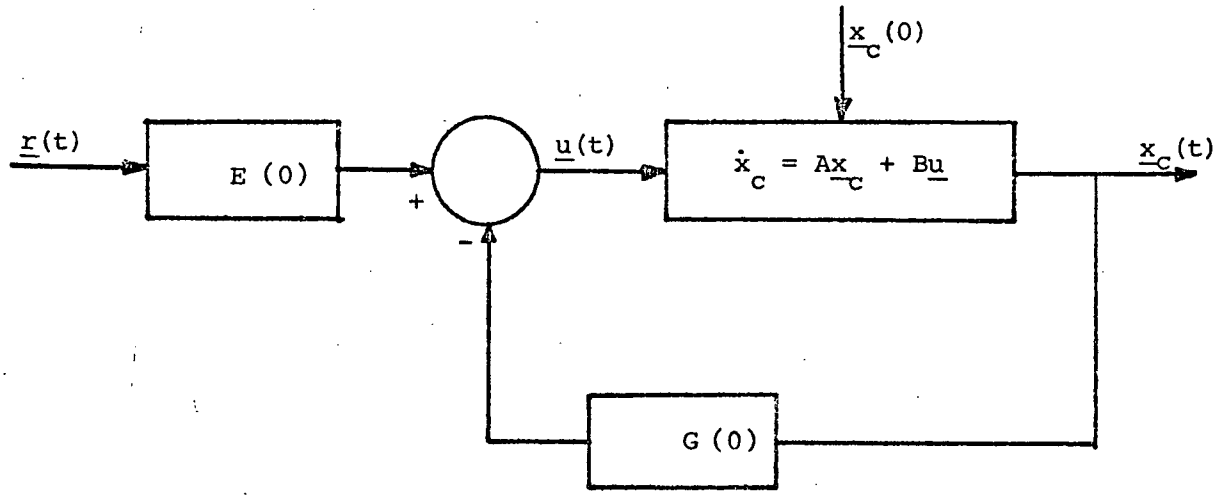

Figure 1-1. A continuous-data system.

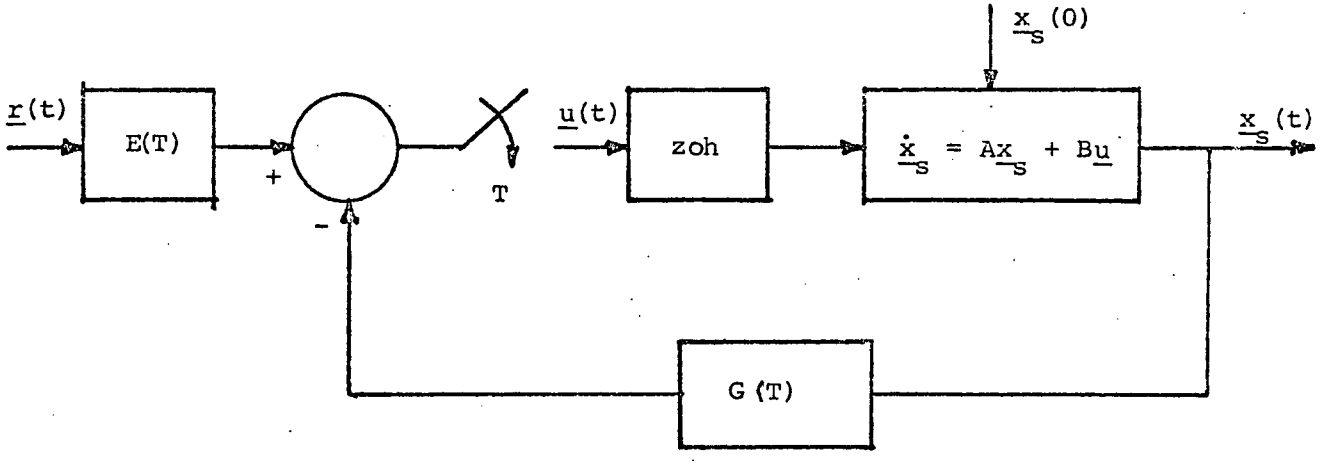

Figure 1-2. Sampled-data system.

1.2 Closed Form Solutions for G(T)

In order that all n states of the continuous system $\underline{x}_c(kT)$ match those of the sampled system $\underline{x}_s(kT)$ at the end of each sampling period it is sufficient that equation (1-13) be satisfied. Equation (1-13) may be written in the simplified matrix form,

$$D(T) = -\theta(T)G(T) \tag{1-14}$$

where

$$D(T) = e^{[A-BG(0)]T} - e^{AT} \tag{1-15}$$

$$\theta(T) = \int_0^T e^{A\lambda} B d\lambda \tag{1-16}$$

Equation (1-14) consists of n^2 scalar equations with mn unknowns. If the number of unknowns equals the number of equations, m = n, and $\theta(T)$ is nonsingular, then a unique solution of Eq.(1-14) exists and is given by

$$G(T) = -\theta^{-1}(T)D(T) \tag{1-17}$$

A Special Case for Exact Matching

If the control system has more states than controls, n > m, which is the case in most control systems, Eq.(1-14) will generally not have a solution. However, if the rank conditions described in the following are satisfied, the system of equations in Eq.(1-14) are consistent and there still is a solution.

Let

$$G(T) = [g_1, g_2, \ldots, g_n] \tag{1-18}$$

$$D(T) = [d_1, d_2, \ldots, d_n] \tag{1-19}$$

where g_i, i = 1, ..., n, are m-dimensional vectors and d_i, i=1, ..., n, are n-dimensional vectors, then if

$$\text{rank } [\theta] = \text{rank } [\theta, d_i] \tag{1-20}$$

for all i=1, ..., n, the system of equations in Eq.(1-14) has at least one solution. If the above conditions are not satisfied the equations are inconsistent and no solution exists.

Partial Matching of States

Generally speaking, the above rank conditions will not be satisfied and thus for the case where n > m not all of the states of the continuous and sampled systems can be made to match at the end of each sampling period.

Although it is not possible to match all of the states it can be shown that it is possible to match some of the states or algebraic sums of the states at each sampling period. Multiplying both sides of Eq. (1-14) by a constant m x n matrix H gives,

$$HD(T) = - H\theta(T)G(T) \tag{1-21}$$

The above equation consists of mn scalar equations and mn unknowns. If H is chosen such that $H\theta(T)$ is nonsingular, Eq. (1-21) may be solved for a solution, $G_w(T)$,

$$G_w(T) = - [H\theta(T)]^{-1}HD(T) \tag{1-22}$$

It should be noted that the above solution for G(T) does not satisfy Eq.(1-14). The reason is that when Eq. (1-14) is premultiplied by the matrix H, it reduces the system of n^2 equations to a system of mn equations. Only if Eq.(1-14) had been multiplied by a nonsingular

matrix would the new system of equations be equivalent to the original system. Since H is a m x n matrix, for n > m the transformation is a singular one, and the solution may not necessarily satisfy the original set of equations.

To understand the consequencies of the transformation and the physical meaning of the solution of Eq.(1-22), we match Eqs. (1-9) and (1-10) in the following form:

$$\underline{x}_c[(k+1)T] = \phi_c(T)\underline{x}_c(kT) + \theta_c(T)E(0)\underline{r}(kT)$$

$$= \underline{x}_s[(k+1)T] = [\phi_0(T) - \theta(T)G(T)]\underline{x}_s(kT) + \theta(T)E(T)\underline{r}(kT) \quad (1\text{-}23)$$

where

$$\phi_c(T) = e^{[A-BG(0)]T} \quad \text{(state transition matrix of the closed-loop continuous-data system)} \quad (1\text{-}24)$$

$$\phi_0(T) = e^{AT} \quad \text{(state transition matrix of the open-loop system)} \quad (1\text{-}25)$$

$$\theta_c(T) = \int_0^T e^{[A-BG(0)]\lambda}\, d\lambda B \quad (1\text{-}26)$$

Premultiplying both sides of Eq.(1-23) by the m x n matrix H gives

$$H\underline{x}_c[(k+1)T] = H\phi_c(T)\underline{x}_c(kT) + H\theta_c(T)E(0)\underline{r}(kT)$$

$$= H\underline{x}_s[(k+1)T] = H[\phi_0(T) - \theta(T)G(T)]\underline{x}_s(kT) + H\theta(T)E(T)\underline{r}(kT) \quad (1\text{-}27)$$

For arbitrary $\underline{x}_c(kT)$, $\underline{x}_s(kT)$, and $\underline{r}(kT)$, the last equation leads to

$$H\phi_c(T)\,\underline{x}_c(kT) = H[\phi_0(T) - \theta(T)G(T)\underline{x}_s(kT) \quad (1\text{-}28)$$

and

$$H\theta_c(T)E(0)\underline{r}(kT) = H\theta(T)E(T)\underline{r}(kT) \tag{1-29}$$

The significant point is that the solution, $G_w(T)$, of Eq. (1-22) satisfies Eq. (1-29) for any arbitrary "initial" state $\underline{x}_c(kT)$. Premultiplying both sides of Eqs. (1-9) and (1-10) by H simply transforms the n-dimensional state vectors $\underline{x}_c[(k + 1)T]$ and $\underline{x}_s[(k + 1)T]$ into a new m-dimensional vector, $\underline{y}[(k + 1)T]$, such that

$$\underline{y}[(k + 1)T] = H\underline{x}_c[k + 1)T] = H\underline{x}_s[(k + 1)T] \tag{1-30}$$

Note that the new states $y_i[(k + 1)T]$, $i = 1, 2, \ldots, m$, are algebraic sums of the original n state variables; that is,

$$y_i[(k + 1)T] = \sum_{j=1}^{n} h_{ij}x_j[(k + 1)T] \qquad i = 1, 2, \ldots m \tag{1-31}$$

Although the solution, $G_w(T)$, of Eq. (1-22) does not match the n states of the continuous system, $\underline{x}_c[(k + 1)T]$, to the n states of the sampled system $\underline{x}_s[(k + 1)T]$, at time $(k + 1)T$, it does match an algebraic sum of these states.

$$\underline{y}[(k + 1)T] = H\underline{x}_c[(k + 1)T] = H\underline{x}_s[(k + 1)T] \tag{1-32}$$

1.3 An Exact Solution for $G_w(T)$

With the understanding of the conditions and limitations as described in the preceding section, we shall derive an exact closed-form solution of the feedback gain $G_w(T)$ which partially matches the states at the end of each sampling period as governed by the weighting matrix H. Starting with Eq. (1-13)

$$e^{[A-BG(0)]T} = e^{AT} - \int_0^T e^{A\lambda}\, d\lambda BG(T) \tag{1-33}$$

Let

$$\theta(T) = \int_0^T e^{A\lambda} d\lambda B = \sum_{j=0}^{\infty} \frac{A^j T^{j+1}}{(j+1)!} B \tag{1-34}$$

then

$$e^{[A-BG(0)]T} = e^{AT} - \theta(T)G(T) \tag{1-35}$$

Premultiplying by a weighting matrix H which is chosen such that $H\theta(T)$ is nonsingular and solving for G(T)

$$G_w(T) = [H\theta(T)]^{-1} H[e^{AT} - e^{[A-BG(0)]T}] \tag{1-36}$$

A special case of interest is when $H = B'$. In this case $H\theta$ may be expressed as a quadratic form

$$H\theta(T) = \int_0^T B' e^{A\lambda} B\, d\lambda \tag{1-37}$$

Since

$$e^{A\lambda} = \sum_{j=0}^{\infty} \frac{A^j T^j}{j!} \tag{1-38}$$

for λ sufficiently small $e^{A\lambda} > 0$ (i.e. a positive definite matrix). Thus it can be argued that there exists a number $\alpha > 0$ such that if $T < \alpha$ then

$$e^{A\lambda} > 0 \quad \text{for } 0 \leq \lambda \leq T$$

and therefore the quadratic form

$$\int_0^T B' e^{A\lambda} B \, d\lambda > 0.$$

Then for $T < \alpha$, $H\theta(T)$ is nonsingular.

1.4 G(T) By Series Expansion

In this section we shall derive a Taylor series expansion for G(T) about T = 0. In general, if this series converges, G(T) can be approximated by taking a finite number of terms of the series expansion.

Let G(T) be represented by a Taylor series about T = 0; that is

$$G(T) = \lim_{K\to\infty} G_K(T) = \lim_{K\to\infty} \sum_{j=0}^{K-1} \frac{1}{j!} G^{(j)}(T) T^j \tag{1-39}$$

where

$$G^{(j)}(T) = \left.\frac{\partial^j G(T)}{\partial T^j}\right|_{T=0} \tag{1-40}$$

Substitute G(T) from Eq. (1-39) into Eq. (1-13), we get

$$e^{[A-BG(0)]T} = e^{AT} - \int_0^T e^{A\lambda} d\lambda B \sum_{j=0}^{\infty} \frac{1}{j!} G^{(j)}(T) T^j \tag{1-41}$$

Or

$$\sum_{j=0}^{\infty} \frac{[A - BG(0)]^j T^j}{j!} = \sum_{j=0}^{\infty} \frac{A^j T^j}{j!} - \sum_{j=0}^{\infty} \frac{A^j T^{j+1}}{(j+1)!} B \sum_{k=0}^{\infty} \frac{G_k(T) T^k}{k!} \tag{1-42}$$

The last equation is written

$$\sum_{j=0}^{\infty} \left[\frac{[A - BG(0)]^j T^j}{j!} - \frac{A^j T^j}{j!} + \frac{A^j B}{(j+1)!} \sum_{k=0}^{\infty} \frac{G^{(k)}(T) T^{k+j+1}}{k!} \right] = \underline{0} \tag{1-43}$$

Now equating the coefficients of T^p ($p = 1, 2, \ldots$) to zero, we have

$$\frac{[A - BG(0)]^p}{p!} - \frac{A^p}{p!} + \sum_{j=0}^{p-1} \frac{A^{p-j-1} B G^{(j)}(T)}{(p-j)!\,j!} = \underline{0} \tag{1-44}$$

In general, it is possible to express $G^{(p-1)}(T)$ in terms of $G^{(p-2)}(T)$, $G^{(p-3)}(T)$, ..., $G^{(1)}(T)$, $G^{(0)}(T)$, where $G^{(0)}(T) = G(0)$.

Equation (1-44) is written

$$\frac{[A-BG(0)]^p}{p!} - \frac{A^p}{p!} + \sum_{j=0}^{p-2} \frac{A^{p-j-1}BG^{(j)}(T)}{(p-1)!j!} + \frac{BG^{(p-1)}(T)}{(p-1)!} \qquad (1\text{-}45)$$

Therefore,

$$\frac{BG^{(p-1)}(T)}{(p-1)!} = \frac{A^p}{p!} - \frac{[A-BG(0)]^p}{p!} - \sum_{j=0}^{m-2} \frac{A^{m-j-1}BG^{(j)}(T)}{(p-j)!j!} \qquad (1\text{-}46)$$

Then, let H be an m x n matrix such that (HB) is nonsingular; Eq. (1-46) leads to the solution of $G^{(p-1)}(T)$,

$$G^{(p-1)}(T) = (HB)^{-1}H\left\{\frac{A^p}{p} - \frac{[A-BG(0)]^p}{p} - (p-1)!\sum_{j=0}^{p-2} \frac{A^{p-j-1}BG^{(j)}(T)}{(p-j)!j!}\right\} \qquad (1\text{-}47)$$

$p = 1, 2, \ldots$.

The following table gives the expressions for $G^{(p-1)}(T)$ for $p = 1, 2,$ and 3. Then, according to Eq. (1-39),

$$G_1(T) = G^{(0)}(T) = G(0) \qquad (1\text{-}48)$$

$$G_2(T) = G(0) + TG^{(1)}(T) \qquad (1\text{-}49)$$

$$G_3(T) = G(0) + TG^{(1)}(T) + \frac{T^2}{2}G^{(2)}(T) \qquad (1\text{-}50)$$

Table 1-1.

p	$G^{(p-1)}(T)$
1	$G(0)$
2	$\frac{1}{2}G(0)[A - BG(0)]$
3	$(HB)^{-1}H\{-\frac{1}{6}ABG(0)[A - BG(0)] + \frac{1}{3}BG(0)[A - BG(0)]^2\}$

It is interesting to note that since $G^{(0)}(T)$ and $G^{(1)}(T)$ are not dependent upon H, the one-term and the two-term series approximations of $G(T)$, $G_1(T)$ and $G_2(T)$, respectively, will attempt to match all the states of the continuous-data and the sampled-data systems. Beyond two terms, the weighting matrix, H, must be used, and only certain states and combinations of states are matched, depending on the H selected. As more terms are added to the series approximation, $G_K(T)$ will approach the exact solution of $G_w(T)$ of Eq. (1-36).

1.5 An Exact Solution For E(T)

The solution of E(T) is obtained from Eq. (1-23),

$$\theta(T)E(T) = \theta_c(T)E(0) \tag{1-51}$$

Similar to the closed-form solution for G(T) discussed in Section 1.2, if m = n, and $\theta(T)$ is nonsingular, a unique solution of Eq. (1-51) exists, and is given by

$$E(T) = \theta^{-1}(T)\theta_c(T)E(0) \tag{1-52}$$

When n > m, the solution of the matrix E(T) which corresponds to the partial matching of states is obtained from Eq. (1-29),

$$H\theta(T)E_w(T) = H\theta_c(T)E(0) \tag{1-53}$$

Therefore,

$$E_w(T) = [H\theta(T)]^{-1} H\theta_c(T)E(0) \tag{1-54}$$

where it is assumed that $H\theta(T)$ is nonsingular.

1.6 E(T) By Series Expansion

Similar to the solution of G(T), the matrix E(T) may be expanded into a Taylor series about T = 0; that is

$$E(T)=\lim_{K\to\infty} E_K(T) \tag{1-55}$$

where

$$E_K(T) = \sum_{j=0}^{K-1} \frac{1}{j!} E^{(j)}(T)T^j \tag{1-56}$$

where

$$E^{(j)}(T) = \left.\frac{\partial^j E(T)}{\partial T^j}\right|_{T=0} \tag{1-57}$$

Substituting the series expansion of E(T) into Eq. (1-51), we get

$$\theta(T) \sum_{j=0}^{\infty} \frac{1}{j!} E^{(j)}(T)T^j = \theta_c(T)E(0) \tag{1-58}$$

Or,

$$\sum_{j=0}^{\infty} \frac{1}{j!} A^j \frac{T^{j+1}}{j+1} B \sum_{k=0}^{\infty} \frac{1}{k!} E^{(k)}(T)T^k = \sum_{j=0}^{\infty} \frac{1}{j!} [A - BG(0)]^j \frac{T^{j+1}}{j+1} BE(0) \tag{1-59}$$

The last equation is simplified to

$$\sum_{j=0}^{\infty} \left[\frac{A^j B}{(j+1)!} \sum_{k=0}^{\infty} \frac{E^{(k)}(T)T^{k+j+1}}{k!} - \frac{[A - BG(0)]^j T^{j+1}}{(j+1)!} BE(0) \right] = \underline{0} \tag{1-60}$$

Equating the coefficients of T^p $(p = 1, 2, \ldots)$ to zero, we have

$$- \frac{[A - BG(0)]^{p-1}BE(0)}{p!} + \frac{A^{p-1}B}{p!} E(0) + \frac{A^{p-2}BE^{(1)}(T)}{(p-1)!} + \frac{A^{p-3}BE^{(2)}(T)}{(p-2)!2!} + \ldots + \frac{A^{0}BE^{(p-1)}(T)}{1!(p-1)!} \quad (1\text{-}61)$$

Or,

$$BE^{(p-1)}(T) = \frac{[A - BG(0)]^{p-1}BE(0)}{p} - (p-1)! \sum_{j=0}^{p-2} \frac{A^{p-j-1}BE^{(j)}(T)}{(p-j)!j!} \quad (1\text{-}62)$$

Now let H be an m x n matrix such that HB is nonsingular, the solution of $E^{(p-1)}(T)$ is given by

$$E^{(p-1)}(T) = (HB)^{-1}H\left\{ \frac{[A - BG(0)]^{p-1}BE(0)}{p} - (p-1)! \sum_{j=0}^{p-2} \frac{A^{p-j-1}BE^{(j)}(T)}{(p-j)!j!} \right\} \quad (1\text{-}63)$$

$p = 1, 2, \ldots$.

The following table gives the expressions for $E^{(p-1)}(T)$ for $p = 1, 2,$ and 3.

Table 1-2.

p	$E^{(p-1)}(T)$
1	$E(0)$
2	$-\frac{1}{2} G(0)BE(0)$
3	$(HB)^{-1}H\left\{ \frac{ABG(0)B}{6} - \frac{BG(0)[A - BG(0)]B}{3} \right\} E(0)$

Notice that, similar to the situation for G(T), if only up to two terms are used in the series approximation for E(T), the H matrix is not needed, and all the states of the sampled-data and the continuous-data systems are apparently matched.

1.7 Computer Program for Computation of Truncated Series, $G_K(T)$ and $E_K(T)$

The power series expansions of $G_w(T)$ and $E_w(T)$ are defined in Eqs. (1-36) and (1-54), respectively. An approximation utilizing the first K terms of the infinite power series can be written as

$$G_w(T) \cong G_K(T) = \sum_{i=0}^{K-1} G^{(i)}(T) \frac{T^i}{i!} \tag{1-64}$$

and

$$E_w(T) \cong E_K(T) = \sum_{i=0}^{K-1} E^{(i)}(T) \frac{T^i}{i!} \tag{1-65}$$

where

$$G^{(i-1)}(T) = (HB)^{-1} H \left\{ \frac{A^i}{j} - \frac{[A - BG(0)]^i}{i} - (i-1)! \sum_{j=0}^{i-2} \frac{A^{i-j-1} BG^{(j)}(T)}{(i-j)!\,j!} \right\} \tag{1-66}$$

(A-3)

$$E^{(i-1)}(T) = (HB)^{-1} H \left\{ \frac{[A - BG(0)]^{i-1}}{i} BE(0) - (i-1)! \sum_{j=0}^{i-2} \frac{A^{i-j-1}}{(i-j)!\,j!} BE^{(j)}(T) \right\}$$

(1-67)

$$G^{(0)} = G(0) \tag{1-68}$$

and

$$E^{(0)} = E(0) \tag{1-69}$$

Equation (1-64)- (1-67) can be modified for computational efficiency, Let

$$\hat{G}^{(m)}(T) = \frac{G^{(m-1)}(T)}{(m-1)!} \tag{1-70}$$

$$\hat{E}^{(m)}(T) = \frac{E^{(m-1)}(T)}{(m-1)!} \tag{1-71}$$

$$\overline{A}_i = \frac{A^i}{i!} \tag{1-72}$$

$$\overline{[A - BG(0)]}_i = \frac{[A - BG(0)]^i}{i!} \tag{1-73}$$

$$\overline{(AB)}_i = \frac{A^i B}{(i+1)!} \tag{1-74}$$

then the K-term series approximations of $G_w(T)$ and $E_w(T)$ become

$$G_K(T) = \sum_{i=0}^{K-1} \hat{G}^{(i+1)}(T) T^i \tag{1-75}$$

and

$$E_K(T) = \sum_{i-0}^{K-1} \hat{E}^{(i+1)}(T) T^i \tag{1-76}$$

with

$$\hat{G}^{(i)}(T) = (HB)^{-1} H \left[\overline{A}_i - \overline{[A - BG(0)]}_i - \sum_{j=2}^{i} \overline{(AB)}_{i-j+1} \hat{G}^{(j-1)}(T) \right] \tag{1-77}$$

$$\hat{E}^{(i)}(T) = (HB)^{-1} H \left[\frac{\overline{[A-BG(0)]}_{i-1} BE(0)}{i} - \sum_{j=2}^{i} \overline{(AB)}_{i-j+1} \hat{E}^{(j-1)}(T) \right] \tag{1-78}$$

$$\hat{G}^{(1)}(T) = G(0) \tag{1-79}$$

and

$$\hat{E}^{(1)}(T) = E(0) \tag{1-80}$$

Figure 1-3 shows the flow chart of the computer program used for implimenting equations (1-75) - (1-80) Two additional quantities, TP and NUM, are defined. These determine the values

of the sampling period T for which the approximations of $G_w(T)$ and $E_w(T)$ are calculated. With TP and NUM given the sampling period T varies from T = TP to T = TP x NUM in NUM increments.

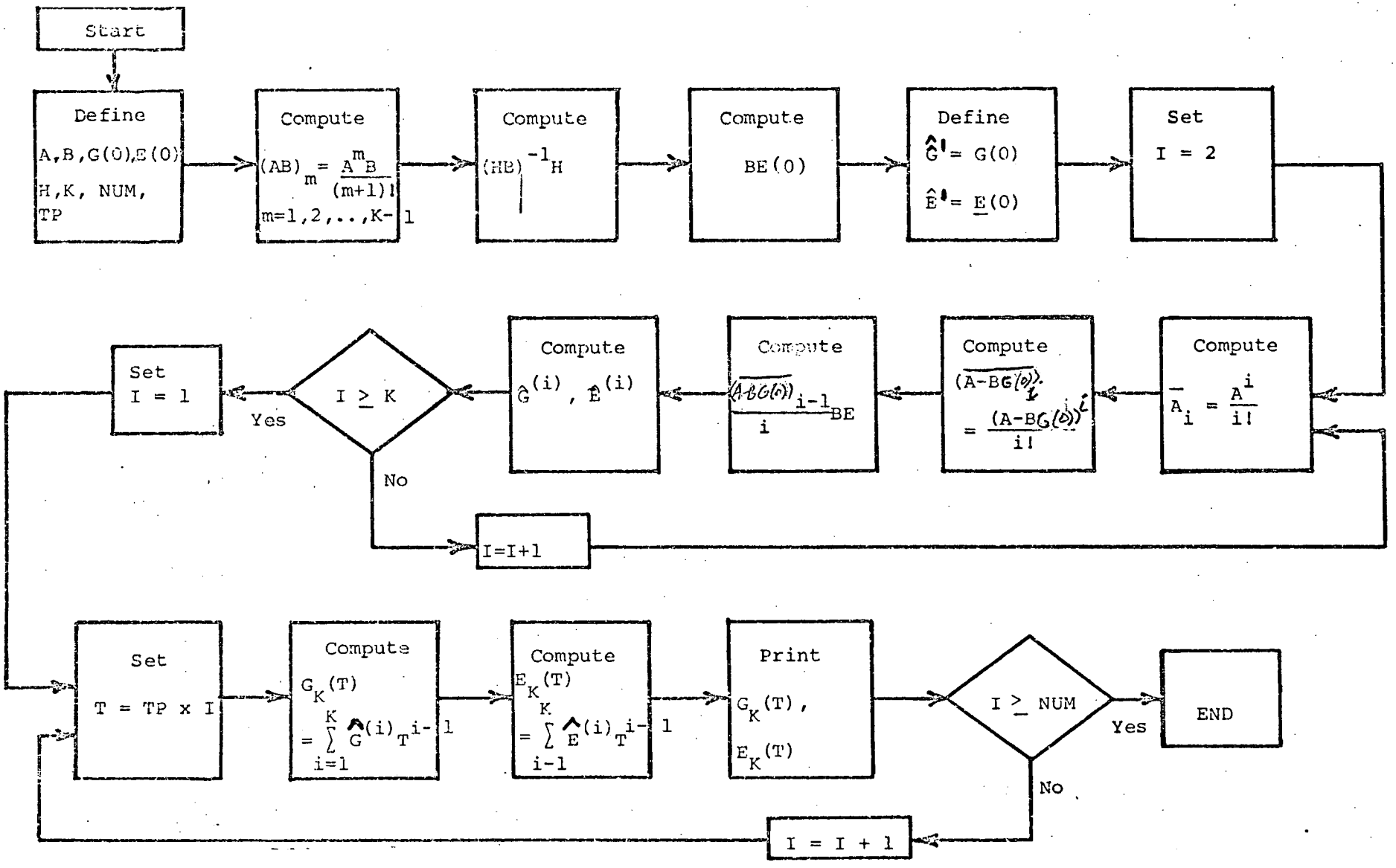

Figure 1-3 Flow Chart for Computation of Series Approximations of $G_w(T)$ and $E_w(T)$.

1.8 Computer Program for Computation of G_W and E_W

The flow diagram for the computer program that calculates G_W and E_W is shown in Fig. 1-4 The program is a straightforward implementation of the formulas(1-47) and (1-63) The subroutine STRMAT is called to calculate the state transition matrix and the integral of the state transition matrix over one sampling period. Its flow diagram is shown in Fig. 1-5 These matrices are calculated by means of the following infinite series.

$$\phi(T) = e^{AT} = \frac{I}{0!} + \frac{AT}{1!} + \frac{A^2T^2}{2!} + \cdots \qquad (1\text{-}81)$$

$$\overline{\theta}(T) = \int_0^T e^{A\lambda} d\lambda = \frac{IT}{1!} + \frac{AT^2}{2!} + \frac{A^2T^3}{3!} + \cdots \qquad (1\text{-}82)$$

Let M be the kth partial sum of the $\phi(\tau)$ series

$$M = \sum_{k=0}^{K} \frac{A^k T^k}{k!} \qquad (1\text{-}83)$$

and R the remainder matrix

$$R = \sum_{k=K+1}^{\infty} \frac{A^k T^k}{k!} \qquad (1\text{-}84)$$

Using the upper bounds established by M. L. Liou [1] and W. Everling [2] the elements, r_{ij}, of R may be bounded by

$$|r_{ij}| \leq \left|\left|\frac{(AT)^K}{K!}\right|\right| \cdot \frac{||A||T}{K+1} \cdot \frac{1}{1-\varepsilon} \qquad (1\text{-}85)$$

where $$\varepsilon = \frac{||A||T}{K+2} \qquad (1\text{-}86)$$

The error test for terminating the summation of the series (1-81) that

$$|r_{ij}| \leq \alpha |m_{ij}| \tag{1-87}$$

where $\alpha = 10^{-6}$ and m_{ij} are the elements of M. The above inequality must hold for all i, j except for elements m_{ij} that are close to zero. If

$$|m_{ij}| < \beta, \qquad \beta = 10^{-30} \tag{1-88}$$

the test(1-87)is bypassed.

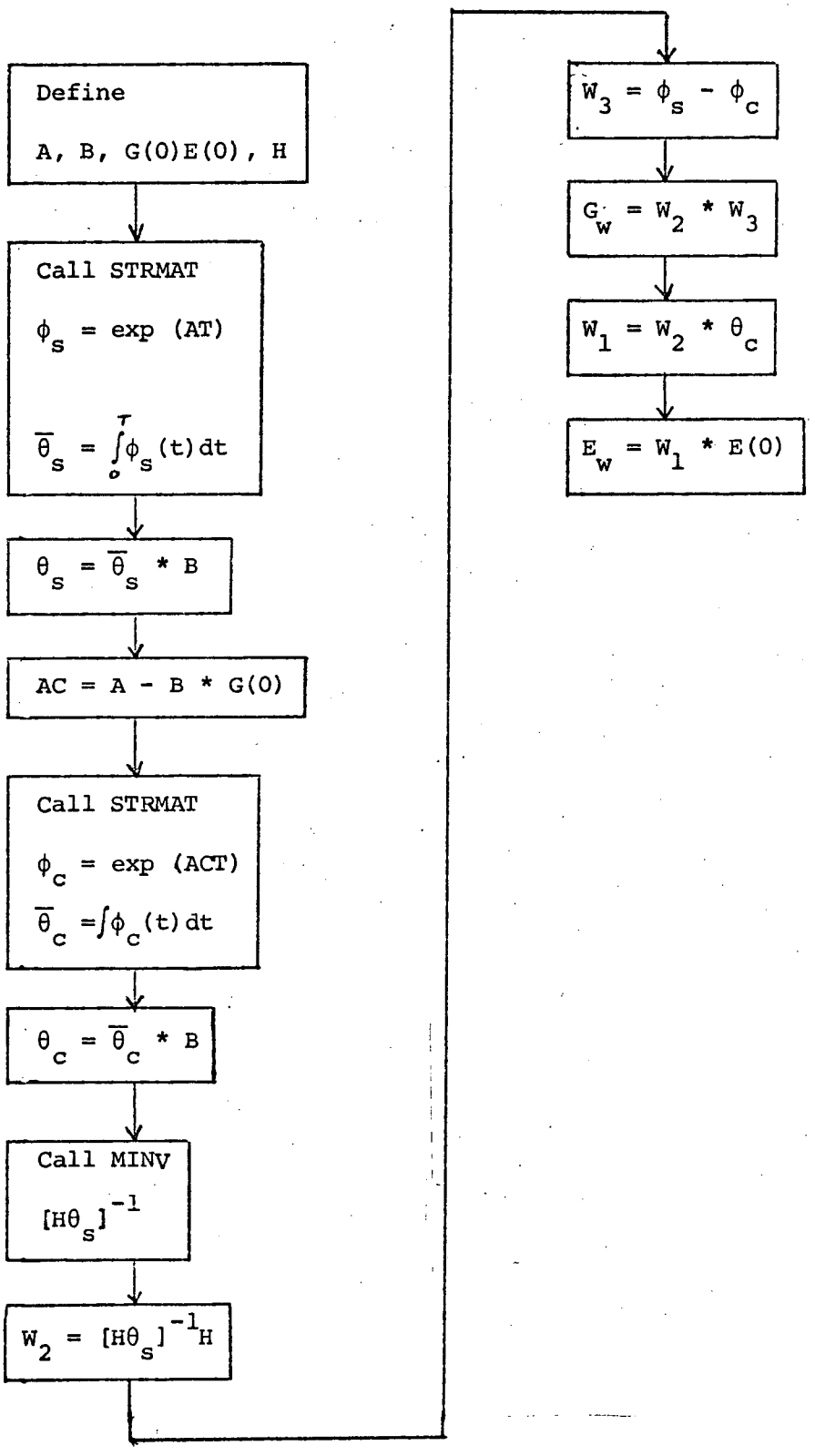

Figure 1-4 Flow chart for the calculation of G_W and E_W.

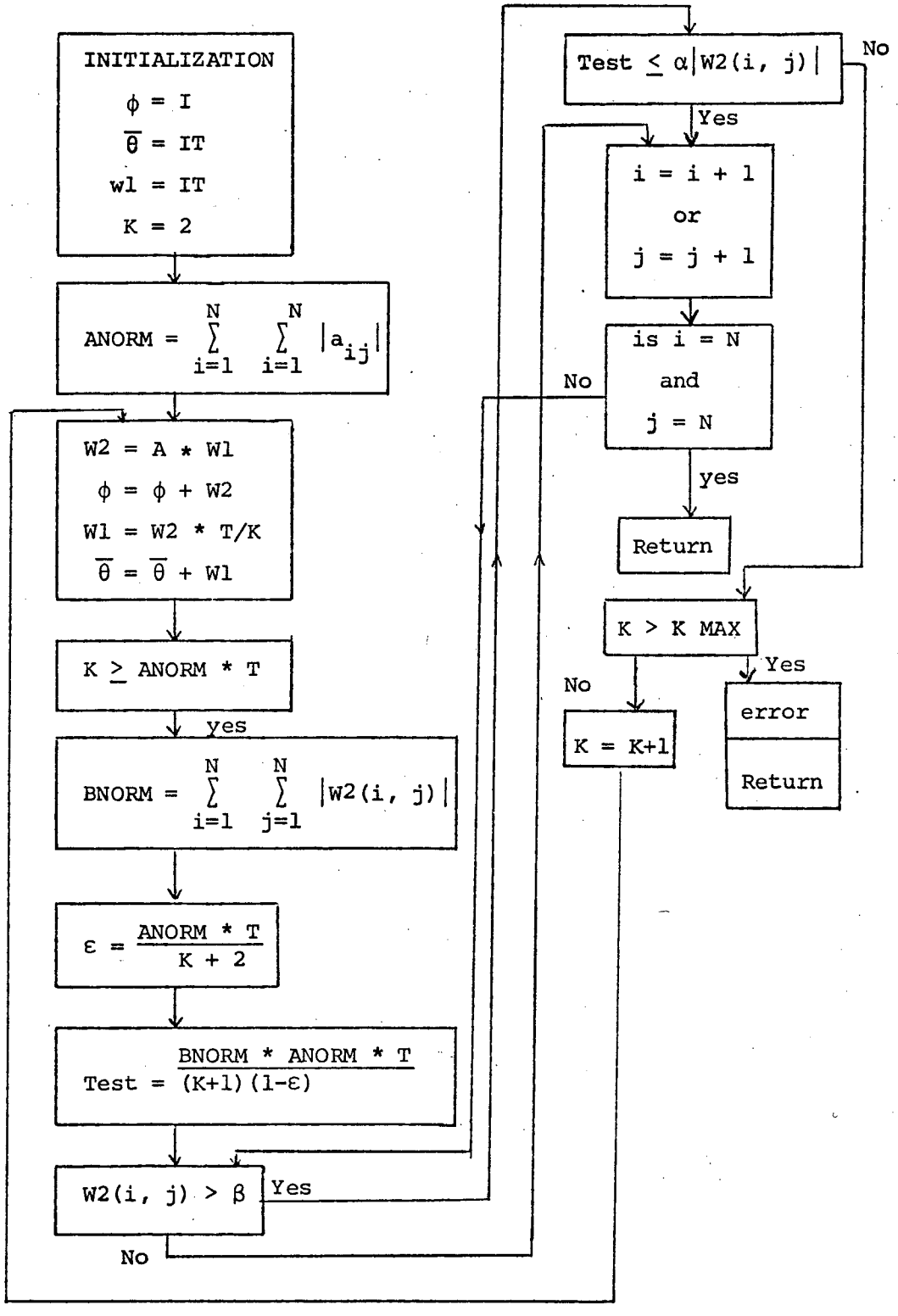

Figure 1-5 Flow chart for calculation of the state transition matrix and its integral, STRMAT.

1.9 Digital Redesign of the Simplified One-Axis Dynamics of the Skylab Satellite.

In this section digital redesign with the partial matching method is applied to the simplified one-axis dynamics of the Skylab Satellite.

The block diagram of the simplified Skylab Satellite is shown in Fig. 1-6. The constants of the system are given as

$$I = 970{,}741 \quad Kg - m^2$$

$$K_0 = 11.8 \times 10^3 \quad n - m/rad$$

$$K_1 = 125.9 \times 10^3 \quad n - m/rad/sec$$

The feedback gains g_1 and g_2 are to be selected so that the damping ratio of the system is 0.707. For zero steady-state error, $g_1 = 1$. The closed-loop transfer function of the system is

$$\frac{X_1(s)}{\psi_c(s)} = \frac{K_0}{Is^2+K_1g_2s+K_0}$$

$$= \frac{11800}{970741s^2+125900g_2s+11800}$$

$$= \frac{0.01215}{s^2+0.129g_2s+0.01215} \qquad (1\text{-}89)$$

Therefore, the natural undamped frequency is 0.11 rad/sec, and $g_2 = 1.205$, $K_1g_2 = 151{,}800$.

The state equations of the system are

$$\dot{x}_1 = x_2$$

$$\dot{x}_2 = \frac{1}{I}u \qquad (1\text{-}90)$$

and

$$u = K_0\psi_c - g_1K_0x_1 - g_2K_1x_2$$

$$= E\psi_c - G_{11}(0)x_1 - G_{12}(0)x_2 \qquad (1\text{-}91)$$

Then,

$$A = \begin{bmatrix} 0 & 1 \\ 0 & 0 \end{bmatrix} \qquad B = \begin{bmatrix} 0 \\ 1/970,741 \end{bmatrix} \qquad (1\text{-}92)$$

$$G(0) = [G_{11}(0) \quad G_{12}(0)] = [11800 \quad 151,800]$$

$$E(0) = 11800 \qquad (1\text{-}93)$$

The block diagram for the continuous model of the Skylab Satellite is shown in Fig. 1-7

The present Skylab Satellite system with the feedback gains of Eq.(1-93) has an undamped natural frequency of 0.11 radians/sec. and a damping ratio of 0.707. For this system the exact gains G_W, E_W are computed for T = 1, 2, 3, 4, 5 seconds and H = [0 1] and H = [1 0]. These gains are listed in Table 1-3. With H = [0 1] the state x_2 is attempted to be matched and with H = [1 0] the state x_1 is attempted to be matched.

The system is simulated on a digital computer for both values of H. A sampling period of T = 2 sec is used for the sampled data system. The gains G(0) and E(0) of Eq.(1-93) are used for the continuous system and the gains G_W and E_W (from Table 1-3 for T = 2 sec) are used for the sampled data system.

Figures 1-8 to 1-13 show the simulation results for T = 2 sec. and H = [0 1] and figures 1-14 to 1-19 show the simulation results for T = 2 sec. and H = [1 0]. Figures 1-8 and 1-14 show the state trajectories $x_{1c}(t)$ and $x_{1s}(t)$ for the two cases of H respectively. Figures 1-9 and 1-15 show the error $(x_{1c}(t) - x_{1s}(t))$ for the two cases of H. The remaining figures show the same results for the state x_2 and control u.

The simulation results show that

i) the states are more closely matched with H = [0 1] than with H[1 0] and

ii) a sampling period of T = 2sec. appears to be adequate for digital redesign of the Skylab Satellite system of Fig. 1-6.

Table 1-3

T(seconds)	H	$G_{W11}(T)$	$G_{W12}(T)$	$E_W(T)$
1	[0 1]	10901.5	145840	10901.5
2	"	10051.2	139921	10051.2
3	"	9248.45	134071	9248.45
4	"	8492.5	128315	8492.5
5	"	7782.34	122674	7782.34
1	[1 0]	11197	147825	11197
2	"	10618.1	143867	10618.1
3	"	10063.1	139937	10063.1
4	"	9531.78	136048	9531.78
5	"	9023.72	132207	9023.72

Also $G_{11}(0) = 11800$

$G_{12}(0) = 151,800$

$G(0) = 11,800$

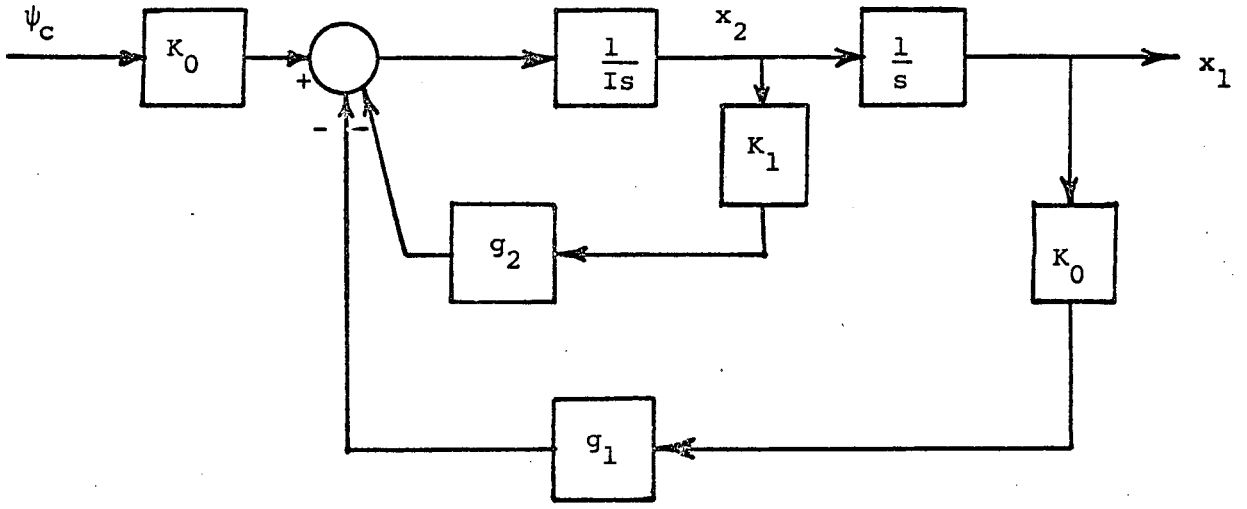

Figure 1-6 Block diagram of a simplified skylab satellite.

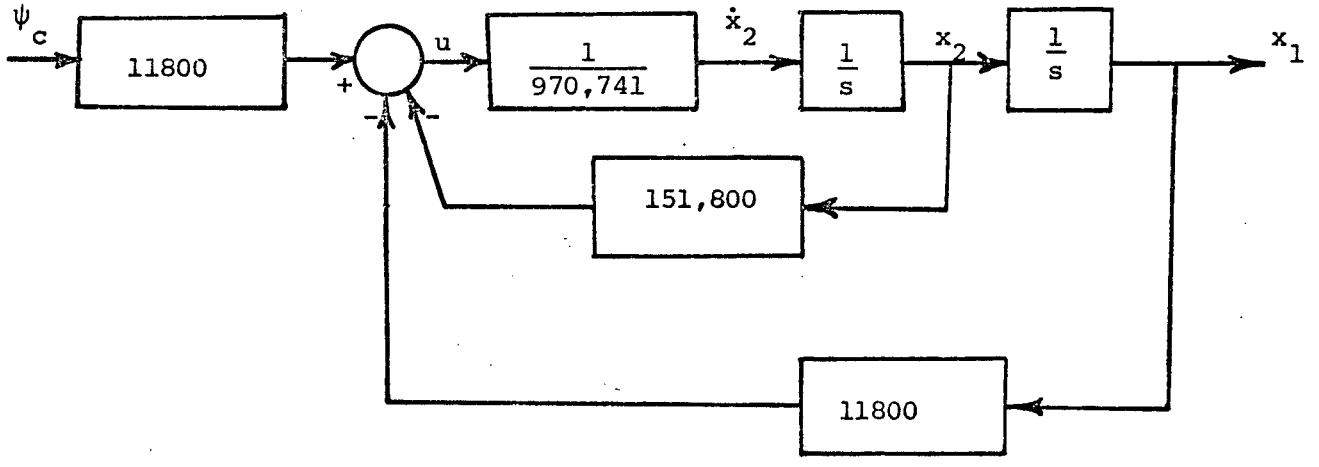

Figure 1-7 Block diagram of the skylab satellite with state feedback for damping ratio of 0.707.

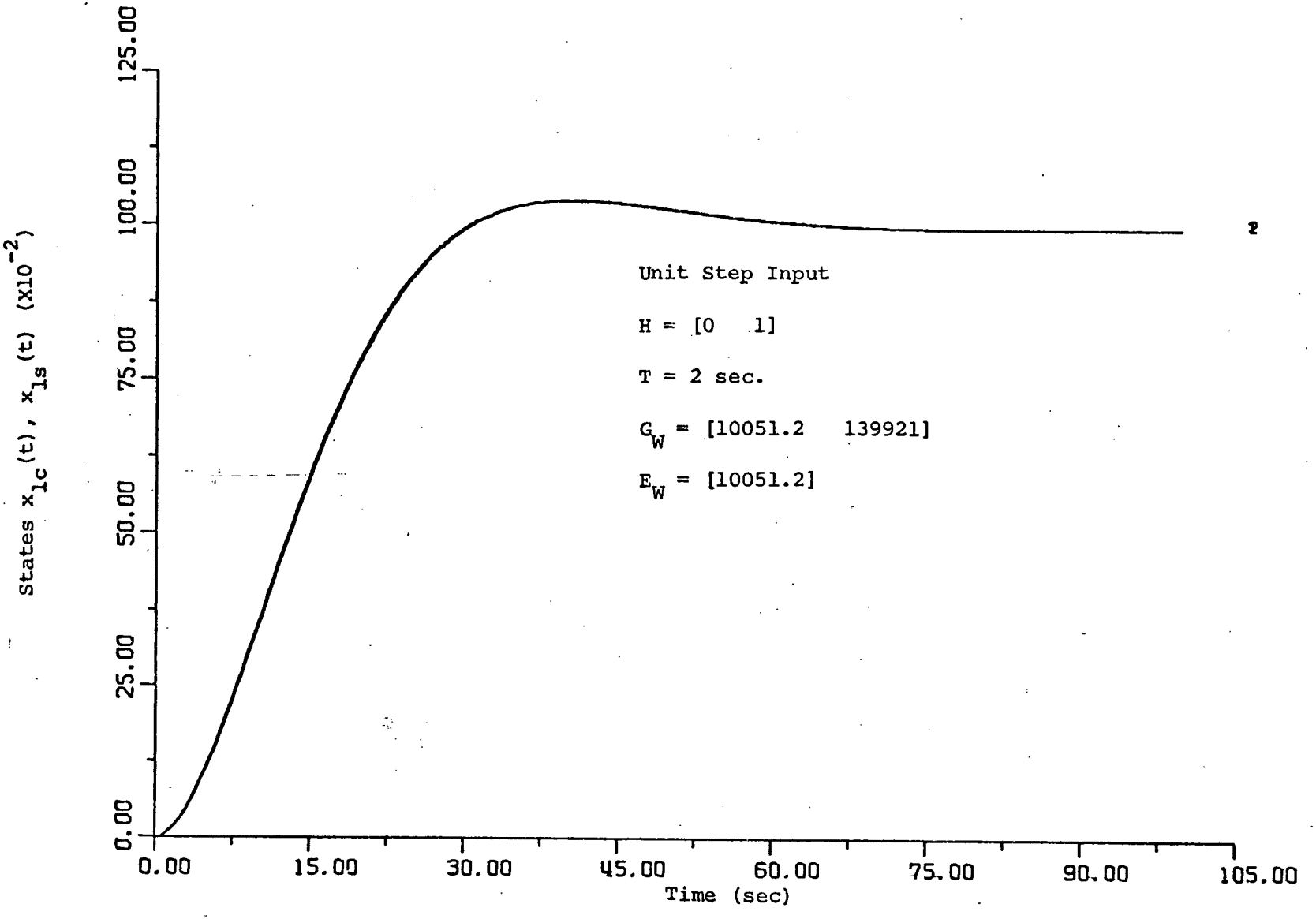

Figure 1-8 State trajectories $x_{1c}(t)$ and $x_{1s}(t)$ for the simplified one axis dynamics of the Skylab Satellite.

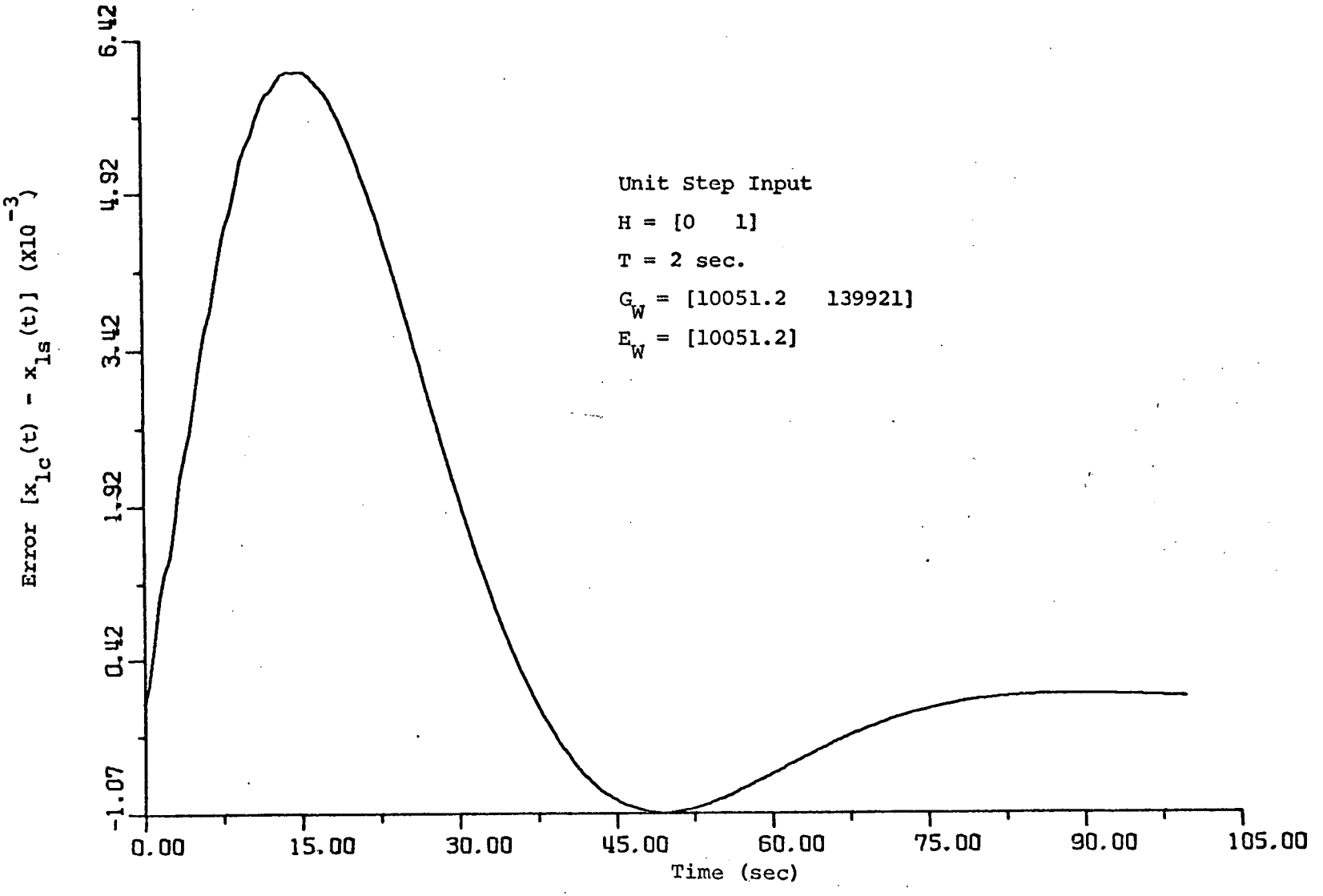

Figure 1-9 Error, $x_{1c}(t) - x_{1s}(t)$, in the state trajectories for the simplified one axis dynamics of the Skylab Satellite.

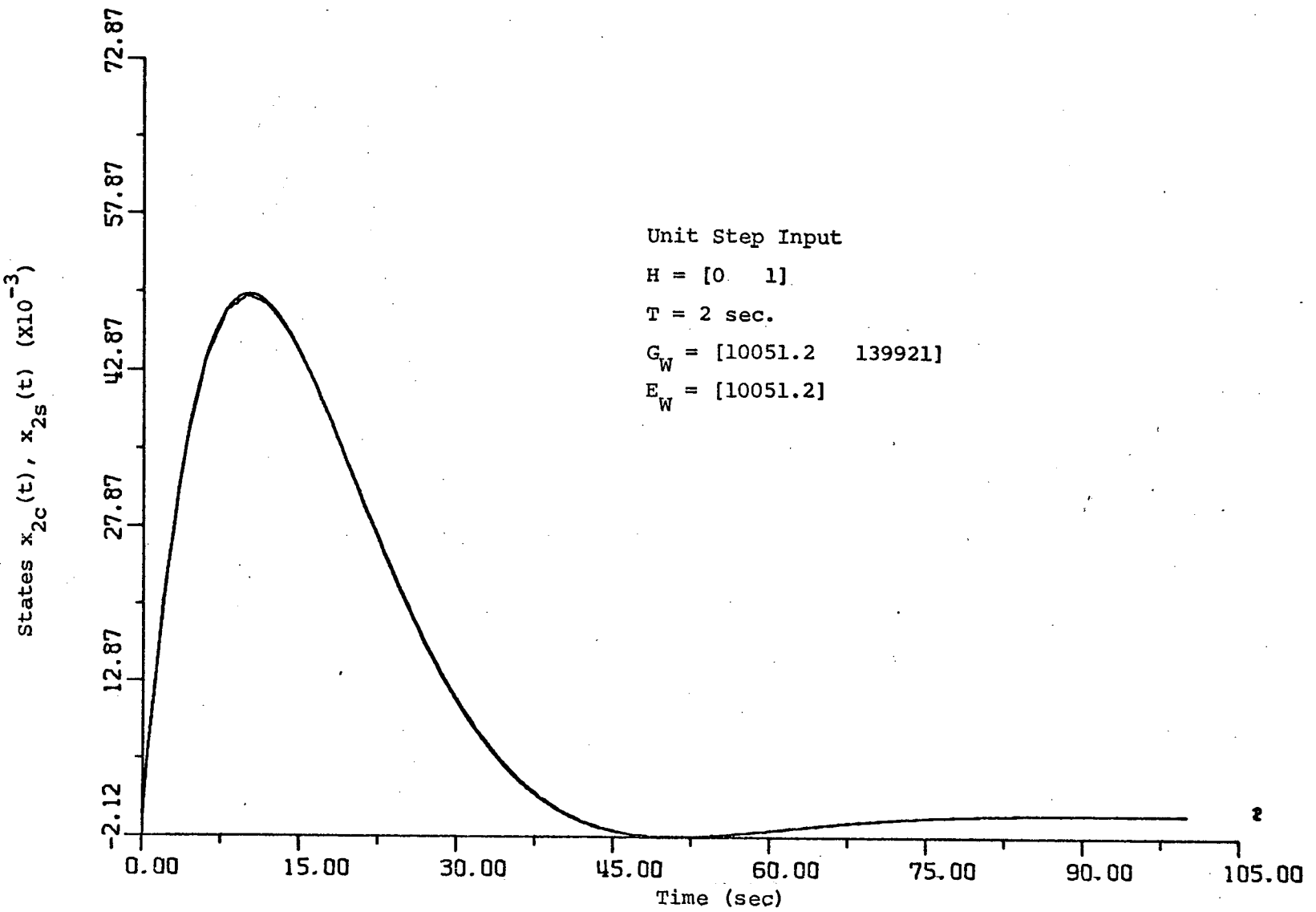

Figure 1-10 State trajectories $x_{2c}(t)$ and $x_{2s}(t)$ for the simplified one axis dynamics of the Skylab Satellite.

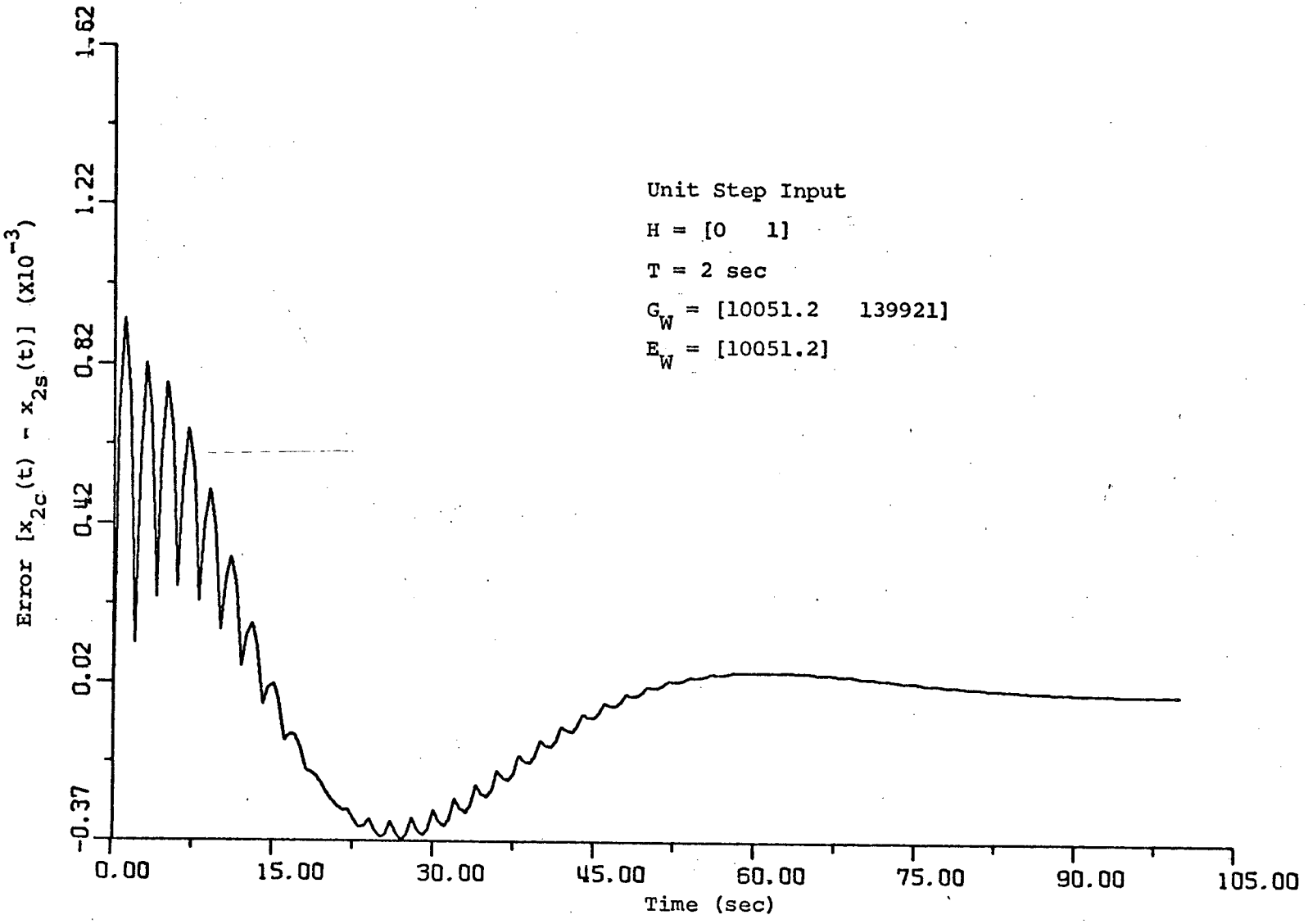

Figure 1-11 Error, $X_{2c}(t) - x_{2s}(t)$, in the state trajectories of the simplified one axis dynamics of the Skylab Satellite.

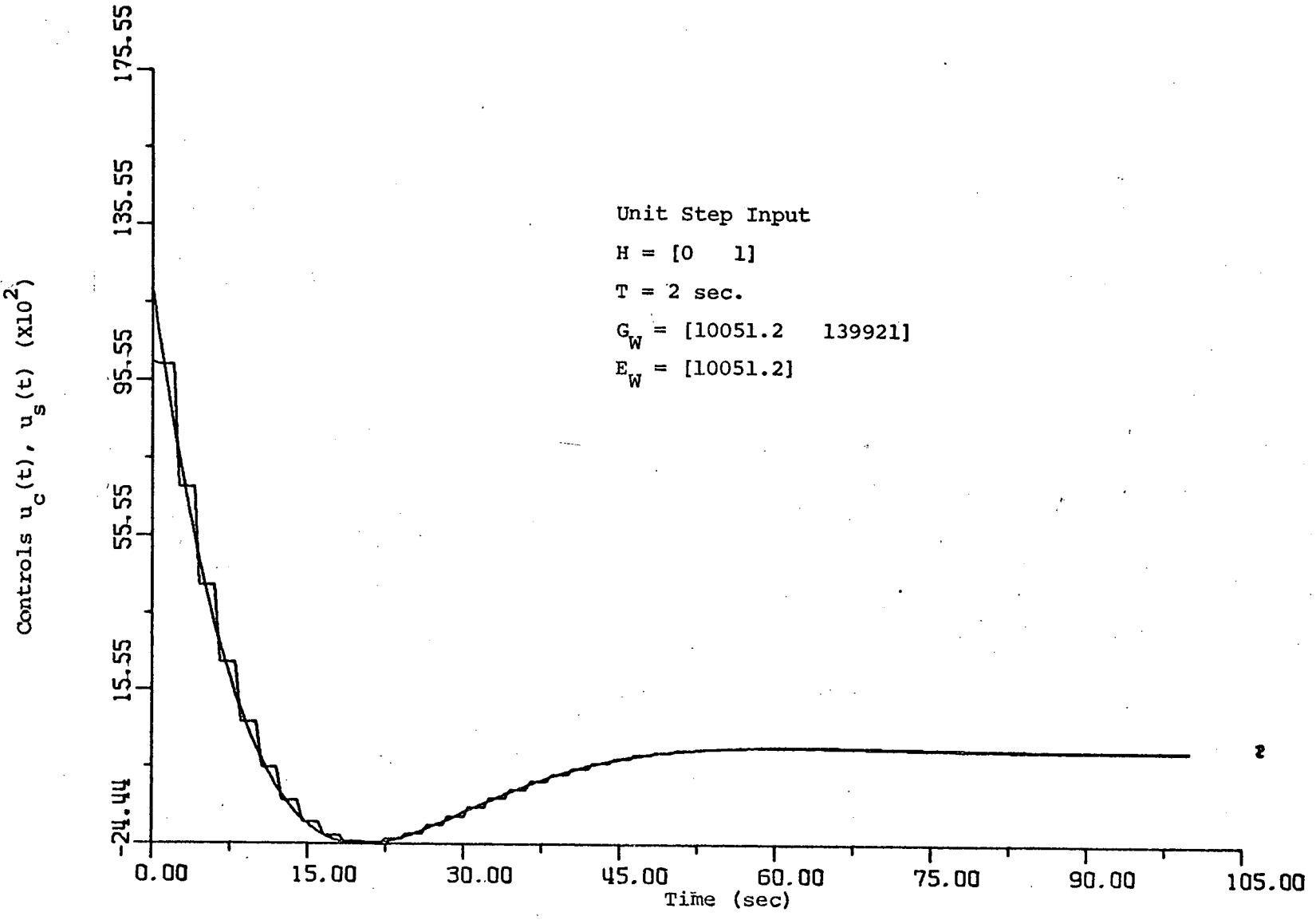

Figure 1-12 Control trajectories $u_c(t)$ and $u_s(t)$ of the simplified one axis dynamics of the Skylab Satellite.

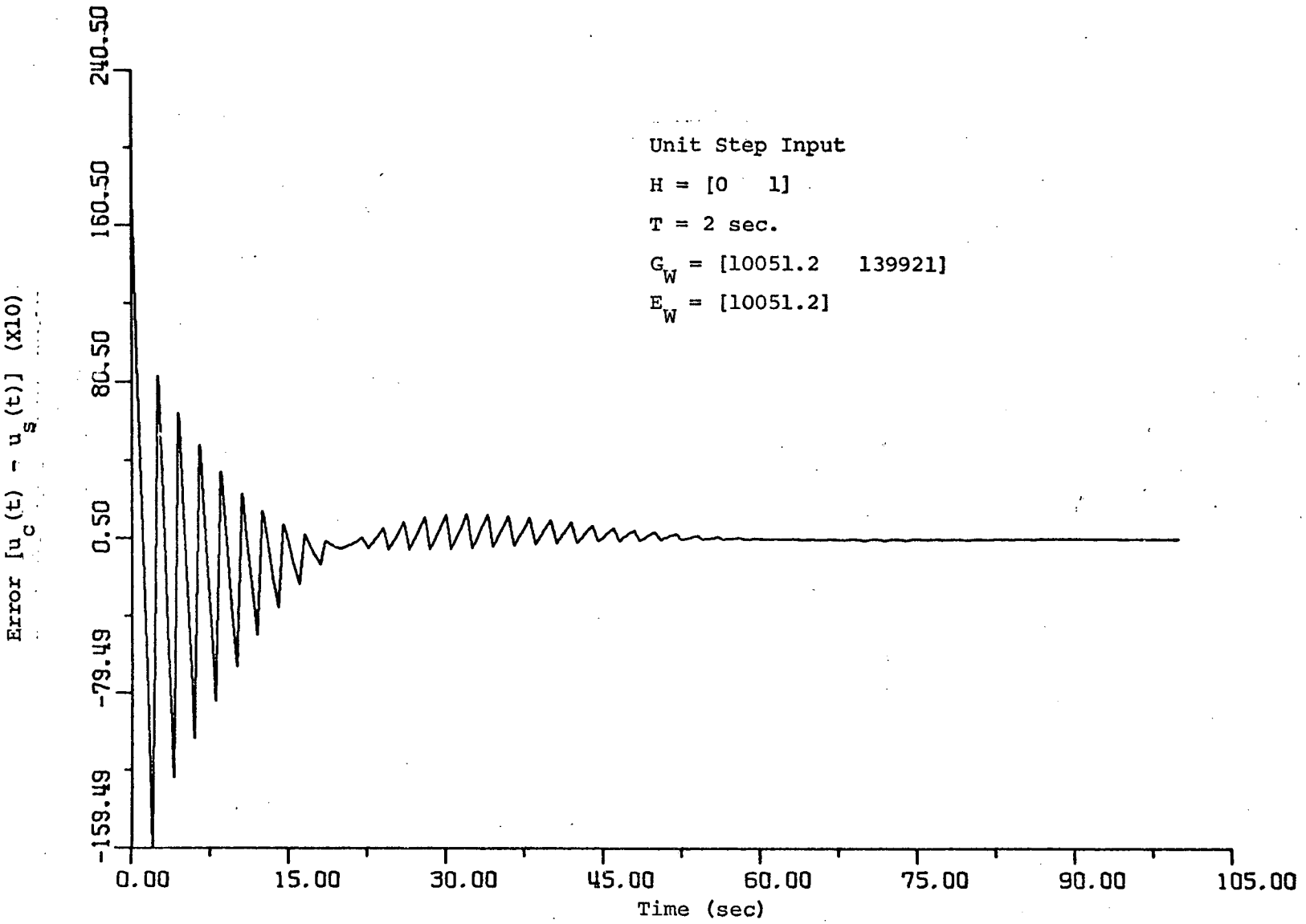

Figure 1-13 Error, $u_c(t) - u_s(t)$, in the control trajectories of the simplified one axis dynamics of the Skylab Satellite.

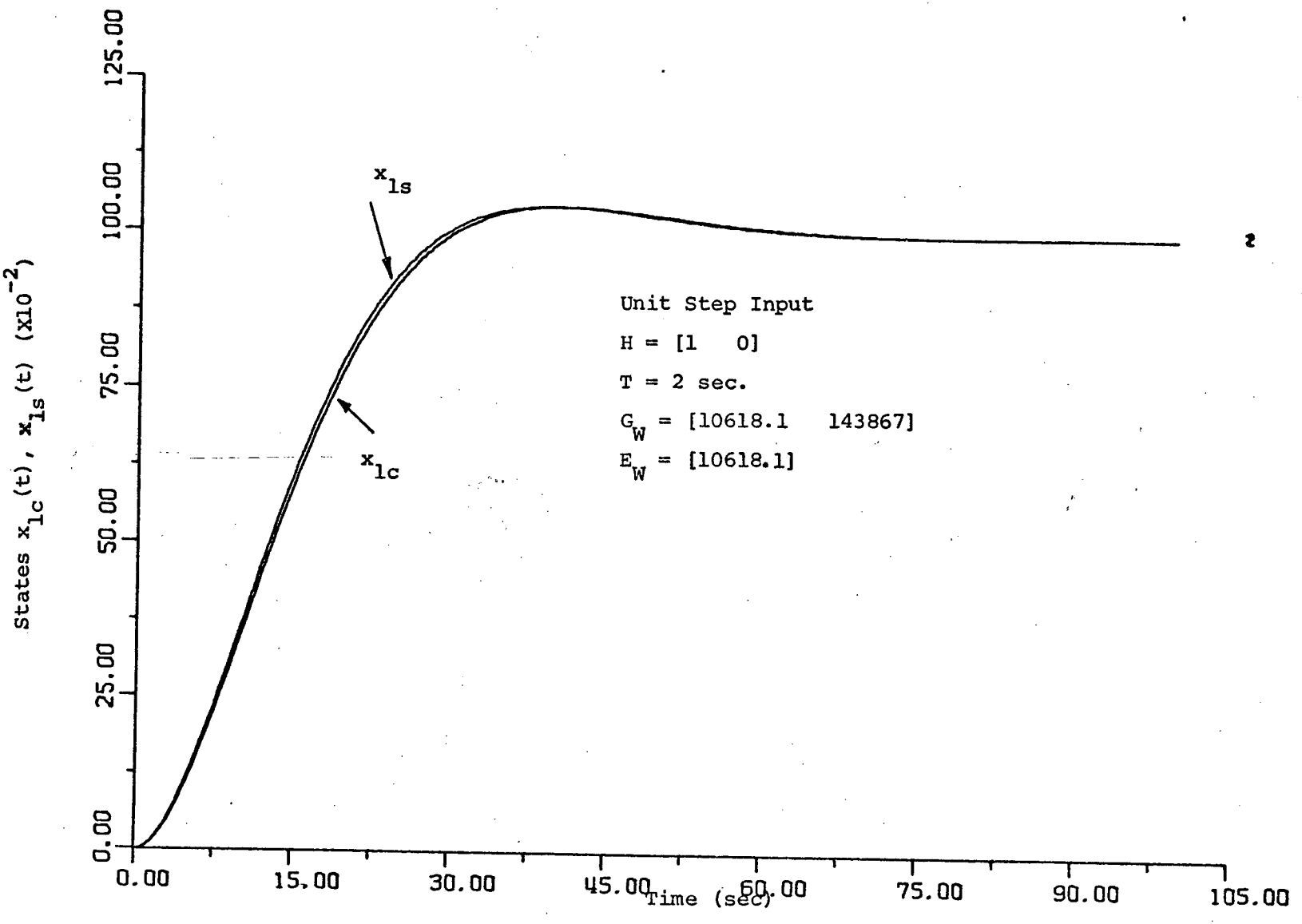

Figure 1-14 State trajectories $x_{lc}(t)$ and $x_{ls}(t)$ for the simplified one axis dynamics of the Skylab Satellite.

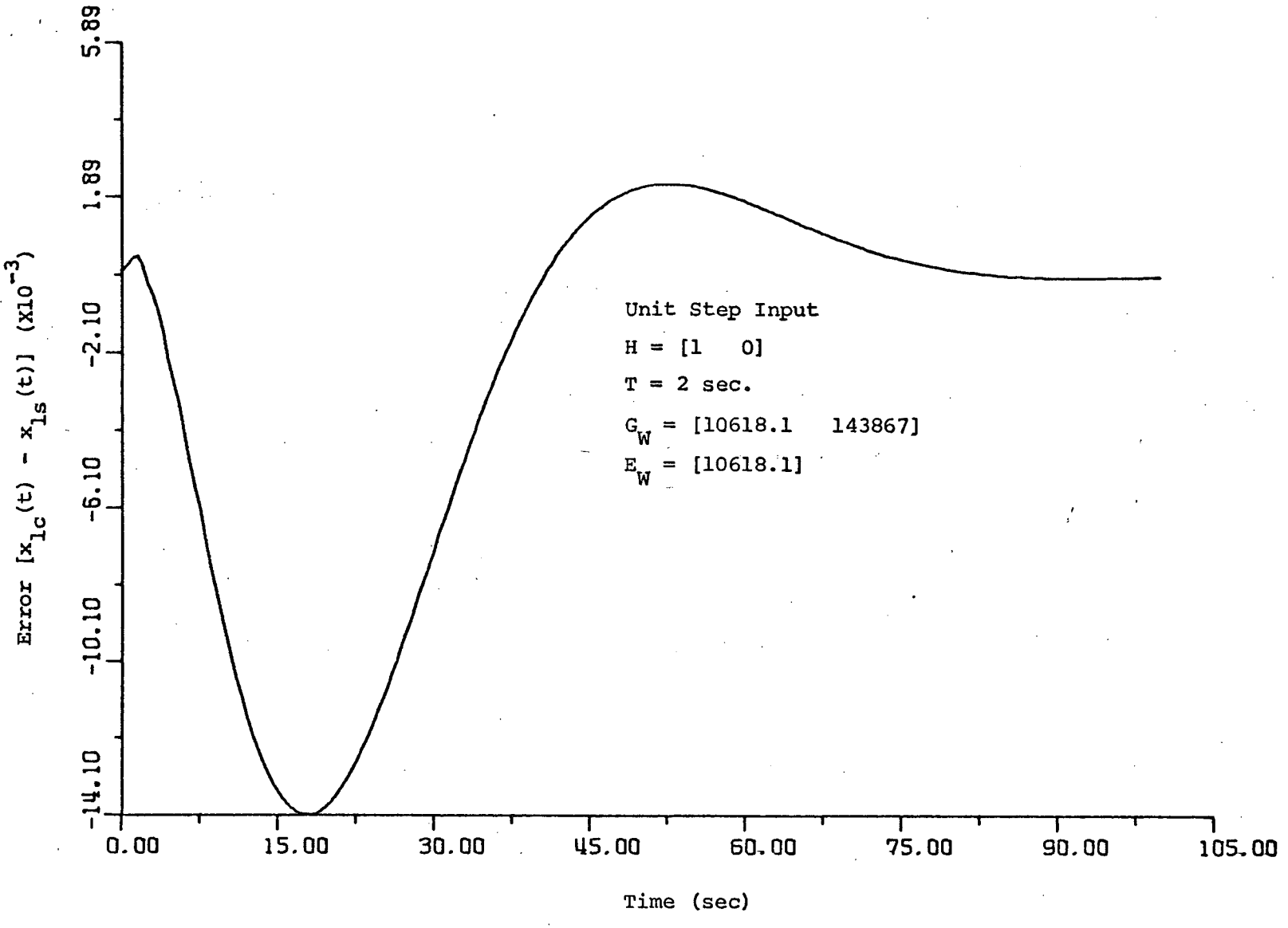

Figure 1-15 Error, $x_{1c}(t) - x_{1s}(t)$, in the state trajectories for the simplified one axis dynamics of the Skylab Satellite.

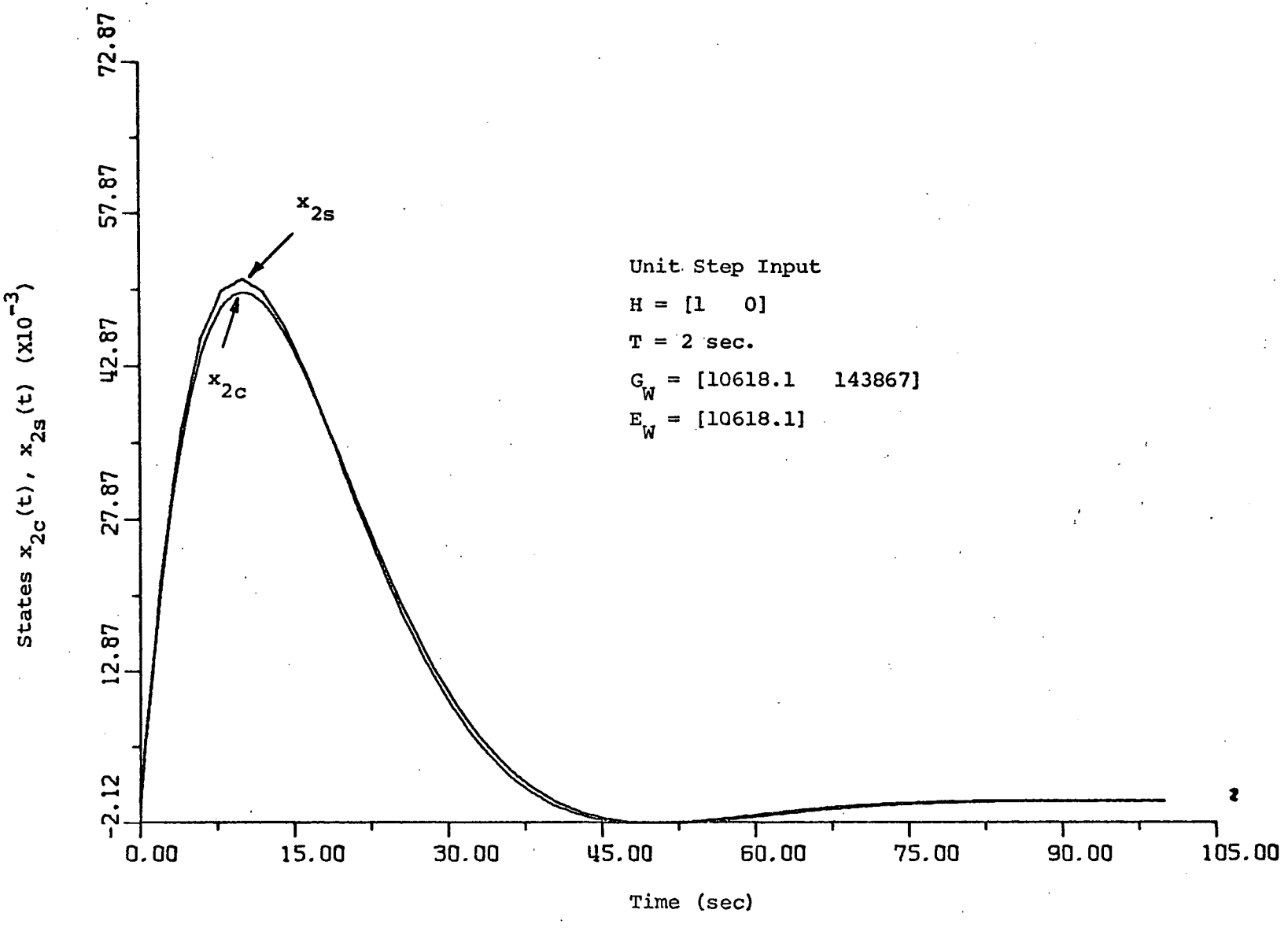

Figure 1-16 State trajectories $x_{2c}(t)$ and $x_{2s}(t)$ for the simplified one axis dynamics of the Skylab Satellite.

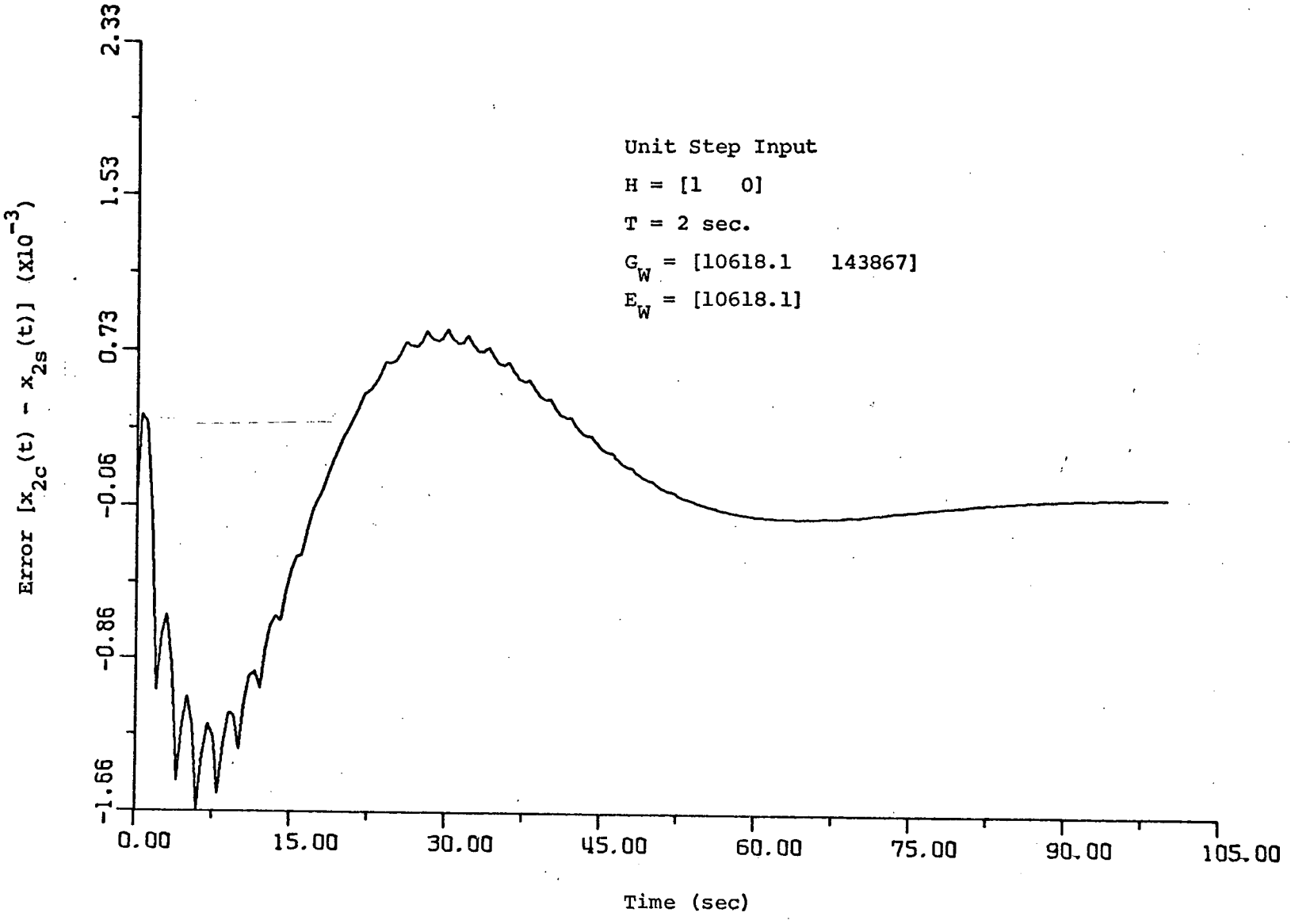

Figure 1-17 Error, $x_{2c}(t) - x_{2s}(t)$, in the state trajectories of the simplified one axis dynamics of the Skylab Satellite.

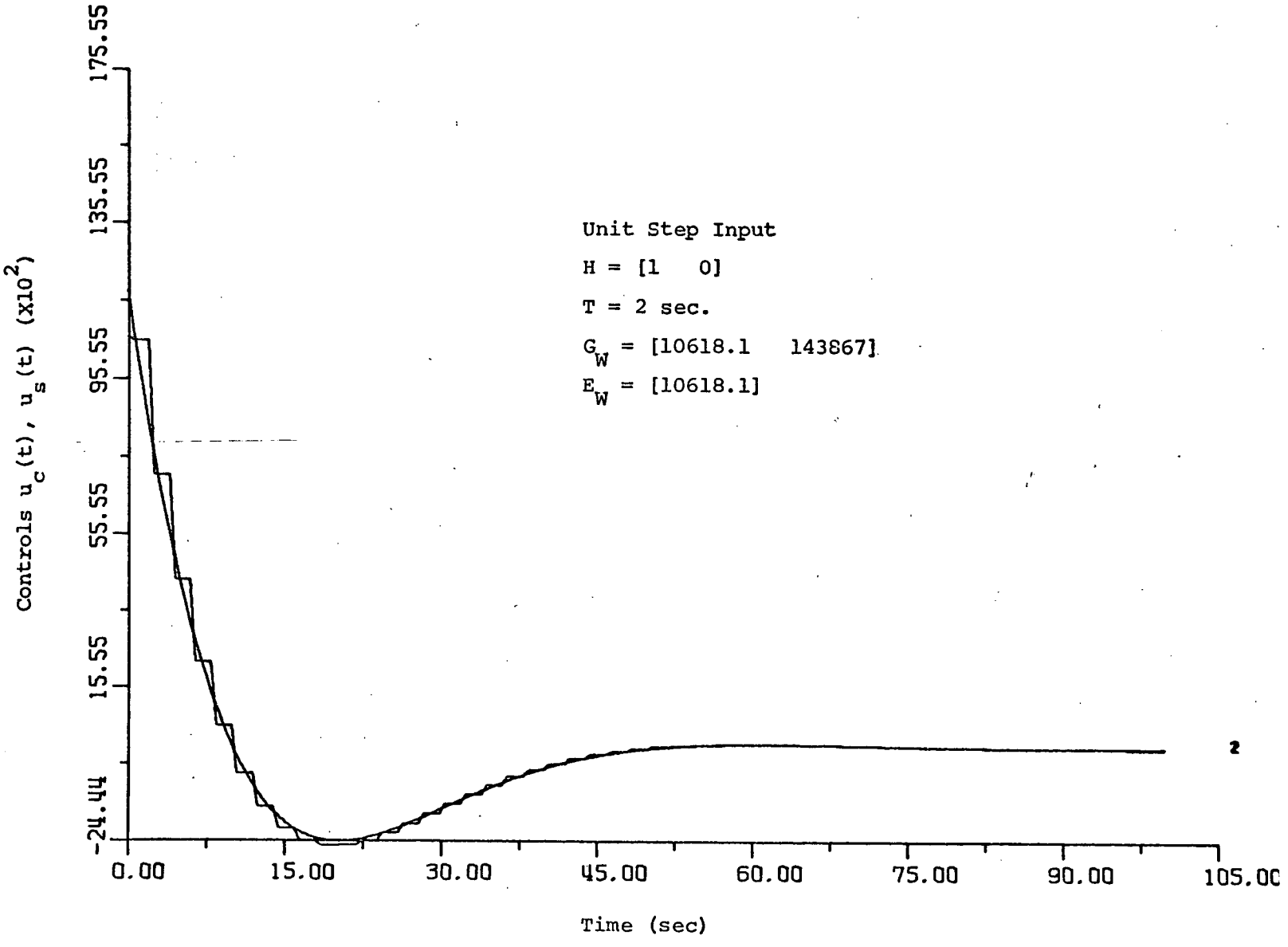

Figure 1-18 Control trajectories $u_c(t)$ and $u_s(t)$ of the simplified one axis dynamics of the Skylab Satellite.

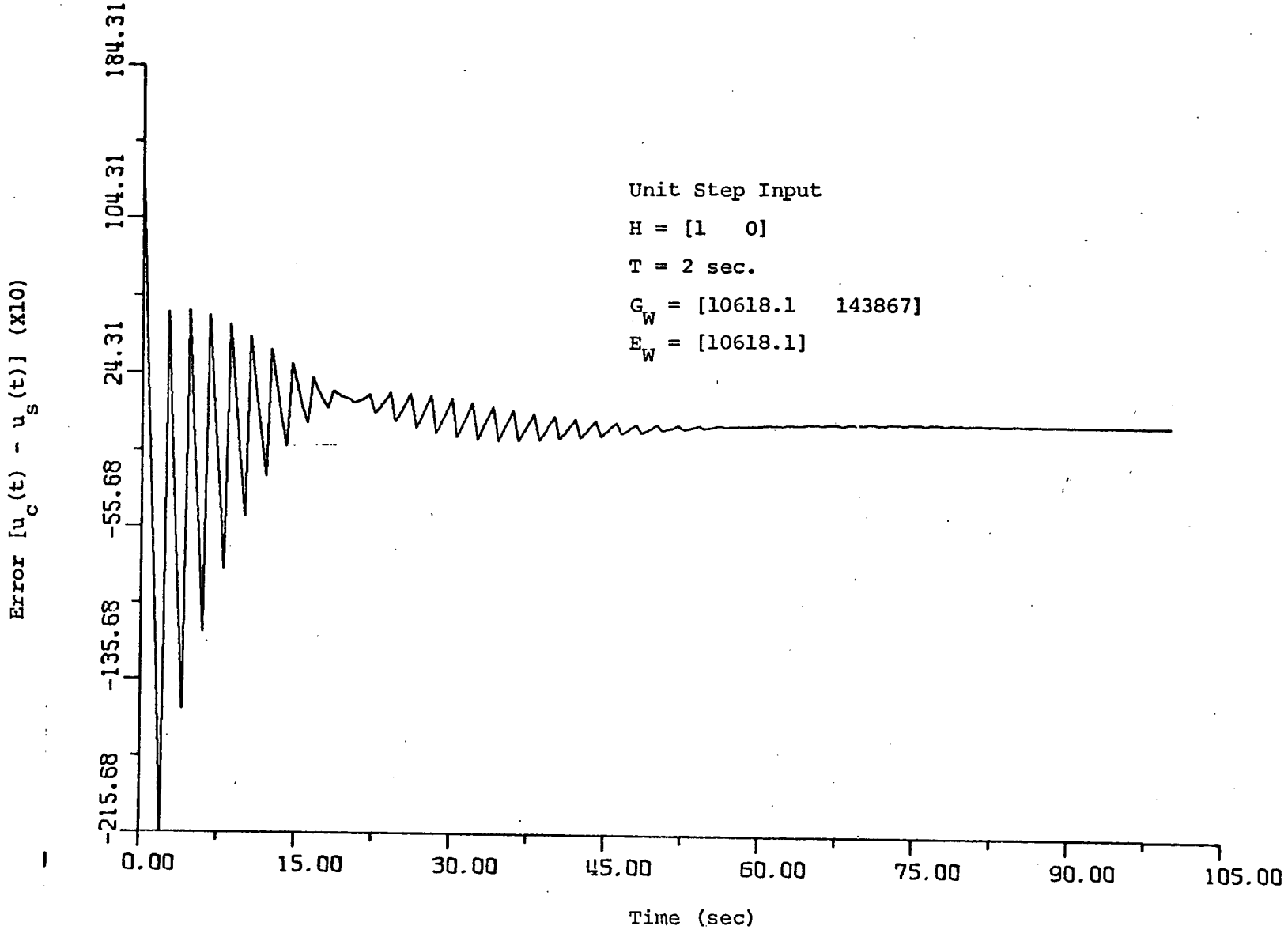

Figure 1-19 Error, $u_c(t) - u_s(t)$, in the control trajectories of the simplified one axis dynamics of the Skylab Satellite.

2. DIGITAL APPROXIMATION BY POINT-BY-POINT STATE COMPARISON WITH EXACT MATCHING AT MULTIPLE SAMPLING PERIODS

2.1 Introduction

The problem is that of approximating a continuous-data system of Fig. 2-1 by a sampled-data model of Fig. 2-2 by comparison of the states of the two systems.

The continuous-data system is described by the following time-invariant dynamic equations:

$$\dot{\underline{x}}_c(t) = A\underline{x}_c(t) + B\underline{u}(t) \tag{2-1}$$

$$\underline{u}(t) = E_c\underline{r}(t) - G_c\underline{x}_c(t) \tag{2-2}$$

where $\underline{x}_c(t)$ denotes an n-vector, $\underline{u}(t)$ and $\underline{r}(t)$ are m-vectors, E_c and G_c are the gains of the forward and the feedback paths, respectively.

The dynamic equations of the sampled-data model are:

$$\dot{\underline{x}}_s(t) = A\underline{x}_s(t) + B\underline{u}_s(t) \tag{2-3}$$

$$\underline{u}_s(kT) = E(T)\underline{r}(kT) - G(T)\underline{x}_s(kT) \tag{2-4}$$

for $kT \leq t \leq (k+1)T$. The sampled-data system is also of the nth order with m inputs. The outputs of the sample-and-hold devices are a series of step functions which are denoted by the vector $\underline{u}_s(kT)$ for $kT \leq t < (k+1)T$.

The objective is to find E(T) and G(T) so that the states of the sampled-data model are as close as possible to that of the continuous-data system.

It was pointed out in Chapter 1 that exact matching of the states of the two systems cannot be achieved in general for an n-state and m-input system, unless n = m and the following matrix is nonsingular.

$$\theta(T) = \int_0^T e^{A\lambda} B d\lambda \tag{2-5}$$

In this chapter we shall show that for a continuous-data system with n states and m inputs, the states can be matched exactly, in principle, subject to approximations, by the states of a sampled-data system every N sampling instants, where

$$n/m \leq N < n/m + 1 \tag{2-6}$$

For instance, for a second-order system with one input, it is possible to match the states of the two systems every two sampling instants. On the other hand, if the sampling period of the sampled-data system, T, has been fixed, it is necessary only to change the forward gain E(T) and the feedback gain G(T) in between the sampling instants, at N equal intervals, to obtain exact matching of states at the sampling instants. It will also be seen that only the values of the states at the sampling instants, kT, k = 1, 2, ..., need to be fed back to generate the control signals k = 1, 2, ...

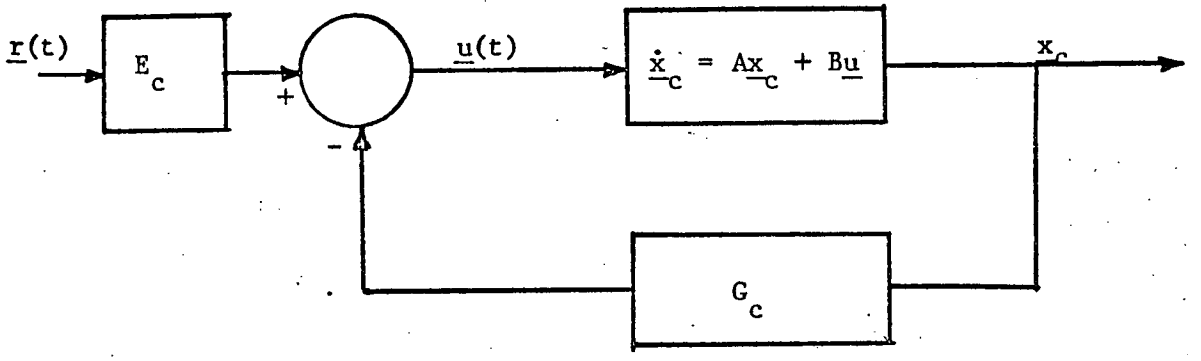

Figure 2-1 Block diagram of continuous-data system.

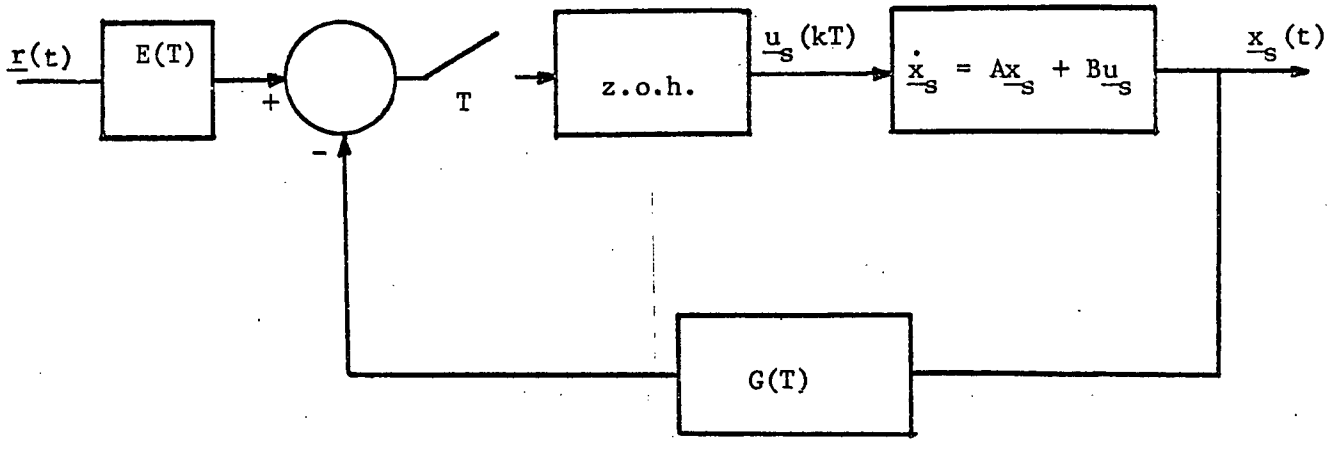

Figure 2-2 Block diagram of sampled-data system.

2.2 Exact Solutions for the Forward and Feedback Gain Matrices (Second-order, single-input system)

In this section we shall derive the optimal gains for the exact matchings of states at multiple sampling instants using a second-order system with a single input (n = 2, m = 1).

Let us define

$$\phi(T) = e^{AT} \tag{2-7}$$

$$\phi_c(T) = e^{(A-BG_c)T} \tag{2-8}$$

$$\theta_c(T) = \int_0^T e^{(A-BG_c)\lambda}\, d\lambda B \tag{2-9}$$

Then, the solution of the state at the sampling instant $t = (k + 1)T$ for the continuous-data system of Eqs. (2-1) and (2-2) is

$$\underline{x}_c[(k + 1)T] = \phi_c(T)\underline{x}_c(kT) + \theta_c(T)E_c r(kT) \tag{2-10}$$

where it is assumed that $r(\tau) = r(kT)$ for $kT \leq \tau < (k + 1)T$. This approximation is necessary so that $r(\tau)$ can be factored out of the integral of $\theta_c(T)$, and the solution will not be input dependent.

Similarly, the state of the continuous-data system at $t = (k + 2)T$ is obtained as

$$\begin{aligned}\underline{x}_c[(k + 2)T] &= \phi_c(T)\underline{x}_c[(k + 1)T] + \theta_c(T)E_c r[(k + 1)T] \\ &= \phi_c(2T)\underline{x}_c(kT) + \phi_c(T)\,\theta_c(T)E_c r(kT) + \theta_c(T)E_c r[(k + 1)T]\end{aligned} \tag{2-11}$$

For the sampled-data system, the solution of Eq. (2-3) for the time interval $kT \leq t \leq (k + 1)T$, $k = 0, 1, 2, \ldots$, is

$$\underline{x}_s[(k + 1)T] = \phi(T)\underline{x}_s(kT) + \theta(T)u_s(kT) \tag{2-12}$$

where $\underline{u}_s(kT)$ denotes the output of the new-order hold for the specific time interval. For analytical reason we are using the control signal $u_s(kT)$ in the derivation instead of expressions involving the input $r(\tau)$.

For two sampling instants, the state vector at $t = (k + 2)T$ is written

$$\underline{x}_s[(k + 2)T] = \phi(2T)\underline{x}_s(kT) + \phi(T)\ \theta(T)\underline{u}_s(kT) + \theta(T)\underline{u}_s[(k + 1)T] \quad (2\text{-}13)$$

where $\underline{u}_s[(k + 1)T]$ denotes the constant output of the zero-order hold for the time interval $kT \leq t < (k + 1)T$.

Now let us assume that the states of the second-order continuous-data system and that of the sampled-data system can be matched at $t = kT$ and at $t = (k + 2)T$, we let

$$\underline{x}_s(kT) = \underline{x}_c(kT) \quad (2\text{-}14)$$

and

$$\underline{x}_s[(k + 2)T] = \underline{x}_c[(k + 2)T] \quad (2\text{-}15)$$

Then Eqs. (2-11) and (2-13) give

$$\phi_c(2T)\underline{x}_s(kT) + \phi_c(T)\theta_c(T)E_c r(kT) + \theta_c(T)E_c r[(k + 1)T]$$

$$= \phi(2T)\underline{x}_s(kT) + \phi(T)\theta(T)u_s(kT) + \theta(T)u_s[(k + 1)T] \quad (2\text{-}16)$$

Let

$$\Gamma(T) = [\phi(T)\theta(T) \quad \theta(T)] \quad (2\text{-}17)$$

$$P(T) = \Gamma^{-1}(T)[\phi_c(2T) - \phi(2T)] \quad (2\text{-}18)$$

$$S_1(T) = \Gamma^{-1}(T)\phi_c(T)\theta_c(T)BE_c \quad (2\text{-}19)$$

$$S_2(T) = \Gamma^{-1}(T)\theta_c(T)BE_c \quad (2\text{-}20)$$

Notice that $\Gamma(T)$ is the "controllability" matrix of the sampled-data system in Eq. (2-12) Therefore, if the sampled-data system is controllable with the sampling period T, $\Gamma(T)$ is nonsingular.

With the matrices defined in Eq. (2-17), (2-18), (2-19), and (2-20), Eq. (2-16) leads to

$$\begin{bmatrix} u_s(kT) \\ u_s[(k+1)T] \end{bmatrix} = P(T)\underline{x}_s(kT) + S_1(T)r(kT) + S_2(T)r[(k+1)T] \qquad (2\text{-}21)$$

where $k = 2j$, $j = 0, 1, 2, \ldots$.

The last equation is also written as

$$u_s(kT) = [1 \quad 0]\{P(T)\underline{x}_s(kT) + S_1(T)r(kT) + S_2(T)r[(k+1)T]\} \qquad (2\text{-}22)$$

$$u_s[(k+1)T] = [0 \quad 1]\{P(T)\underline{x}_s(kT) + S_1(T)r(kT) + S_2(T)r[(k+1)T]\} \qquad (2\text{-}23)$$

Let

$$u_s(kT) = -G_0\underline{x}_s(kT) + E_0 r(kT) + F_0 r[(k+1)T] \qquad (2\text{-}24)$$

where G_0, E_0, and F_0 represent the constant gains which are effective during the time intervals of $2kT \leq t < (2k+1)T$, $k = 0, 1, 2, \ldots$. Comparing Eqs. (2-22) and (2-24), we have

$$G_0 = -[1 \quad 0]P(T) \qquad (2\text{-}25)$$

$$E_0 = [1 \quad 0]S_1(T) \qquad (2\text{-}26)$$

$$F_0 = [1 \quad 0]S_2(T) \qquad (2\text{-}27)$$

However, Eq. (2-24) indicates that $u_s(kT)$ is a function of both $r(kT)$ and $r[(k+1)T]$, which means that in order to determine the control $u_s(kT)$ at $t = kT$, the input $r(t)$ must be known at the next sampling instant $t = (k+1)T$. This implies that either the input signal must be known in advance over each interval $[kT, (k+2)T]$ or a predictor must be constructed to predict $r[(k+1)T]$ on line.

In a similar fashion, Eq. (2-23) is written

$$u_s[(k+1)T] = -G_1\underline{x}_s[(k+1)T] + E_1 r(kT) + F_1 r[(k+1)T] \quad (2\text{-}28)$$

where G_1, E_1, and F_1 represent the constant gains for the time interval $(2k+1)T \leq t < 2(k+1)T$, $k = 0, 1, 2, \ldots$.

Substituting Eqs. (2-24) and (2-12) into the last equation, we have,

$$u_s[(k+1)T] = -G_1[\phi(T) - \theta(T)G_0]\underline{x}_s(kT) + [E_1 - G_1\theta(T)E_0]r(kT) + [F_1 - G_1\theta(T)F_0]r[(k+1)T] \quad (2\text{-}29)$$

Comparing Eqs. (2-17) and (2-23) yields

$$G_1 = -[0 \quad 1]P(T)[\phi(T) - \theta(T)G_0]^{-1} \quad (2\text{-}30)$$

$$E_1 = [0 \quad 1]S_1(T) + G_1\theta(T)E_0 \quad (2\text{-}31)$$

$$F_1 = [0 \quad 1]S_2(T) + G_1\theta(T)F_0 \quad (2\text{-}32)$$

It can be shown that the condition for the matrix $[\phi(T) - \theta(T)G_0]$ to be nonsingular is that the sampled-data system be completely controllable.

Note that the control $u_s[(k+1)T]$ may be expressed in terms of the state $\underline{x}_s(kT)$ as in Eq. (2-23), or in terms of the state $\underline{x}_s[(k+1)T]$ as in Eq. (2-28). Thus, the state variable can be sampled either every kT or every 2kT, $k = 0, 1, 2, \ldots$, for feedback purpose.

A simpler solution which does not require the use of a predictor can be obtained if we assume that

$$r[(k+1)T] = r(kT) = r(\tau) \quad (2\text{-}33)$$

for $kT \leq \tau < (k+2)T$. Then Eq. (2-16) becomes

$$\phi_c(2T)\underline{x}_s(kT) + \theta_c(2T)E_c r(kT) = \phi(2T)\underline{x}_s(kT) + \phi(T)\theta(T)u_s(kT) + \theta(T)u_s[(k+1)T] \quad (2\text{-}34)$$

where

$$\theta_c(2T) = \int_0^{2T} e^{(A-BG_c)\lambda} d\lambda B \tag{2-35}$$

Therefore, Eq. (2-34) is written

$$\begin{bmatrix} u_s(kT) \\ \\ u_s[(k+1)T] \end{bmatrix} = P(T)\underline{x}_s(kT) + S(T)r(kT) \tag{2-36}$$

where $k = 2j$, $j = 0, 1, 2, \ldots$, and

$$S(T) = \theta_c(2T)E_c \tag{2-37}$$

Equation (2-36) can be written as

$$u_s(kT) = - G_0\underline{x}_s(kT) + E_0 r(kT) \tag{2-38}$$

$$u_s[(k+1)T] = - G_1\underline{x}_s[(k+1)T] + E_1 r(kT) \tag{2-39}$$

Comparing Eq. (2-36) with Eq. (2-38) yields

$$G_0 = - [1 \quad 0]P(T) \tag{2-40}$$

$$E_0 = [1 \quad 0]S(T) \tag{2-41}$$

Equation (2-39) is rewritten as

$$u_s[(k+1)T] = - G_1[\phi(T) - \theta(T)G_0]\underline{x}_s(kT) + [E_1 - G_1\theta(T)E_0]r(kT) \tag{2-42}$$

Thus, comparing Eq. (2-36) with Eq. (2-42), we have

$$[0 \quad 1]P(T) = - G_1[\phi(T) - \theta(T)G_0] \tag{2-43}$$

$$[0 \quad 1]S(T) = - G_1\theta(T)E_0 + E_1 \tag{2-44}$$

Solving for G_1 from Eq. (2-43) and E_1 from Eq. (2-44), we get

$$G_1 = - [0 \quad 1]P(T)[\phi(T) - \theta(T)G_0]^{-1} \tag{2-45}$$

$$E_1 = [0 \quad 1]S(T) + G_1\theta(T)E_0 \tag{2-46}$$

Therefore, for the second-order system with single input, if the states can be matched every two sampling periods, the gains G(T) and E(T) must change twice during each basic period of 2T. Then, during the subsequent sampling periods these gains go through the same sequences repeatedly. In other words, referring to Eq. (2-4),

$$G(T) = G_0 \qquad 2kT \leq t < (2k + 1)T \tag{2-47}$$

$$G(T) = G_1 \qquad (2K + 1)T \leq t < 2(k + 1)T \tag{2-48}$$

$k = 0, 1, 2, \ldots$. In general, if the states of the continuous-data system are exactly matched with those of the sampled-data system every NT seconds, where N is an integer greater than unity, the feedback gain would have to assume N different values, $G_0, G_1, \ldots, G_{N-1}$, over the basic period, NT, with changes occuring at the sampling instants T. Furthermore,

$$G_k = G_{k+N} \tag{2-49}$$

for $k = 0, 1, 2, \ldots$. Similar properties may be stated for the forward gain E(T) of Eq. (2-4)

As an alternative to sampling and feeding back the states at every sampling period T, we can assume that the gain matrices are changed every T but the states are sampled only at $t = 2kT$. Then, in addition to Eq. (2-38) Eq. (2-39) is written as

$$u_s[(k + 1)T] = - \hat{G}_1\underline{x}_s(kT) + \hat{E}_1 r(kT) \tag{2-50}$$

where $k = 2j$, $j = 0, 1, 2, \ldots$. The gains G_0 and E_0 in Eq. (2-38) are still given by Eqs. (2-40) and (2-41), respectively, but comparing Eq. (2-50) with Eq. (2-36), we have

$$\hat{G}_1 = - [0 \quad 1]P(T) \tag{2-51}$$

and

$$\hat{E}_1 = [0 \quad 1]S(T) \tag{2-52}$$

It should be noted that feeding back the states every T seconds and feeding back the states every 2T would yield the same responses for the system at the sampling instants, although the control signals and the gains for the two schemes are different. However, using $\underline{x}_s(kT)$ $k = 0, 2, 4, \ldots$ means that the states may be sampled only half as frequently in the second-order system, but the gain matrices must be changed during the sampling period. In practice the choice of either method may depend upon the applicability of the methods. For instance, if the sampling period T is fixed a priori, then we may say that for the second-order system considered it is possible to match the states at every other sampling instants only, by feeding back the state variables and changing the gains at each sampling instant. However, in order to match the states at every sampling instant we can change the forward and feedback gain matrices once in between the sampling instants. If we use Eqs. (2-51) and (2-52) for this purpose no additional samplings of the states are necessary.

Although it may be more convenient to sample the states every N sampling periods and change the feedback and forward gains every sampling period to match the states every N sampling periods, it should be noted that the system is operating open loop over these N sampling periods. If the states and gains are changed at the end of every sampling period the system will only be operating open loop over a single sampling period. This second method requires that the

states be sampled more frequently but, in general, it should be less susceptible to noise perturbations and variations of system parameters.

Another interesting observation is that the digital point-by-point state matching problem considered here is closely related to the time-optimal control of sampled-data control systems. For simplicity of illustration, we may consider the regulator problem by setting $r(kT) = 0$ for all k. Then, the optimal control for point-by-point state matching for the second-order system is obtained from Eq. (2-21)

$$\begin{bmatrix} u_s(kT) \\ \\ u_s[(k+1)T] \end{bmatrix} = P(T)\underline{x}_s(kT)$$

$$= [\phi(T)\theta(T) \quad \theta(T)]^{-1} [\phi_c(2T) - \phi(2T)]\underline{x}_s(kT) \qquad (2\text{-}53)$$

In sampled-data systems theory, it is well known that given a second-order system with initial state $\underline{x}_s(kT)$, the optimal control to bring $\underline{x}_s(kT)$ to the equilibrium state $\underline{0}$ in minimum time is

$$\underline{u}_s = [\phi(T)\theta(T) \quad \theta(T)]^{-1}\underline{x}_s(kT) \qquad (2\text{-}54)$$

Therefore, Eq. (2-47) can be interpreted as the optimal control which brings the difference of $\phi_c(2T)\underline{x}_c(kT)$ and $\phi(2T)\underline{x}_s(kT)$ to zero in minimum time. For a second-order system, if the amplitudes of the controls at various sampling instants are unconstrained, the mimimum (and maximum) time to achieve state matching is two. However, if the controls are subject to amplitude constraint, more sampling periods are required for matching.

2.3 Exact Solutions for the Forward and Feedback Gain Matrices (General Case)

Now consider that the continuous-data system of Eqs.(2-1) and (2-2) has n states and m inputs. Then, if the sampled-data system of Eqs. (2-3) and (2-4) is controllable for the sampling period T, the states of the two systems may be exactly matched every N sampling instants; where N is given by Eq. (2-6).

The states of the continuous-data system evaluated at t = (k + N)T are expressed as

$$\underline{x}_c[(k + N)T] = \phi_c(NT)\underline{x}_c(kT) + \theta_c(NT)E_c\underline{r}(kT) \tag{2-55}$$

where

$$\phi_c(NT) = e^{N(A-BG_c)T}$$

$$\theta_c(NT) = \int_0^{NT} e^{(A-BG_c)\lambda}\, d\lambda B \tag{2-56}$$

and

By recursion, the solution of Eq. (2-16) at (k + N)T is

$$\underline{x}_s[(k + N)T] = \phi(NT)\underline{x}_s(kT) + \sum_{i=0}^{N-1} \phi[(N - i - 1)T]\theta(T)\underline{u}_s[(k + i)T] \tag{2-57}$$

Now equating Eq. (2-55) to Eq. (2-57) and letting $\underline{x}_c(kT) = \underline{x}_s(kT)$, we have

$$[\phi_c(NT) - \phi(NT)]\underline{x}_s(kT) + \theta_c(NT)E_c\underline{r}(kT) = \sum_{i=0}^{N-1} \phi[(N - i - 1)T]\theta(T)\underline{u}_s[(k + i)T] \tag{2-58}$$

The last equation can be written as

$$[\phi[(N-1)T]\theta(T) \quad \phi[(N-2)T]\theta(T) \ldots \phi(T)\theta(T) \quad \theta(T)] \begin{bmatrix} \underline{u}_s(kT) \\ \underline{u}_s[(k+1)T] \\ \vdots \\ \underline{u}_s[(k+N-2)T] \\ \underline{u}_s[(k+N-1)T] \end{bmatrix}$$

$\longleftarrow n \times Nm \longrightarrow$ $\longleftarrow Nm \times 1 \longrightarrow$

$$= [\phi_c(NT) - \phi(NT)]\underline{x}_s(kT) + \theta_c(NT)E_c\underline{r}(kT) \tag{2-59}$$

Let

$$\Gamma(T) = [\phi[(N-1)T]\theta(T) \quad \phi[(N-2)T]\theta(T) \ldots \phi(T)\theta(T) \quad \theta(T)] \tag{2-60}$$

which is not a square matrix unless $n = Nm$. However, if the sampled-data system is completely controllable, $\Gamma(T)$ must be of rank n. Let $\Lambda(T)$ be an $n \times n$ matrix which is formed by use of n linearly independent columns of $\Gamma(T)$. In general, there may be a nonuniqueness in the selection of $\Lambda(T)$ if $NM > n$ and there are more than n independent columns in $\Gamma(T)$. Now let $\underline{U}$ represent at $n \times 1$ vector which contains the elements of the control vector of Eq. (2-59) that correspond to the columns of $\Lambda(T)$ taken from $\Gamma(T)$, which means that $Nm - n$ elements of the control vector can be set arbitrarily. Then, Eq. (2-59) leads to

$$\underline{U} = \Lambda^{-1}(T)[\phi_c(NT) - \phi(NT)]\underline{x}_s(kT) + \Lambda^{-1}(T)\theta_c(NT)E_c\underline{r}(kT) \tag{2-61}$$

The procedure of expressing the elements of $\underline{U}$ in terms of state feedback in the form of the following equations is conceptually simple:

$$\underline{u}_s[(k+j)T] = -\hat{G}_j\underline{x}_s(kT) + \hat{E}_j\underline{r}(kT) \tag{2-62}$$

or

$$\underline{u}_s[(k + j)T] = - G_j \underline{x}_s[(k + j)T] + E_j \underline{r}(kT) \tag{2-63}$$

$j = 0, 1, 2, \ldots, N - 1.$

However, because of the nonuniqueness in the solution general closed form solutions for the gains are difficult to express.

Let us consider the case when n/m is an integer; then $N = n/m$. In this case, $\Gamma(T)$ is an $n \times n$ square matrix, and the N optimal control vectors, $\underline{u}_s(kT)$, $\underline{u}_s[(k + 1)T]$, ..., $\underline{u}_s[(k + N - 1)T]$, are uniquely determined from

$$n \times 1 \begin{pmatrix} \underline{u}_s(kT) \\ \underline{u}_s[(k + 1)T] \\ \vdots \\ \underline{u}_s[(k + N - 2)T] \\ \underline{u}_s[(k + N - 1)T] \end{pmatrix} = P(T)\underline{x}_s(kT) + S(T)\underline{r}(kT) \tag{2-64}$$

where

$$P(T) = \Gamma^{-1}(T)[\phi_c(NT) - \phi(NT)] \tag{2-65}$$

$$S(T) = \Gamma^{-1}(T)\theta_c(NT)E_c \tag{2-66}$$

Then the control vector, $\underline{u}_s[(k + j)T]$, $j = 0, 1, 2, \ldots, N - 1$, can be expressed by Eq. (2-62)or Eq. (2-63) The matrices, G_j, $\hat{G}_j$, E_j, and $\hat{E}_j$, represent the gain matrices which must change N times during each sampling period NT. During subsequent matching periods of NT to 2NT, 2NT to 3NT, ..., etc., these gain matrices go through the same N sequences of variations for each period.

Let us define the $m \times n$ matrix I_j as

$$I_j = \left[\begin{array}{c|c|c} \underset{m(j+1)\text{ columns}}{\begin{matrix} 0 & \cdots & 0 \\ \vdots & & \vdots \\ 0 & & 0 \end{matrix}} & \underset{m\text{ columns}}{\begin{matrix} 1 & \cdots & 0 \\ \vdots & & \vdots \\ 0 & & 1 \end{matrix}} & \underset{n-2m-mj\text{ columns}}{\begin{matrix} 0 & \cdots & 0 \\ \vdots & & \vdots \\ 0 & & 0 \end{matrix}} \end{array}\right] \begin{matrix} \uparrow \\ m \\ \downarrow \end{matrix} \qquad (2\text{-}67)$$

$j=0,1,\ldots.$

then the control vectors of Eq. (2-64) can be written as

$$\underline{u}_s[(k+j)T] = I_j[P(T)\underline{x}_s(kT) + S(T)\underline{r}(kT)] \qquad (2\text{-}68)$$

Now comparing Eq. (2-62) with Eq. (2-68), we have

$$\hat{G}_j = -I_j P(T) \qquad (2\text{-}69)$$

and

$$\hat{E}_j = I_j S(T) \qquad (2\text{-}70)$$

for $j = 0, 1, 2, \ldots, N-1$,

which are relatively simple solutions for the gain matrices.

However, if the control vector is defined by Eq. (2-63), the solution is more complex.

For $j = 0$, comparison of Eqs. (2-63) and (2-68) gives

$$G_0 = -I_0 P(T) \qquad (2\text{-}71)$$

$$E_0 = I_0 S(T) \qquad (2\text{-}72)$$

As expected, when the exact matching of states can be accomplished in one sampling period, the solutions from Eqs. (2-62) and (2-63) are identical.

For $j = 1$, Eq. (2-63) gives

$$\underline{u}_s[(k+1)T] = -G_1[\phi(T) - \theta(T)G_0]\underline{x}_s(kT) + [E_1 - G_1E_0]\underline{r}(kT) \qquad (2\text{-}73)$$

Comparing Eq. (2-73) with Eq. (2-68), with j = 1, we have

$$G_1 = -I_1 P(T)[\phi(T) - \theta(T)G_0]^{-1} \tag{2-74}$$

$$E_1 = I_1 S(T) + G_1 E_0 \tag{2-75}$$

For the general case,

$$\underline{x}_s[(k + j)T] = \prod_{i=1}^{j} [\phi(T) - \theta(T)G_{j-i}]\underline{x}_s(kT) + \sum_{p=1}^{j-1} \prod_{i=1}^{j-p} [\phi(T) - \theta(T)G_{j-i}]\theta(T)E_{p-1}\underline{r}(kT) + \theta(T)E_{j-1}\underline{r}(kT) \tag{2-76}$$

Substituting Eq. (2-76) into Eq. (2-63), we have

$$\underline{u}_s[(k + j)T] = - G_j \prod_{i=1}^{j} [\phi(T) - \theta(T)G_{j-i}]\underline{x}_s(kT) - G_j \sum_{p=1}^{j-1} \prod_{i=1}^{j-p} [\phi(T) - \theta(T)G_{j-i}]\theta(T)E_{p-1}\underline{r}(kT) - G_j\theta(T)E_{j-1}\underline{r}(kT) + E_j\underline{r}(kT) \tag{2-77}$$

Comparing Eq. (2-77) with Eq. (2-68) the gain matrices are obtained as

$$G_j = - I_j P(T) \left\{ \prod_{i=1}^{j} [\phi(T) - \theta(T)G_{j-i}] \right\}^{-1} \tag{2-78}$$

$$E_j = I_j S(T) + G_j \sum_{p=1}^{j-1} \prod_{i=1}^{j-p} [\phi(T) - \theta(T)G_{j-i}]\theta(T)E_{p-1} + G_j\theta(T)E_{j-1} \tag{2-79}$$

j = 0, 1, 2, ..., N - 1.

2.4 The General Gamma Matrix

In section 2.3 we considered the case when n = Nm and the system was controllable in N sampling periods. A more general case is when n/m is not an integer or when n = Nm but the system is not controllable in N sampling periods. In both these cases N must be chosen such that Nm > n. The matrix $\Gamma(T)$ given by Eq. (2-60) is then nonsquare. As mentioned previously if an integer N can be found such that the system is controllable in N sampling periods and Nm > n then a nonsingular matrix $\Lambda(T)$ of dimension n × n can be formed by selecting n linearly independent columns of $\Gamma(T)$. Equation (2-59) is then written as

$$\Lambda(T)\underline{U}(T) + \overline{\Lambda}(T)\overline{\underline{U}}(T) = [\phi_c(NT) - \phi(NT)]\underline{x}_s(kT) + \theta_c(NT)E_c\underline{r}(kT) \quad (2\text{-}80)$$

where $\underline{U}(T)$ is an n-dimensional control vector whose elements correspond to the n linearly independent columns of $\Gamma(T)$ that were selected to form $\Lambda(T)$. The remaining Nm - n columns of $\Gamma(T)$ form the n × (Nm - n) matrix $\overline{\Lambda}(T)$, and the remaining Nm - n controls form the corresponding control vector $\overline{\underline{U}}(T)$. Since the controls $\overline{\underline{U}}(T)$ may be set arbitrarily, let $\overline{\underline{U}}(T) = 0$. Solving Eq. (2-80) gives

$$\underline{U}(T) = P(T)\underline{x}_s(kT) + S(T)\underline{r}(kT) \quad (2\text{-}81)$$

where

$$P(T) = \Lambda^{-1}(T)[\phi_c(NT) - \phi(NT)]$$

$$S(T) = \Lambda^{-1}(T)\theta_c(NT)E_c$$

First consider the case when the control is expressed as

$$\underline{u}_s[(k + j)T] = -\hat{G}_j\underline{x}_s(kT) + \hat{E}_j\underline{r}(kT) \quad (2\text{-}82)$$

j = 0, 1, 2, ..., N - 1.

It is sufficient to consider $\underline{u}_s(t)$ over the first sampling period since the gains $\hat{G}_j$ and $\hat{E}_j$ repeat themselves every sampling period.

In section III we equated the first m columns of $\underline{U}(T)$ with $\underline{u}_s(0)$ to find $\hat{G}_0$ and $\hat{E}_0$. However here the vector $\underline{U}(T)$ in Eq. (4-2) may not contain all the controls for the first sampling period, $\underline{u}_i(0)$ $i = 1, 2, \ldots m$. Some of these controls are contained in the $\underline{U}(T)$ vector and some the $\overline{\underline{U}}(T)$ vector. The ones that are in the $\overline{\underline{U}}(T)$ vector have been set to zero. In order to compare the controls in equations (4-2) and (4-3) it is necessary to add back to the $\underline{U}(T)$ vector the controls that have been set to zero. That is, we form the Nm - vector

$$\tilde{\underline{U}}(T) = \begin{bmatrix} \underline{u}_s(kT) \\ \underline{u}_s[(k+1)T] \\ \vdots \\ \underline{u}_s[(k+N-1)T] \end{bmatrix} \qquad (2\text{-}83)$$

by adding back the Nm - n controls that formed the $\overline{\underline{U}}$ vector. We also construct an Nm × n matrix $\tilde{P}(T)$ by inserting rows of zero corresponding to the additional Nm - n controls. Similarly we construct an Nm × m matrix $\tilde{S}(T)$. Then

$$\tilde{\underline{U}}(T) = \tilde{P}(T)\underline{x}_s(kT) + \tilde{S}(T)\underline{r}(kT)$$

The control vectors of Eq.(2-83) can then be written as

$$\underline{u}_s[(k+j)T] = I_j[\tilde{P}(T)\underline{x}_s(kT) + \tilde{S}(T)\underline{r}(kT)] \qquad (2\text{-}84)$$

Comparing Eq. (4-3) and Eq. (2-84) we have

$$\hat{G}_j = I_j\tilde{P}(T) \qquad (2\text{-}85)$$

$$\hat{E}_j = I_j\tilde{S}(T) \qquad (2\text{-}86)$$

for $j = 0, 1, 2, \ldots, (N-1)$.

Next we consider the case when the control is expressed as

$$\underline{u}_s[(k + j)T] = - G_j\underline{x}_s[(k + j)T] + E_j r(kT) \tag{2-87}$$

for $j = 0, 1, 2, \ldots, (n - 1)$.

Equating the control given by Eq. (2-77) and the control given by Eq. (2-84) gives expressions identical to Eq. (2-78) and Eq. (2-79) except that the matrices $P(T)$ and $S(T)$ are replaced by $\tilde{P}(T)$ and $\tilde{S}(T)$.

In order to illustrate the matrix manipulations discussed in this section we will consider the case of a third-order system having two inputs.

Equation Eq. (2-59) is written as

$$\begin{bmatrix} \lambda_{11} & \lambda_{12} & \lambda_{13} & \lambda_{14} \\ \lambda_{21} & \lambda_{22} & \lambda_{23} & \lambda_{24} \\ \lambda_{31} & \lambda_{31} & \lambda_{33} & \lambda_{34} \end{bmatrix} \begin{bmatrix} u_1(0) \\ u_2(0) \\ u_1(T) \\ u_2(T) \end{bmatrix} = [\phi_c(NT) - \phi(NT)]\underline{x}_s(kT) + \theta_c(NT)E_c\underline{r}(kT) \tag{2-88}$$

Since $n = 3$ and $m = 2$ the $\Gamma(T)$ matrix is nonsquare. If the first three columns of $\Gamma(T)$ constitute a nonsingular matrix, we can define $\Lambda(T)$ as

$$\Lambda(T) = \begin{bmatrix} \lambda_{11} & \lambda_{12} & \lambda_{13} \\ \lambda_{21} & \lambda_{22} & \lambda_{23} \\ \lambda_{31} & \lambda_{32} & \lambda_{33} \end{bmatrix} \tag{2-89}$$

Also

$$\underline{U}'(T) = [u_1(0) \quad u_2(0) \quad u_1(T)] \tag{2-90}$$

Setting $u_2(T) = 0$, Eq. (2-88) is written as

$$\Lambda(T)\underline{U}(T) = [\phi_c(NT) - \phi(NT)]\underline{x}_s(kT) + \theta_c(NT)E_c\underline{r}(kT) \tag{2-91}$$

then

$$\underline{U}(T) = P(T)\underline{x}_s(kT) + S(T)\underline{r}(kT) \tag{2-92}$$

where

$$P(T) = \Lambda^{-1}(T)[\phi_c(NT) - \phi(NT)] \tag{2-93}$$

$$S(T) = \Lambda^{-1}(T)\theta_c(NT)E_c \tag{2-94}$$

By adding a row of zeros to the P(T) and S(T) matrices Eq. (2-92) may be written for the complete control vector for both sampling periods.

$$\begin{bmatrix} u_1(kT) \\ u_2(kT) \\ u_1[(k+1)T] \\ u_2[(k+1)T] \end{bmatrix} = \tilde{P}(T)\underline{x}_s(kT) + \tilde{S}(T)\underline{r}(kT)$$

where

$$\tilde{P}(T) = \begin{bmatrix} P_{11} & P_{12} & P_{13} \\ P_{21} & P_{22} & P_{23} \\ P_{31} & P_{32} & P_{33} \\ 0 & 0 & 0 \end{bmatrix} \qquad \tilde{S}(T) = \begin{bmatrix} S_{11} & S_{12} \\ S_{21} & S_{22} \\ S_{31} & S_{32} \\ 0 & 0 \end{bmatrix}$$

The $\hat{G}_j$, $\hat{E}_j$ and G_j, E_j gains may then be found by using Eqs. (2-69), (2-70) and (2-72), (2-73) respectively.

2.5 Simulation of Systems

Digital Redesign of the Simplified One-Axis Dynamics of the Skylab Satellite

The dynamic equations of the simplified one-axis model of the skylab satellite were discussed in detail in Chapter 1.

The state equations for the continuous system are

$$\frac{d\underline{x}}{dt} = [A - BG_c]\underline{x}(t) + BE_c r(t)$$

where

$r(t)$ = unit step function,

$$A = \begin{bmatrix} 0 & 1 \\ 0 & 1 \end{bmatrix} \qquad B = \begin{bmatrix} 0 \\ 1/970{,}741 \end{bmatrix}$$

$$G_c = [11800 \quad 151{,}800]$$

$$E_c = 11800$$

The method of multiple sampling periods discussed in sections 2.2 - 2.4 was used for the digital redesign of the above system. Since the system is of the second order with one control, the responses of the continuous and digital systems can at best be matched at the end of two sampling periods. For the skylab example the digital system was controllable in two sampling periods so that exact matching could take place at the end of the second period. The sampling period was chosen as T = 1 sec and N = 2. Therefore, matching occurs at t = 2, 4, 6, ... sec. The feedback gains and the forward gains are

$$G_0 = [11185. \quad 147812.]$$

$$G_1 = [10639.6 \quad 144149.]$$

$$E_0 = [11185.]$$

$$E_1 = [10639.6]$$

G_0 and E_0 are used over the sampling periods kT for k = 0, 2, 4, ..., and G_1 and E_1 are used over the sampling periods kT for k = 1, 3, 5 ... .

The simulation results are shown in Figs. 2-4 through 2-9 for the states and controls and the errors between the states of the digital and continuous systems. The matching of the states can best be seen in Fig. 2-7 At the end of the first sampling period the error is negative, however, at the end of the second sampling period the error is close to zero.

Table 3-1 in the next chapter compares the method of partial matching to the method of multiple sampling periods by giving the maximum error between the states of the digital and continuous systems at the end of one sampling period for the method of partial matching and at the end of two sampling periods for the method of multiple sampling periods.

3. DIGITAL APPROXIMATION BY POINT-BY-POINT STATE COMPARISON WITH HIGHER ORDER HOLDS

3.1 Introduction

The problem is that of approximating a continuous-data system of Fig. 3-1 by a sampled-data model of Fig. 3-2 by comparison of the states of the systems.

The continuous-data system is described by the following time-invariant dynamic equations:

$$\dot{\underline{x}}_c(t) = A\underline{x}_c(t) + B\underline{u}(t) \tag{3-1}$$

$$\underline{u}(t) = E_c\underline{r}(t) - G_c\underline{x}_c(t) \tag{3-2}$$

where $\underline{x}_c(t)$ denotes an n-vector, $\underline{u}(t)$ and $\underline{r}(t)$ are m-vectors, E_c and G_c are the gain matrices of the forward and the feedback paths, respectively.

The dynamic equations of the sampled-data system which is to replace the continuous-data model are

$$\dot{\underline{x}}_c(t) = A\underline{x}_s(t) + B\underline{u}_s(t) \tag{3-3}$$

where $\underline{u}_s(t)$ is an m-vector and is defined as the output of an (N-1)st-order hold, N=1, 2, ...

It will be shown that it is possible to match all the states of the system in one sampling period if a hold device of sufficiently high order is utilized. The order of the hold which is necessary to match the states, depends upon the ratio of the number of states and the number of controls of the system. For the system considered which is of the nth order with m inputs, it is possible to match all the states at every sampling instant with at least an (N - 1)st-order hold, where $n/m \leq N < n/m + 1$.

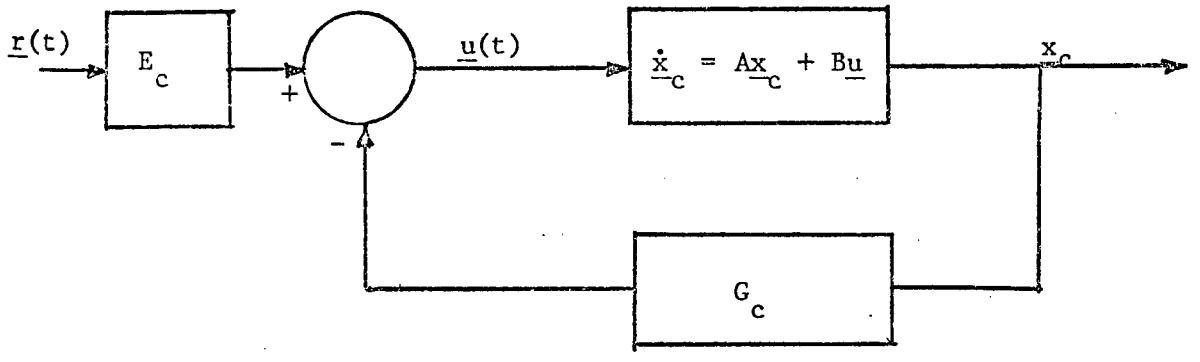

Figure 3-1 Block diagram of continuous-data system.

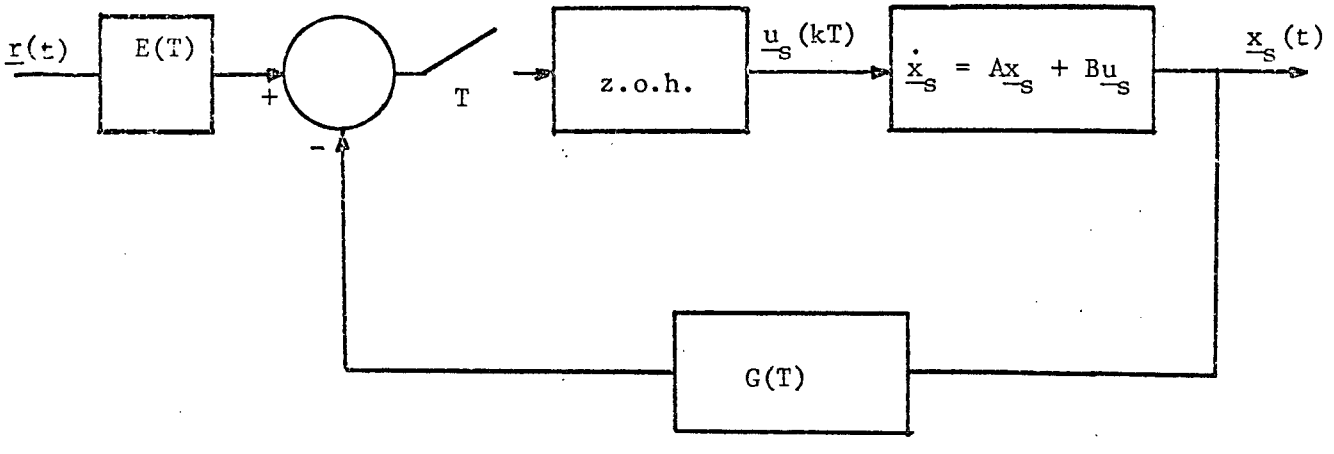

Figure 3-2 Block diagram of sampled-data system.

Let us consider, for the time being, that an (N - 1)st-order hold is adequate for exact matching of states at every sampling instant. (The case when a higher than (N - 1)st-order hold is necessary will be discussed later.) The control input of the sampled-data system with an (N - 1)st-order hold is expressed as

$$\underline{u}_s(t) = [E_0 + (t - kT)E_1 + \ldots + \frac{(t - kT)^{N-1}}{(N - 1)!} E_{N-1}]\underline{r}(kT)$$

$$- [G_0 + (t - kT)G_1 + \ldots + \frac{(t - kT)^{N-1}}{(N - 1)!} G_{N-1}]\underline{x}_s(kT) \qquad (3\text{-}4)$$

for $kT \leq t < (k + 1)T$, where E_0, E_1, ..., E_{N-1} are m x m coefficient matrices, and G_0, G_1, ..., G_{N-1} are m x n coefficient matrices.

Let us define the following matrices:

$$\underline{E} = \begin{bmatrix} E_0 \\ E_1 \\ . \\ . \\ . \\ E_{N-1} \end{bmatrix} \qquad (mN \times m) \qquad (3\text{-}5)$$

$$\underline{G} = \begin{bmatrix} G_0 \\ G_1 \\ . \\ . \\ . \\ G_{N-1} \end{bmatrix} \qquad (mN \times n) \qquad (3\text{-}6)$$

Then, Eq. (3-4) is written

$$\underline{u}_s(t) = [I_m \vdots (t - kT)I_m \vdots \ldots \frac{(t - kT)^{N-1}}{(N - 1)!} I_m][\underline{Er}(kT)$$

$$- \underline{Gx}_s(kT)] \qquad kT \leq t < (k + 1)T \qquad (3\text{-}7)$$

where I_m is the indentity matrix of dimension m x m.

Now let us define the m x mN matrix

$$L_{mN}(t - kT) = [I_m \quad (t - kT)I_m \quad . \; . \; . \quad \frac{(t - kT)^{N-1}}{(N - 1)!} I_m] \tag{3-8}$$

Equation (3-7) is written as

$$\underline{u}_s(t) = E(t - kT)\underline{r}(kT) - G(t - kT)\underline{x}_s(kT) \tag{3-9}$$

where

$$E(t - kT) = L_{mN}(t - kT)\underline{E} \tag{3-10}$$

$$G(t - kT) = L_{mN}(t - kT)\underline{G} \tag{3-11}$$

$kT \leq t < (k + 1)T$.

3.2 Derivation of the Optimal Gains

The necessary conditions for the exact matching of all the states of the continuous-data and the discrete-data systems at $t = (k + 1)T$, $k = 0, 1, 2, \ldots$, for arbitrary inputs $\underline{r}(t)$ and initial conditions, $\underline{x}_c(kT) = \underline{x}_s(kT)$, are given by Eqs. (1-11) and (1-12),

$$e^{(A-BG_c)T} = e^{AT} - \int_{kT}^{(k+1)T} e^{A(kT+T-\tau)} BG(\tau - kT)\,d\tau \tag{3-12}$$

where G_c denotes the feedback gain matrix of the continuous-data system, and $G(\tau - kT)$ is given by Eq. (3-11)

$$\int_{kT}^{(k+1)T} e^{(A-BG_c)(kT+T-\tau)} BE_c\,d\tau = \int_{kT}^{(k+1)T} e^{A(kT+T-\tau)} BE(\tau - kT)\,d\tau \tag{3-13}$$

where E_c denotes the forward gain matrix of the continuous-data system, and $E(\tau - kT)$ is given by Eq. (3-10). Also, in arriving at Eq. (3-13) it has been assumed that $\underline{r}(t) \cong \underline{r}(kT)$ for $kT \leq t < (k+1)T$.

If we let $\lambda = (k + 1)T - \tau$, Eqs. (3-12) and (3-13) become

$$e^{AT} - e^{\hat{A}T} = \int_0^T e^{A\lambda} BG(T - \lambda)\,d\lambda \tag{3-14}$$

$$\theta_c(T) = \int_0^T e^{A\lambda} BE(T - \lambda)\,d\lambda \tag{3-15}$$

where

$$\hat{A} = A - BG_c \tag{3-16}$$

and

$$\theta_c(T) = \int_0^T e^{\hat{A}\lambda} BE_c\,d\lambda \tag{3-17}$$

Substituting Eq. (3-11) into Eq. (3-14) we have

$$e^{AT} - e^{\hat{A}T} = \int_0^T e^{A\lambda} B L_{mN}(T - \lambda)\underline{G}d\lambda \tag{3-18}$$

Similarly, substituting Eq. (3-10) into Eq. (3-15)gives

$$\theta_c(T) = \int_0^T e^{A\lambda} B L_{mN}(T - \lambda)\underline{E}d\lambda \tag{3-19}$$

Equation(3-18) represents n^2 equations in nmN unknown variables in $\underline{G}$, and Eq.(3-19) represents nm equations in m^2N unknown variables in $\underline{E}$. From the assumption that $n/m \leq N < n/m + 1$, there are at least n^2 variables in Eq.(3-18) and at least nm variables in Eq.(3-19). Thus, it is possible under certain conditions to solve for $\underline{G}$ and $\underline{E}$ from these equations.

If we define

$$q_i(T) = \int_0^T e^{A\lambda} B \frac{(T - \lambda)^i}{i!} d\lambda \tag{3-20}$$

i=0, ..., N - 1, then Eqs.(3-18) and (3-19)become

$$\begin{aligned} e^{AT} - e^{\hat{A}T} &= [q_0(T) \quad q_1(T) \ \cdots \ q_{N-1}(T)]\underline{G} \\ &= Q(T)\underline{G} \end{aligned} \tag{3-21}$$

$$\theta_c(T) = Q(T)\underline{E} \tag{3-22}$$

Note that

$$q_0(T) = \int_0^T e^{A\lambda} B d\lambda = \theta(T) \tag{3-23}$$

The matrix $q_i(T)$, i = 0, 1, ..., N-1, is of dimension n x m, and Q(T) is of dimension n x Nm.

The expression for $q_i(T)$ in Eq. (3-20) can be simplified when $i \geq 1$. Let

$$v = (t - \lambda)^i / i! \tag{3-24}$$

$$dw = e^{A\sigma} d\sigma \tag{3-25}$$

then

$$dv = - \frac{(T - \lambda)^{i-1}}{(i - 1)!} d\lambda \tag{3-26}$$

$$w = \int_a^{\lambda} e^{A\sigma} d\sigma \tag{3-27}$$

where, in general, a is an arbitrary constant.

Substituting the last four equations into eq. (3-20), and applying integration by parts, we get

$$q_i(T) = \frac{(T - \lambda)^i}{i!} \int_a^{\lambda} e^{A\sigma} d\sigma \Big|_{\lambda=0}^{\lambda=T} B + \int_0^T \left(\int_a^{\lambda} e^{A\sigma} d\sigma \right) \frac{(T - \lambda)^{i-1}}{(i - 1)!} d\lambda B \tag{3-28}$$

Or,

$$q_i(T) = - \frac{T^i}{i!} \int_a^0 e^{A\sigma} d\sigma B + \int_0^T \left(\int_a^0 e^{A\sigma} d\sigma + \int_0^{\lambda} e^{A\sigma} d\sigma \right) \frac{(T - \lambda)^{i-1}}{(i-1)!} d\lambda B$$

$$= - \frac{T^i}{i!} \int_a^0 e^{A\sigma} d\sigma B + \frac{T^i}{i!} \int_a^0 e^{A\sigma} d\sigma B + \int_0^T \int_0^{\lambda} e^{A\sigma} d\sigma \frac{(T - \lambda)^{i-1}}{(i-1)} d\lambda B$$

$$= \int_0^T \int_0^{\lambda} e^{A\sigma} d\sigma \frac{(T - \lambda)^{i-1}}{(i-1)!} d\lambda B \tag{3-29}$$

Now using Eq. (3-23), the last equation is written

$$q_i(T) = \int_0^T \theta(\lambda) \frac{(T - \lambda)^{i-1}}{(i-1)!} d\lambda \tag{3-30}$$

Thus, Q(T) is given by

$$Q(T) = [q_0(T) \vdots q_1(T) \vdots \cdots q_{N-1}(T)]$$

$$= [\theta(\tau) \vdots \int_0^T \theta(\lambda)d\lambda \vdots \int_0^T \theta(\lambda)(T-\lambda)d\lambda \vdots \cdots \vdots \int_0^T \theta(\lambda)\frac{(T-\lambda)^{N-2}}{(N-2)!}d\lambda] \tag{3-31}$$

If $\theta(\lambda)$ and $e^{A\lambda}$ are available in explicit form, Eqs. (3-30) and (3-31) are useful for evaluating Q(T). However, if $\theta(\lambda)$ and $e^{A\lambda}$ have to be calculated numerically using an infinite series, an alternate form for $q_i(\tau)$ and Q(T) is more useful. This alternate form is now derived as follows.

The infinite series expression for $e^{A\lambda}$ is written

$$e^{A\lambda} = \sum_{j=0}^{\infty} \frac{A^j\lambda^j}{j!} \tag{3-32}$$

Substituting Eq. (3-32) into Eq. (3-20) yields

$$q_i(T) = \int_0^T \sum_{j=0}^{\infty} \frac{A^j\lambda^j}{j!}\frac{(T-\lambda)^i}{i!}Bd\lambda$$

$$= \sum_{j=0}^{\infty} A^j \int_0^T \frac{\lambda^j(T-\lambda)^i}{i!j!}Bd\lambda \tag{3-33}$$

In order to carry out the integration in the last equation, for $i \geq 1$, we choose

$$v = (T-\lambda)^i/i! \tag{3-34}$$

$$dw = \frac{\lambda^j}{j!}d\lambda \tag{3-35}$$

then

$$dv = -\frac{(T-\lambda)^{i-1}}{(i-1)!}d\lambda \tag{3-36}$$

$$w = \frac{\lambda^{j+1}}{(j+1)!} \tag{3-37}$$

Substituting the last four equations into Eq. (3-33), and carrying out the integration by parts, we have

$$q_i(T) = \sum_{j=0}^{\infty} \frac{A^j \lambda^{j+1}}{(j+1)!} \frac{(T-\lambda)^i}{i!} \Bigg|_{\lambda=0}^{\lambda=T} B + \sum_{j=0}^{\infty} A^j \int_0^T \frac{\lambda^{j+1}}{(j+1)!} \frac{(T-\lambda)^{i-1}}{(i-1)!} \, d\lambda B$$

$$= \sum_{j=0}^{\infty} A^j \int_0^T \frac{\lambda^{j+1}}{(j+1)!} \frac{(T-\lambda)^{i-1}}{(i-1)!} \, d\lambda B \tag{3-38}$$

For $i \geq 2$, the above process can be repeated with

$$v = \frac{(T-\lambda)^{i-1}}{(i-1)!} \tag{3-39}$$

and

$$dw = \frac{\lambda^{j+1}}{(j+1)!} \tag{3-40}$$

to give

$$q_i(T) = \sum_{j=0}^{\infty} A^j \int_0^T \frac{\lambda^{j+2}}{(j+2)!} \frac{(T-\lambda)^{i-2}}{(i-2)!} \, d\lambda B \tag{3-41}$$

Generalizing the above described process, it can be seen that the expression for $q_i(T)$ in Eq. (3-33) needs to be integrated by parts a total of i times, to yield the result

$$q_i(T) = \sum_{j=0}^{\infty} A^j \int_0^T \frac{\lambda^{j+i}}{(i+j)!} \, d\lambda B$$

$$= \sum_{j=0}^{\infty} \frac{A^j T^{j+i+1}}{(i+j+1)!} B \tag{3-42}$$

Thus,

$$q_0(T) = \sum_{j=0}^{\infty} \frac{A^j T^{j+1}}{(j+1)!} B \tag{3-43}$$

$$q_1(T) = \sum_{j=0}^{\infty} \frac{A^j T^{j+2}}{(j+2)!} B \tag{3-44}$$

$$\vdots$$

$$q_{N-1}(T) = \sum_{j=0}^{\infty} \frac{A^j T^{j+N}}{(j+N)!} B \tag{3-45}$$

and

$$Q(T) = \sum_{j=0}^{\infty} A^j T^{j+1} \left[\frac{1}{(j+1)!} I_n \vdots \frac{T}{(j+2)!} I_n \vdots \cdots \vdots \frac{T^{N-1}}{(j+N)!} I_n \quad B \right] \tag{3-46}$$

where I_n is the n x n identity matrix.

The above expressions for Q(T) can be readily implemented on a digital computer.

The desired solutions for $\underline{G}$ and $\underline{E}$ are to be obtained from Eqs. (3-21) and (3-22), respectively. To solve these equations, two cases have to be considered:

Case 1. $n/m = N$.

In this case Q(T) is of dimension n x n and $\underline{G}$ is also of dimension n x n If $[Q(T)]^{-1}$ exists, then the desired solutions of Eqs. (3-21) and (3-22) are

$$\underline{G} = [Q(T)]^{-1}[e^{AT} - e^{\hat{A}T}] \tag{3-47}$$

and

$$\underline{E} = [Q(T)]^{-1}\theta_c(T) \tag{3-48}$$

where $\underline{E}$ and $\theta_c(T)$ are n x m matrices. Substituting these solutions into Eqs. (3-10) and (3-11) yields the optimal feedback and forward gains

$$G(\tau) = L_{mN}(\tau)[Q(T)]^{-1}[e^{AT} - e^{\hat{A}T}]$$

$$E(\tau) = L_{mN}(\tau)[Q(T)]^{-1}\ {}_{c}(T) \qquad (3\text{-}49)$$

where $\tau = t - kT$, $kT \leq t \leq (k+1)T$, $0 \leq \tau < T$.

Case 2. $n/m < N < n/m + 1$.

In this case $Q(T)$ is of dimension $n \times Nm$, $\underline{G}$ and $\underline{E}$ are of dimensions $Nm \times n$ and $Nm \times m$, respectively. Since $Nm > n$ and $Nm > m$, Eqs. (3-21) and (3-22) have more variables then the number of scalar equations.

Let

$$Nm - n = k \qquad (3\text{-}50)$$

Then, the number of excess variables in Eqs. (3-21) and (3-22) are kn and km, respectively, and the number of columns to be deleted from $Q(T)$ to yield an $n \times n$ matrix is k. If the rank of $Q(T)$ is n, then k dependent columns of $Q(T)$ may be deleted and the corresponding k rows of $\underline{G}$ and $\underline{E}$ may be chosen arbitrarily.

Let the $n \times Nm$-dimensional $Q(T)$ be written as

$$Q(T) = [Q_n(T) \vdots Q_k(T)] \qquad (3\text{-}51)$$

where

$Q_n(T) = n \times n$ nonsingular matrix

$Q_k(T) = n \times k$ matrix

and k is given by Eq. (3-50) In general, given $Q(T)$ with rank n, there is a degree of arbitrariness in the selection of $Q_n(T)$ which is nonsingular and is $n \times n$.

Let $\underline{G}_n$ be the $n \times n$ matrix which contains the n rows of $\underline{G}$ that correspond to the columns of $Q_n(T)$, Also $\underline{G}_k$ is the $k \times n$ matrix which contains the remaining rows of $\underline{G}$ that correspond to the columns of $Q_k(T)$. Then, Eq. (3-21) is written

$$e^{AT} - e^{\hat{A}T} = Q(T)\underline{G}$$

$$= [Q_n(T) \vdots Q_k(T)] \begin{pmatrix} \underline{G}_n \\ \cdots \\ \underline{G}_k \end{pmatrix} \tag{3-52}$$

Similarly, let $\underline{E}_n$ and $\underline{E}_k$ be the matrices which contain the rows of $\underline{E}$ that correspond to the columns of $Q_n(T)$ and $Q_k(T)$, respectively; $\underline{E}_n$ is n x n and $\underline{E}_k$ is k x m. Then, Eq. (3-22) is written

$$\theta_c(T) = Q(T)\underline{E}$$

$$= [Q_n(T) \vdots Q_k(T)] \begin{pmatrix} \underline{E}_n \\ \cdots \\ \underline{E}_k \end{pmatrix} \tag{3-53}$$

Since the nk elements of $\underline{G}_k$ may be chosen arbitrarily, Eq. (3-52) is written as

$$e^{AT} - e^{\hat{A}T} - Q_k(T)\underline{G}_k = Q_n(T)\underline{G}_n \tag{3-54}$$

Similarly, the mk elements of $\underline{E}_k$ are chosen arbitrarily; thus Eq. (3-53) becomes

$$\theta_c(T) - Q_k(T)\underline{E}_k = Q_n(T)\underline{E}_n \tag{3-55}$$

Since it is assumed that $Q_n(T)$ is nonsingular, $\underline{G}_n$ and $\underline{E}_n$ are solved from the last two equations,

$$\underline{G}_n = [Q_n(T)]^{-1}[e^{AT} - e^{\hat{A}T} - Q_k(T)\underline{G}_k] \tag{3-56}$$

$$\underline{E}_n = [Q_n(T)]^{-1}[\theta_c(T) - Q_k(T)\underline{E}_k] \tag{3-57}$$

Now using Eqs. (3-10) and (3-11) the optimal feedback and forward gain matrices are written

$$G(\tau) = L_{mN}(\tau)\underline{G} = L_{mN}(\tau) \begin{pmatrix} \underline{G}_n \\ \underline{G}_k \end{pmatrix}$$

$$= L_{mN}(\tau) \begin{pmatrix} [Q_n(T)]^{-1}[e^{AT} - e^{\hat{A}T} - Q_k(T)\underline{G}_k] \\ \underline{G}_k \end{pmatrix} \tag{3-58}$$

$$E(\tau) = L_{mN}(\tau)\underline{E} = L_{mN}(\tau)\begin{pmatrix}\underline{E}_n \\ \underline{E}_k\end{pmatrix}$$

$$= L_{mN}(\tau)\begin{pmatrix}[Q_n(T)]^{-1}[\theta_c(T) - Q_k(T)\underline{E}_k] \\ \underline{E}_k\end{pmatrix} \tag{3-59}$$

where $\tau = t - kT$, $kT \leq t < (k+1)T$, $0 \leq \tau < T$.

In general, if there are no amplitude constraints on the control inputs, we may set the elements of $\underline{G}_k$ and $\underline{E}_k$ arbitrarily to zero. Then, Eqs. (3-58) and (3-59) become

$$G(\tau) = L_{mN}(\tau)\begin{pmatrix}[Q_n(T)]^{-1}[e^{AT} - e^{\hat{A}T}] \\ \underline{0}\end{pmatrix} \tag{3-60}$$

$$E(\tau) = L_{mN}(\tau)\begin{pmatrix}[Q_n(T)]^{-1}\theta_c(T) \\ 0\end{pmatrix} \tag{3-61}$$

3.3 Example of Digital Redesign with the Method of Point by Point State Comparison by use of Higher-Order Holds.

In this chapter the simplified one-axis dynamics of the Skylab Satellite System is digitally redesigned by the point-by-point method using higher than zero-order holds. The optimal gain matrices $G(\tau)$ and $E(\tau)$ are computed, and the system responses are simulated with unit-step inputs.

This system has been simulated earlier and its system and control matrices are

$$A = \begin{pmatrix} 0 & 1 \\ 0 & 0 \end{pmatrix}, \quad B = \begin{pmatrix} 0 \\ \frac{1}{970,741} \end{pmatrix} \tag{3-62}$$

The continuous system gains are

$$G_c = [11800 \quad 151,800], \; E_c = [11800] \tag{3-63}$$

Since $n = 2$ and $m = 1$ a first-order hold should be adequate to match the states at every sampling instant. The feedback and forward gains of the digital system are defined by use of Eqs. (3-4) and (3-9),

$$G(t - kT) = G_0 + (t - kT)G_1 \tag{3-64}$$

$$E(t - kT) = E_0 + (t - kT)E_1$$

$$kT \leq t \leq (k + 1)T \tag{3-65}$$

Thus

$$\underline{G} = \begin{pmatrix} G_0 \\ G_1 \end{pmatrix}, \; \underline{E} = \begin{pmatrix} E_0 \\ E_1 \end{pmatrix} \tag{3-66}$$

The state transition matrix is

$$e^{AT} = \begin{pmatrix} 1 & T \\ 0 & 1 \end{pmatrix} \tag{3-67}$$

and from Eq. (2-23)

$$q_0(T) = \theta(T) = \int_0^T e^{A\lambda} B d\lambda = \frac{1}{970,741} \begin{pmatrix} \frac{T^2}{2} \\ T \end{pmatrix} \tag{3-68}$$

Also, from Eq. (2-30)

$$q_1(T) = \int_0^T q_0(\lambda) d\lambda = \frac{1}{970,741} \begin{pmatrix} \frac{T^3}{6} \\ \frac{T^2}{2} \end{pmatrix} \tag{3-69}$$

Using Eq. (2-31), we have

$$Q(T) = [q_0(T) \quad q_1(T)] = \frac{1}{970,741} \begin{pmatrix} \frac{T^2}{2} & \frac{T^3}{6} \\ T & \frac{T^2}{2} \end{pmatrix} \tag{3-70}$$

Thus,

$$[Q(T)]^{-1} = 970,741 \begin{pmatrix} \frac{6}{T^2} & \frac{-2}{T} \\ \frac{12}{T^3} & \frac{6}{T^2} \end{pmatrix} \tag{3-71}$$

The solutions for $\underline{G}$ and $\underline{E}$ are obtained from Eqs. (2-47) and (2-48), respectively;

$$\underline{G} = [Q(T)]^{-1}[e^{AT} - e^{\hat{A}T}]$$

$$= 970,741 \begin{pmatrix} \frac{6}{T^2} & \frac{-2}{T} \\ \frac{-12}{T^3} & \frac{6}{T^2} \end{pmatrix} [e^{AT} - e^{\hat{A}T}] \tag{3-72}$$

$$\underline{E} = [Q(T)]^{-1}\theta_c(T)$$

$$= 970{,}741\begin{pmatrix} \frac{6}{T^2} & \frac{-2}{T} \\ \frac{-12}{T^3} & \frac{6}{T^2} \end{pmatrix}\theta_c(T) \qquad (3\text{-}73)$$

For T = 2, we have

$$\underline{G} = \begin{pmatrix} 11752 & 151758 \\ -1700.7 & -11837 \end{pmatrix} = \begin{pmatrix} G_0 \\ G_1 \end{pmatrix} \qquad (3\text{-}74)$$

$$\underline{E} = \begin{pmatrix} 11752 \\ -1700.7 \end{pmatrix} = \begin{pmatrix} E_0 \\ E_1 \end{pmatrix} \qquad (3\text{-}75)$$

Thus,

$$G_0 = [11752 \quad 151758]$$

$$G_1 = [-1700.7 \quad -11837] \qquad (3\text{-}76)$$

$$E_0 = [11752]$$

$$E_1 = [-1700.7]$$

The optimal gains are obtained from Eqs. (3-64) and (3-68)

$$G(t - kT) = [11752 - 1700.7\,(t - kT) \qquad 151758 - 11837\,(t - kT)] \qquad (3\text{-}77)$$

$$E(t - kT) = [11752 - 1700.7\,(t - kT)]$$

$$kT \leq t < (k + 1)T$$

The continuous and digital data systems are simulated on a digital computer. A unit-step input is applied in both cases and a sampling period of T = 2 sec. is used for the sampled-data system. The results of the simulation are shown in Figs. 3-3 through 3-8 These include the state trajectories, control trajectories and the errors in the state and control trajectories.

Comparing these simulation results with those of the partial matching method of Chapter 1, it can be seen that the error between the states and the controls of the continuous and sampled-data systems is lower with this method. Theoretically, the errors should be zero at each sampling period but due to the numerical processes of simulation a small amount of error is still present. Table 3-1 shows the maximum errors at the sampling instants and in between the sampling instants for the exact as well as the partial matching cases.

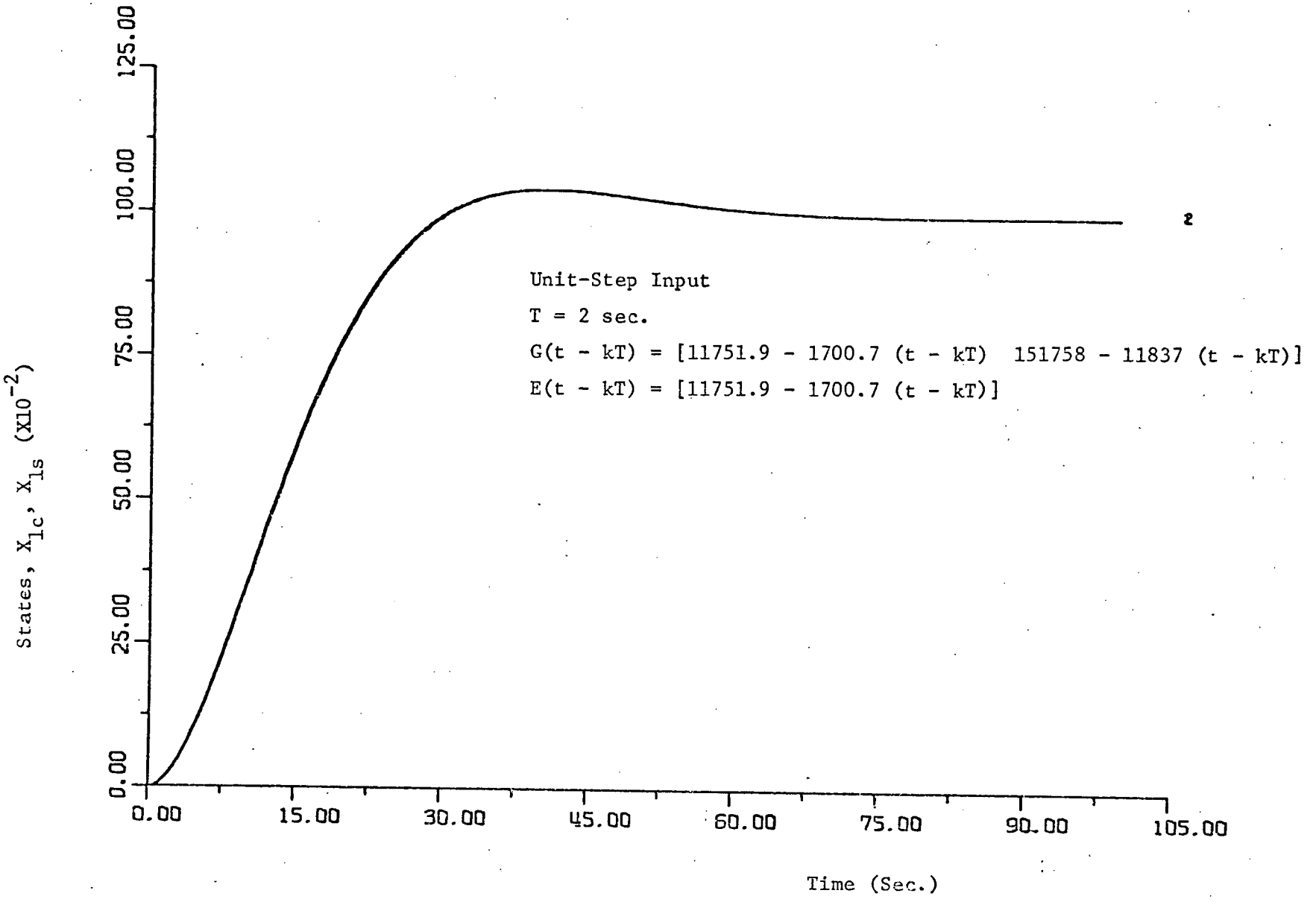

Figure 3-3 Simplified Skylab Satellite Comparison of states, X_{ic} (continuous) and X_{ls} (sampled).

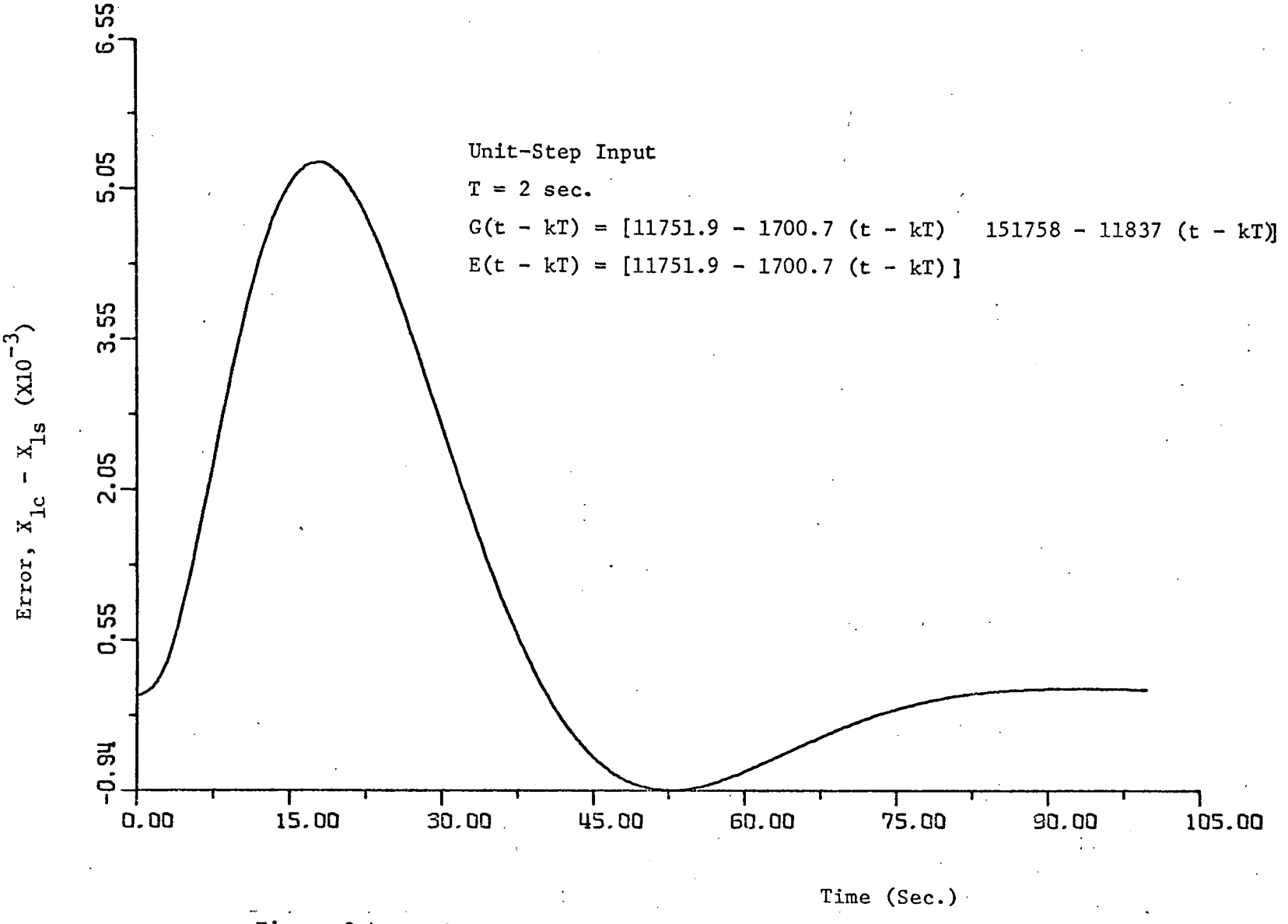

Figure 3-4 Simplified Skylab Satellite. Error, $X_{1c} - X_{1s}$.

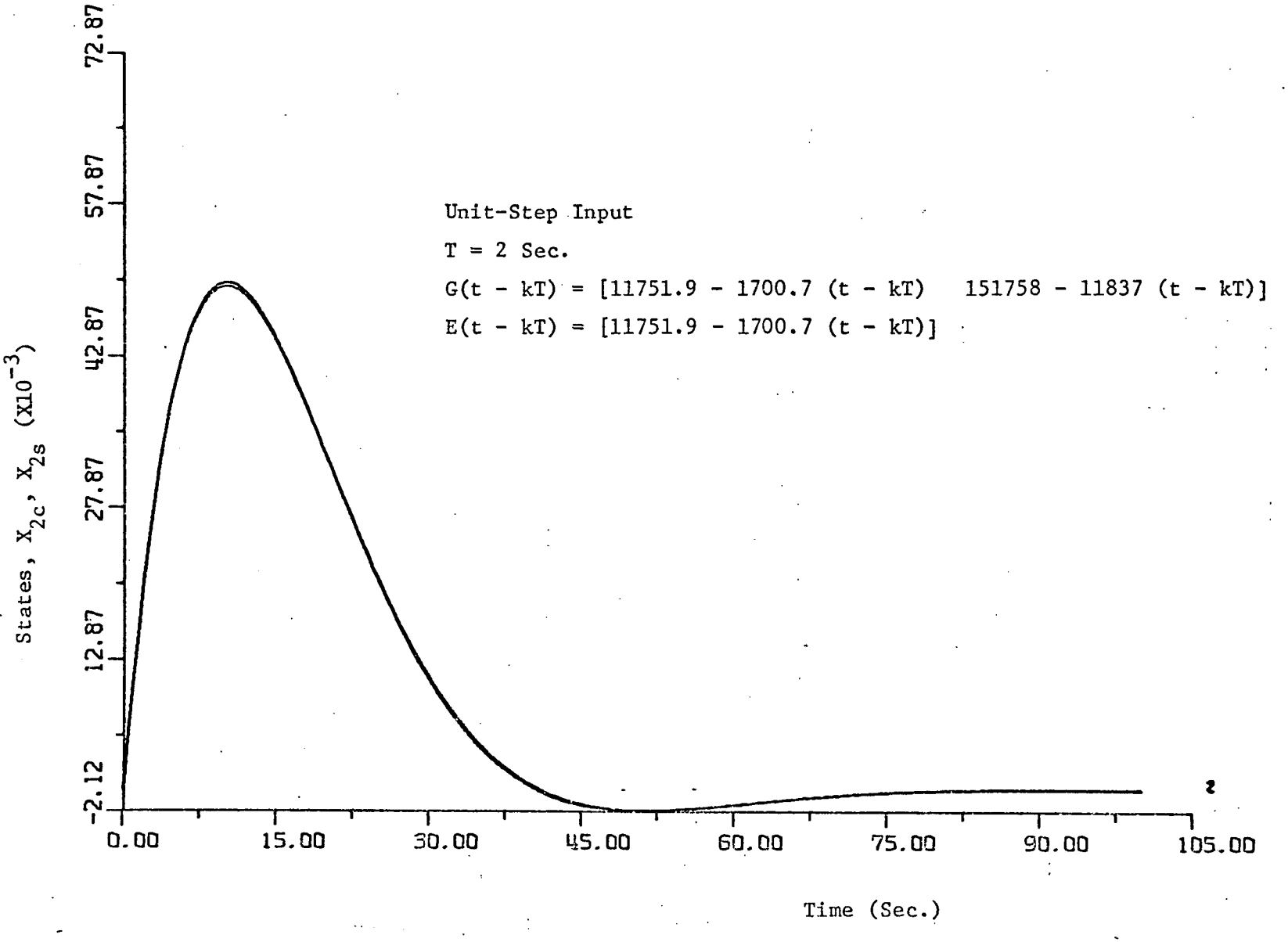

Figure 3-5 Simplified Skylab Satellite.
Comparison of X_{2c} and X_{2s}.

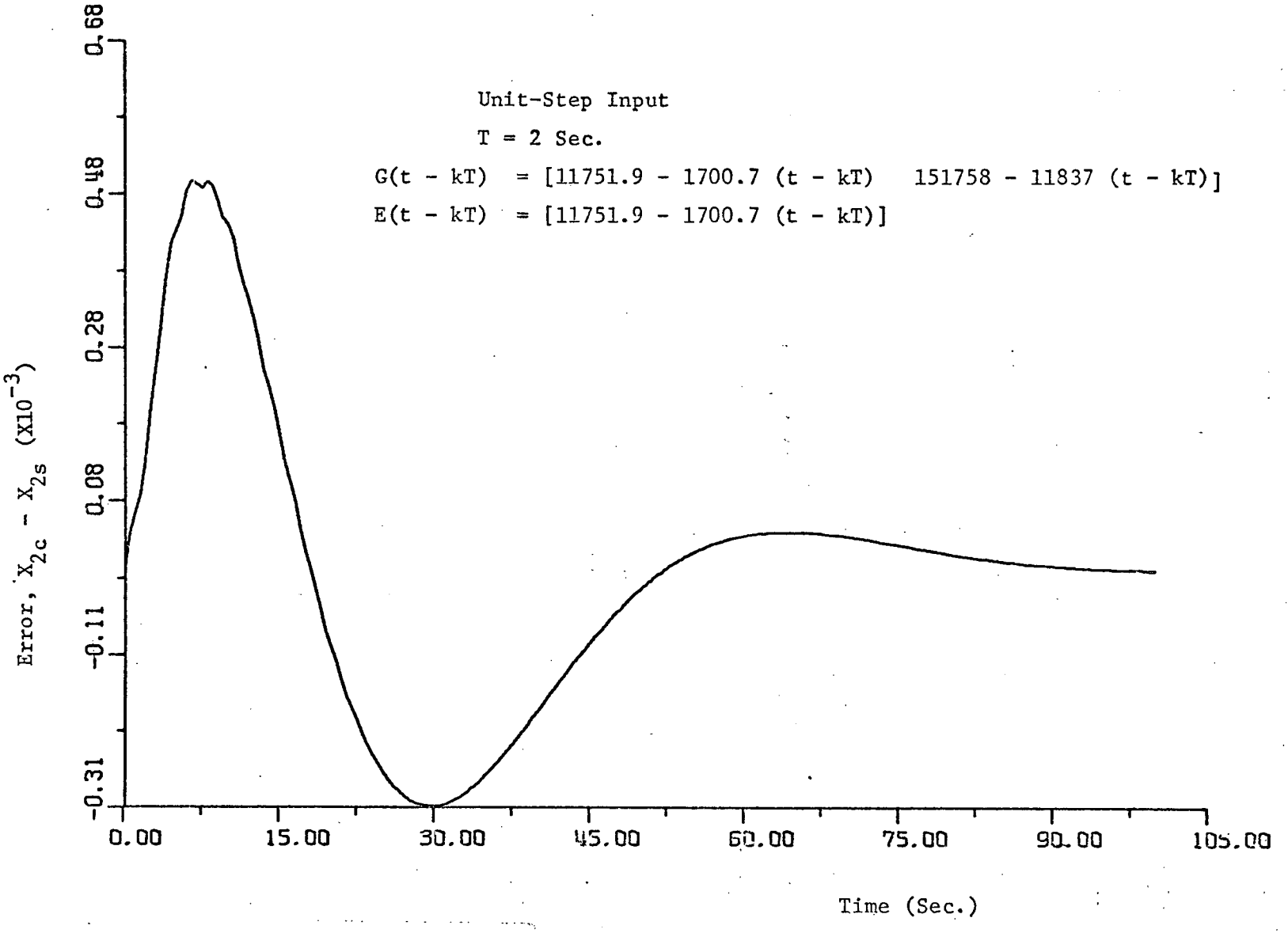

Figure 3-6 Simplified Skylab Satellite.
Error, $X_{2c} - X_{2s}$.

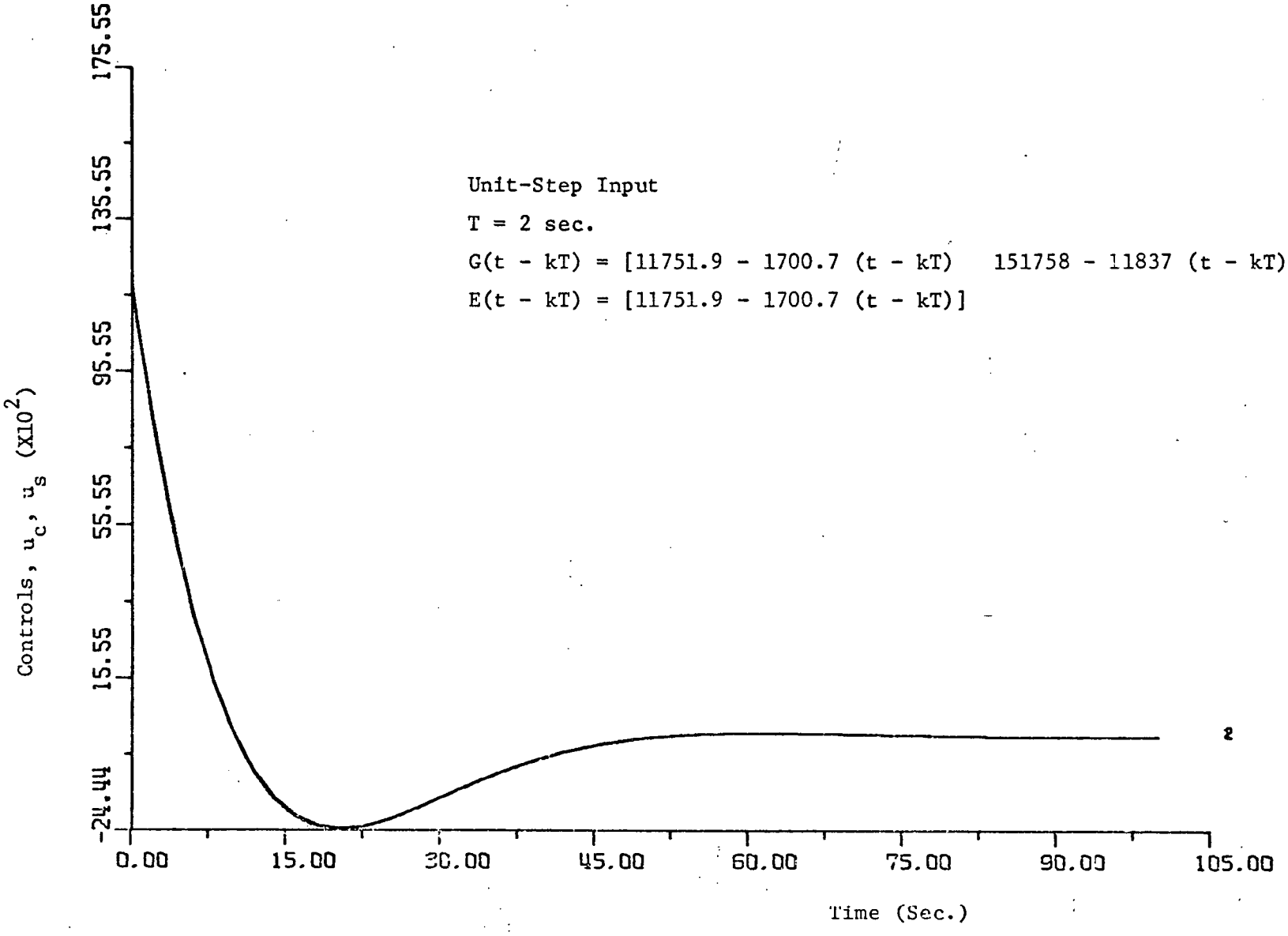

Figure 3-7. Simplified Skylab Satellite
Comparison of Controls, u_c and u_s.

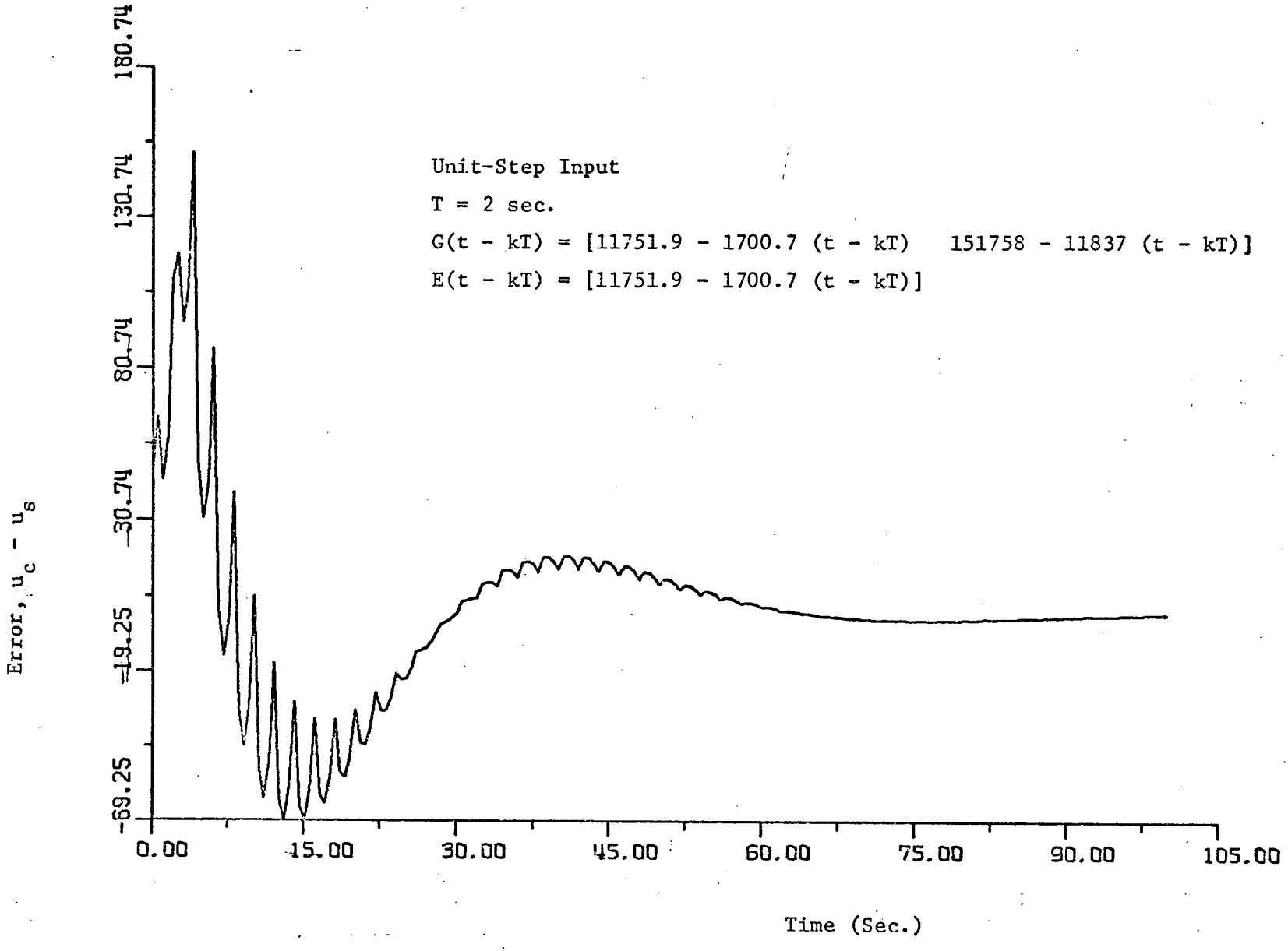

Figure 3-8 Simplified Skylab Satellite. Error, $u_c - u_s$.

Table 3.1. Comparison of errors between the states of the continuous and digital systems for the Simplified Skylab Satellite

Method of Digital Redesign	Maximum Error at the Sampling Instants				Maximum error at points within sampling instants			
	Error in X_1		Error in X_2		Error in X_1		Error in X_2	
	Error	Time of Occurence	Error	Time of Occurence	Error	Time of Occurence	Error	Time of Occurence
Partial Matching H = [0 1], T = 2 sec	6.12×10^{-3}	t = 7T	-3.28×10^{-4}	t = 13T	6.12×10^{-3}	15.5 sec.	9.35×10^{-4}	1 sec.
Partial Matching H = [1 0], T = 2 sec	1.41×10^{-2}	t = 9T	-1.66×10^{-3}	t = 3T	-1.41×10^{-3}	17.5 sec.	-1.66×10^{-3}	6.
Method of High Order Hold, T = 2 sec. N = 2	5.3×10^{-3}	t = 9T	5×10^{-4}	t = 4T	5.3×10^{-3}	18. sec.	5×10^{-4}	6.5
Method of Multiple Sampling Periods T = 1. sec., N = 2	1.267×10^{-3}	t = 9T	1.308×10^{-4}	t = 4T	1.269×10^{-3}	18.5 sec.	-2.92×10^{-4}	1.

4. DIGITAL REDESIGN OF THE CONTROL OF THE WOBBLE DYNAMICS OF THE SPINNING SKYLAB

4.1 Introduction

This report presents the results of the digital redesign of the control of a spinning Skylab space station. The dynamics of the spinning Skylab are first described. Only the wobble dynamics are considered however. The optimal feedback gains and the forward gains of the digital control are determined by use of the following point-by-point methods:

a. Partial matching of states

b. Exact matching at multiple sampling periods

c. Exact matching with higher-order holds

The simulation of the spinning Skylab system was carried out using the partial matching method and the multiple sampling period method. In practice, since the digital control as derived from the partial matching method is the easiest one to implement, and the simulation results are quite good, it is the recommended solution.

4.2 Modeling of the Spinning Skylab

A detailed description of the spinning Skylab space station can be found in the literature [3,4]. A simplified model for the spinning Skylab vehicle is shown in Figure 4-1 The variables of the system are indicated on the diagram.

The mission of a spinning Skylab makes it necessary to point the 3-axis at the sun rather than to passively stabilize the steady-state rotation of the vehicle about its 3-axis. This will place the solar panels, which are lying in the 1-2 plane of the vehicle, normal to the impinging rays of the sun, making maximum use of solar energy. The control torques may be provided by three control moment gyros (CMG's).

The dynamic equations of the system are expressed in vector form:

$$M\ddot{\underline{z}} + D\ddot{\underline{z}} + K\underline{z} = -\underline{v} \qquad (4\text{-}1)$$

where the dots represent derivatives with respect to $\tau = \Omega t$.

$$\underline{z} = [\phi_1 \quad \phi_2 \quad \phi_3 \quad \mu_1 \quad \mu_2 \quad \mu_3]' \qquad (4\text{-}2)$$

The control vector is given by

$$\underline{v} = [v_1 \quad v_2 \quad v_3 \quad v_4 \quad v_5 \quad v_6]'$$

$$= [\frac{T_1}{I_1\Omega^2} \quad \frac{T_2}{I_2\Omega^2} \quad 0 \quad \frac{T_3}{I_3\Omega^2} \quad 0 \quad 0]' \qquad (4\text{-}3)$$

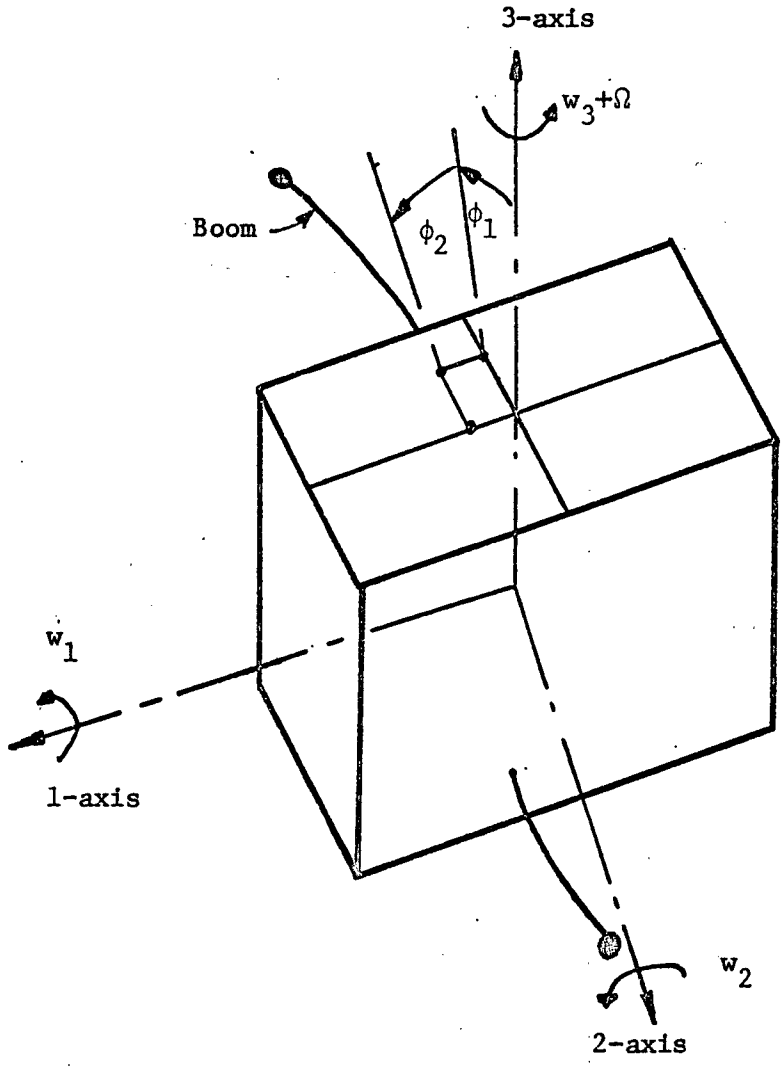

Figure 4-1 A simplified model of the spinning Skylab.

$$M = \begin{pmatrix} 1 & 0 & 0 & 0 & \xi\gamma_1 & -\gamma_1 \\ 0 & \frac{1+K_1}{1-K_2} & 0 & -\xi\gamma_1 & 0 & 0 \\ -\gamma_1 & 0 & 0 & 0 & 0 & \gamma_1 \\ 0 & 0 & 1 & \gamma_3 & 0 & 0 \\ 0 & -\xi & 1 & 1 & 0 & 0 \\ \xi & 0 & 0 & 0 & 1 & 0 \end{pmatrix} \qquad (4\text{-}4)$$

$$D = \begin{pmatrix} 0 & -(1+K_1) & 0 & 2\xi\gamma_1 & 0 & 0 \\ 1+K_1 & 0 & 0 & 0 & 2\xi\gamma_1 & 0 \\ 0 & 0 & 0 & 0 & 0 & \gamma_1\Delta_3 \\ 0 & 0 & 0 & 0 & -2\gamma_3 & 0 \\ -2\xi & 0 & 0 & \Delta_1 & -2 & 0 \\ 0 & -2\xi & 2 & 2 & \Delta_2 & 0 \end{pmatrix} \qquad (4\text{-}5)$$

$$K = \begin{pmatrix} -K_1 & 0 & 0 & 0 & -\xi\gamma_1 & -\gamma_1 \\ 0 & K_2(\frac{1+K_1}{1-K_2}) & 0 & \xi\gamma_1 & 0 & 0 \\ -\gamma_1 & 0 & 0 & 0 & 0 & \gamma_1(\sigma_3^2+1) \\ 0 & 0 & 0 & 0 & 0 & 0 \\ 0 & \xi & 0 & \sigma_1^2 & 0 & 0 \\ -\xi & 0 & 0 & 0 & \sigma_2^2-1 & 0 \end{pmatrix} \qquad (4\text{-}6)$$

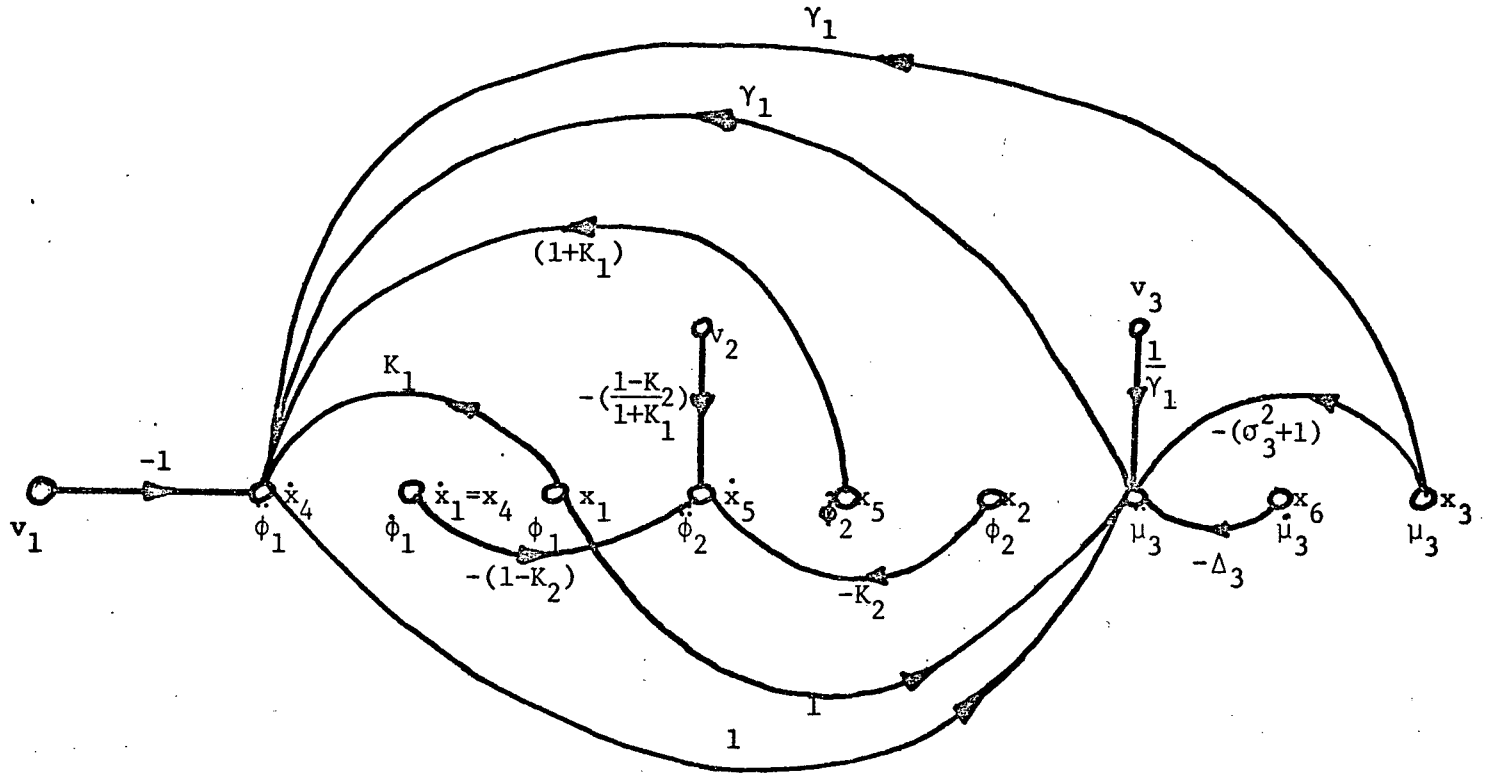

Figure 4-2 State diagram for the wobble dynamics of the spinning Skylab.

If the value of Γ_3 is neglected, and $\xi = \Gamma_3/\Gamma_2 = 0$, the wobble motion is separated from the spin velocity motion. In other words, the differential equations represented by Eq. (4-1) are now divided into two sets of uncoupled equations.

Wobble Dynamics

$$\ddot{\phi}_1 - \gamma_1\ddot{\mu}_3 - (1 + K_1)\dot{\phi}_2 - K_1\phi_1 - \gamma_1\mu_3 = -v_1 \tag{4-7}$$

$$\left(\frac{1+K_1}{1-K_2}\right)\ddot{\phi}_2 + (1 + K_1)\dot{\phi}_1 + K_2\left(\frac{1+K_1}{1-K_2}\right)\phi_2 = -v_2 \tag{4-8}$$

$$-\gamma_1\ddot{\phi}_1 + \gamma_1\ddot{\mu}_3 + \gamma_1\Delta_3\dot{\mu}_3 - \gamma_1\phi_1 + \gamma_1(\sigma_3^2 + 1)\mu_3 = -v_3 \tag{4-9}$$

Spin Velocity Model

$$\ddot{\phi}_3 + \gamma_3\ddot{\mu}_1 - 2\gamma_3\dot{\mu}_2 = -v_4 \tag{4-10}$$

$$\ddot{\phi}_3 + \ddot{\mu}_1 + \Delta_1\dot{\mu}_1 - 2\dot{\mu}_2 + \sigma_1^2\mu_1 = -v_5 \tag{4-11}$$

$$\ddot{\mu}_2 + 2\dot{\phi}_3 + 2\dot{\mu}_1 + \Delta_2\dot{\mu}_2 + (\sigma_2^2 - 1)\mu_2 = -v_6 \tag{4-12}$$

In this study only the wobble dynamics will be considered.

In order to obtain the state equations of the wobble dynamics, a state diagram is constructed in Figure 4-2 using Eqs. (4-7),(4-8) , and (4-9) Applying Mason's gain formula to the state diagram of Figure 4-2 we have

$$\begin{pmatrix} \dot{\phi}_1 \\ \dot{\phi}_2 \\ \dot{\mu}_3 \\ \ddot{\phi}_1 \\ \ddot{\phi}_2 \\ \ddot{\mu}_3 \end{pmatrix} = \left(\begin{array}{ccc|ccc} 0 & 0 & 0 & 1 & 0 & 0 \\ 0 & 0 & 0 & 0 & 1 & 0 \\ 0 & 0 & 0 & 0 & 0 & 1 \\ \hline \frac{K_1+\gamma_1}{1-\gamma_1} & 0 & \frac{-\gamma_1\sigma_3^2}{1-\gamma_1} & 0 & \frac{1+K_1}{1-\gamma_1} & \frac{-\gamma_1\Delta_3}{1-\gamma_1} \\ 0 & -K_2 & 0 & -(1-K_2) & 0 & 0 \\ \frac{1+K_1}{1-\gamma_1} & 0 & \frac{\gamma_1-(\sigma_3^2+1)}{1-\gamma_1} & 0 & \frac{1+K_1}{1-\gamma_1} & \frac{-\Delta_3}{1-\gamma_1} \end{array}\right) \begin{pmatrix} \phi_1 \\ \phi_2 \\ \mu_3 \\ \dot{\phi}_1 \\ \dot{\phi}_2 \\ \dot{\mu}_3 \end{pmatrix}$$

$$+ \begin{pmatrix} 0 \\ 0 \\ 0 \\ \frac{-1}{1-\gamma_1} \\ 0 \\ \frac{-1}{1-\gamma_1} \end{pmatrix} v_1 \qquad (4\text{-}13)$$

where it has been assumed that $v_2 = v_3 = v_4 = v_5 = v_6 = 0$.

The physical characteristics of the spinning skylab are given below:

$I_1 = 1.25 \times 10^6$ kg-m^2

$I_2 = 6.90 \times 10^6$ kg-m^2

$I_3 = 7.10 \times 10^6$ kg-m^2

$\Gamma_1 = 0$

$\Gamma_2 = 23.3$ m

$\Gamma_3 = -1.53$ m

$m = 227$ kg

$$k_1 = k_3 = 146 \text{ N/m}$$

$$k_2 = 7.4 \times 10^4 \text{ N/m}$$

$$d_1 = d_3 = 0.04\,(k_3 m)^{1/2} = 7.28$$

$$d_2 = 0.04\,(k_2 m)^{1/2} = 164$$

$$\Omega = 0.6 \text{ s}^{-1}$$

$$K_1 = \frac{I_2 - I_3}{I_1} = -0.16$$

$$K_2 = \frac{I_3 - I_1}{I_2} = 0.8478$$

$$\gamma_1 = \frac{2m\Gamma_2^2}{I_1} = 0.19717$$

$$\gamma_3 = \frac{2m\Gamma_2^2}{I_1} = 0.03471$$

$$\Delta_1 = \frac{d_1}{m\Omega} = 0.0534$$

$$\Delta_2 = \frac{d_2}{m\Omega} = 1.20$$

$$\Delta_3 = \frac{d_3}{m\Omega} = \Delta_1 = 0.0534$$

$$\sigma_1^2 = \frac{k_1}{m\Omega^2} = 1.787$$

$$\sigma_2^2 = \frac{k_2}{m\Omega^2} = 905.53$$

$$\sigma_3^2 = \sigma_1^2 = 1.787$$

Substituting the values of these parameters into Eq.(4-13) , we have

$$\begin{pmatrix} \dot{\phi}_1 \\ \dot{\phi}_2 \\ \dot{\mu}_3 \\ \ddot{\phi}_1 \\ \ddot{\phi}_2 \\ \ddot{\mu}_3 \end{pmatrix} = \left(\begin{array}{ccc|ccc} 0 & 0 & 0 & 1 & 0 & 0 \\ 0 & 0 & 0 & 0 & 1 & 0 \\ 0 & 0 & 0 & 0 & 0 & 1 \\ \hline 0.0463 & 0 & -0.4388 & 0 & 1.0462 & -0.01313 \\ 0 & -0.8478 & 0 & -0.1522 & 0 & 0 \\ 1.0462 & 0 & -3.22 & 0 & 1.0462 & -0.06657 \end{array}\right) \begin{pmatrix} \phi_1 \\ \phi_2 \\ \mu_3 \\ \dot{\phi}_1 \\ \dot{\phi}_2 \\ \dot{\mu}_3 \end{pmatrix} + \begin{pmatrix} 0 \\ 0 \\ 0 \\ -1.245 \\ 0 \\ -1.245 \end{pmatrix} v_1 \qquad (4\text{-}14)$$

4.3 Optimal Control Laws for the Continuous-Data Controllers

A total of three control laws were provided by NASA which represent the solution of the control of the wobble dynamics of the spinning Skylab vehicle by continuous-data controllers. These control laws are described as follows:

Control Law No. 1.

$$\underline{T} = \alpha\underline{\phi} + \beta\underline{\omega} \tag{4-15}$$

where

$$\underline{T} = [T_1 \quad T_2 \quad T_3]' \tag{4-16}$$

$$\underline{\phi} = [\phi_1 \quad \phi_2 \quad 0]' \tag{4-17}$$

$$\underline{\omega} = [w_1 \quad w_2 \quad w_3 + \Omega]' \tag{4-18}$$

$$\alpha = \begin{bmatrix} \alpha_{11} & \alpha_{12} & 0 \\ \alpha_{21} & \alpha_{22} & 0 \\ 0 & 0 & 0 \end{bmatrix} \tag{4-19}$$

$$\beta = \begin{bmatrix} \beta_{11} & \beta_{12} & 0 \\ \beta_{21} & \beta_{22} & 0 \\ 0 & 0 & 0 \end{bmatrix} \tag{4-20}$$

$$\underline{\omega} = \begin{bmatrix} -1 & 0 & 0 \\ 0 & -1 & 0 \\ 0 & 0 & -1 \end{bmatrix} \frac{d\underline{\phi}}{dt} + \begin{bmatrix} 0 & \Omega & 0 \\ -\Omega & 0 & 0 \\ 0 & 0 & 0 \end{bmatrix} \underline{\phi} \tag{4-21}$$

$$\alpha_{12} = I_1\Omega^2\varepsilon \qquad \text{all other } \alpha_{ij} = 0$$

$$\beta_{11} = I_1\Omega\delta \qquad \text{all other } \beta_{ij} = 0$$

Then

$$T_1 = \alpha_{12}\phi_2 + \beta_{11}w_1 = (\alpha_{12} + \beta_{11}\Omega)\phi_2 - \beta_{11}\dot{\phi}_1\Omega \tag{4-22}$$

(a) Linear case A: $\delta = -1.27$, $\varepsilon = 5.9$

Then

$$\alpha_{12} = I_1\Omega^2\varepsilon = 2.655 \times 10^6 \tag{4-23}$$

$$\beta_{11} = I_1\Omega\delta = -0.9525 \times 10^6 \tag{4-24}$$

Thus

$$T_1 = 2.0835 \times 10^6\phi_2 + 0.5715 \times 10^6\dot{\phi}_1 \tag{4-25}$$

$$v_1 = \frac{T_1}{I_1\Omega^2} = 4.63\phi_2 + 1.27\dot{\phi}_1 \tag{4-26}$$

In terms of state feedback, $v_1 = -G(0)\underline{x}$,

$$v_1 = [0 \quad 4.63 \quad 0 \quad 1.27 \quad 0 \quad 0] \begin{pmatrix} \phi_1 \\ \phi_2 \\ \mu_3 \\ \dot{\phi}_1 \\ \dot{\phi}_2 \\ \dot{\mu}_3 \end{pmatrix} \tag{4-27}$$

(b) Linear case B: $\delta = -1$, $\varepsilon = 2$.

$$\alpha_{12} = I_1\Omega^2\varepsilon = 0.9 \times 10^6$$

$$\beta_{11} = I_1\Omega\delta = -0.75 \times 10^6$$

Thus

$$T_1 = 0.45 \times 10^6\dot{\phi}_1 + 0.45 \times 10^6\phi_2 \tag{4-28}$$

$$v_1 = \frac{T_1}{I_1\Omega^2} = \dot{\phi}_1 + \phi_2$$

$$v_1 = [0 \quad 1 \quad 0 \quad 1 \quad 0 \quad 0] \begin{pmatrix} \phi_1 \\ \phi_2 \\ \mu_3 \\ \dot{\phi}_1 \\ \dot{\phi}_2 \\ \dot{\mu}_3 \end{pmatrix} \tag{4-29}$$

Control Law No. 2 (Linear Quadratic Law)

The optimal control as obtained by the linear quadratic law is

$$v_1 = [1.263 \quad -0.777 \quad -0.172 \quad 2.768 \quad -1.792 \quad -0.095] \begin{pmatrix} \phi_1 \\ \phi_2 \\ \mu_3 \\ \dot{\phi}_1 \\ \dot{\phi}_2 \\ \dot{\mu}_3 \end{pmatrix} \tag{4-30}$$

4.4 Digital Redesign and Simulation

The digital redesign of the control for thw wobble dynamics of the spinning Skylab vehicle is performed by three different point-by-point methods:

a. Partial matching of states

b. Exact matching at multiple sampling periods

c. Exact matching at higher order holds.

In each case the feedback and forward gains are determined for the various control laws. The imulation is performed using the method of partial matching and the method of multiple sampling periods.

From Eq. (4-14) the state equations of the system are

$$\dot{\underline{x}} = A\underline{x} + B\underline{u} \tag{4-31}$$

with $\underline{x} = [\phi_1 \quad \phi_2 \quad \mu_3 \quad \dot{\phi}_1 \quad \dot{\phi}_2 \quad \dot{\mu}_3]'$

$\underline{u} = v_1$

$$A = \left[\begin{array}{ccc|ccc} 0 & 0 & 0 & 1 & 0 & 0 \\ 0 & 0 & 0 & 0 & 1 & 0 \\ 0 & 0 & 0 & 0 & 0 & 1 \\ \hline 0.0463 & 0 & -0.4388 & 0 & 1.0462 & -.01313 \\ 0 & & 0 & -.1522 & 0 & 0 \\ 1.0462 & 0 & -3.22 & 0 & 1.0462 & -.06657 \end{array}\right]$$

$$B = [0 \quad 0 \quad 0 \quad -1.245 \quad 0 \quad -1.245]'$$

The control vector $\underline{u}$ for the continuous system is

$$\underline{u}_c = E_c r - G_c \underline{x}_c \tag{4-32}$$

where the feedback and forward gains of the continuous system for the three control laws are

Control Law 1A

G_c = [0 4.63 0 1.27 0 0]

E_c = 1.

Control Law 1B

G_c = [0 1. 0 1. 0 0]

E_c = 1.

Control Law 2

G_c = [1.263 -0.777 -0.172 2.768 -1.792 -0.095]

E_c = 1.

The results obtained by performing the digital redesign of this system with the three different methods are described below.

a. Partial Matching of States.

The method of partial matching was used on control law 2 with a sampling period of T = 1 and a weighting matrix

H = [1 1 1 1 1 1]

The sampled-data gains are:

$G_s(1)$ = -.286054 T = 1

$G_s(2)$ = .0711766

$G_s(3)$ = .161217

$G_s(4)$ = -.946105

$G_s(5)$ = -.113347

$G_s(6)$ = .121896

$E_s(1)$ = .246084

The continuous and sampled-data systems were simulated and the results are shown in Figure 4-3 through 4-9. The states and controls, and the errors between the continuous and sampled states and controls are shown. The results show that for T = 1 the point-by-point method of partial matching yields an acceptable redesign.

Time Interval	Feedback Gains from States						Forward Gain
	x_1	x_2	x_3	x_4	x_5	x_6	r
.0	-4.92398	-801.398	55.8475	-826.826	-283.221	9.22254	830.723
.5	-14.5192	-594.385	153.307	-549.619	-706.054	-1.40256	546.516
1.0	-13.3919	-867.241	17.1915	-1058.39	37.3406	74.8695	870.569
1.5	40.4243	-619.488	68.0836	-342.295	-929.208	-51.2130	291.012
2.0	35.3183	-859.229	85.9373	-1008.44	-64.9085	22.6930	597.738
2.5	.156333	-624.771	83.1258	-662.564	-514.606	22.8996	516.595

Table 4-1 Forward gain $E_s X10^{-3}$ and Feedback gains $G_s X10^{-3}$ for the sixth order model of the wobble dynamics of the Spinning Skylab.

b. Exact Matching by Multiple Sampling Periods.

The method of Multiple Sampling Periods was used on control law 1B for T = 0.5. That is the gains are changed every 0.5 seconds and all the states are to be matched every 6 x 0.6 = 3 seconds. The sampled-data gains are given in Table 4-1 for G_s and E_s. The continuous and sampled systems were simulated and the states, controls, and the errors between the states and controls of the sampled and continuous systems are shown in Figures 4-10 to 4-16. The states of the two systems are reasonably well matched considering the size of the sampling period.

c. Exact Matching with Higher-Order Holds.

This method for digital redesign has been described in Chapter 3. With n/m = 6, it appears that a 5th-order hold is adequate. Thus, N = 6 is used and the coefficients of the various terms of the gain matrices are calculated with T = 0.2. Table 4-2 lists the gains for control law 1A.

The simulation has not been performed with this method of digital redesign, but it is expected that the results will be similar to those obtained by the method of multiple sampling periods.

Table 4-2 Feedback and Forward Gains for the wobble dynamics of the Spinning Skylab, Control Law 1A. Method of Higher-Order Holds.

Coefficients of	Feedback Gains: Feedback from States						Forward Gains	Scale Factor
	x_1	x_2	x_3	x_4	x_5	x_6		
1	.29116	-464.55	-.2666	-127.72	2.3438	-.08154	100.56	$X10^{-2}$
$t - kT$	-.57297	10.953	1.0845	3.4844	-10.7695	.17682	-2.75	-
$\frac{(t - kT)^2}{2!}$	.41414	-3,52	-,45875	-1.36	4.29	-.13752	1.05	$X10^{2}$
$\frac{(t - kT)^3}{3!}$	-.18961	2.1888	.2446	.7616	-2.3768	.07324	-.5888	$X10^{4}$
$\frac{(t - kT)^4}{4!}$	.48	-6.922	-.68544	-2.2682	6.8147	-.2046	1.6947	$X10^{5}$
$\frac{(t - kT)^5}{5!}$	-.5382	9.699	.88064	3.0556	-8.966	.26099	-2.2364	$X10^{6}$

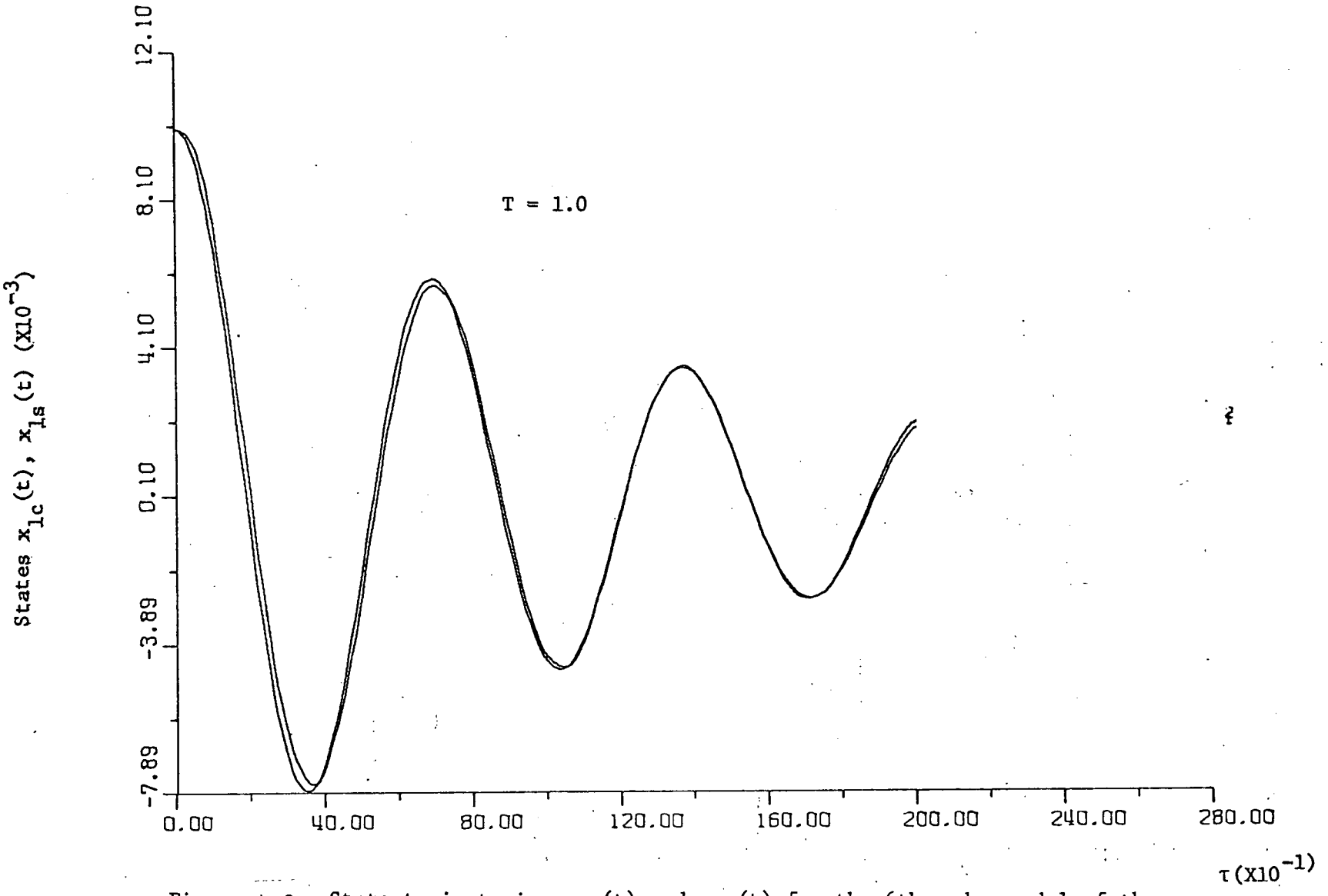

Figure 4-3 State trajectories $x_{1c}(t)$ and $x_{1s}(t)$ for the 6th order model of the Spinning Skylab Satellite. Digital redesign by the point by point method of partial matching.

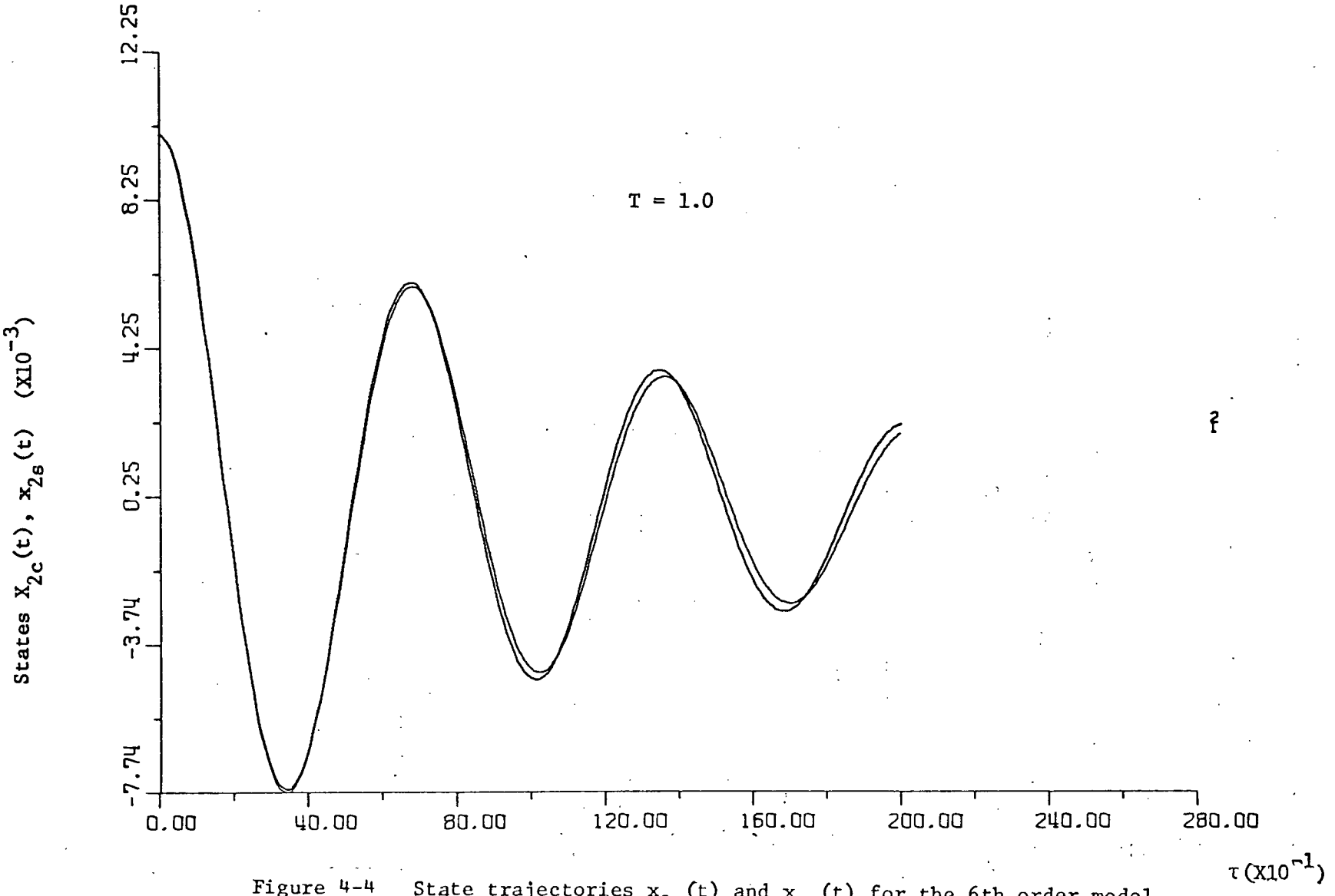

Figure 4-4 State trajectories $x_{2c}(t)$ and $x_{2s}(t)$ for the 6th order model of the Spinning Skylab Satellite. Digital redesign by the point by point method of partial matching.

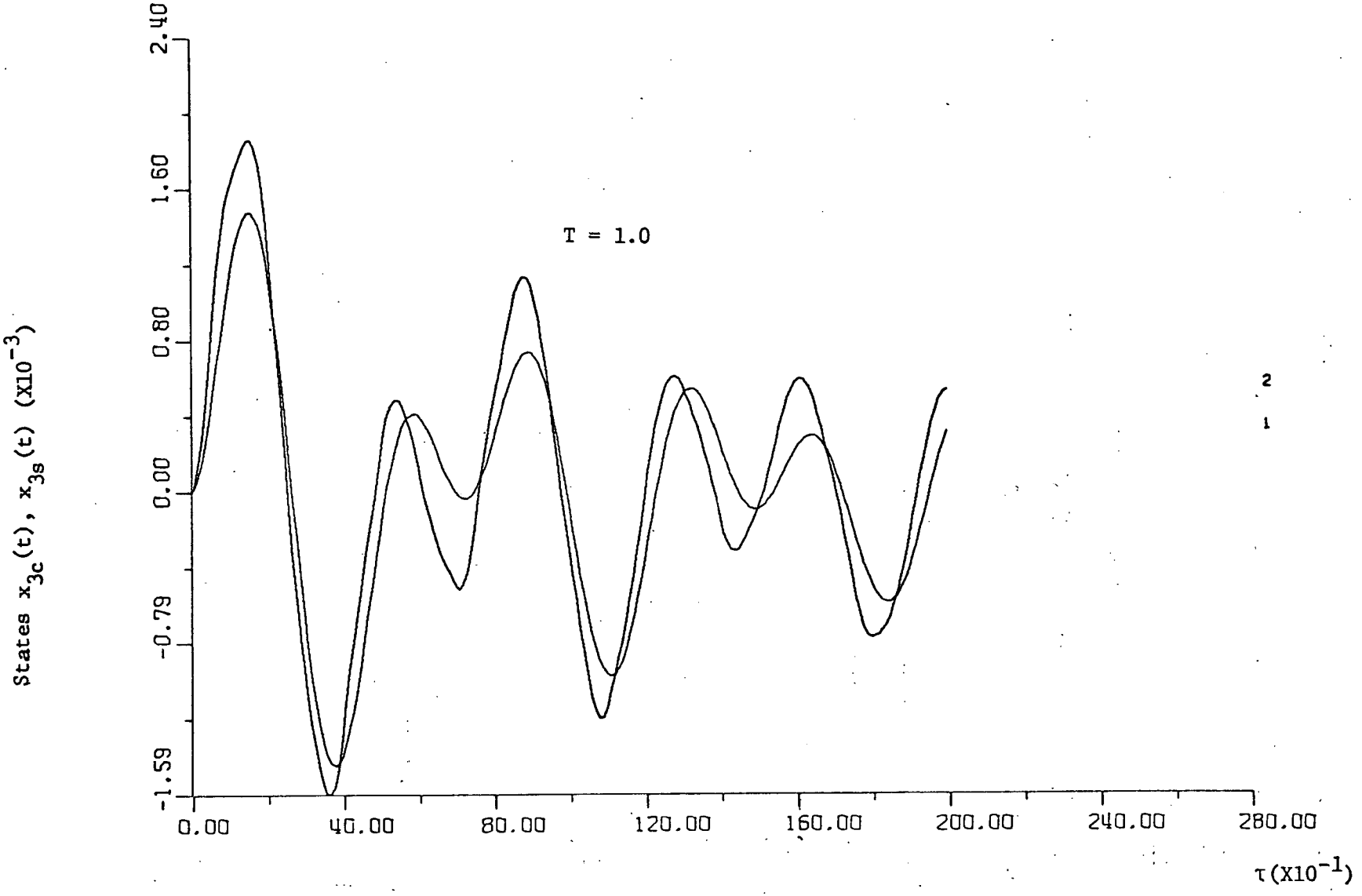

Figure 4-5 State trajectories $x_{3c}(t)$ and $x_{3s}(t)$ for the 6th order model of the Spinning Skylab Satellite. Digital redesign by the point by point method of partial matching.

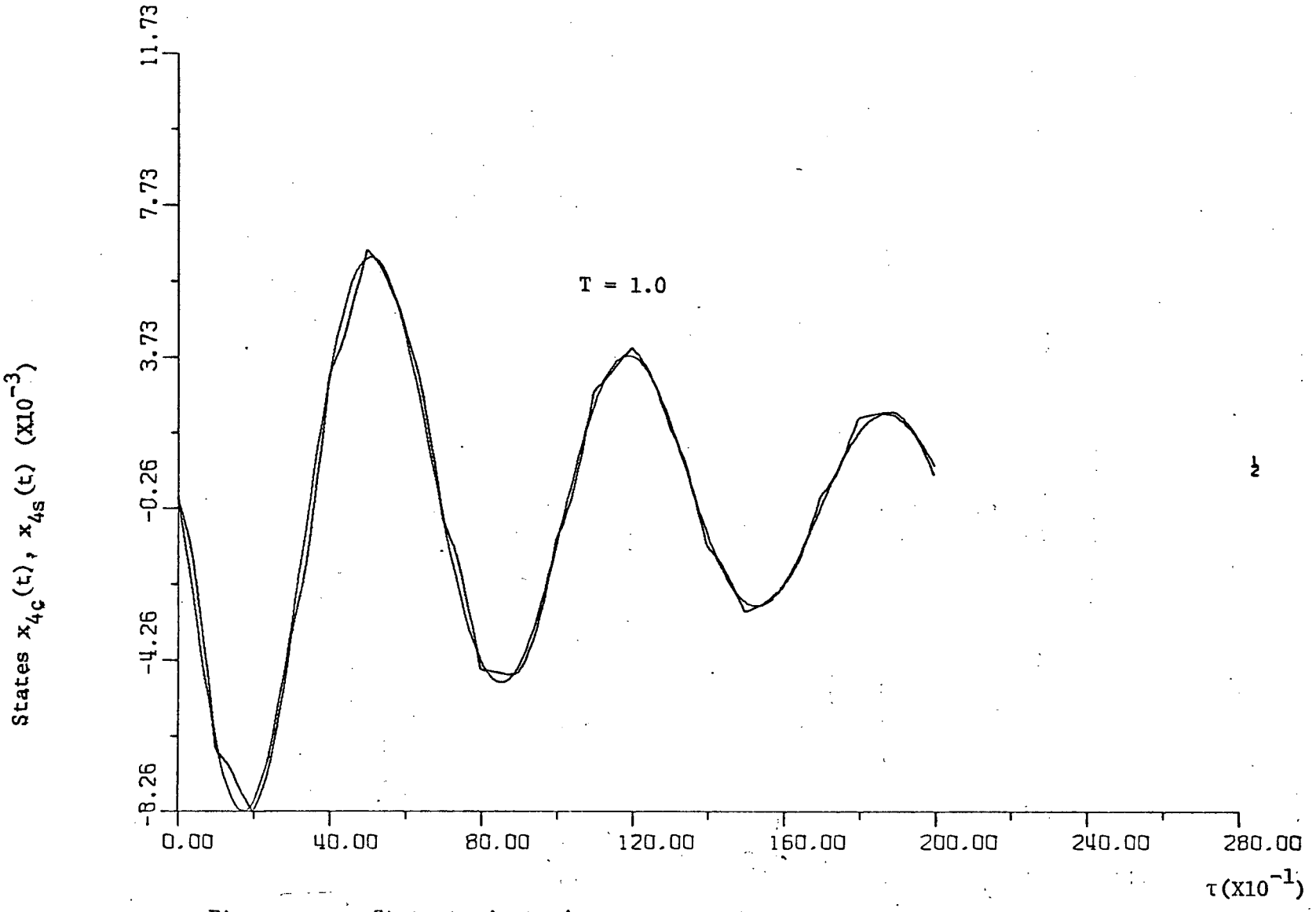

Figure 4-6 State trajectories $x_{4c}(t)$ and $x_{4s}(t)$ for the 6th order model of the Spinning Skylab Satellite. Digital redesign by the point by point method of partial matching.

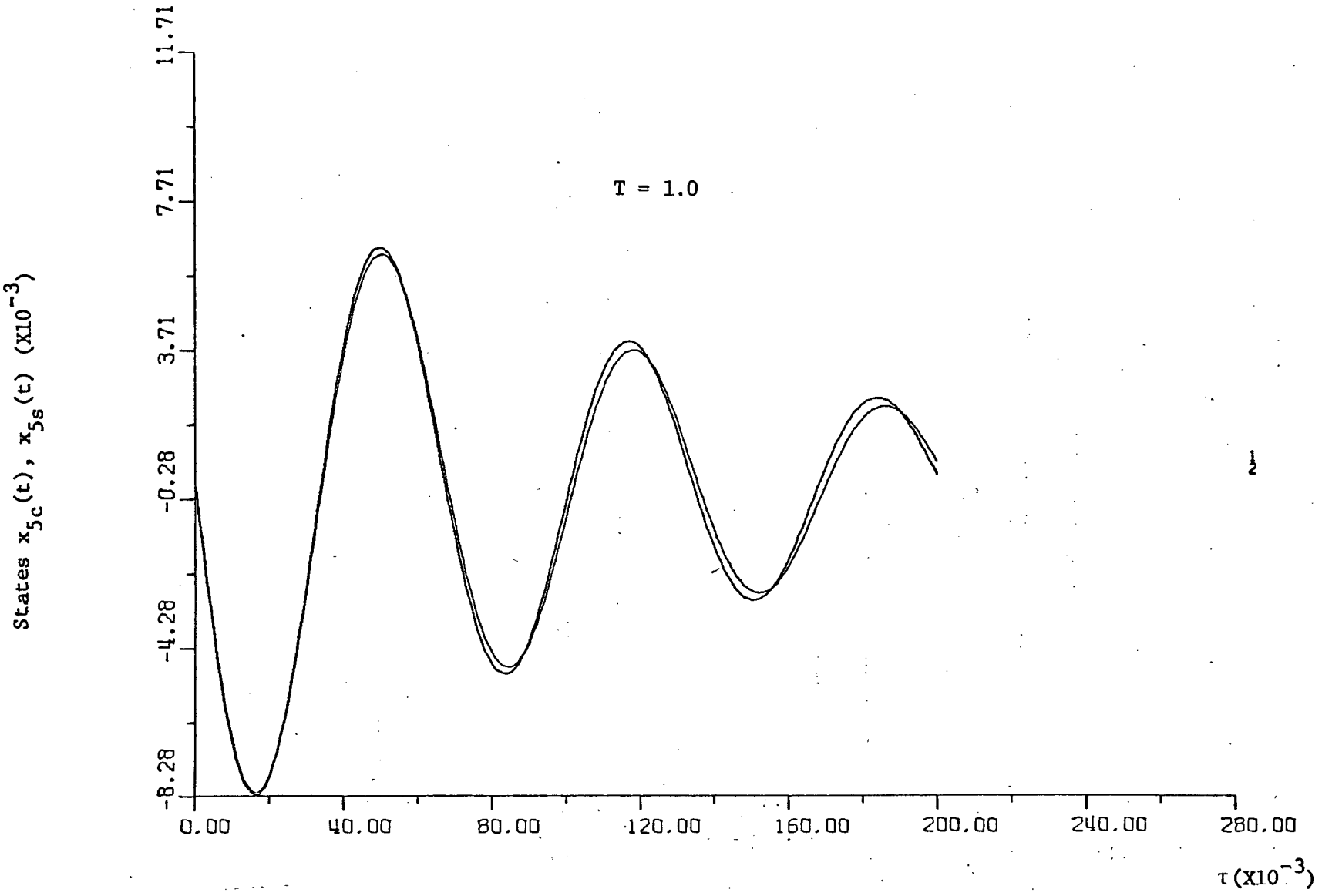

Fig. 4-7 State trajectories $x_{5c}(t)$ and $x_{5s}(t)$ for the 6th order model of the Spinning Skylab Satellite. Digital redesign by the point by point method of partial matching.

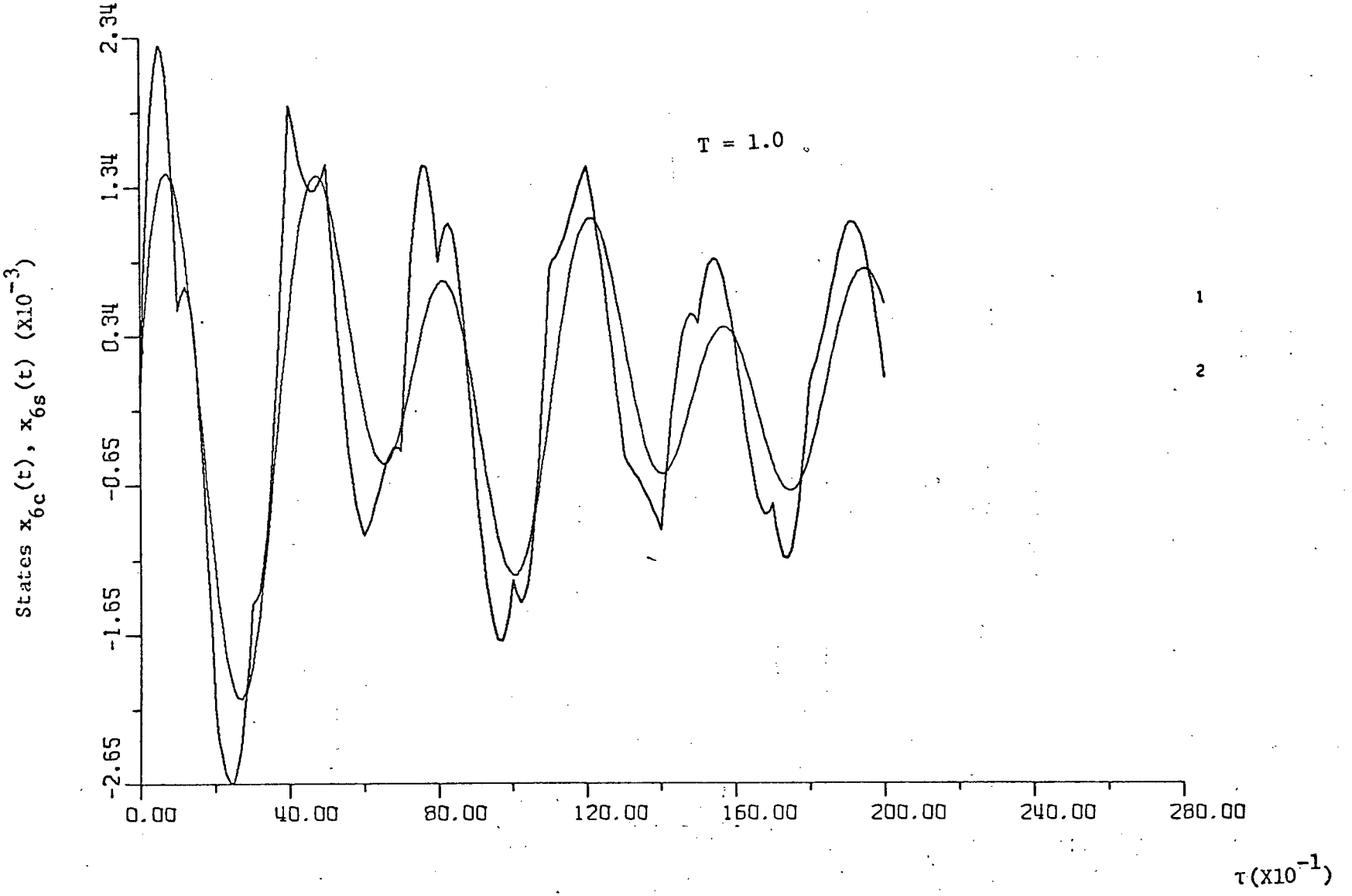

Figure 4-8 State trajectories $x_{6c}(t)$ and $x_{6s}(t)$ for the 6th order model of the Spinning Skylab Satellite. Digital redesign by the point by point method of partial matching.

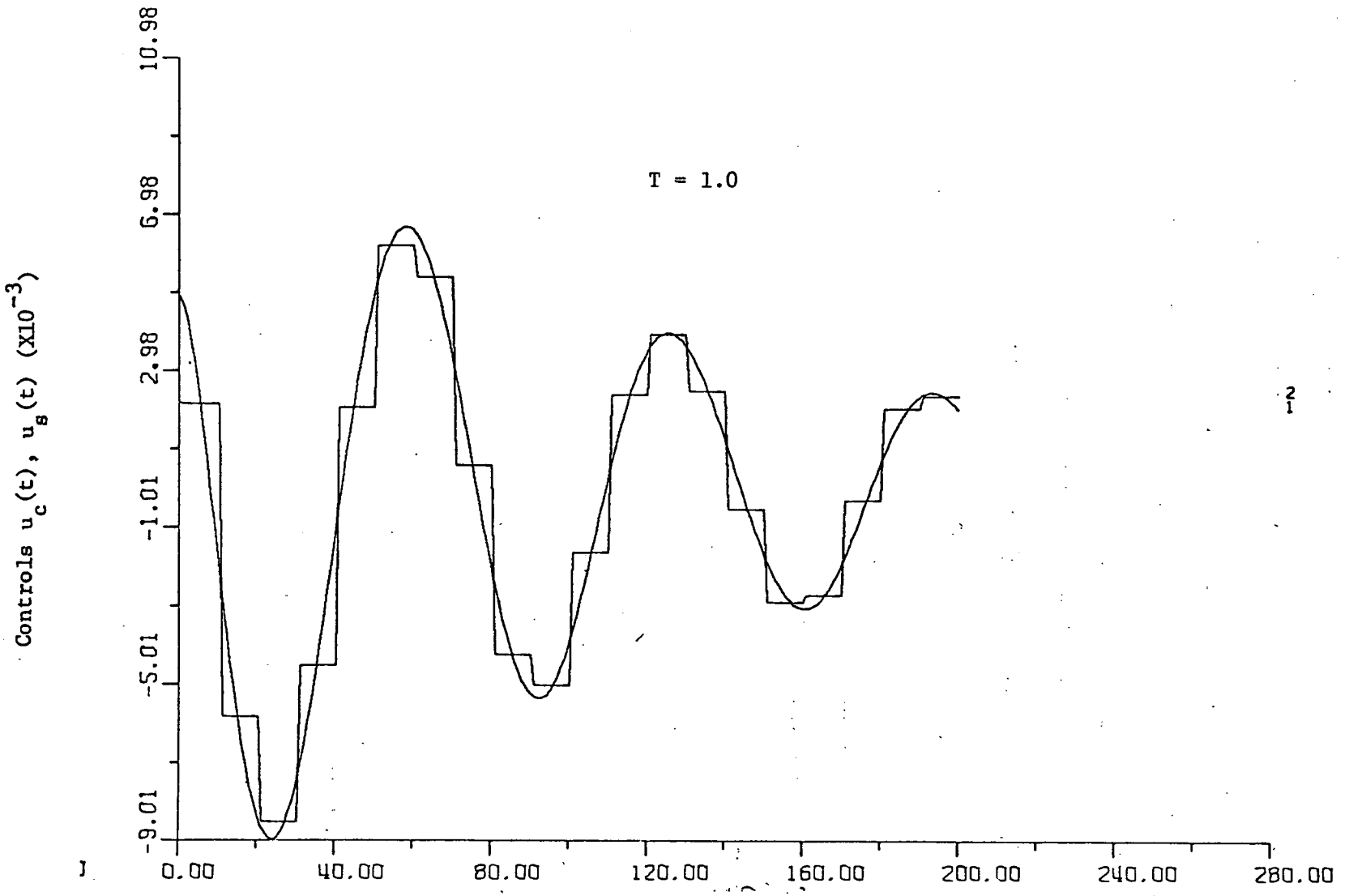

Figure 4-9 Control trajectories $u_c(t)$ and $u_s(t)$ for the 6th order model of the Spinning Skylab Satellite. Digital redesign by the point by point method of partial matchint.

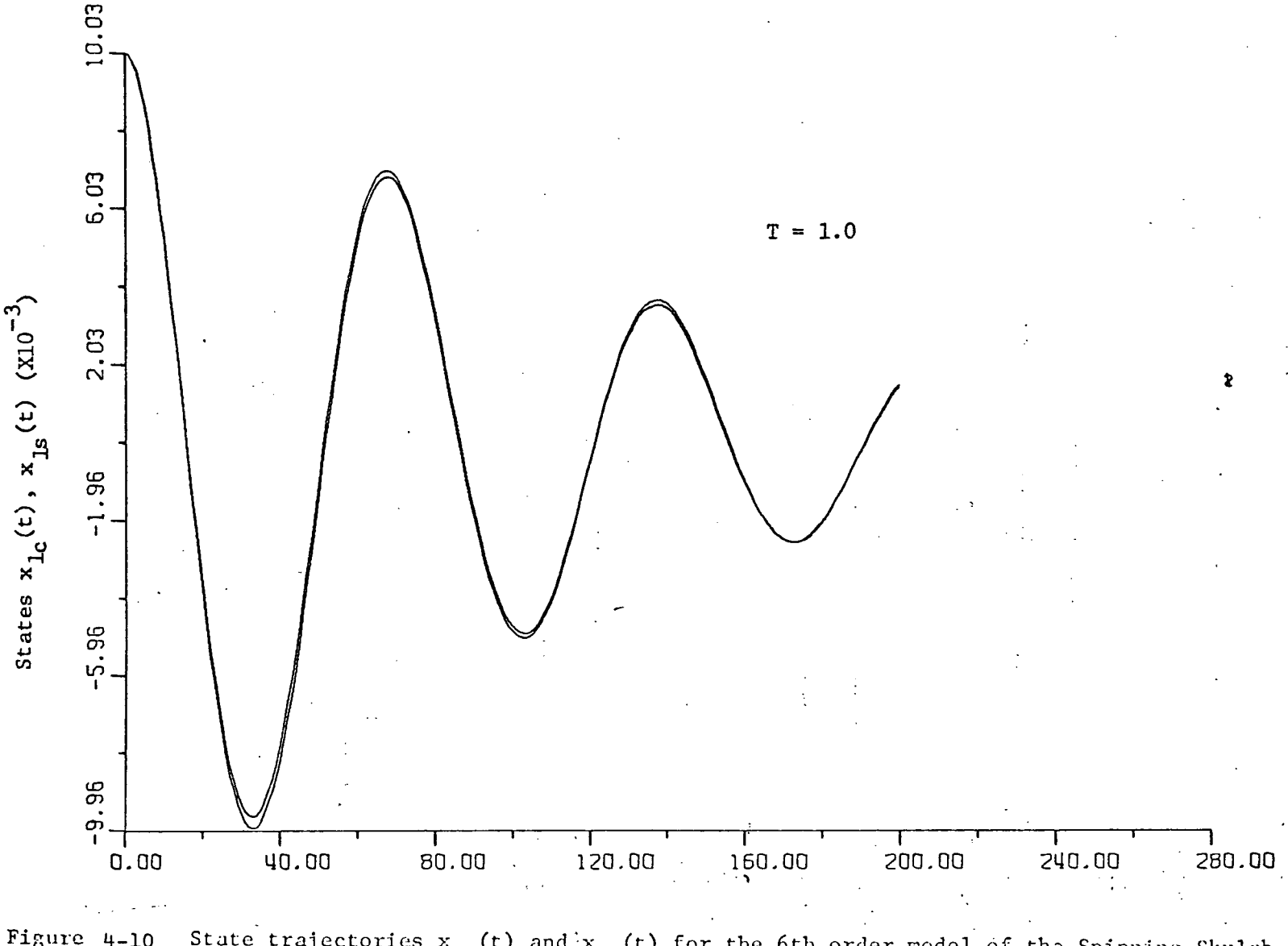

Figure 4-10 State trajectories $x_{lc}(t)$ and $x_{ls}(t)$ for the 6th order model of the Spinning Skylab Satellite. Digital redesign by the method of exact matching at multiple sampling periods.

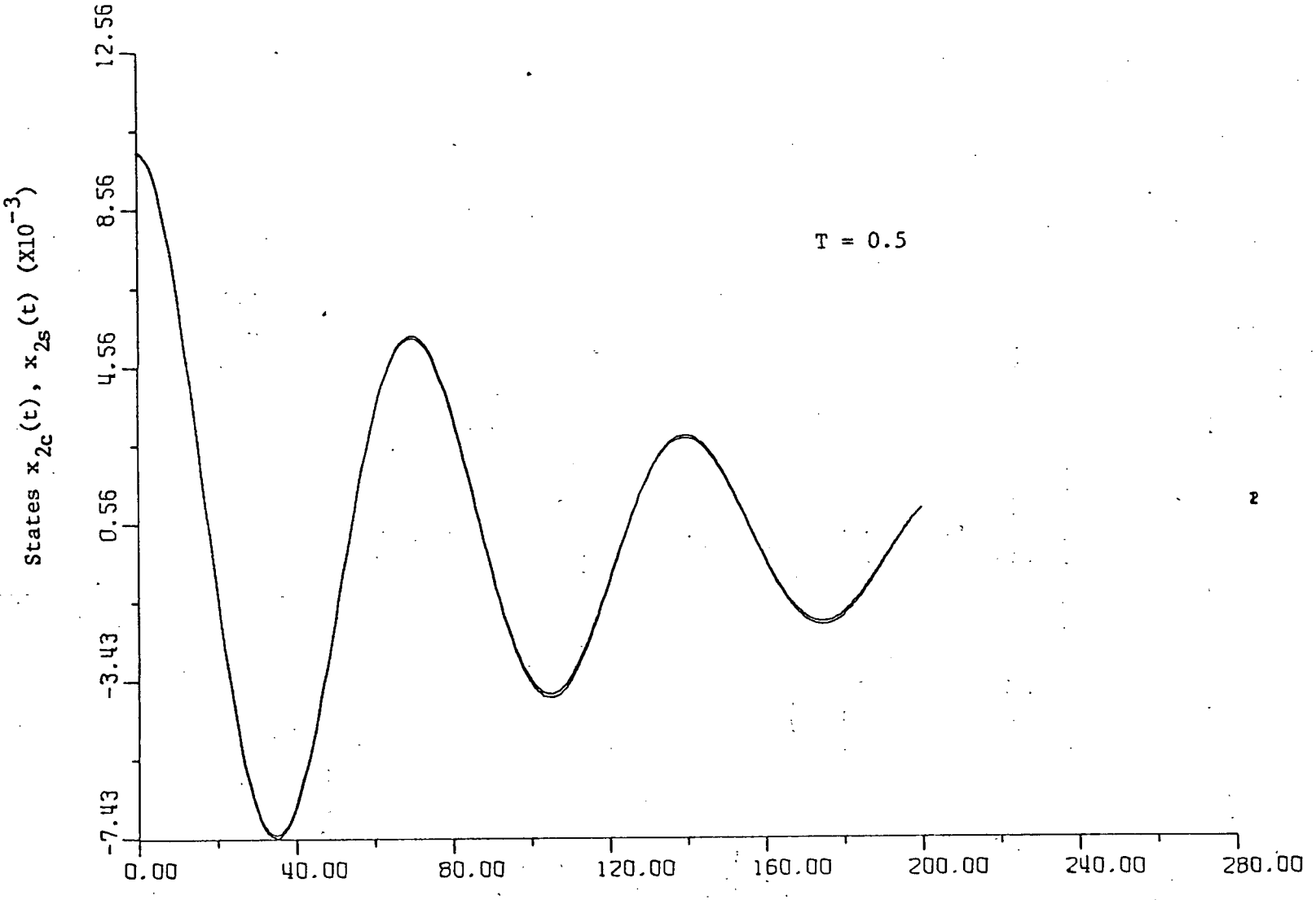

Figure 4-11 State trajectories $x_{2c}(t)$ and $x_{2s}(t)$ for the 6th order model of the Spinning Skylab Satellite. Digital redesign by the method of exact matching at multiple sampling periods.

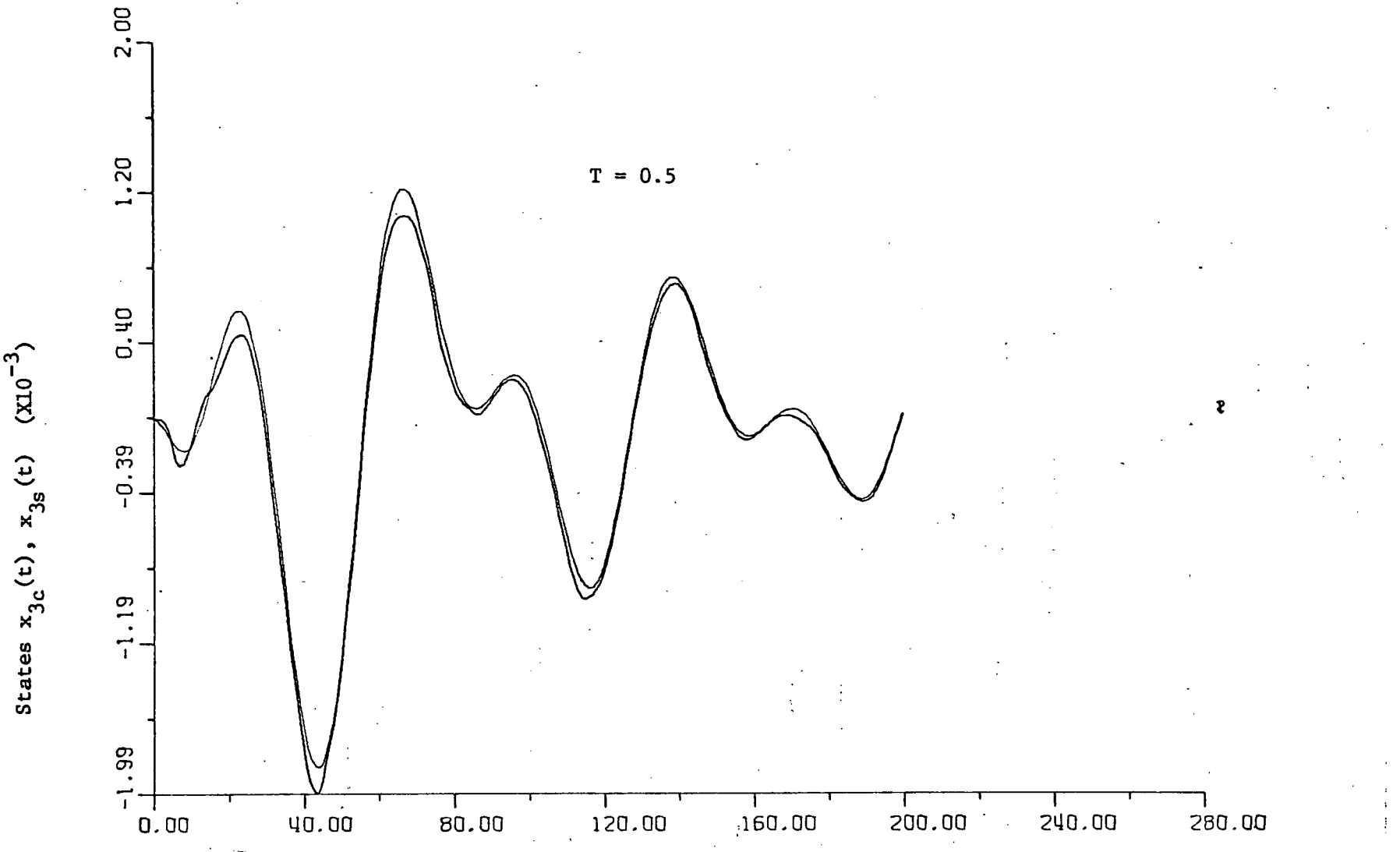

Figure 4-12 State trajectories $x_{3c}(t)$ and $x_{3s}(t)$ for the 6th order model of the Spinning Skylab Satellite. Digital redesign by the method of exact matching at multiple sampling periods.

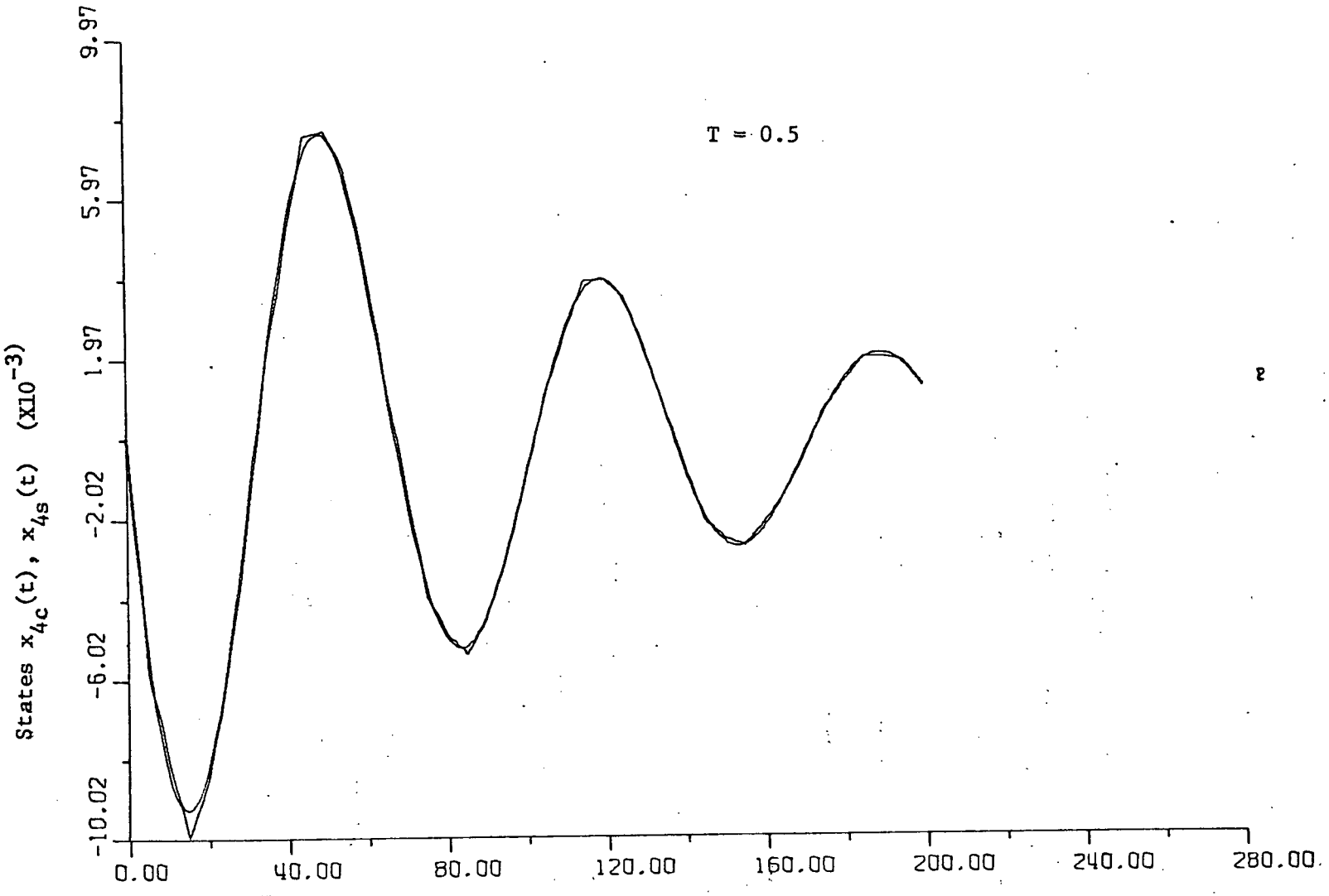

Figure 4-13 State trajectories $x_{4c}(t)$ and $x_{4s}(t)$ for the 6th order model of the Spinning Skylab Satellite. Digital redesign by the method of exact matching at multiple sampling periods.

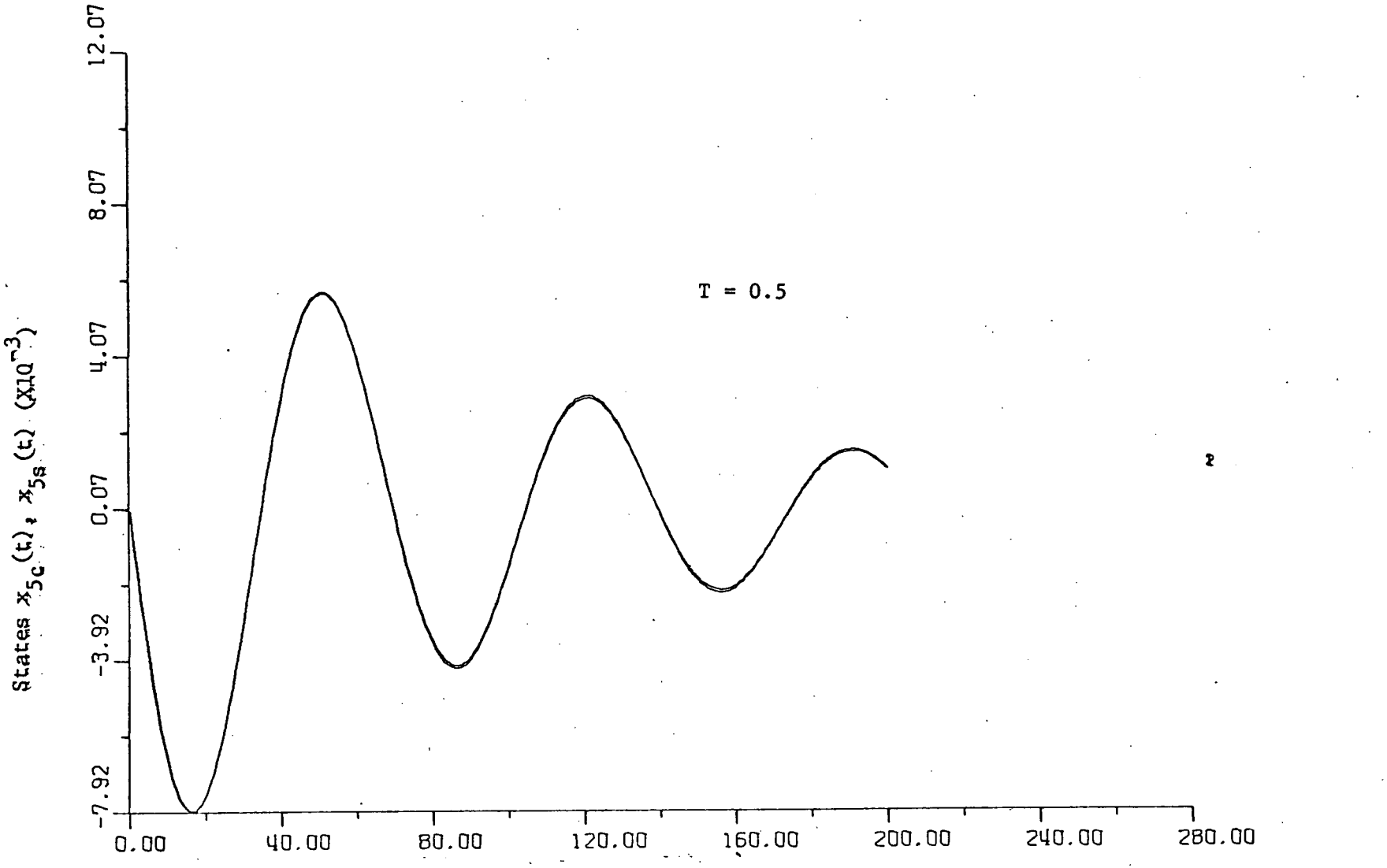

Figure 4-14. State trajectories $x_{5c}(t)$ and $x_{5s}(t)$ for the 6th order model of the Spinning Skylab Satellite. Digital redesign by the method of exact matching at multiple sampling periods.

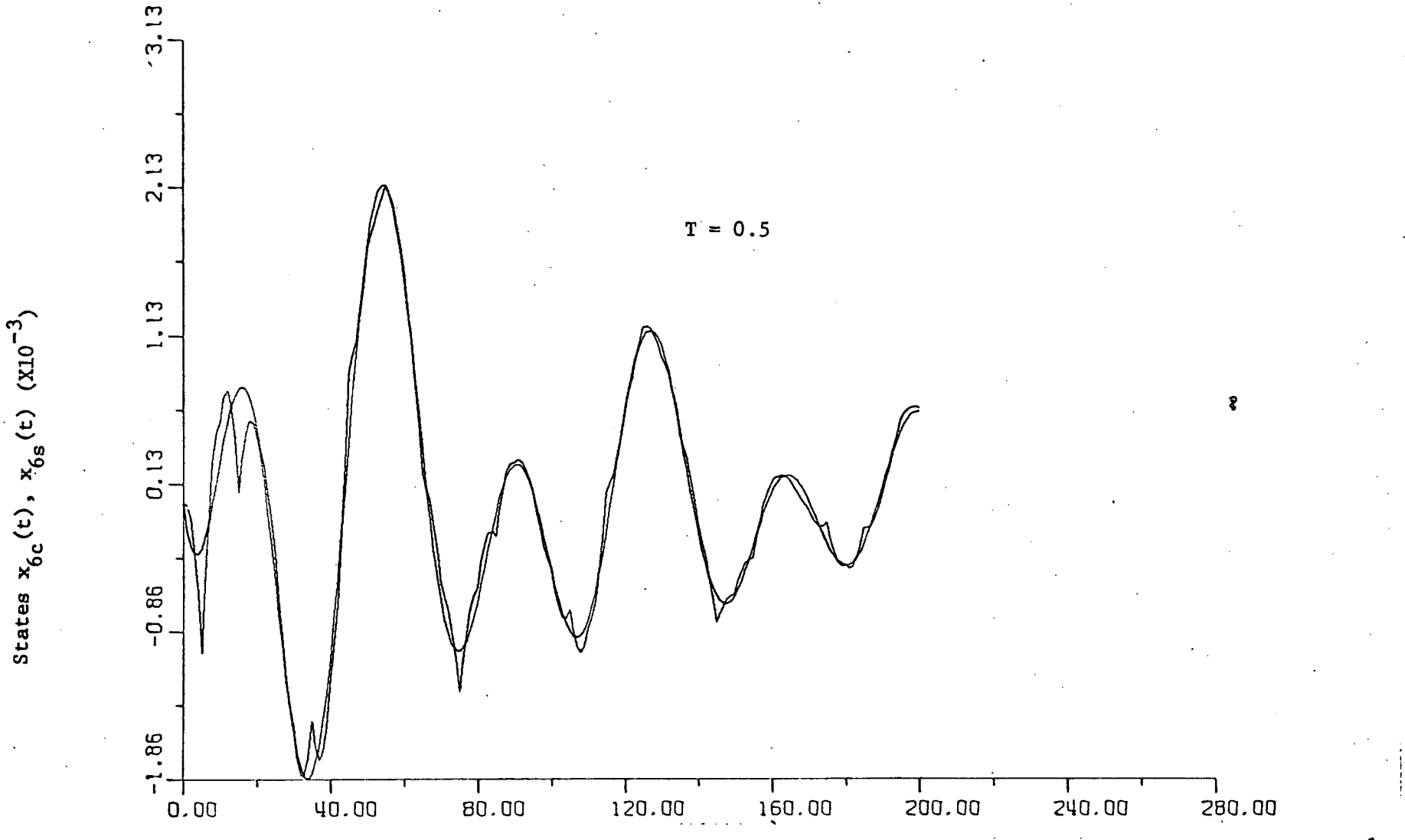

Figure 4-15 State trajectories $x_{6c}(t)$ and $x_{6s}(t)$ for the 6th order model of the Spinning Skylab Satellite. Digital redesign by the method of exact matching at multiple sampling periods.

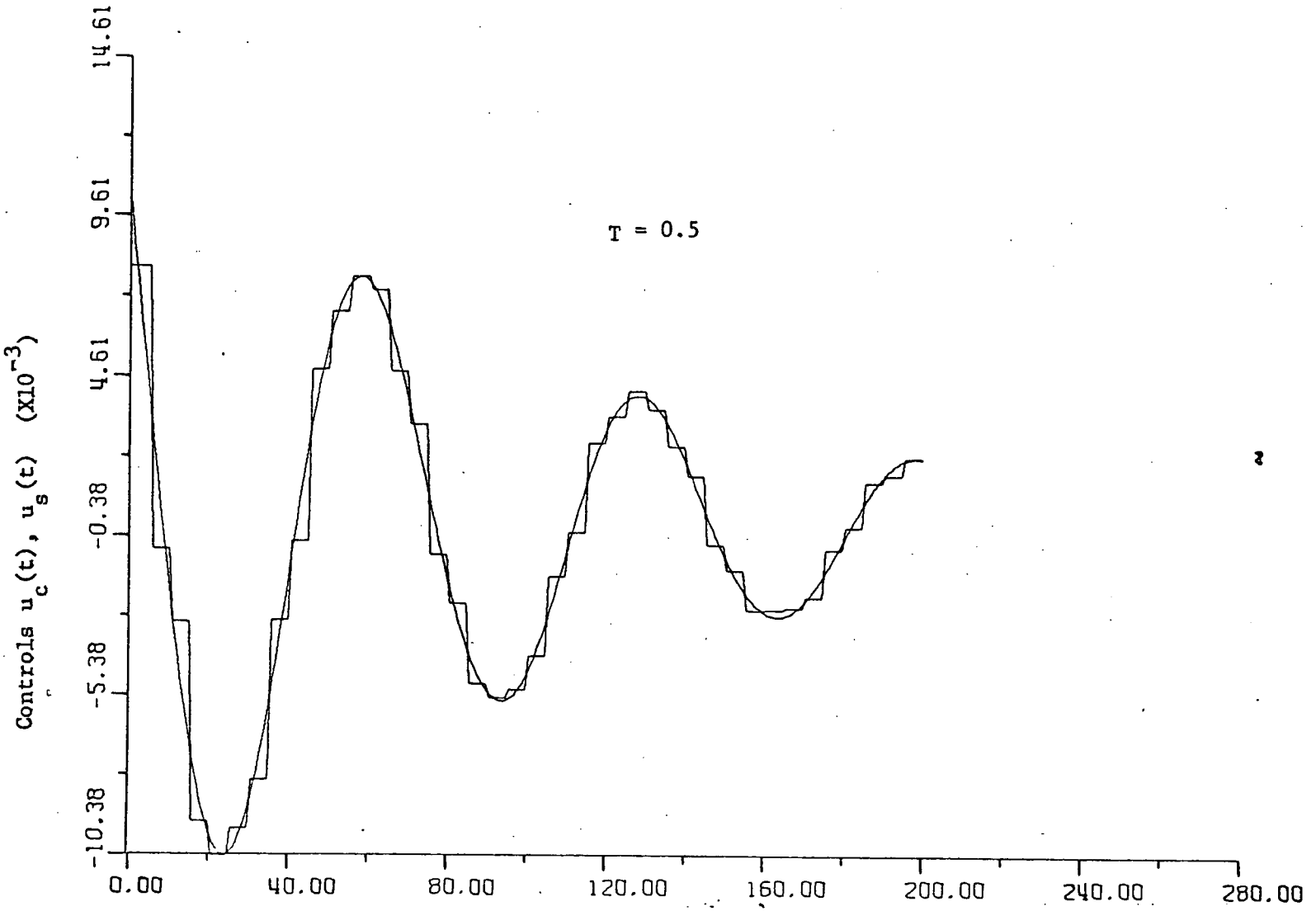

Figure 4-16 Control trajectories $u_c(t)$ and $u_s(t)$ for the 6th order model of the Spinning Skylab Satellite. Digital redesign by the method of exact matching at multiple sampling periods.

5. OPTIMAL REGULATION OF THE TWELFTH-ORDER SPINNING SKYLAB

5.1 Introduction

This report considers the calculation of the optimal feedback gains and simulations of the closed-loop system of the twelfth-order spinning skylab. The linear quadratic law (LQL) method is used for the optimal design of the skylab system.

It has been determined that the overall skylab system is uncontrollable with only one input to one of the wobble axes. An additional input to one of the spin axes has been found necessary to provide controllability of the system.

The optimal feedback gains have been obtained by feeding back eleven of the states, with two different weighting matrices for Q.

Simulation results are presented for the twelfth-order system using the optimal gains as obtained from the design of the sixth-order wobble dynamics, as well as using the optimal gains designed with the eleventh-order model. The eleventh-order model was used by deleting the state ϕ_3 which is the cummulative deviation of the position of the spin axis. Since it is of interest only to regulate $\dot{\phi}_3$ about its zero reference, the state ϕ_3 is not necessary in the optimal design.

5.2 Modeling of the Twelfth-Order Spinning Skylab

The dynamic equations of the spinning skylab space station are expressed in vector form:

$$\underline{M}\ddot{\underline{z}} + \underline{D}\dot{\underline{z}} + \underline{K}\underline{z} = -\underline{v} \tag{5-1}$$

where the dots represent derivatives with respect to $\tau = \Omega t$

$$\underline{z} = [\phi_1 \quad \phi_2 \quad \phi_3 \quad \mu_1 \quad \mu_2 \quad \mu_3]' \tag{5-2}$$

The control vector is given by

$$\underline{v} = [v_1 \quad v_2 \quad v_3 \quad v_4 \quad v_5 \quad v_6]'$$

$$= [\frac{T_1}{I_1\Omega^3} \quad \frac{T_2}{I_2\Omega^2} \quad 0 \quad \frac{T_3}{I_3\Omega^3} \quad 0 \quad 0]' \tag{5-3}$$

$$M = \begin{pmatrix} 1 & 0 & 0 & 0 & \xi\gamma_1 & -\gamma_1 \\ 0 & \frac{1+K_1}{1-K_2} & 0 & -\xi\gamma_1 & 0 & 0 \\ -\gamma_1 & 0 & 0 & 0 & 0 & \gamma_1 \\ 0 & 0 & 1 & \gamma_3 & 0 & 0 \\ 0 & -\xi & 1 & 1 & 0 & 0 \\ \xi & 0 & 0 & 0 & 1 & 0 \end{pmatrix} \qquad (5\text{-}4)$$

$$D = \begin{pmatrix} 0 & -(1+K_1) & 0 & 2\xi\gamma_1 & 0 & 0 \\ 1+K_1 & 0 & 0 & 0 & 2\xi\gamma_1 & 0 \\ 0 & 0 & 0 & 0 & 0 & \gamma_1\Delta_3 \\ 0 & 0 & 0 & 0 & -2\gamma_3 & 0 \\ -2\xi & 0 & 0 & \Delta_1 & -2 & 0 \\ 0 & -2\xi & 2 & 2 & \Delta_2 & 0 \end{pmatrix} \qquad (5\text{-}5)$$

$$K = \begin{pmatrix} -K_1 & 0 & 0 & 0 & -\xi\gamma_1 & -\gamma_1 \\ 0 & K_2\left(\frac{1+K_1}{1-K_2}\right) & 0 & \xi\gamma_1 & 0 & 0 \\ -\gamma_1 & 0 & 0 & 0 & 0 & \gamma_1(\sigma_3^2+1) \\ 0 & 0 & 0 & 0 & 0 & 0 \\ 0 & \xi & 0 & \sigma_1^2 & 0 & 0 \\ -\xi & 0 & 0 & 0 & \sigma_2^2-1 & 0 \end{pmatrix} \qquad (5\text{-}6)$$

We shall consider the wobble motion together with the spin velocity motion so that Eq. (5-1) represents a twelfth-order system.

In order to obtain the state equations of the overall system, a state diagram is constructed as shown in Figure (5-1) The state equations are determined from Figure(5-1)by use of Mason's gain formula. We have

$$\begin{pmatrix} \dot{\phi}_1 \\ \dot{\phi}_2 \\ \dot{\phi}_3 \\ \dot{\mu}_1 \\ \dot{\mu}_2 \\ \dot{\mu}_3 \\ \hline \ddot{\phi}_1 \\ \ddot{\phi}_2 \\ \ddot{\phi}_3 \\ \ddot{\mu}_1 \\ \ddot{\mu}_2 \\ \ddot{\mu}_3 \end{pmatrix} = \left(\begin{array}{cccccc|cccccc} 0 & 0 & \cdot & \cdot & \cdot & 0 & 1 & 0 & \cdot & \cdot & \cdot & 0 \\ 0 & 0 & \cdot & \cdot & \cdot & 0 & 0 & 1 & \cdot & \cdot & \cdot & 0 \\ \cdot & \cdot & \cdot & \cdot & \cdot & \cdot & \cdot & \cdot & \cdot & \cdot & \cdot & \cdot \\ \cdot & \cdot & \cdot & \cdot & \cdot & \cdot & \cdot & \cdot & \cdot & \cdot & \cdot & \cdot \\ 0 & 0 & \cdot & \cdot & \cdot & 0 & 0 & 0 & \cdot & \cdot & 1 & 0 \\ 0 & 0 & \cdot & \cdot & \cdot & 0 & 0 & 0 & \cdot & \cdot & \cdot & 1 \\ \hline & & & & & & & & & & & \\ & & & -M^{-1}K & & & & & -M^{-1}D & & & \\ & & & & & & & & & & & \end{array}\right) \begin{pmatrix} \phi_1 \\ \phi_2 \\ \phi_3 \\ \mu_1 \\ \mu_2 \\ \mu_3 \\ \hline \dot{\phi}_1 \\ \dot{\phi}_2 \\ \dot{\phi}_3 \\ \dot{\mu}_1 \\ \dot{\mu}_2 \\ \dot{\mu}_3 \end{pmatrix} + \begin{pmatrix} 0 \\ 0 \\ 0 \\ 0 \\ 0 \\ 0 \\ \hline -d_1 \\ 0 \\ 0 \\ 0 \\ \xi d_1 \\ -d_1 \end{pmatrix} v_1 \tag{5-7}$$

where

$$M^{-1} = \begin{bmatrix} d_1 & 0 & d_1 & 0 & 0 & -\xi\gamma_1 d_1 \\ 0 & (1-\gamma_3)cd_2 & 0 & -\xi\gamma_1 cd_2 & \xi\gamma_1 d_2 c & 0 \\ 0 & -\gamma_3\xi cd_2 & 0 & (1-\xi^2\gamma_1 c)d_2 & -\gamma_3 d_2 & 0 \\ 0 & \xi cd_2 & 0 & -d_2 & d_2 & 0 \\ -\xi d_1 & 0 & -\xi d_1 & 0 & 0 & (1-\gamma_1)d_1 \\ d_1 & 0 & (\frac{1}{\gamma_1} - \xi^2)d_1 & 0 & 0 & -\xi\gamma_1 d_1 \end{bmatrix} \quad (5\text{-}8)$$

$$M^{-1}K = \begin{bmatrix} a_{71} & a_{72} & a_{73} & a_{74} & a_{75} & a_{76} \\ a_{81} & a_{82} & a_{83} & a_{84} & a_{85} & a_{86} \\ a_{91} & a_{92} & a_{93} & a_{94} & a_{95} & a_{96} \\ a_{10,1} & a_{10,2} & a_{10,3} & a_{10,4} & a_{10,5} & a_{10,6} \\ a_{11,1} & a_{11,2} & a_{11,3} & a_{11,4} & a_{11,5} & a_{11,6} \\ a_{12,1} & a_{12,2} & a_{12,3} & a_{12,4} & a_{12,5} & a_{12,6} \end{bmatrix} \quad (5\text{-}9)$$

$$M^{-1}D = \begin{bmatrix} a_{77} & a_{78} & a_{79} & a_{7,10} & a_{7,11} & a_{7,12} \\ a_{87} & a_{88} & a_{89} & a_{8,10} & a_{8,11} & a_{8,12} \\ a_{97} & a_{98} & a_{99} & a_{9,10} & a_{9,11} & a_{9,12} \\ a_{10,7} & a_{10,8} & a_{10,9} & a_{10,10} & a_{10,11} & a_{10,12} \\ a_{11,7} & a_{11,8} & a_{11,9} & a_{11,10} & a_{11,11} & a_{11,12} \\ a_{12,7} & a_{12,8} & a_{12,9} & a_{12,10} & a_{12,11} & a_{12,12} \end{bmatrix} \quad (5\text{-}10)$$

$$d_1 = \frac{1}{1 - \gamma_1(1 + \xi^2)} \tag{5-11}$$

$$d_2 = \frac{1}{1 - \gamma_3 - \xi^2\gamma_1 c} \tag{5-12}$$

$$c = (1 - K_2)/(1 + K_1) \tag{5-13}$$

$$a_{71} = -K_1 d_1 - \gamma_1 d_1 + \xi^2 \gamma_1 d_1$$

$$a_{72} = 0$$

$$a_{73} = 0$$

$$a_{74} = 0$$

$$a_{75} = -\xi\gamma_1 d_1 \sigma_2^2$$

$$a_{76} = \gamma_1 d_1 \sigma_3^2$$

$$a_{81} = 0$$

$$a_{82} = (1 - \gamma_3) K_2 d_2 + \xi^2 \gamma_1 d_2 c$$

$$a_{83} = 0$$

$$a_{84} = (1 - \gamma_3) c\xi\gamma_1 d_2 + \xi\gamma_1 d_2 c\sigma_1^2$$

$$a_{85} = 0$$

$$a_{86} = 0$$

$$a_{91} = 0$$

$$a_{92} = -\gamma_3 \xi K_2 d_2 - \xi\gamma_3 d_2$$

$$a_{93} = 0$$

$$a_{94} = -\xi^2 \gamma_1 \gamma_3 c d_2 - \gamma_3 d_2 \sigma_1^2$$

$$a_{95} = 0$$

$$a_{96} = 0$$

$$a_{10,1} = 0$$

$$a_{10,2} = \xi K_2 d_2 + \xi d_2$$

$$a_{10,3} = 0$$

$$a_{10,4} = \xi^2 \gamma_1 c d_2 + d_2 \sigma_1^2$$

$$a_{10,5} = 0$$

$$a_{10,6} = 0$$

$$a_{11,1} = K_1 \xi d_1 + \gamma_1 \xi d_1 - (1 - \gamma_1)\xi d_1$$

$$a_{11,2} = 0$$

$$a_{11,3} = 0$$

$$a_{11,4} = 0$$

$$a_{11,5} = \xi^2 \gamma_1 d_1 + (\sigma_2^2 - 1)(1 - \gamma_1) d_1$$

$$a_{11,6} = -\xi \gamma_1 d_1 \sigma_3^2$$

$$a_{12,1} = -K_1 d_1 - (1 - \xi^2 \gamma_1) d_1 + \xi^2 \gamma_1 d_1$$

$$a_{12,2} = 0$$

$$a_{12,3} = 0$$

$$a_{12,4} = 0$$

$$a_{12,5} = -\xi \gamma_1 d_1 \sigma_2^2$$

$$a_{12,6} = -\gamma_1 d_1 + (1 - \xi^2 \gamma_1)(\sigma_3^2 + 1) d_1$$

$$a_{77} = 0$$

$$a_{78} = -(1 + K_1)d_1 + 2\xi^2\gamma_1 d_1$$

$$a_{79} = -2\xi\gamma_1 d_1$$

$$a_{7,10} = 0$$

$$a_{7,11} = -\xi\gamma_1 d_1 \Delta_2$$

$$a_{7,12} = \gamma_1 \Delta_3 d_1$$

$$a_{87} = (1 + K_1)(1 - \gamma_3)cd_2 - 2\xi^2\gamma_1 d_2 c$$

$$a_{88} = 0$$

$$a_{89} = 0$$

$$a_{8,10} = \xi\gamma_1 d_2 c\Delta_1$$

$$a_{8,11} = 0$$

$$a_{8,12} = 0$$

$$a_{97} = 2\xi\gamma_3 d_2 - (1 + K_1)\gamma_3 \xi c d_2$$

$$a_{98} = 0$$

$$a_{99} = 0$$

$$a_{9,10} = -\gamma_3 d_2 \Delta_1$$

$$a_{9,11} = 0$$

$$a_{9,12} = 0$$

$$a_{10,7} = (1 + K_1)\xi c d_2 - 2\xi d_2$$

$$a_{10,8} = 0$$

$$a_{10,9} = 0$$

$$a_{10,10} = \Delta_1 d_2$$

$$a_{10,11} = -2$$

$$a_{10,12} = 0$$

$$a_{11,7} = 0$$

$$a_{11,8} = (1 + K_1)\xi d_1 - 2\xi(1 - \gamma_1)d_1$$

$$a_{11,9} = 2(1 - \gamma_1)d_1$$

$$a_{11,10} = 2(1 - \gamma_1)d_1 - 2\xi^2\gamma_1 d_1$$

$$a_{11,11} = (1 - \gamma_1)d_1\Delta_2$$

$$a_{11,12} = -\xi d_1\gamma_1\Delta_3$$

$$a_{12,7} = 0$$

$$a_{12,8} = 2\xi^2\gamma_1 d_1 - (1 + K_1)d_1$$

$$a_{12,9} = -2\xi\gamma_1 d_1$$

$$a_{12,10} = 0$$

$$a_{12,11} = -\xi\gamma_1 d_1\Delta_2$$

$$a_{12,12} = (1 - \gamma_1\xi^2)d_1\Delta_3$$

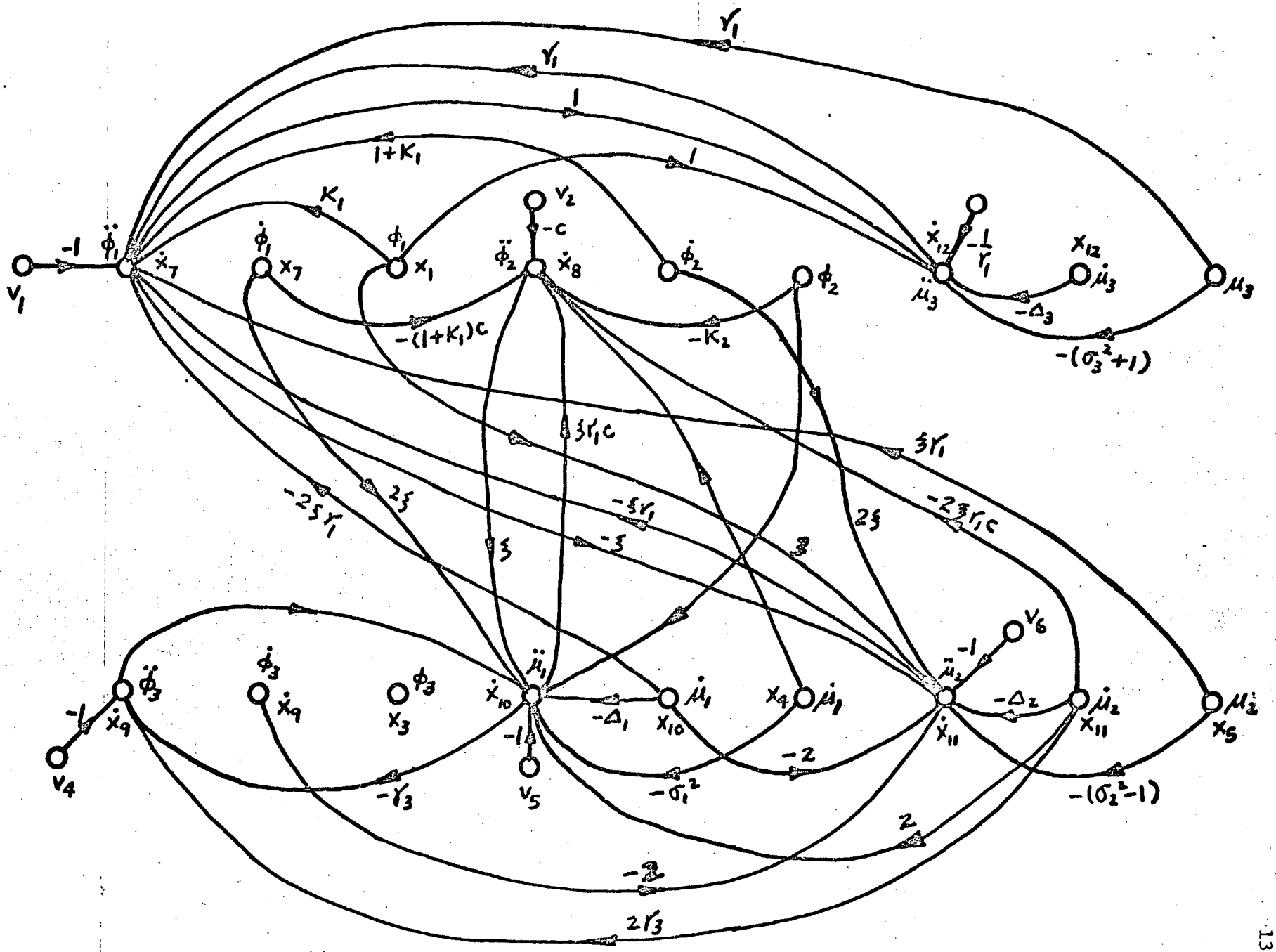

Figure 5-1 State diagram of the 12th-order skylab.

5.3 Controllability of the Skylab System

Given a linear time-invariant system

$$\dot{\underline{x}} = A\underline{x} + B\underline{u} \tag{5-14}$$

where $\underline{x}$ is n-dimensional, and $\underline{u}$ is m-dimensional. A common method of checking the controllability of the system is to see if the following rank condition is satisfied:

$$\text{Rank } [B \quad AB \quad A^2B \quad \ldots \quad A^{n-1}B] = n \tag{5-15}$$

For the skylab system with one input, $V_1 = T_1/I_1\Omega^2$, the above matrix is square and thus the rank condition can be checked by calculating the determinant of the matrix. Using the numerical values of the system parameters given in Chapter 4, section 4.2 of this report, the determinant of the matrix of Eq. (5-15) is found to be 4.46×10^{18}. Therefore, it would appear that the system is completely controllable. However, due to the numerical difficulties encountered in calculating the Riccati gains as well as in shifting the closed-loop eigenvalues, it was decided to perform an alternate check on the controllability of the system. An alternate test on the controllability can be made by performing the similarity transformation

$$\underline{x} = P\underline{y} \tag{5-16}$$

on Eq. (5-14) where P is an n x n nonsingular matrix. The new system of state equations are written

$$\dot{\underline{y}} = \Lambda\underline{y} + \Gamma\underline{u} \tag{5-17}$$

where

$$\Lambda = P^{-1}AP \tag{5-18}$$

and

$$\Gamma = P^{-1}B \tag{5-19}$$

For A with r pairs of distinct complex eigenvalues and n - 2r distinct real eigenvalues, Λ is written

$$\Lambda = \text{diag.}\ [S_1 \quad S_2 \quad \ldots S_r \quad \lambda_{2r+1} \ldots \lambda_n] \tag{5-20}$$

where

$$S_i = \begin{pmatrix} \sigma_i & \omega_i \\ -\omega_i & \sigma_i \end{pmatrix} \tag{5-21}$$

with $\sigma_i \pm j\omega_i$, i = 1, 2, ... r, denoting the ith-pair of complex eigenvalues; and λ_i, i = 2r+1, ..., n denotes the n-2r real eigenvalues.

For complete controllability, the rows of Γ which correspond to the distinct real eigenvalues must not contain all zeros, and at least one of the two rows which corresponds to the rows of S_i for i = 1, 2, ..., r, does not contain all zeros.

For the eleventh-order system, the eigenvalues of A are given in Table 5-1.

The Γ matrix which corresponds to the same order as these eigenvalues is obtained as

$$\Gamma = \begin{pmatrix} -8.16 \times 10^{-2} \\ 1.67 \times 10^{-3} \\ -9.32 \times 10^{-1} \\ 2.99 \times 10^{-2} \\ -1.32 \times 10^{-3} \\ 9.0 \times 10^{-2} \\ -1.76 \times 10^{-1} \\ 1.54 \times 10^{-10} \\ 1.97 \times 10^{-3} \\ -3.19 \\ -2.79 \times 10^{-16} \end{pmatrix} \qquad (5\text{-}22)$$

Since the last element of Γ is practically zero, the system is uncontrollable. In fact, the state which corresponds to the eigenvalue at the origin, $s = 0$, is the uncontrollable one. This explains the difficulty in attempting to move this eigenvalue into the left-half plane. This alternate controllability test also shows the interesting fact that in practice, when there are very large and very small parameter values in a large-scale system, the controllability check using Eq. (5-15) may be unreliable, due to the repeated products of very large and very small numbers.

When the control $V_4 = T_3/I_3\Omega^2$ is used in addition to the control V_1, carrying out the similarity transformation, we have

$$\Gamma = \begin{bmatrix} -8.2 \times 10^{-2} & -1.2 \times 10^{-4} \\ 1.7 \times 10^{-3} & -7 \times 10^{-5} \\ -9.3 \times 10^{-1} & 1.2 \times 10^{-3} \\ 3 \times 10^{-2} & 3 \times 10^{-2} \\ -1.3 \times 10^{-3} & 1.03 \\ 9.0 \times 10^{-2} & -2 \times 10^{-2} \\ -1.8 \times 10^{-1} & -2.9 \times 10^{-10} \\ 1.5 \times 10^{-10} & 3.6 \times 10^{-9} \\ 1.9 \times 10^{-3} & 1.6 \times 10^{-2} \\ -3.2 & 1.2 \times 10^{-4} \\ -2.8 \times 10^{-16} & 9.9 \times 10^{-1} \end{bmatrix} \quad (5\text{-}23)$$

Now since all the elements of the last row of Γ are not zero, and not all rows which correspond to the complex eigenvalues are zero, the system is completely controllable.

5.4 The Eigenvector Method of Calculating Riccati Gains

Consider the matrix quadratic equation.

$$-KA - A'K + KSK - Q = 0 \tag{5-24}$$

where the coefficient matrices A, S, and Q are given n x n matrices. The solution K is also an n x n matrix.

It will be shown later that (5-24) possesses many solutions one of which is positive definite, one negative definite and the rest indefinite. We will be concerned with the positive definite solution which is denoted by K^+.

Let us form the 2n x 2n matrix

$$M = \begin{pmatrix} -A & -Q \\ -S & A' \end{pmatrix} \tag{5-25}$$

and denote the 2n eigenvalues of M by λ_i, i = 1, ... 2n and the 2n eigenvectors of M by a_i, i = 1.... 2n. Partitioning the eigenvectors we have

$$a_i = \begin{pmatrix} b_i \\ \hline c_i \end{pmatrix} \tag{5-26}$$

where a_i is a 2n vector, b_i is an n vector and c_i is an n vector.

The following properties which are proven in [5] form the basis for the computation of K.

i) If λ_i is an eigenvalue of M, there is an eigenvalue λ_j of M such that

$$\lambda_j = -\lambda_i^* \quad i,j = 1,2,\ldots,2n \tag{5-27}$$

where the asterik denotes complex conjugate.

ii) M has no purely imaginary eigenvalues.

iii) If the coefficient matrices A, S and Q are real, eigenvalues off of the real axis appear in conjugate pairs

$$\lambda_i = \lambda_j^*$$

The eigenvectors corresponding to the above eigenvalues also appear in conjugate pairs.

$$a_i = a_j^*$$

iv) The n eigenvalues of M with negative real parts correspond to the eigenvalues of $(A - SK^+)$.

v) If $a_1, a_2, \ldots, a_n$ are the eigenvectors corresponding to the n eigenvalues with negative real parts, then

$$K^+ = [b_1\ b_2\ \ldots\ b_n]\ [c_1\ c_2\ \ldots\ c_n]^{-1} \qquad (5\text{-}28)$$

vi) Every solution of $F(K) = 0$ is the form

$$K + [b_1\ b_2\ \ldots\ b_n][c_1\ c_2\ \ldots\ c_n]^{-1} \qquad (5\text{-}29)$$

If the inverse exists, where the eigenvectors correspond to any n eigenvalues of M.

vii) Any linear combinations of the vectors $b_1, b_2, \ldots, b_n$ can be used in (5-28) and (5-29) without affecting the result if the same linear transformation is applied to the vectors $c_1, c_2, \ldots, c_n$.

The computer algorithm then consists of the following steps:

i) Form the M matrix from A, S, and Q.

ii) Calculate the eigenvalues and eigenvectors of M. A University of Illinois subroutine using the QR iteration technique is used for this calculation.

iii) Using a sifting routine separate out the n eigenvectors of M corresponding to the eigenvalues with negative real parts. Form a real 2n x n matrix, D, from these eigenvectors. For complex pairs one column of D consists of the real part of the eigenvector and one column consists of the imaginary part.

iv) Separate the D matrix into two n x n matrices, B and C, as shown in (5-26)

v) The solution is given as

$$K^{+} = BC^{-1} \tag{5-30}$$

Note that the eigenvectors a_i either appear as purely real or in conjugate pairs. Therefore it is always possible to take linear combinations of a_i to form the real matrix D. To see this let E be the 2n x n matrix consisting of the n eigenvectors of M corresponding to eigenvalues with negative real parts. Let the n x n matrix G be the complex linear transformation on E which results in the matrix D.

$$EG = D = \begin{pmatrix} B \\ --- \\ C \end{pmatrix}$$

For example let the first column of E be a real eigenvector and the next two columns consist of a complex pair of eigenvectors. The G matrix would then be of the form

$$G = \begin{pmatrix} 1 & 0 & 0 & \cdots \\ 0 & \frac{1}{2} & \frac{1}{2}j & \cdots \\ 0 & \frac{1}{2} & -\frac{1}{2}j & \\ \cdot & & & \\ \cdot & & & \\ \cdot & & & \end{pmatrix}$$

If we partition E into two n x n matrices E_1 and E_2 it can be seen that the final solution, K^{+}, does not depend on the transformation G.

$$EG = \begin{pmatrix} E_1 \\ --- \\ E_2 \end{pmatrix} \qquad G = \begin{pmatrix} E_1 & G \\ ----- \\ E_2 & G \end{pmatrix} = \begin{pmatrix} B \\ --- \\ C \end{pmatrix}$$

$$K^{+} = BC^{-1} = E_1 G (E_2 G)^{-1} = E_1 E_2^{-1}$$

5.5 Numerical Results

The eigenvalues of the uncontrolled eleventh order open loop system are shown in Table 5-1 Note here that in all cases the coupling parameter between the spin and wobble dynamics in nonzero $\Gamma_3 = 1.56$. By investigating the eigenvectors associated with these eigenvalues, it can be seen that major contributions of the zero eigenvalue is to the state $\dot{\phi}_3$. Therefore the use of a control law which cannot shift this zero eigenvalue will result in a steady state error in $\dot{\phi}_3$.

The eigenvalues of the eleventh order closed loop system using control law 2 given in Chapter 4, Eq. (4-16) are shown in Table 5-1. Since this is a linear quadratic control law for the regulation of the wobble dynamics of the Spinning Skylab, it might be expected that it will not adequately control the spin dynamics. This is indicated in Table 5-1 by the continued presence of the zero eigenvalue. By examining the eigenvectors corresponding to the closed loop eigenvalues we may again see that the major contribution of the zero eigenvalue is to the state $\dot{\phi}_3$.

Since it is shown in the last section that the zero eigenvalue mode is uncontrollable from the input V_1, the additional input V_4 is used when calculating the optimal Riccati gains for the eleventh order system. The Riccati gains are calculated for the following two cases of weighting matrices:

Case 1 $R = I$, $Q = I$

Case 2 $R = I$, $Q = \text{diagonal}\,[10 \quad 10 \quad 1 \quad 1 \quad 1 \quad 10 \quad 10 \quad 1 \quad 1 \quad 1 \quad 1]$

The feedback gains for these two cases are shown in Table 5-2 The closed loop eigenvalues for case 1 and case 2 are shown in Table 5-1 In both cases the zero eigenvalue has been shifted into the left half plane resulting in an asymptotically stable eleventh order system.

THE EIGENVALUES OF THE OPEN AND CLOSED LOOP SYSTEMS			
Open Loop A Matrix	Control Law 2 (LQL design of wobble dynamics)	Case 1	Case 2
-0.603 ± j30.15	-.604 ± j30.15	-0.604 ± j30.15	-0.604 ± j30.15
-.0328 ± j1.76	-.048 ± j1.68	-0.369 ± j1.56	-0.159 ± j1.64
-.0276 ± j1.36	-.0277 ± j1.36	-0.52 ± j1.24	-0.516 ± j1.24
0.0 ± j1.0	-.078 ± j0.92	-0.080 ± j0.938	-0.077 ± j0.92
-.00056 ± j0.29	-2.53	-0.974 ± j0.653	-3.82
0.0	-0.611	-1.01	-1.06
	0.0		-1.01

Table 5-1 The eigenvalues of the open and closed loop for the eleventh order skylab.

States	CASE 1		CASE 2	
	Control V_1	Control V_4	Control V_1	Control V_4
1	-.0513	-.043	-2.67	-.0054
2	.030	-.053	2.15	-.09
3	-.009	.930	.041	.930
4	-.094	-1.82	.077	-1.83
5	-1.29	.052	-1.28	.0254
6	-1.78	-.016	-4.4	-.0176
7	.828	-.058	3.27	.175
8	.023	-1.0	-.001	-1.0
9	.034	.918	.015	0.919
10	.0021	.0043	.0338	.0043
11	-.46	.0082	.155	.01

Table5-2 The optimal Feedback Gains for the eleventh order Skylab.

5.6 Simulation

The 12th order model for the Spinning Skylab is simulated with the following two feedback gains

a.

$$G_c = \begin{bmatrix} -.051 & .03 & 0 & -.009 & -.094 & -1.29 & -1.78 & .828 & .023 & .034 & .002 & -.46 \\ -.043 & -.053 & 0 & .930 & -1.82 & .052 & -.016 & -.058 & -1.0 & .918 & .004 & .008 \end{bmatrix}$$

This gain is obtained by solving the Riccati equation for the eleventh order system with two control inputs and with the weighting matrices Q = [I] and R = [I], (see Case 1 in Table 5-2).

b.

$$G_c = [-1.263 \quad .777 \quad 0 \quad 0 \quad 0 \quad .172 \quad -2.78 \quad 1.792 \quad 0 \quad 0 \quad 0 \quad .095]$$

This gain is obtained by applying the linear quadratic law (LQL) method to the 6th order wobble dynamics of the Spinning Skylab.

In both simulations the initial states are

$$\underline{x}(0) = [.01 \quad .01 \quad 0 \quad 0 \quad 0 \quad 0 \quad 0 \quad 0 \quad .01 \quad 0 \quad 0 \quad 0]'$$

Figures 5-2 through 5-9 show the state and control trajectories for case a and Figures 5-10 through 5-17 show the state trajectories for case b.

As can be seen from the simulation results, in case a all the states are regulated about the zero reference except x_3 which undergoes a constant shift in its steady state magnitude. In case b all states, except x_3 and x_9, are regulated about the zero reference; x_9 undergoes a constant shift in its steady state magnitude and x_3 continually increases.

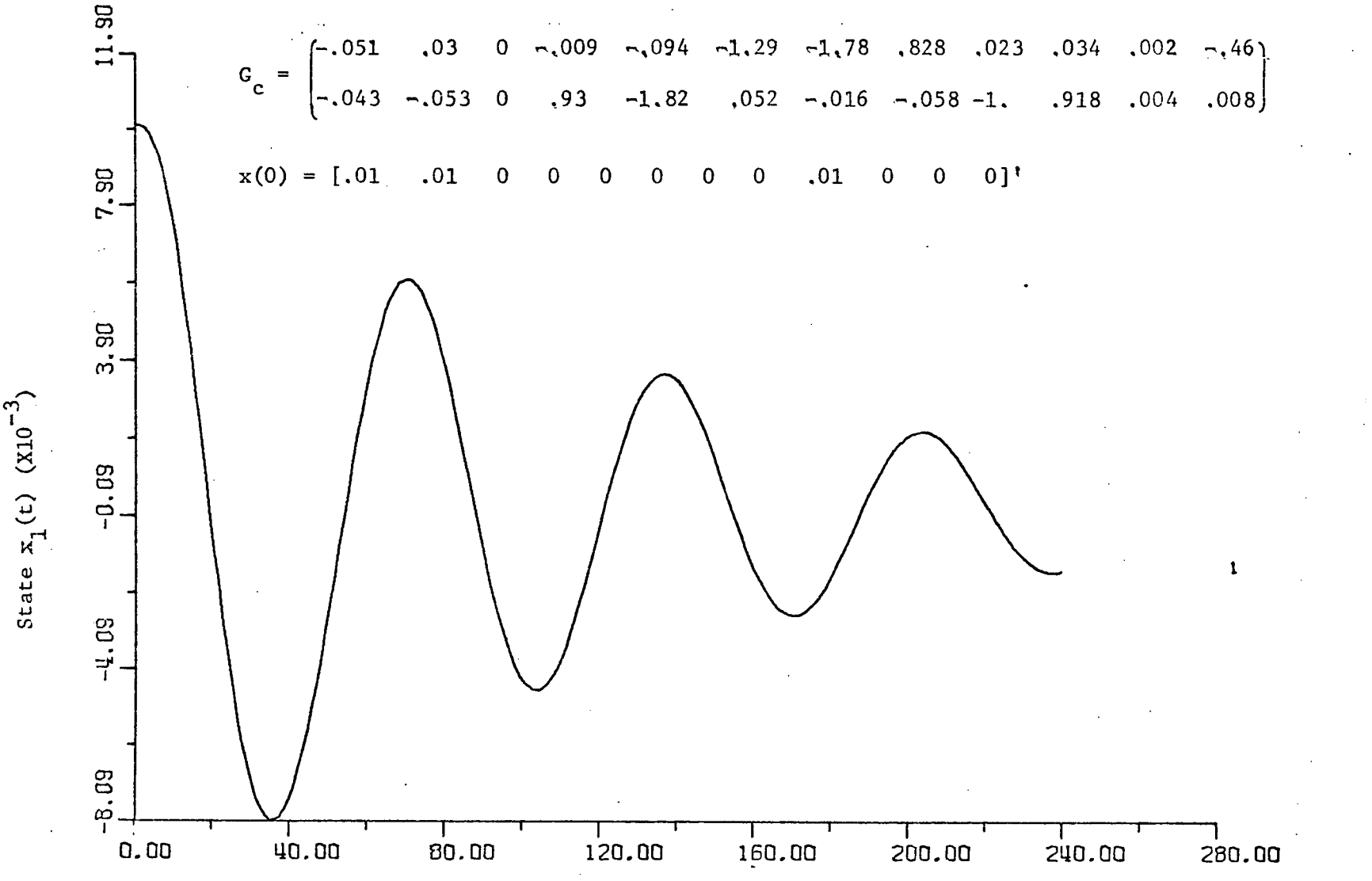

Figure 5-2 State trajectory $x_1(t)$ of the 12th order model for the Spinning Skylab Satellite.

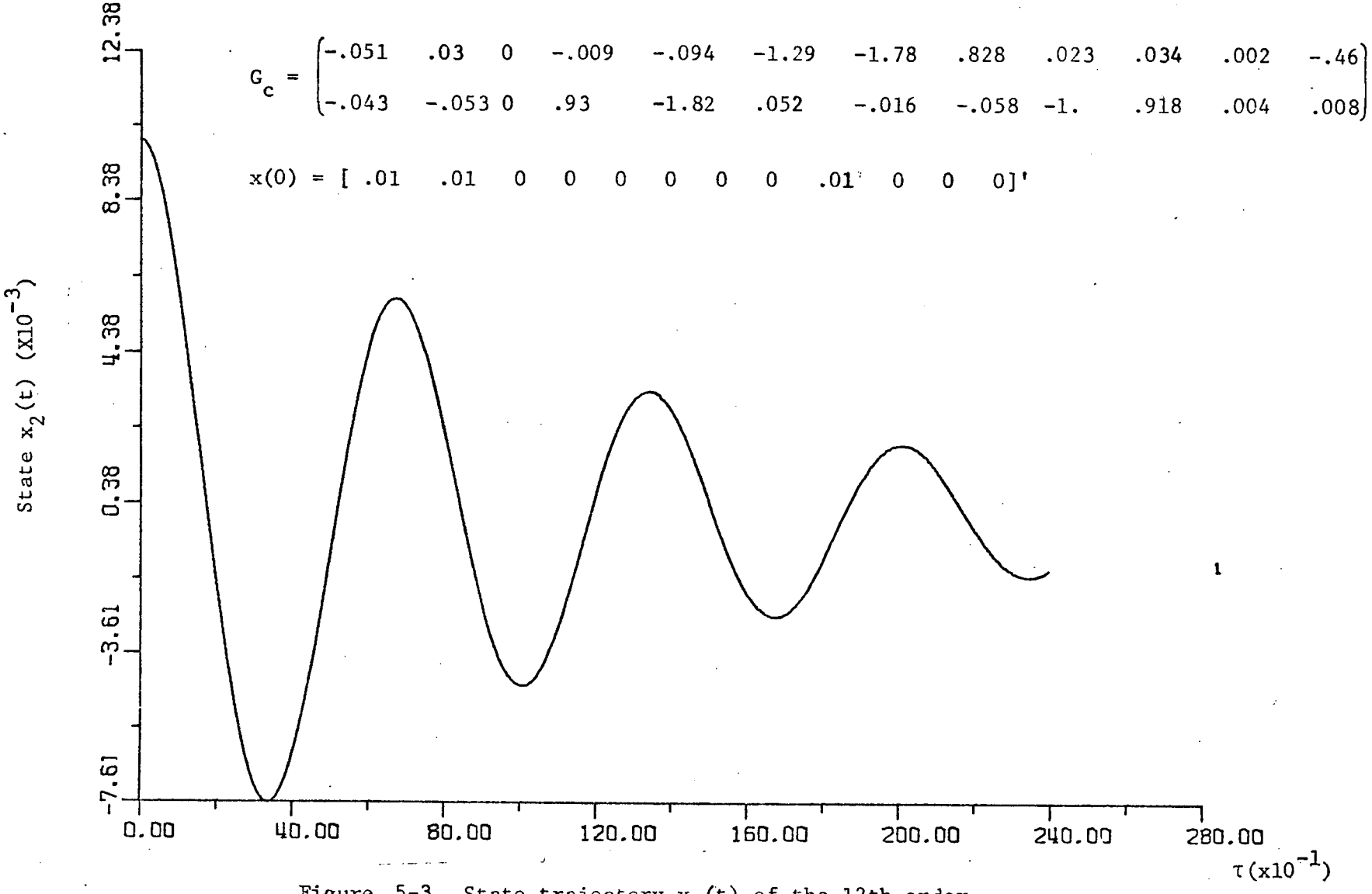

Figure 5-3 State trajectory $x_2(t)$ of the 12th order model for the Spinning Skylab Satellite.

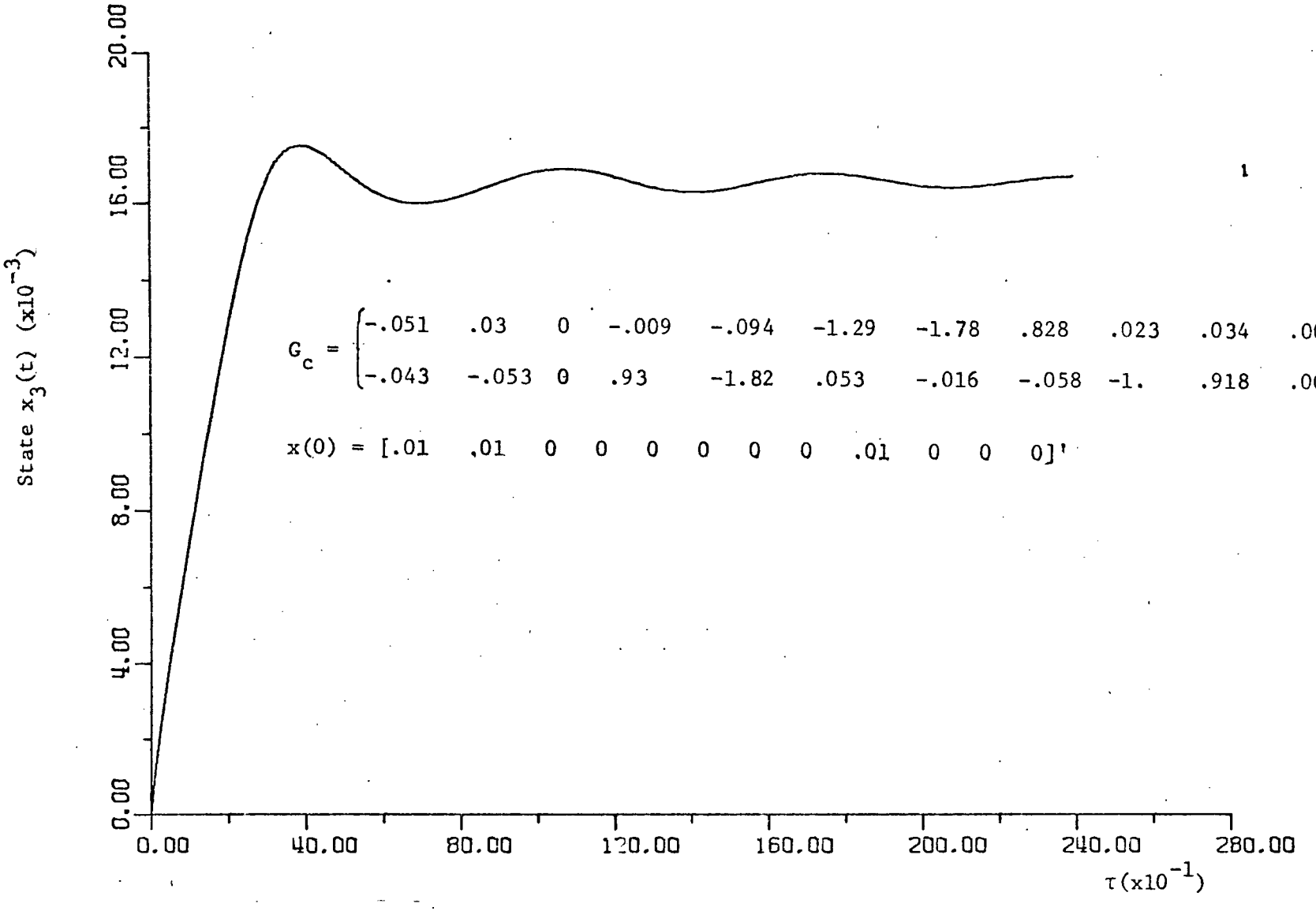

Figure 5-4 State trajectory $x_3(t)$ of the 12th order model for Spinning Skylab Satellite

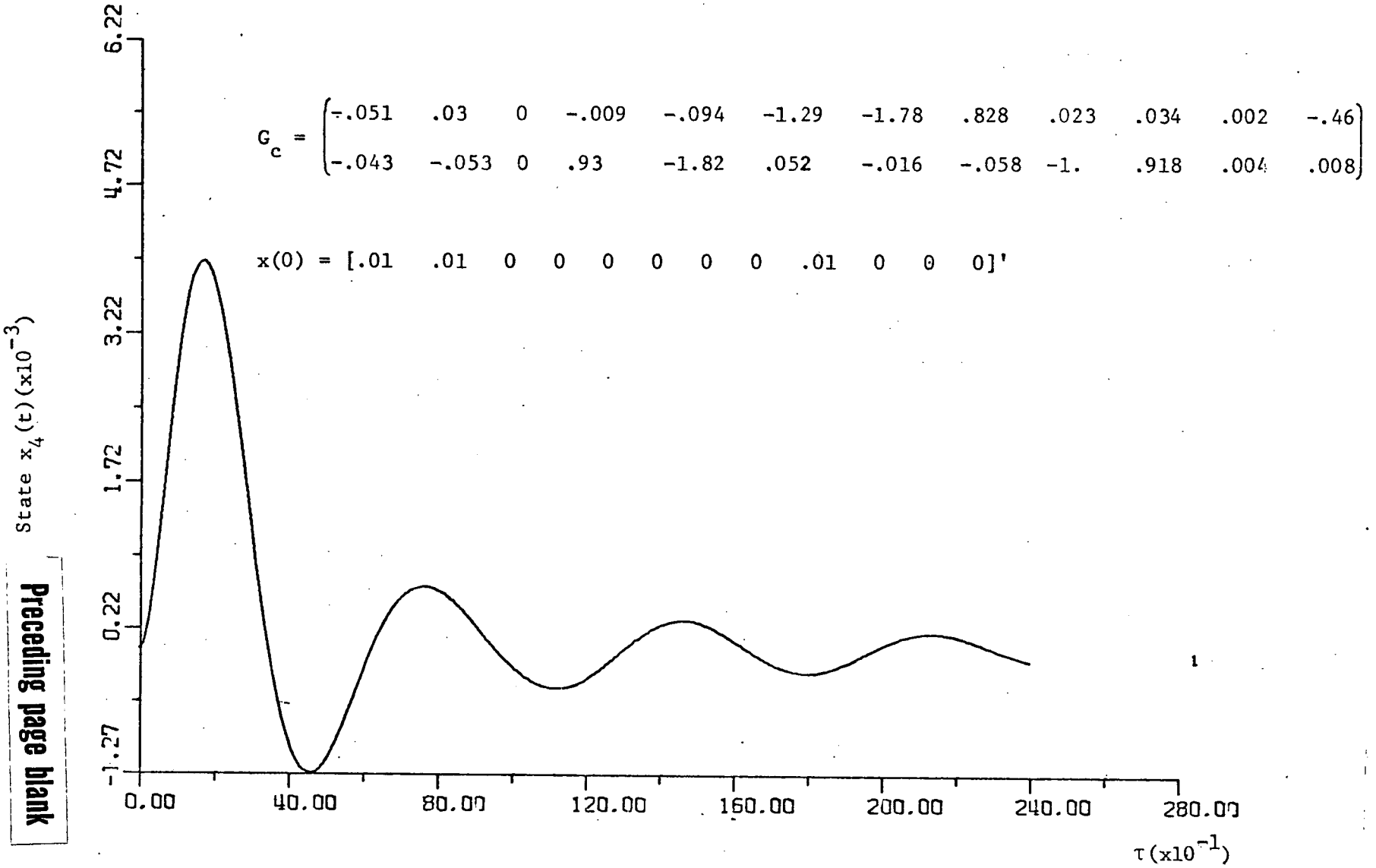

Figure 5-5 State trajectory $x_4(t)$ of the 12th order model for the Spinning Skylab Satellite.

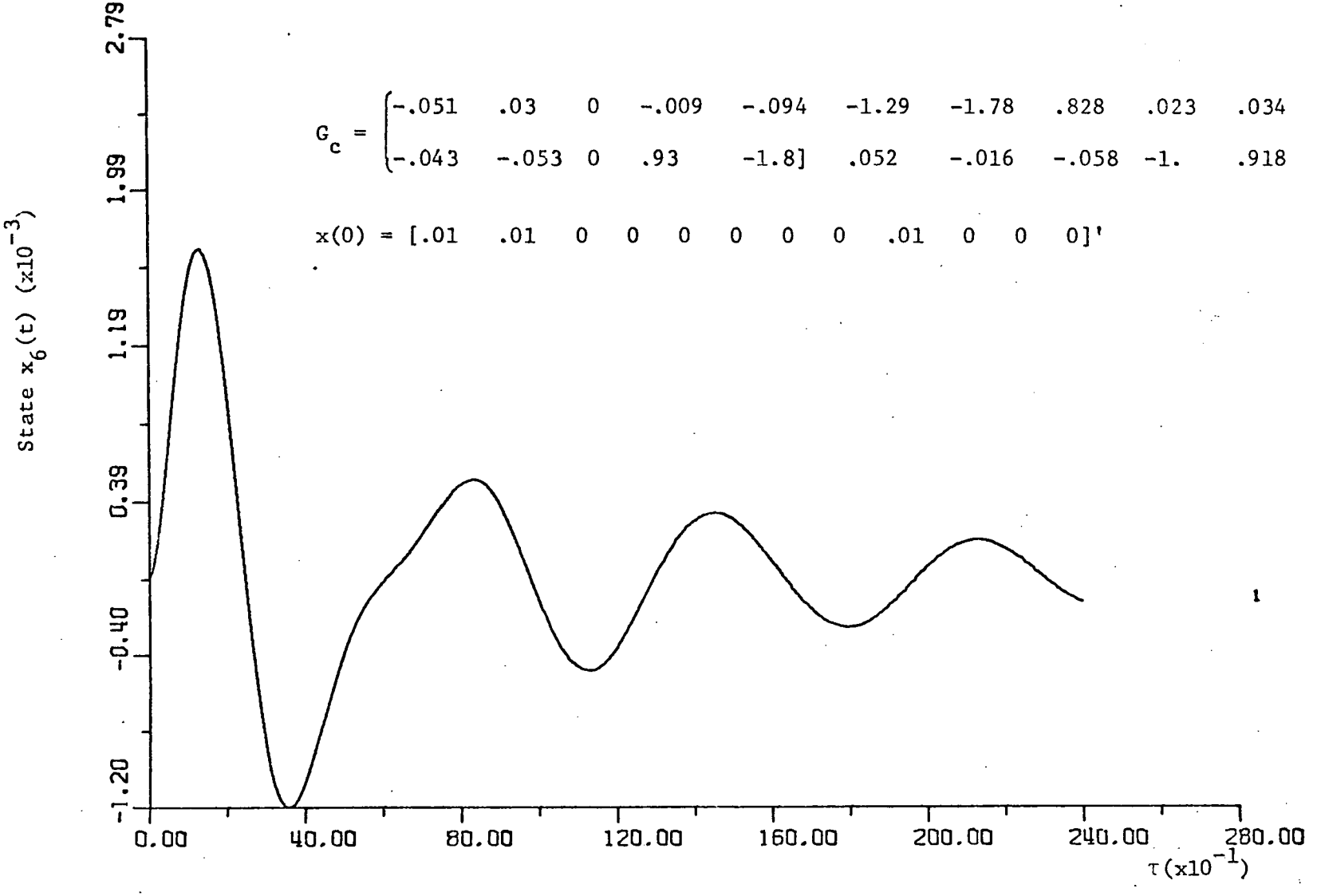

Figure 5-7 State trajectory $x_6(t)$ of the 12th order model for the Spinning Skylab Satellite.

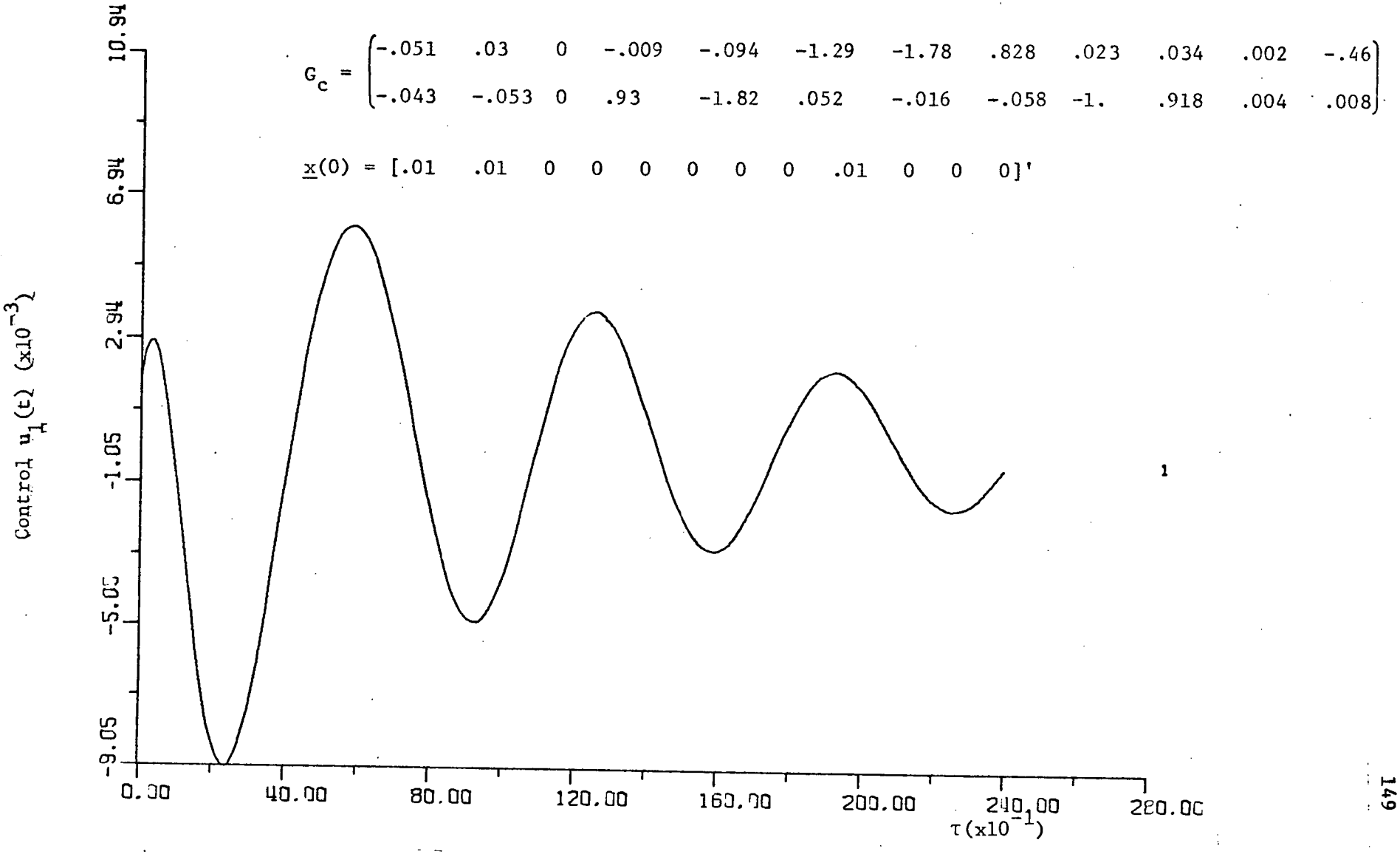

Figure 5-8 Control trajectory $u_1(t)$ of the 12th order model for the Spinning Skylab Satellite.

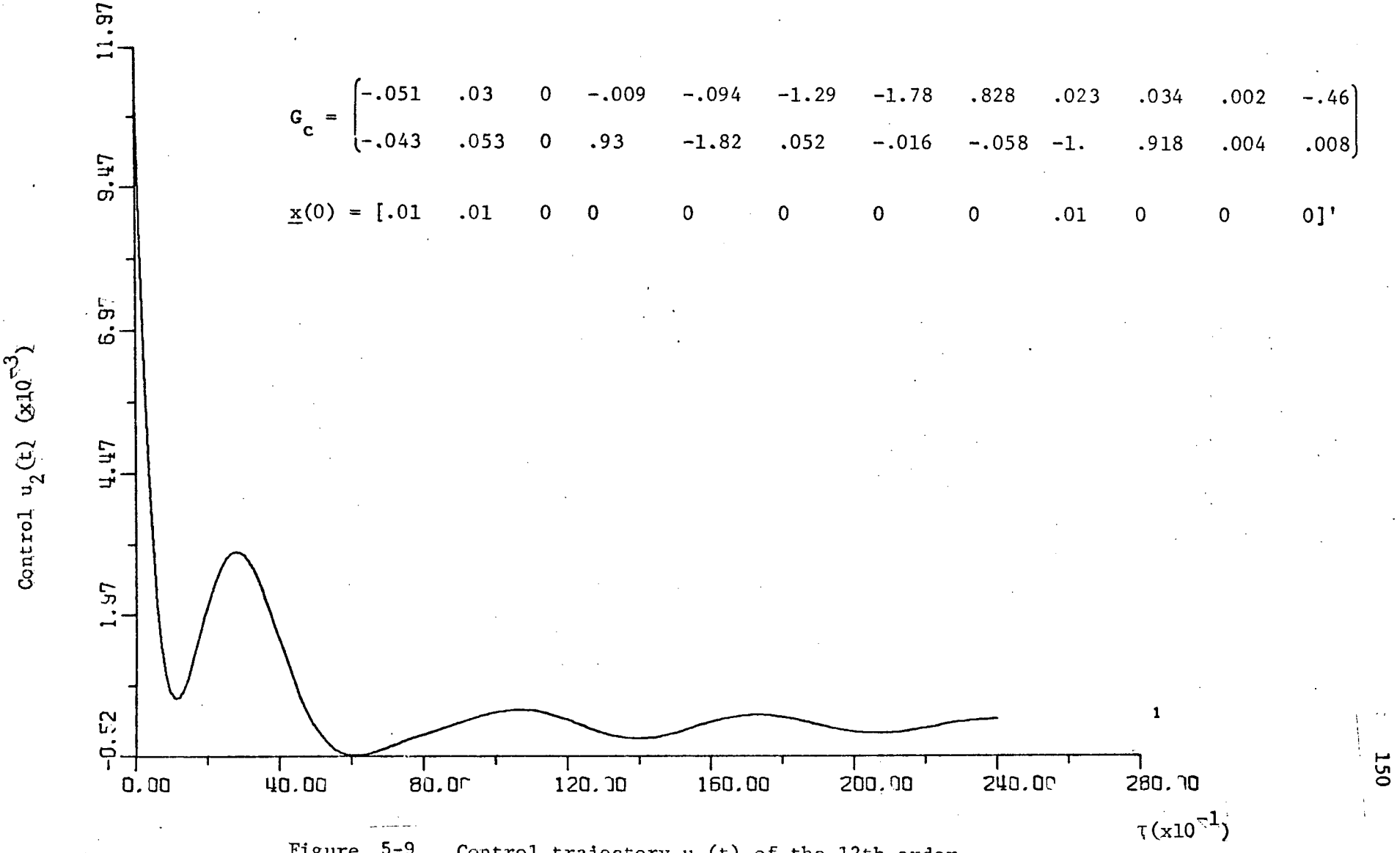

Figure 5-9 Control trajectory $u_2(t)$ of the 12th order model for the Spinning Skylab Satellite.

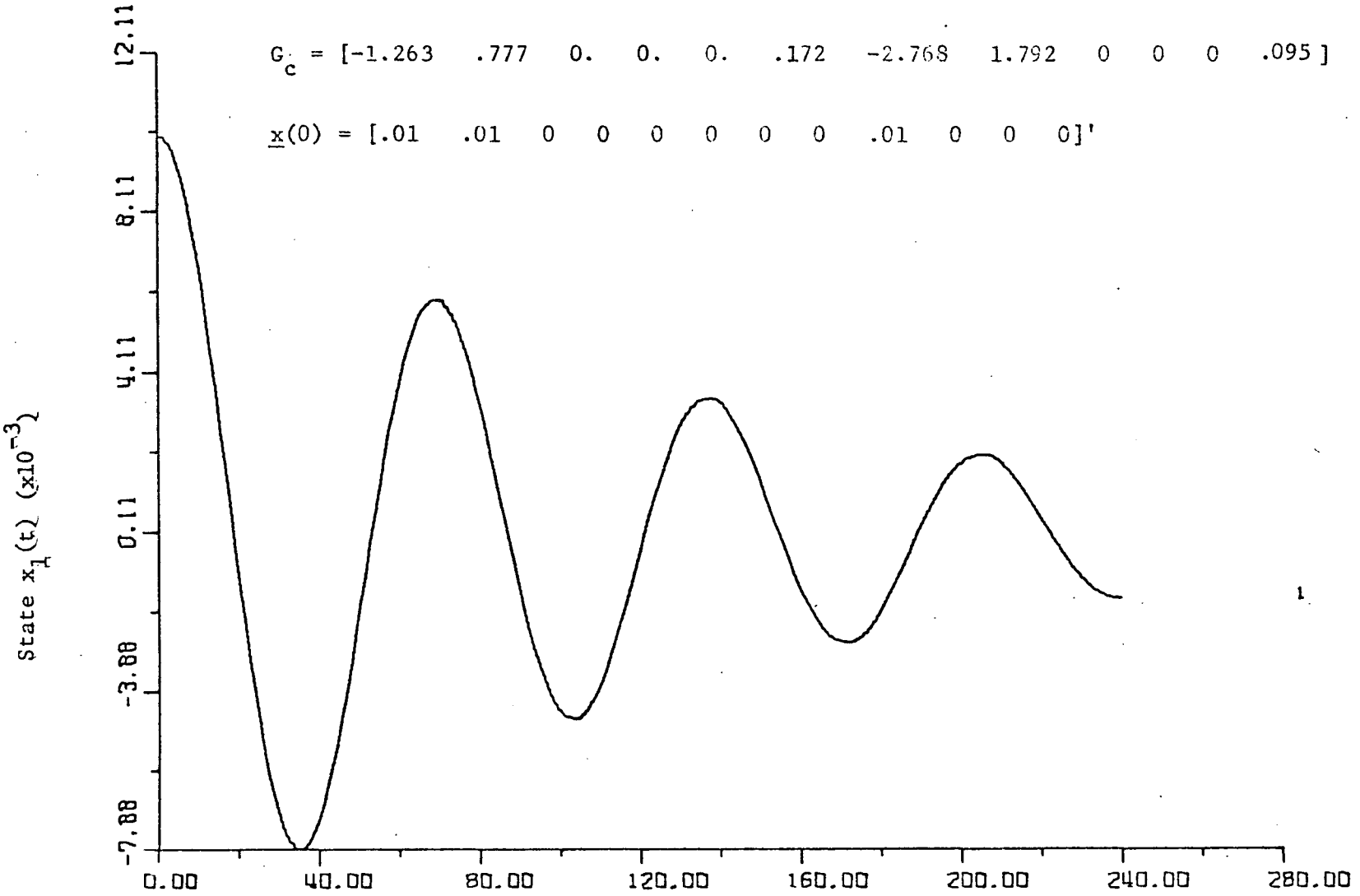

Figure 5-10 State trajectory $x_1(t)$ of the 12th order model for the Spinning Skylab Satellite

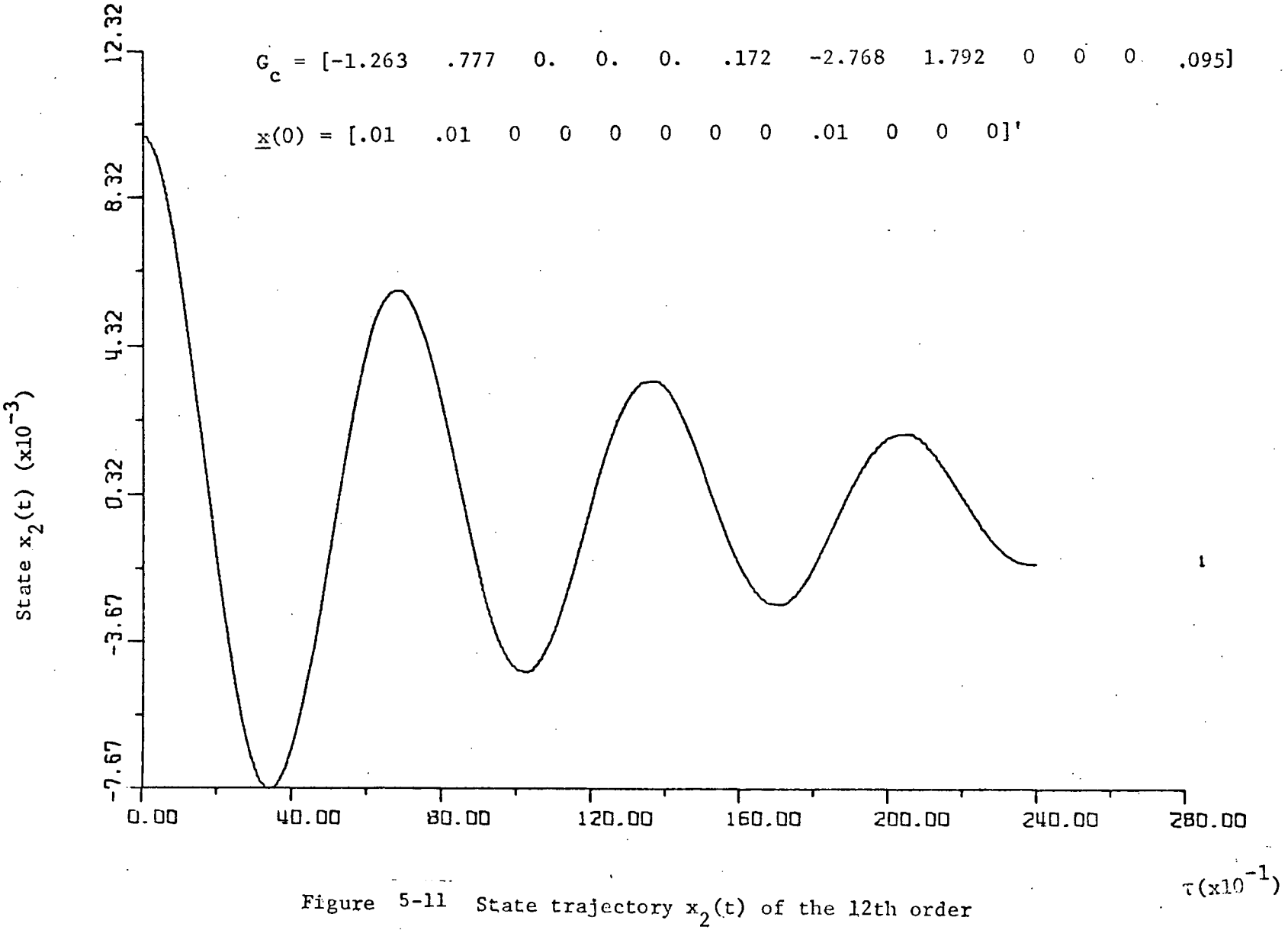

Figure 5-11 State trajectory $x_2(t)$ of the 12th order model for the Spinning Skylab Satellite.

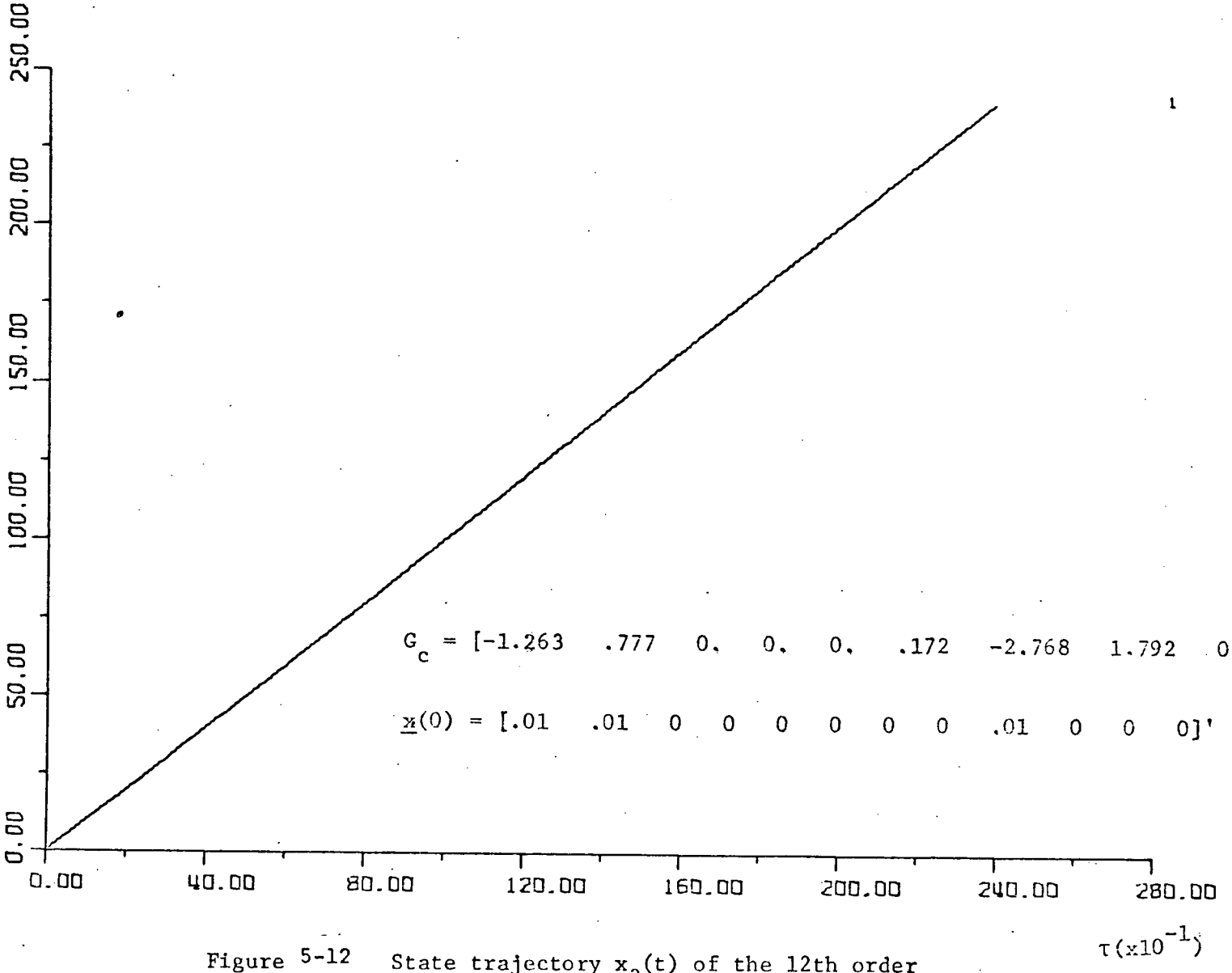

Figure 5-12 State trajectory $x_3(t)$ of the 12th order model for the Spinning Skylab Satellite.

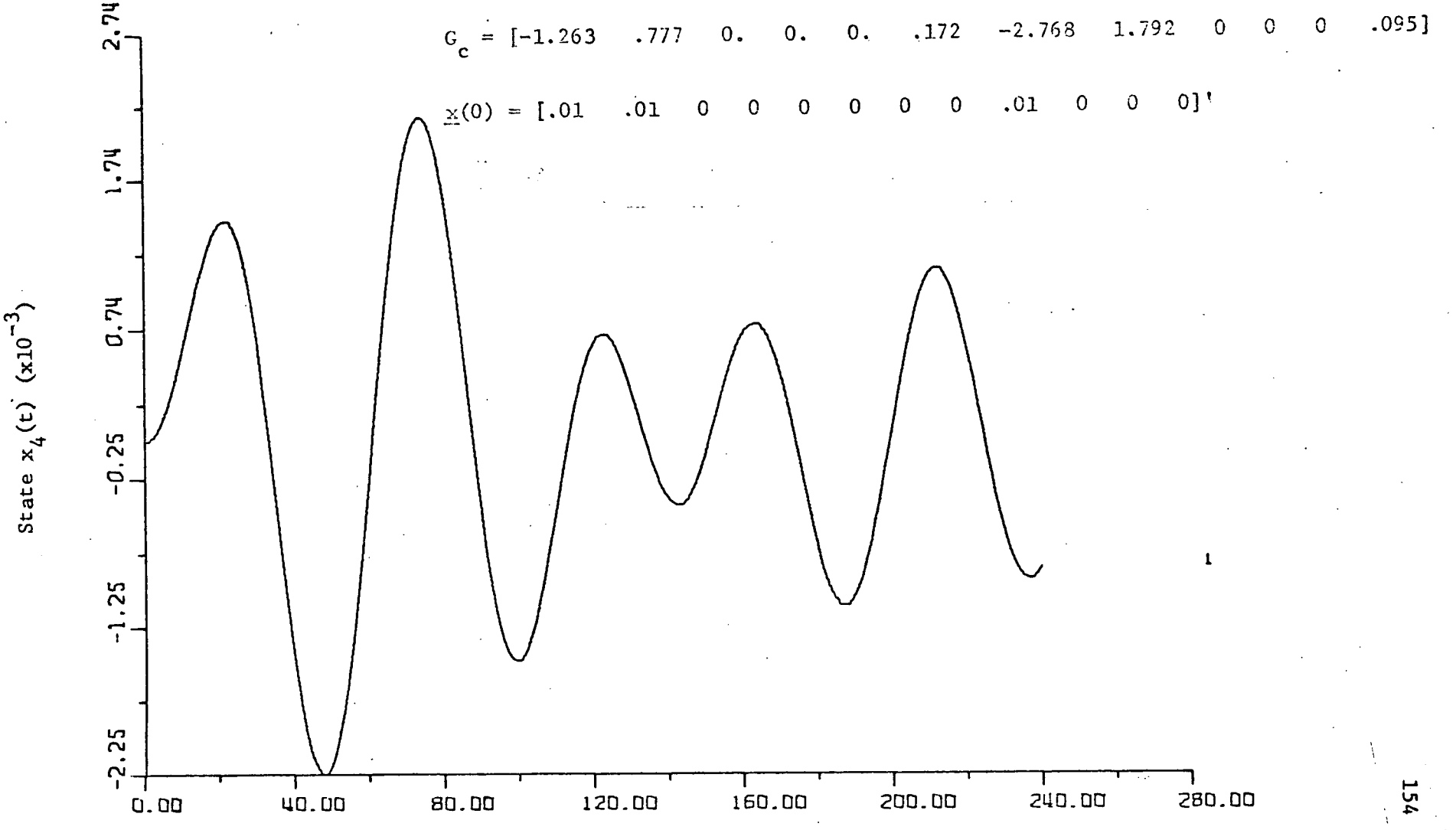

Figure 5-13 State trajectory $x_4(t)$ of the 12th order model for the Spinning Skylab Satellite.

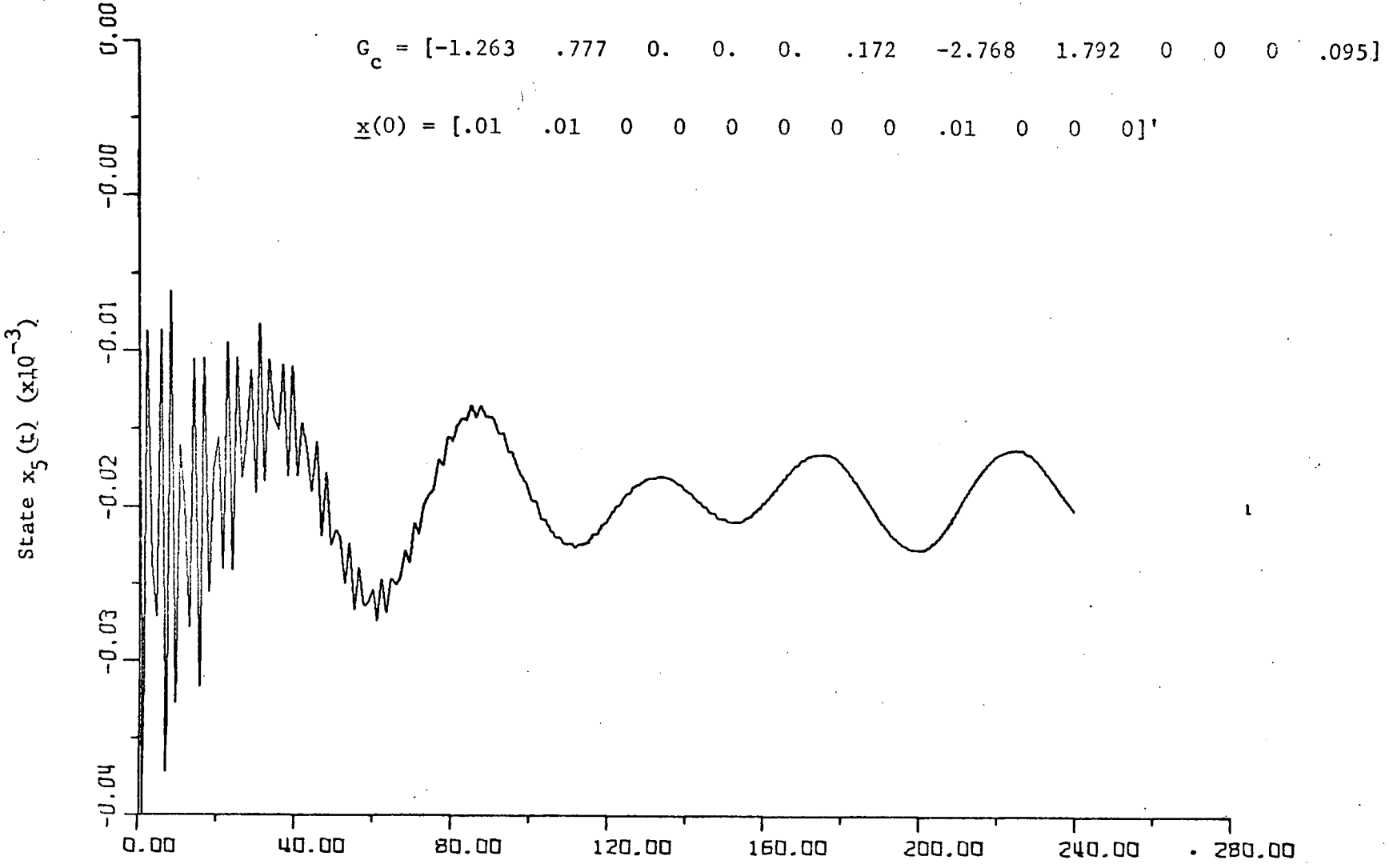

Figure 5-14 State trajectory $x_5(t)$ of the 12th order model for the Spinning Skylab Satellite.

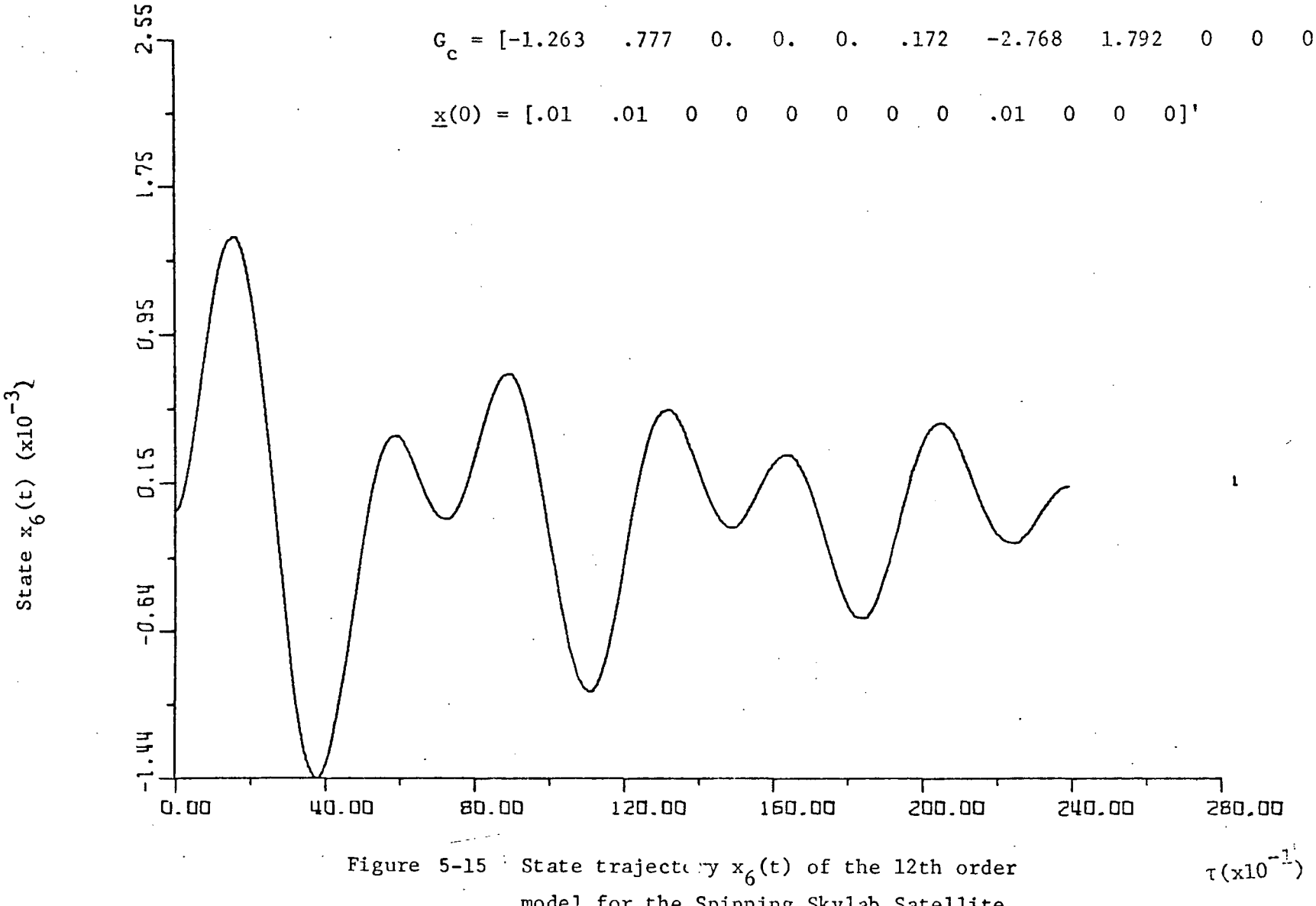

Figure 5-15 State trajectory $x_6(t)$ of the 12th order model for the Spinning Skylab Satellite.

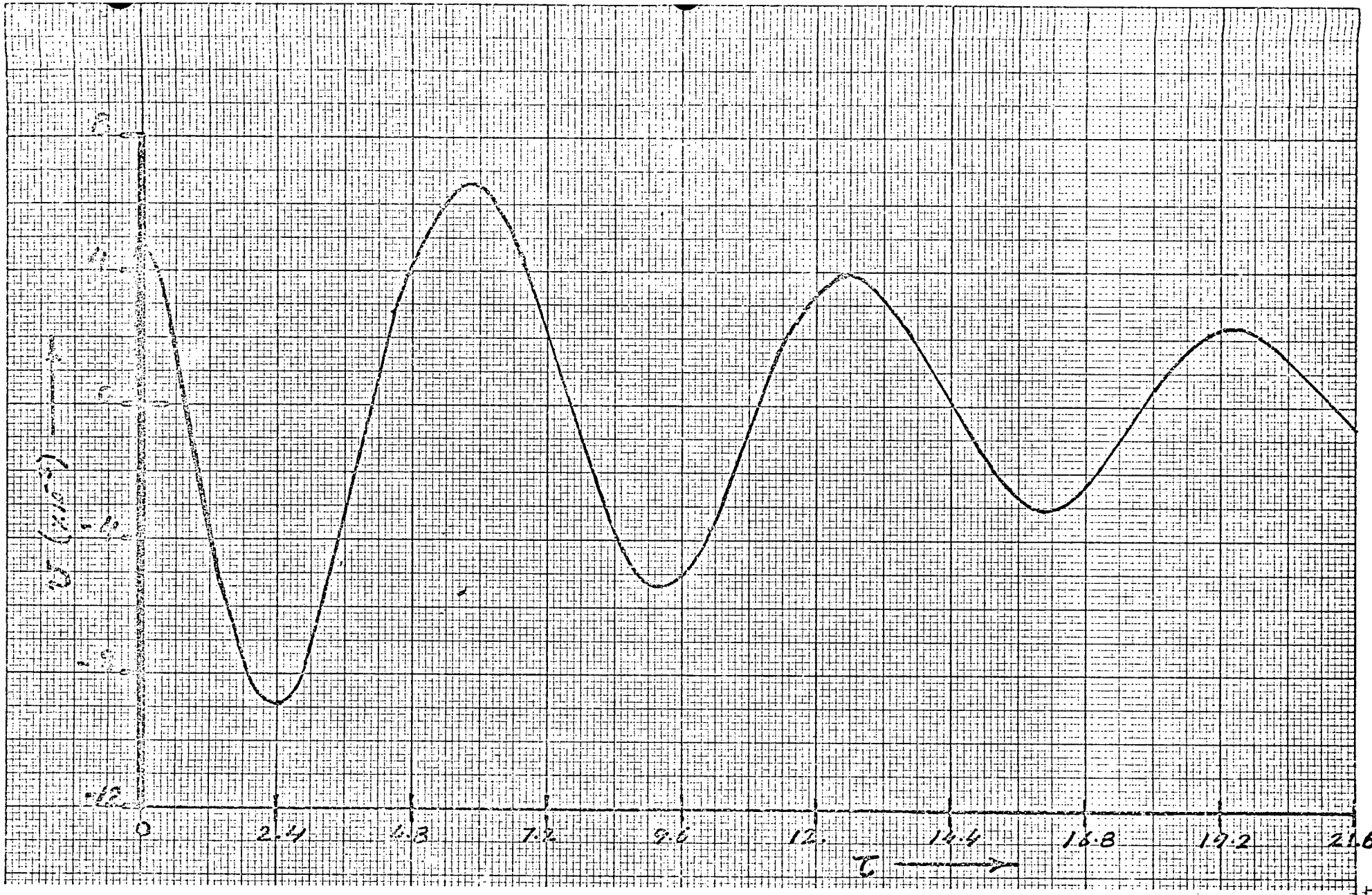

Figure 5-16 Control trajectory $u(\tau)$ for the 12th order model of the Spinning Skylab. Feedback gain obtained from the LQL design of the wobble dynamics (6th order model).

6. DIGITAL REDESIGN OF THE 11th ORDER MODEL OF THE SPINNING SKYLAB

The design of the continuous system for the 11th order model of the Spinning Skylab was performed by use of the LQL method. The feedback gain matrix G_c for Q = I, R = I was found to be (see Chapter 5, Table 5-2).

$$G_c = \begin{pmatrix} -.513 & .302 & -.009 & -.094 & -1.29 & -1.783 & .828 & .0229 & .034 & .0021 & -.457 \\ -.043 & -.053 & .93 & -1.82 & -.0515 & -.016 & -.058 & -1.0 & .918 & .0043 & .0082 \end{pmatrix}$$

The digital redesign of this system is performed by use of the point by point method of partial matching. The weighting matrix H is chosen as

$$H = \begin{pmatrix} 1 & 1 & 0 & 0 & 1 & 1 & 1 & 0 & 0 & 0 & 1 \\ 0 & 0 & 1 & 1 & 0 & 0 & 0 & 1 & 1 & 1 & 0 \end{pmatrix}$$

and the feedback gains for the digital system are determined for two different sampling periods, T = .2 and T = .8. The choice of H was made such that matching is obtained for the sum of the states of the wobble dynamics as well as the sum of the states of the spin dynamics for each sampling instant (See Chapter 1, Section 1.) for a discussion on how H should be chosen). With T = .2 the feedback gain matrix of the sampled data system is

$$G_w = \begin{pmatrix} -.442 & .183 & -.011 & -.0495 & -.777 & -1.41 & .450 & .0178 & .019 & .031 & -.434 \\ -.043 & -.025 & .696 & -1.53 & -.013 & -.063 & -.014 & -.875 & .85 & .015 & .004 \end{pmatrix}$$

with T = .8 we have

$$G_w = \begin{pmatrix} -.332 & .095 & -.0045 & .0055 & .128 & .775 & .21 & .006 & -.0057 & .0017 & -.22 \\ -.032 & .026 & -.0015 & -.66 & -.125 & -.137 & .066 & -.51 & .548 & -.009 & -.025 \end{pmatrix}$$

The simulation of the 12th order model of the Spinning Skylab is performed with each of the above gains. Figures 6-1 through 6-14 show the results with T = 0.2. These figures show the state, control and errors in state

and control trajectories. Figures 6-15 through 6-22 show the results for T = 0.8.

It is apparent that the point by point state comparison method of partial matching yields acceptable redesign with T = .2 as well as T = .8.

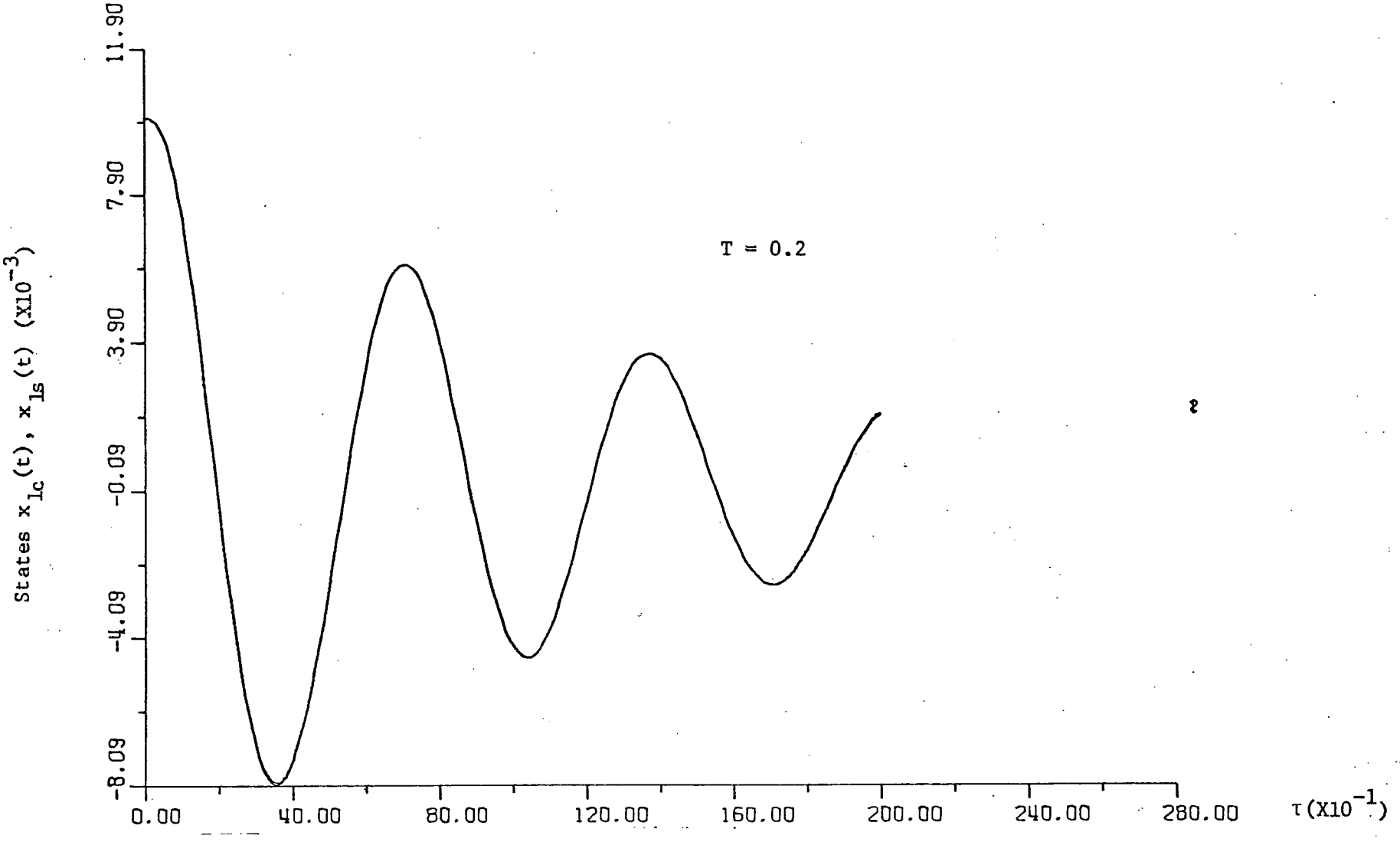

Figure 6-1 State trajectories $x_{lc}(t)$ and $x_{ls}(t)$ for the 12th order model of the Spinning Skylab Satellite. Digital redesign by the point by point method of partial matching.

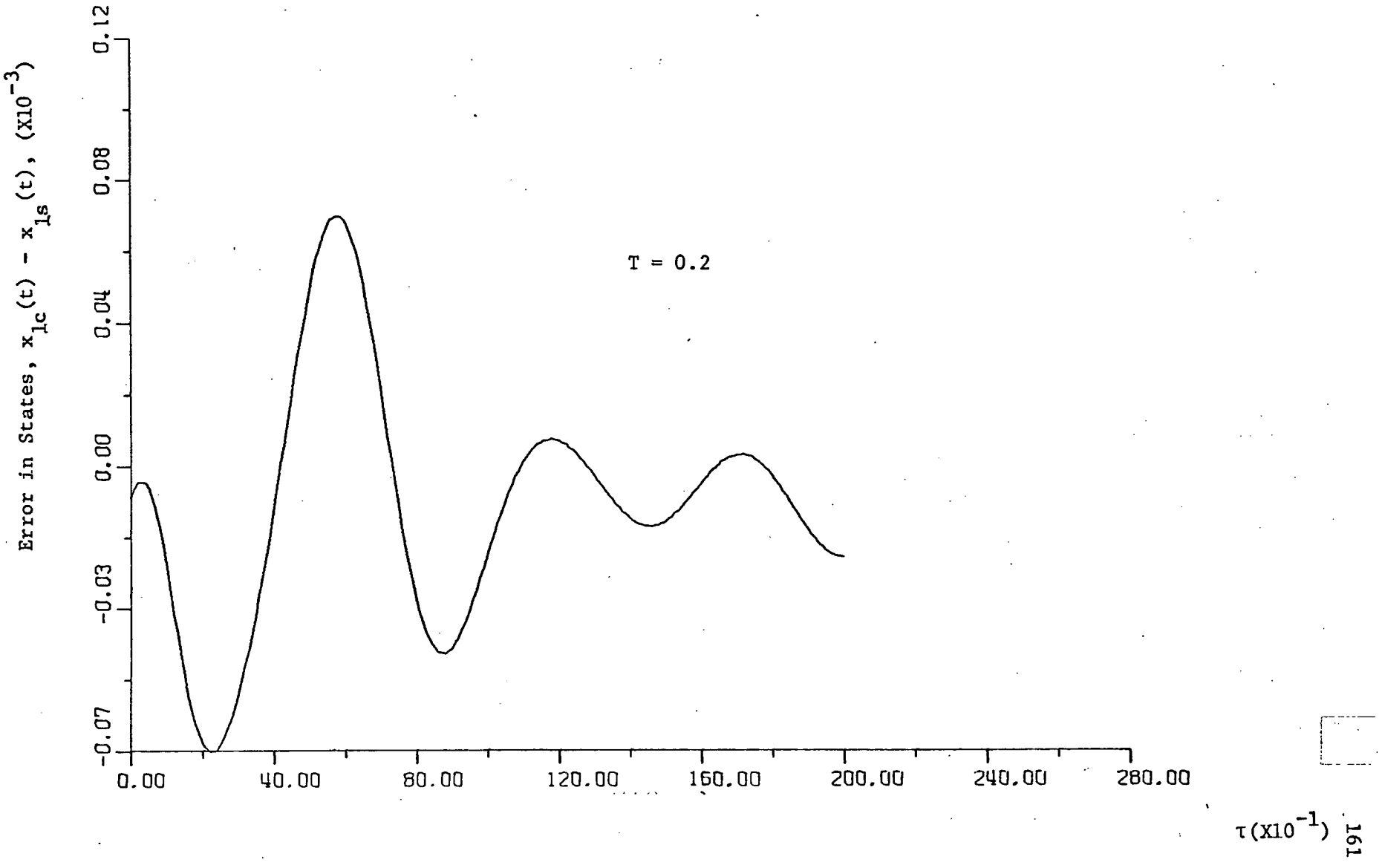

Figure 6-2 Error in state trajectories, $x_{1c}(t) - x_{1s}(t)$, for the 12th order model of the Spinning Skylab Satellite. Digital redesign by the point by point method of partial matching.

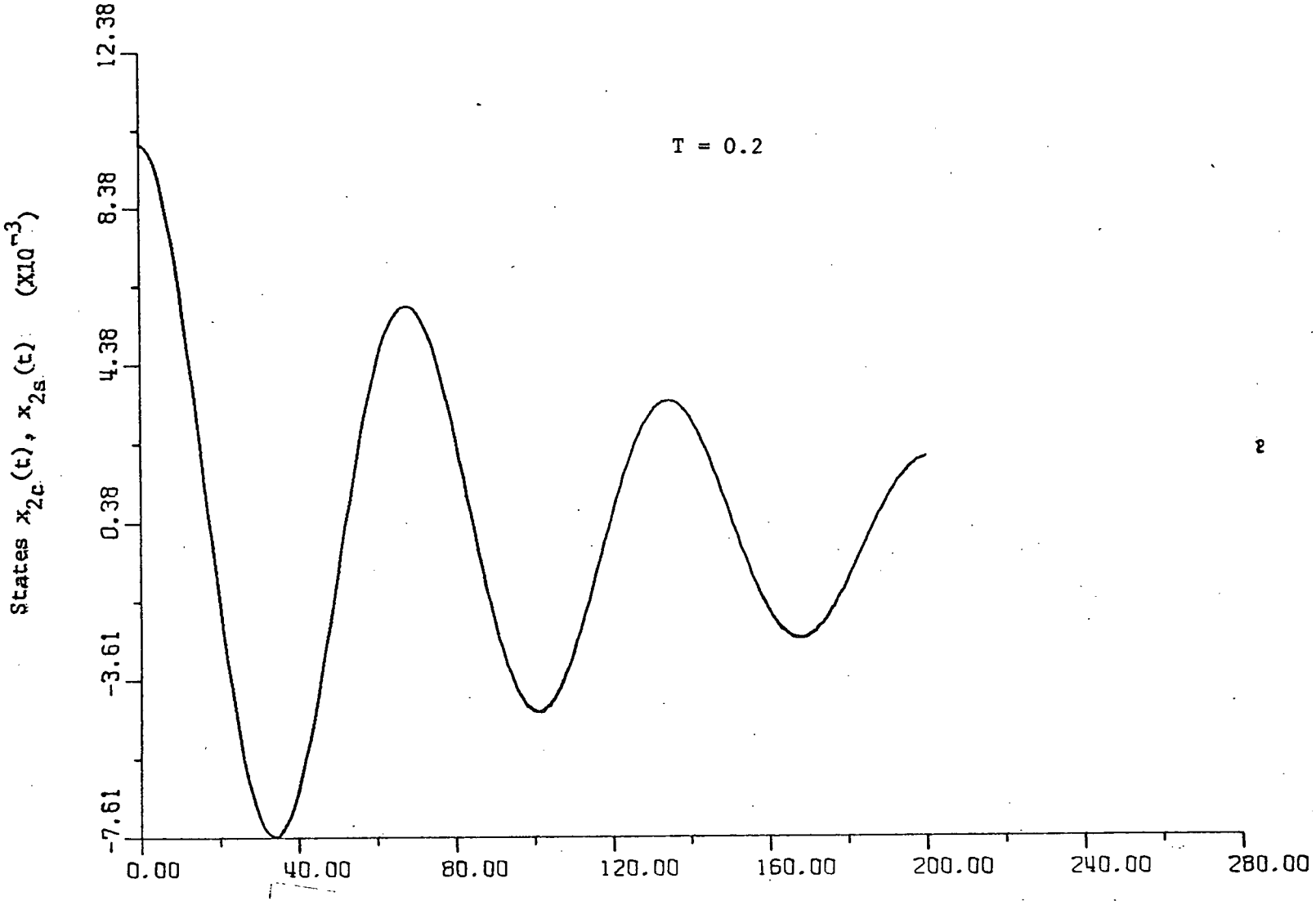

Figure 6-3 State trajectories $x_{2c}(t)$ and $x_{2s}(t)$ for the 12th order model of the Spinning Skylab Satellite. Digital Redesign by the point by point method of partial matching.

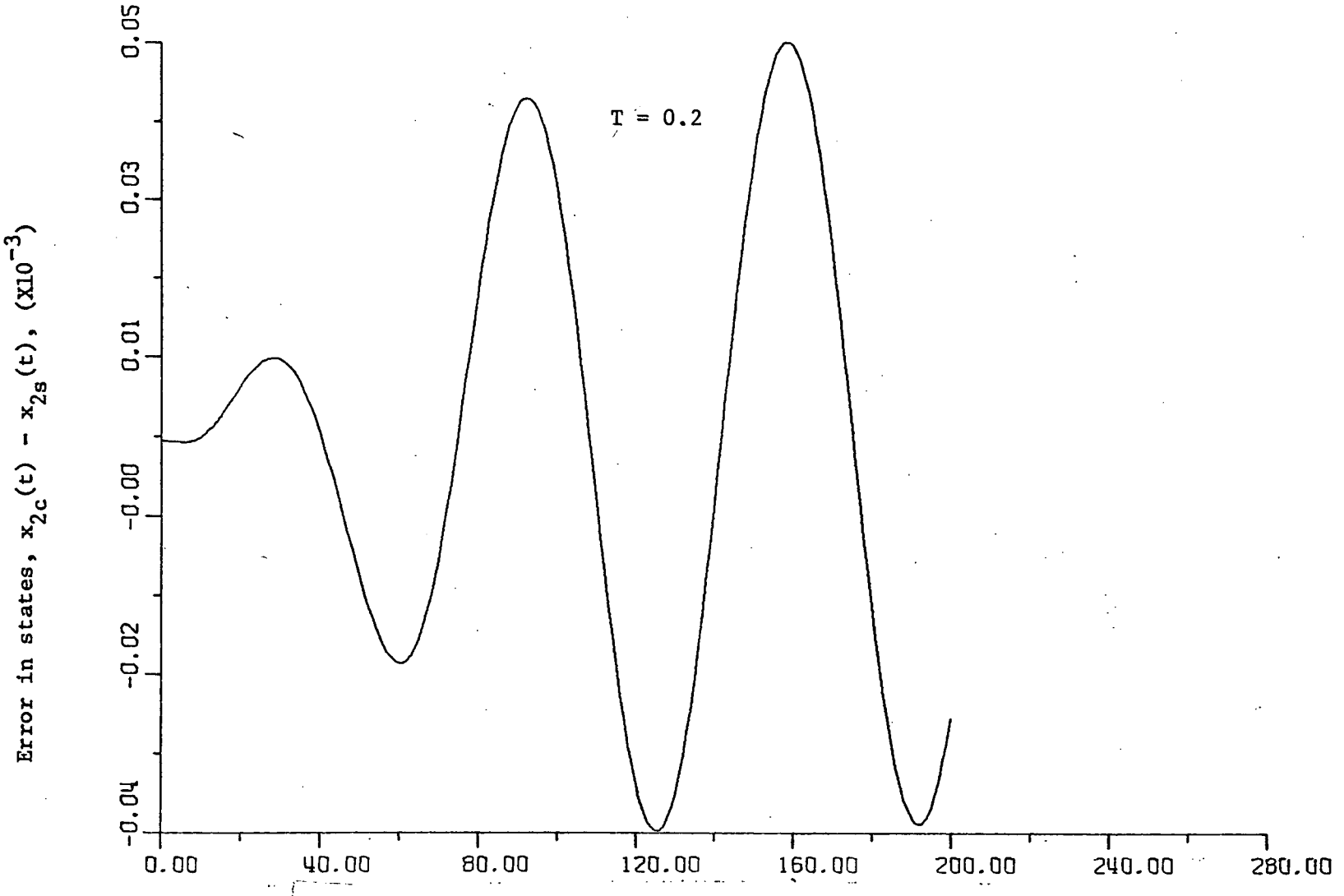

Figure 6-4 Error in state trajectories, $x_{2c}(t) - x_{2s}(t)$, for the 12th order model of the Spinning Skylab Satellite. Digital redesign by the point by point method of partial matching.

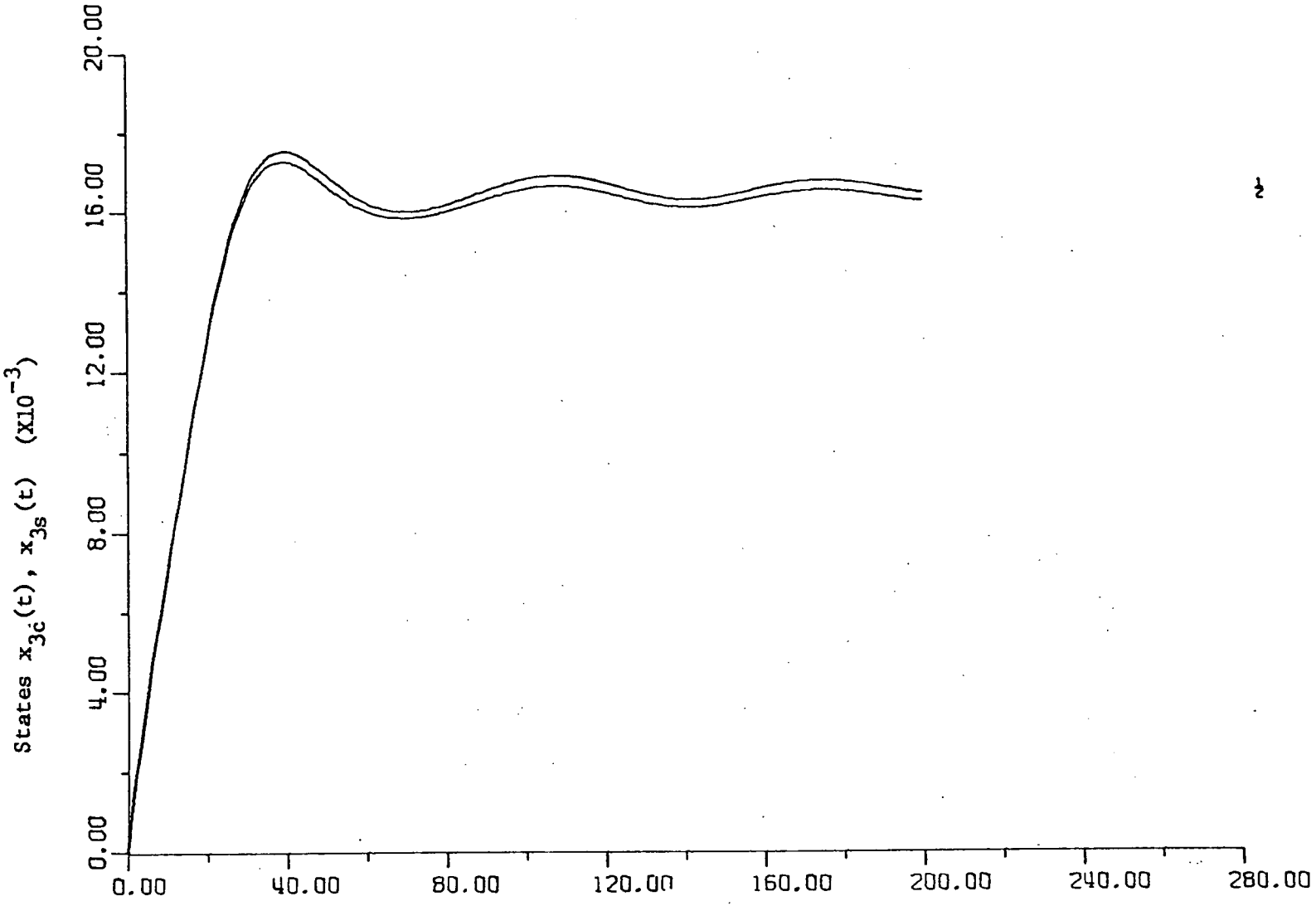

Figure 6-5 State trajectories $x_{3c}(t)$ and $x_{3s}(t)$ for the 12th order model of the Spinning Skylab Satellite. Digital Redesign by the point by point method of partial matching.

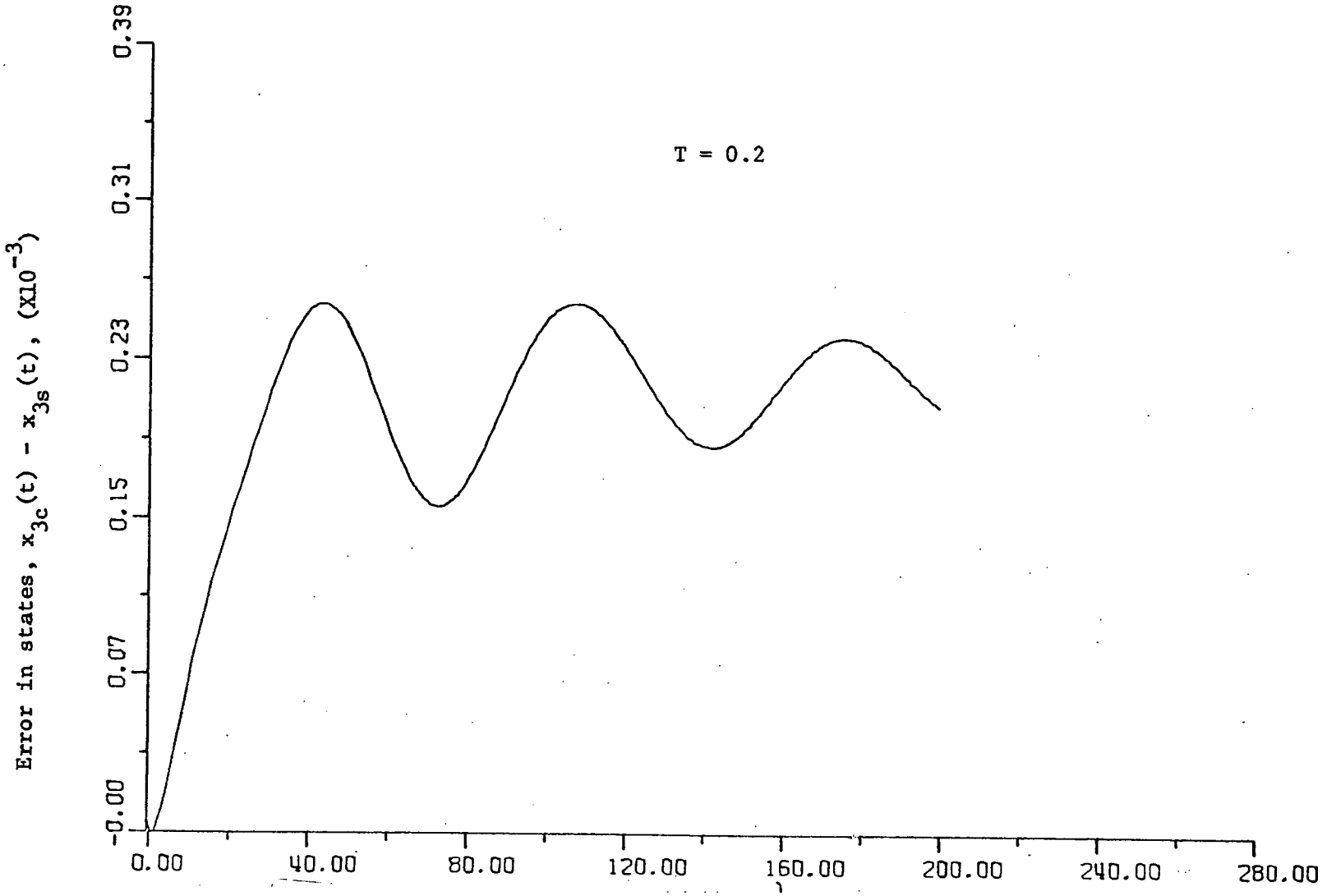

Figure 6-6 Error in state trajectories, $x_{3c}(t) - x_{3s}(t)$ for the 12th order model of the Spinning Skylab Satellite. Digital redesign by the point by point method of partial matching.

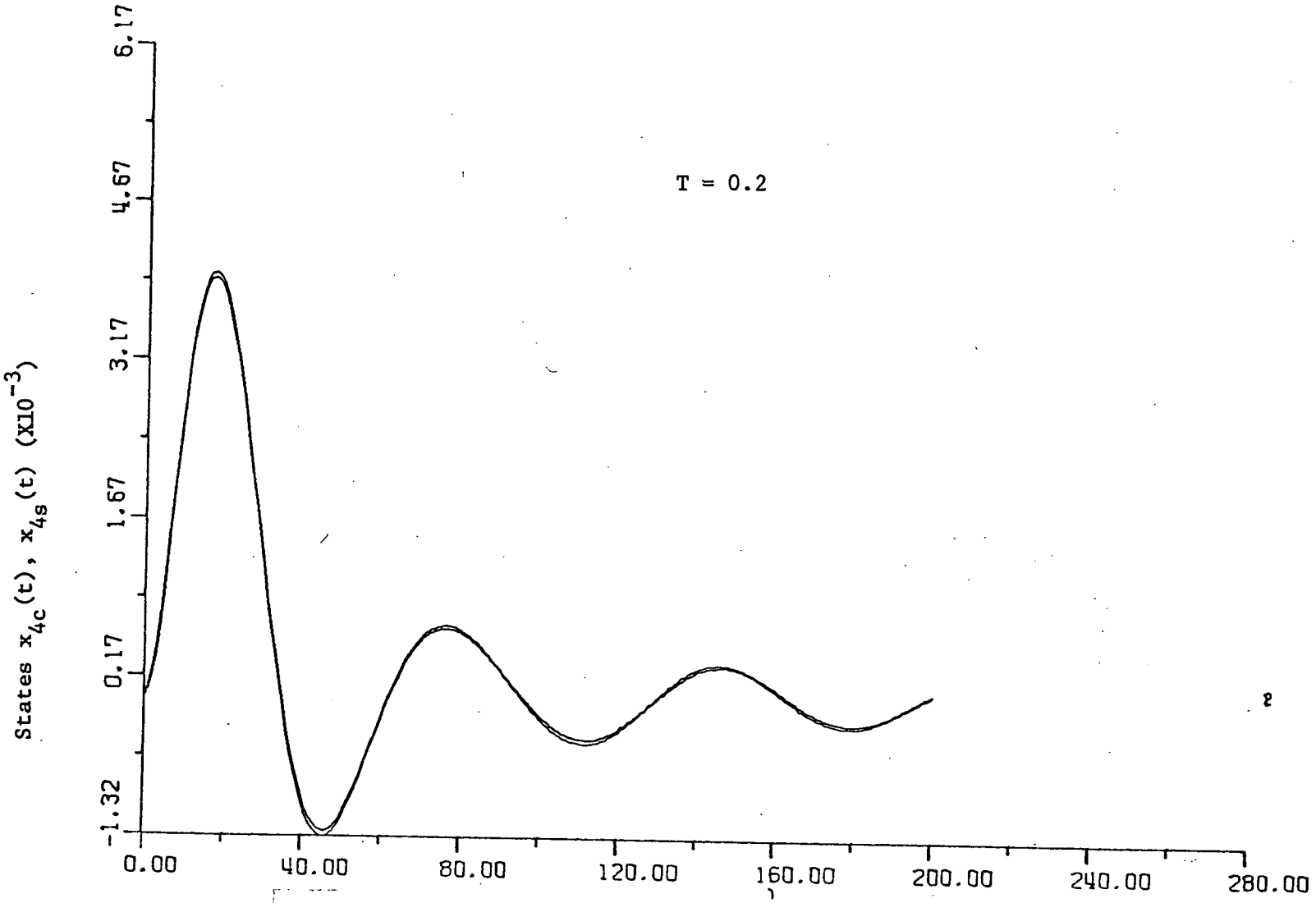

Figure 6-7 State trajectories $x_{4c}(t)$ and $x_{4s}(t)$ for the 12th order model of the Spinning Skylab Satellite. Digital Redesign by the point by point method of partial matching.

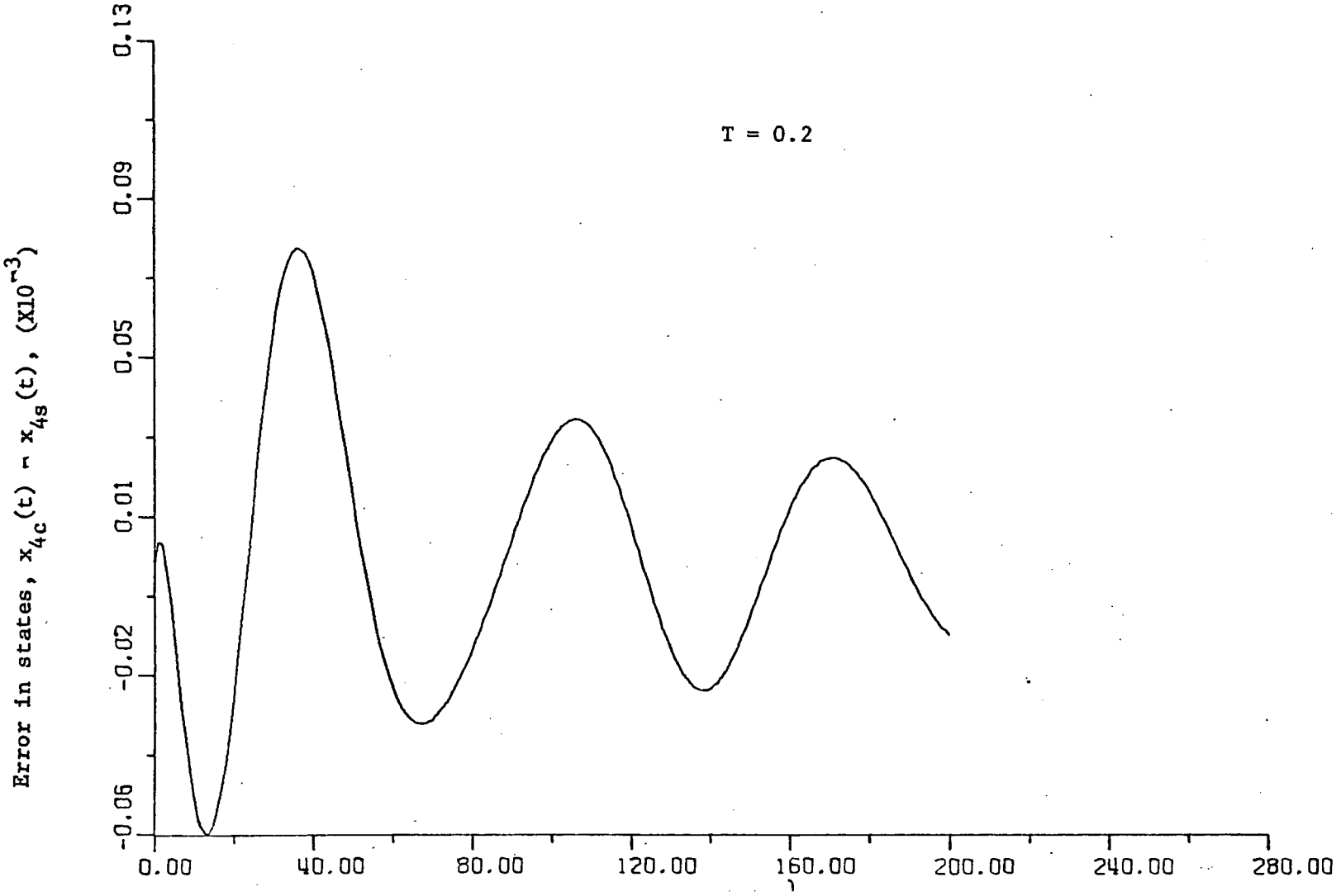

Figure 6-8 Error in state trajectories, $x_{4c}(t) - x_{4s}(t)$, for the 12th order model of the Spinning Skylab Satellite. Digital redesign by the point by point method of partial matching

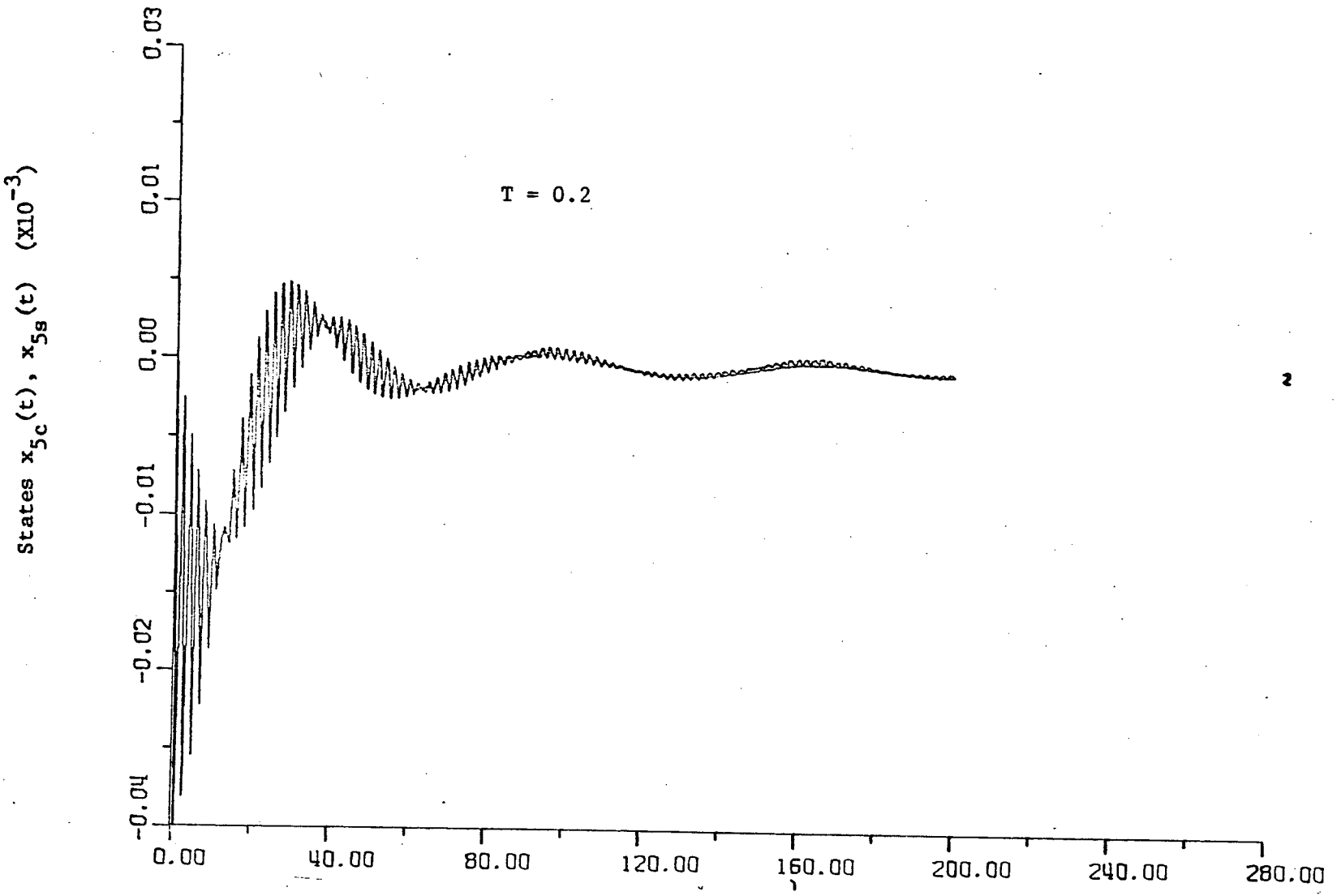

Figure 6-9 State trajectories $x_{5c}(t)$ and $x_{5s}(t)$ for the 12th order model of the Spinning Skylab Satellite. Digital Redesign by the point by point method of partial matching.

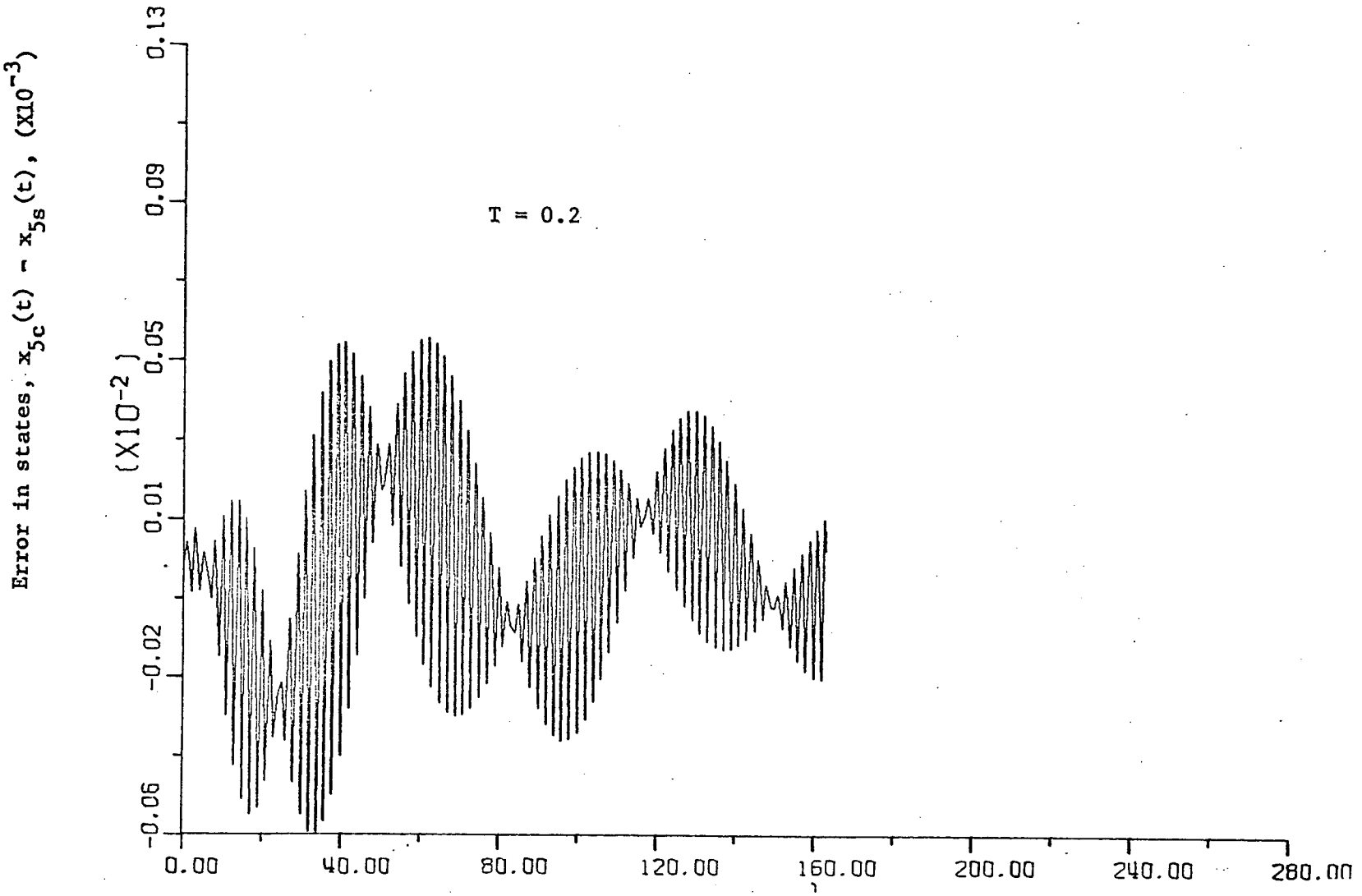

Figure 6-10 Error in state trajectories, $x_{5c}(t) - x_{5s}(t)$, for the 12th order model of the Spinning Skylab Satellite. Digital redesign by the point by point method of partial matching.

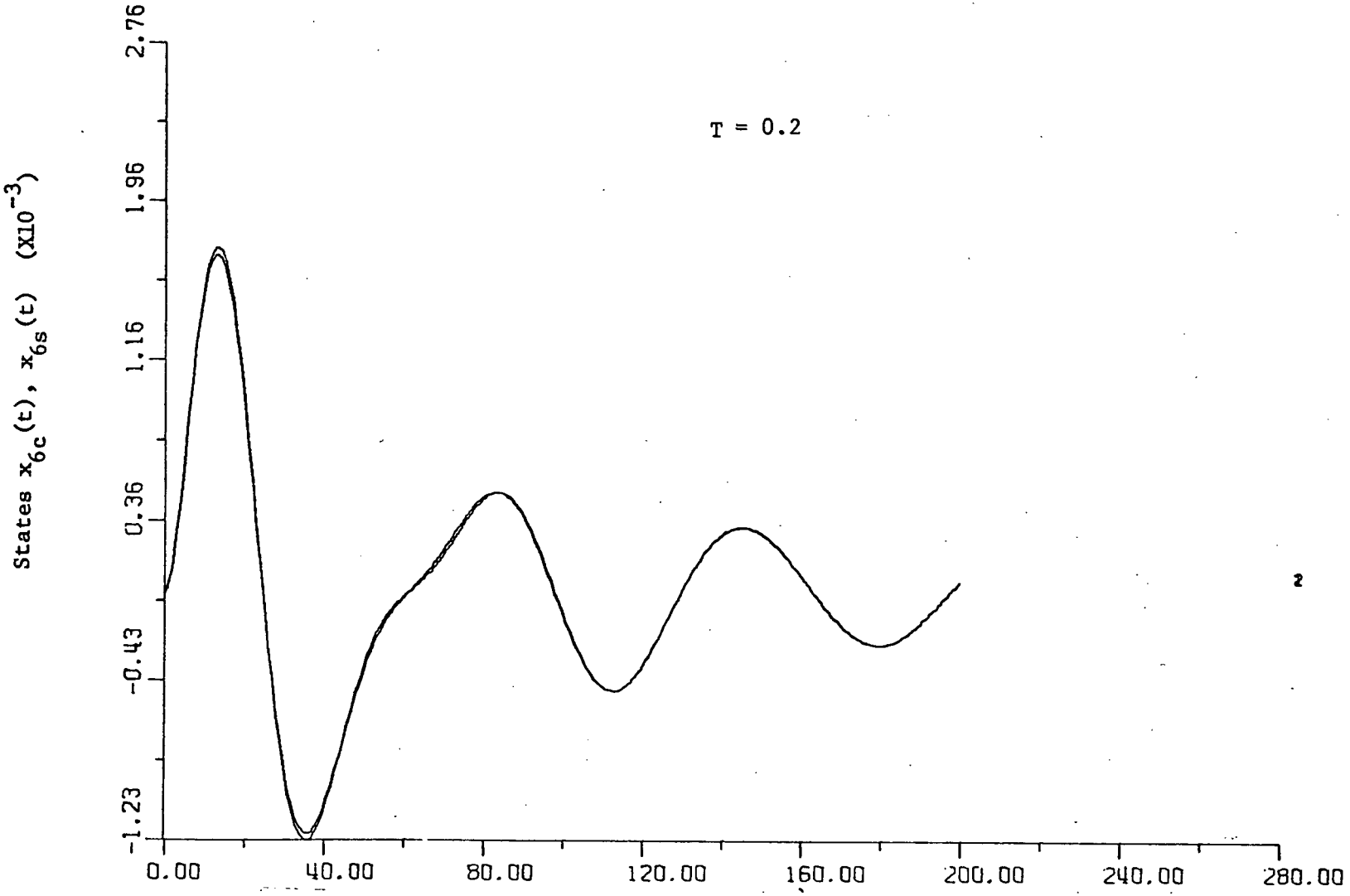

Figure 6-11 State trajectories $x_{6c}(t)$ and $x_{6s}(t)$ for the 12th order model of the Spinning Skylab Satellite. Digital redesign by the point by point method of partial matching.

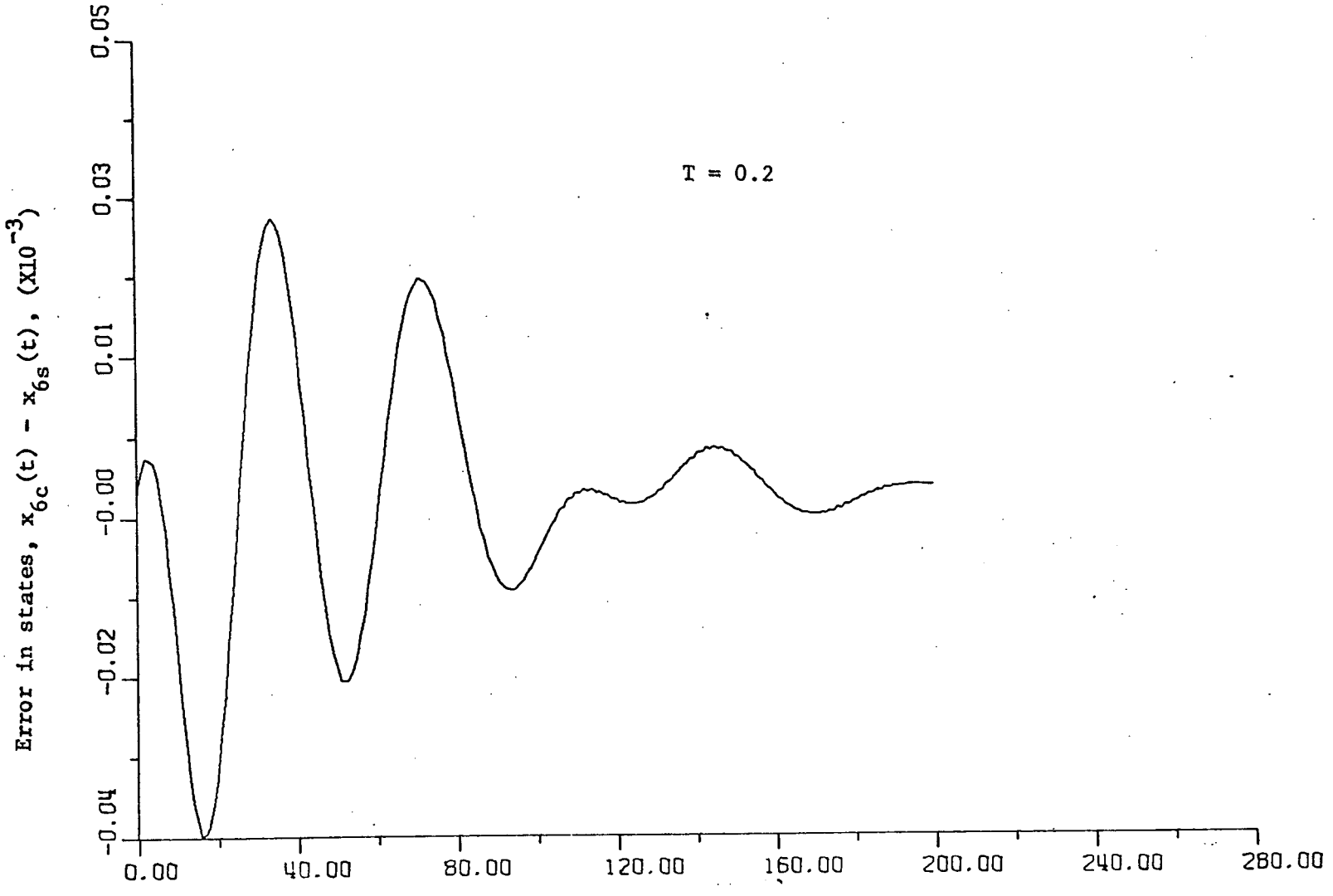

Figure 6-12 Error in state trajectories, $x_{6c}(t) - x_{6s}(t)$, for the 12th order model of the Spinning Skylab Satellite. Digital redesign by the point by point method of partial matching.

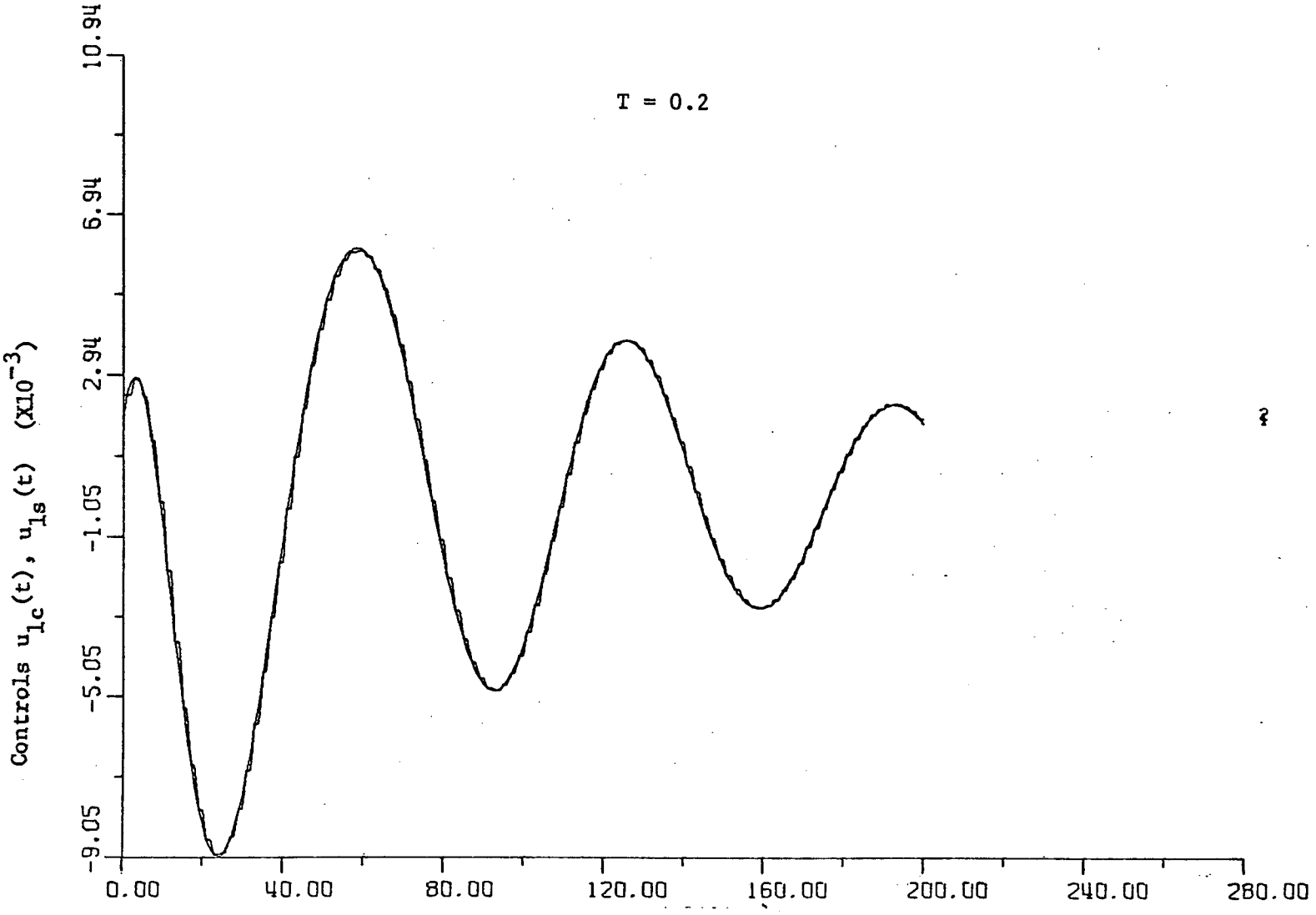

Figure 6-13 Control trajectories $u_{1c}(t)$ and $u_{1s}(t)$ for the 12th order model of the Spinning Skylab Satellite. Digital Redesign by the point by point method of partial matching.

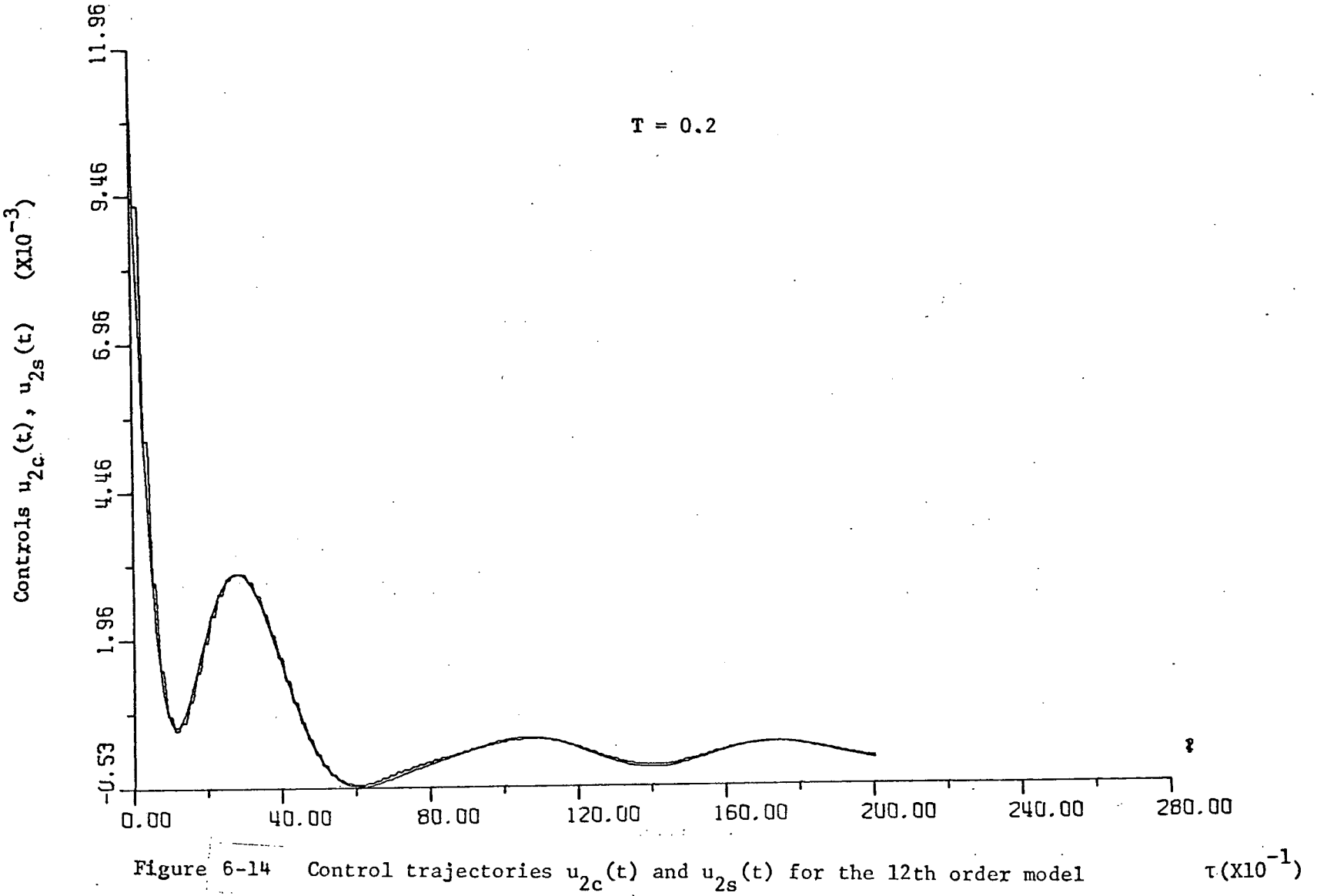

Figure 6-14 Control trajectories $u_{2c}(t)$ and $u_{2s}(t)$ for the 12th order model of the Spinning Skylab Satellite. Digital Redesign by the point by point method of partial matching.

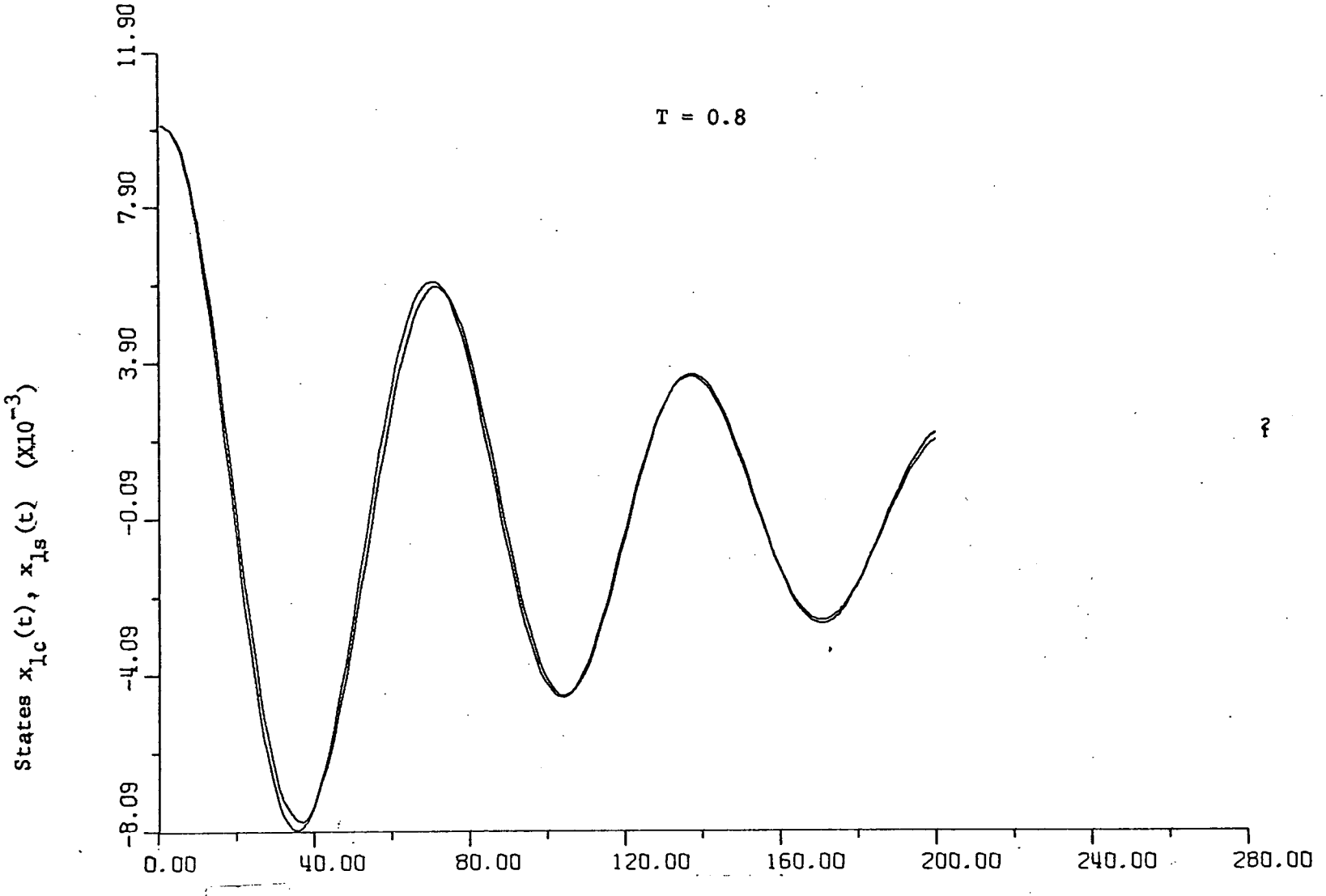

Figure 6-15 State trajectories $x_{1c}(t)$ and $x_{1s}(t)$ for the 12th order model of the Spinning Skylab Satellite. Digital Redesign by the point by point method of partial matching.

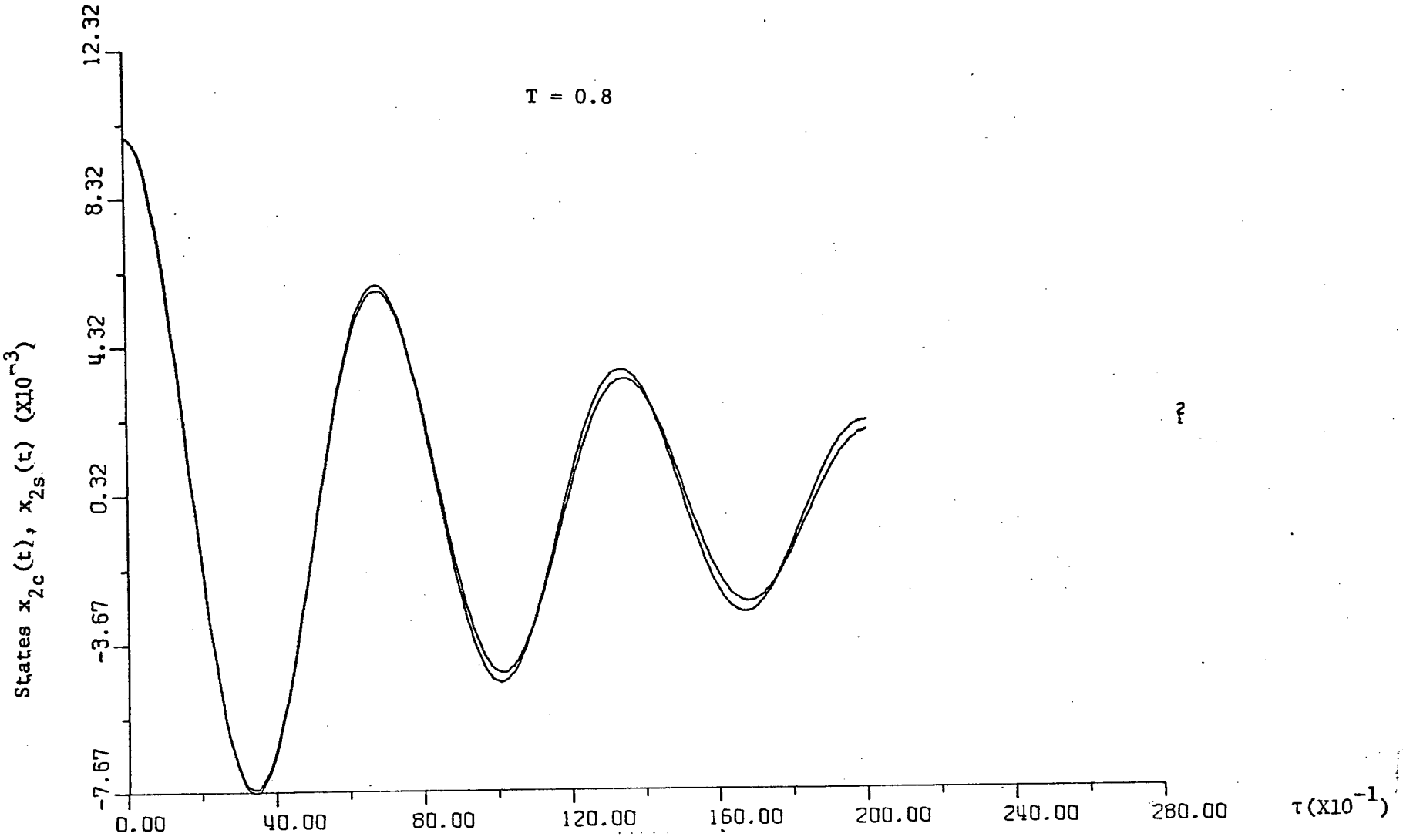

Figure 6-16 State trajectories $x_{2c}(t)$ and $x_{2s}(t)$ for the 12th order model of the Spinning Skylab Satellite. Digital Redesign by the point by point method of partial matching.

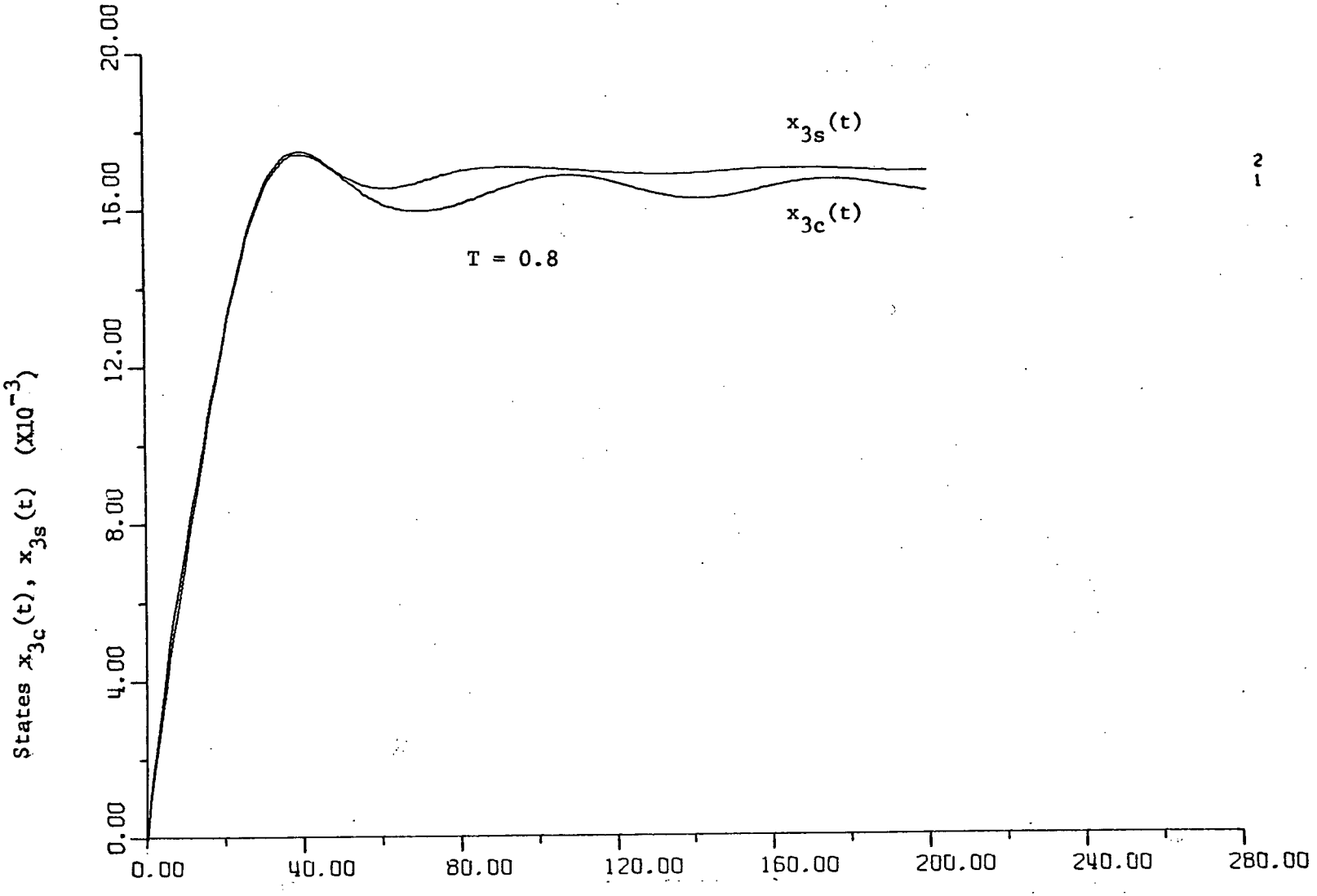

Figure 6-17 State trajectories $x_{3c}(t)$ and $x_{3s}(t)$ for the 12th order model of the Spinning Skylab Satellite. Digital Redesign by the point by point method of partial matching.

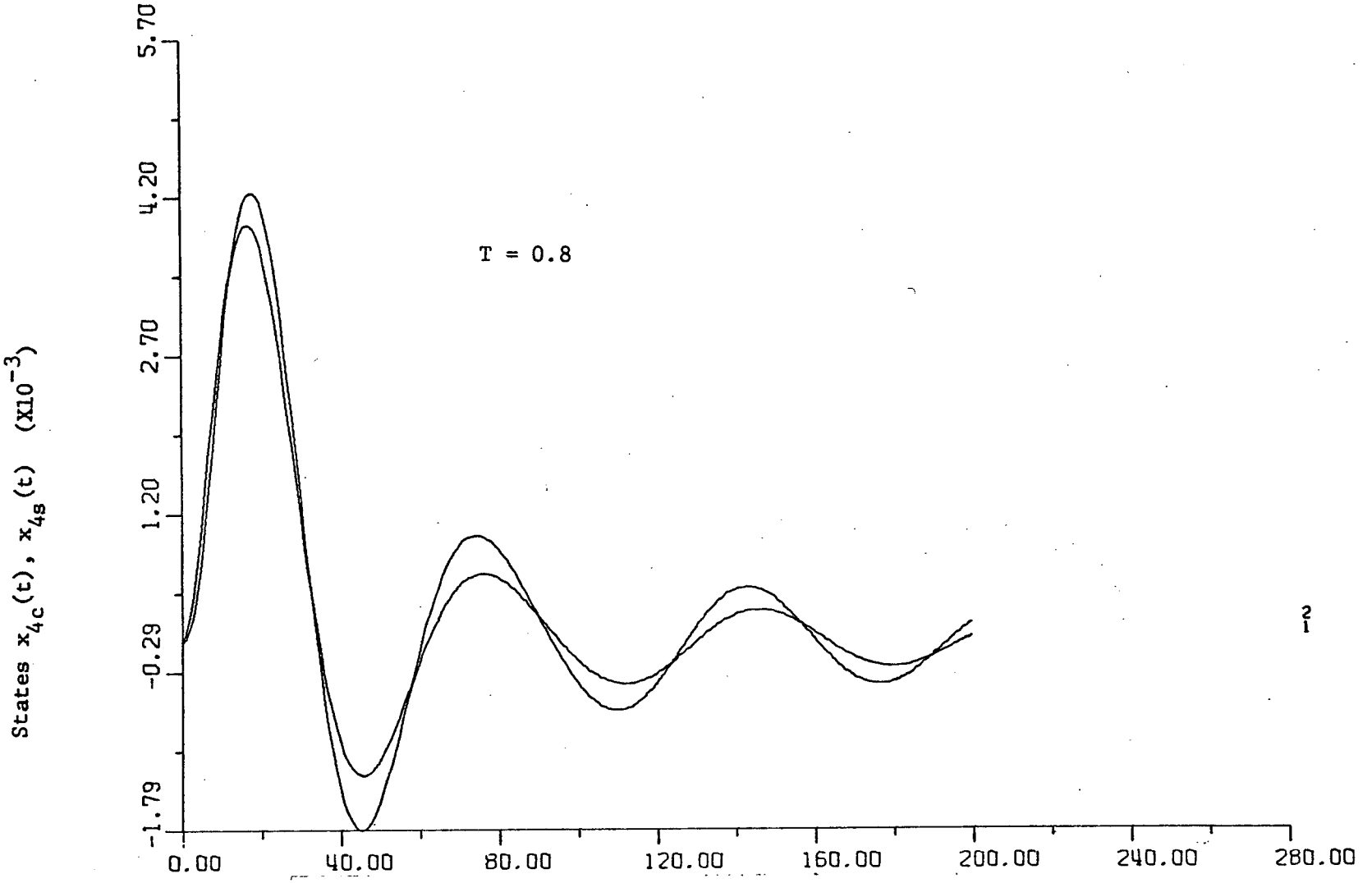

Figure 6-18 State trajectories $x_{4c}(t)$ and $x_{4s}(t)$ for the 12th order model of the Spinning Skylab Satellite. Digital Redesign by the point by point method of partial matching.

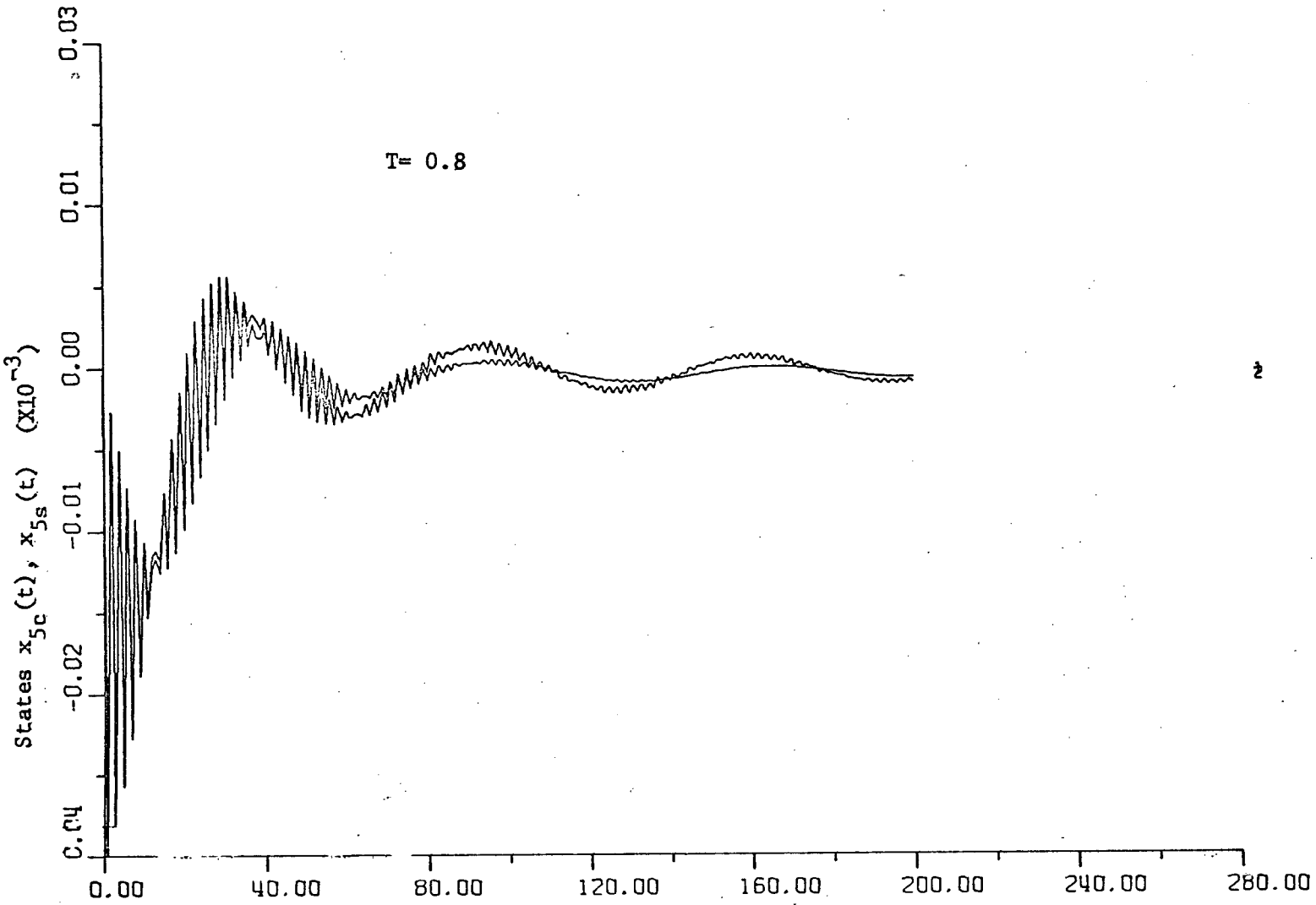

Figure 6-19 State trajectories $x_{5c}(t)$ and $x_{5s}(t)$ for the 12th order Spinning Skylab Satellite. Digital Redesign by the point by point method of partial matching.

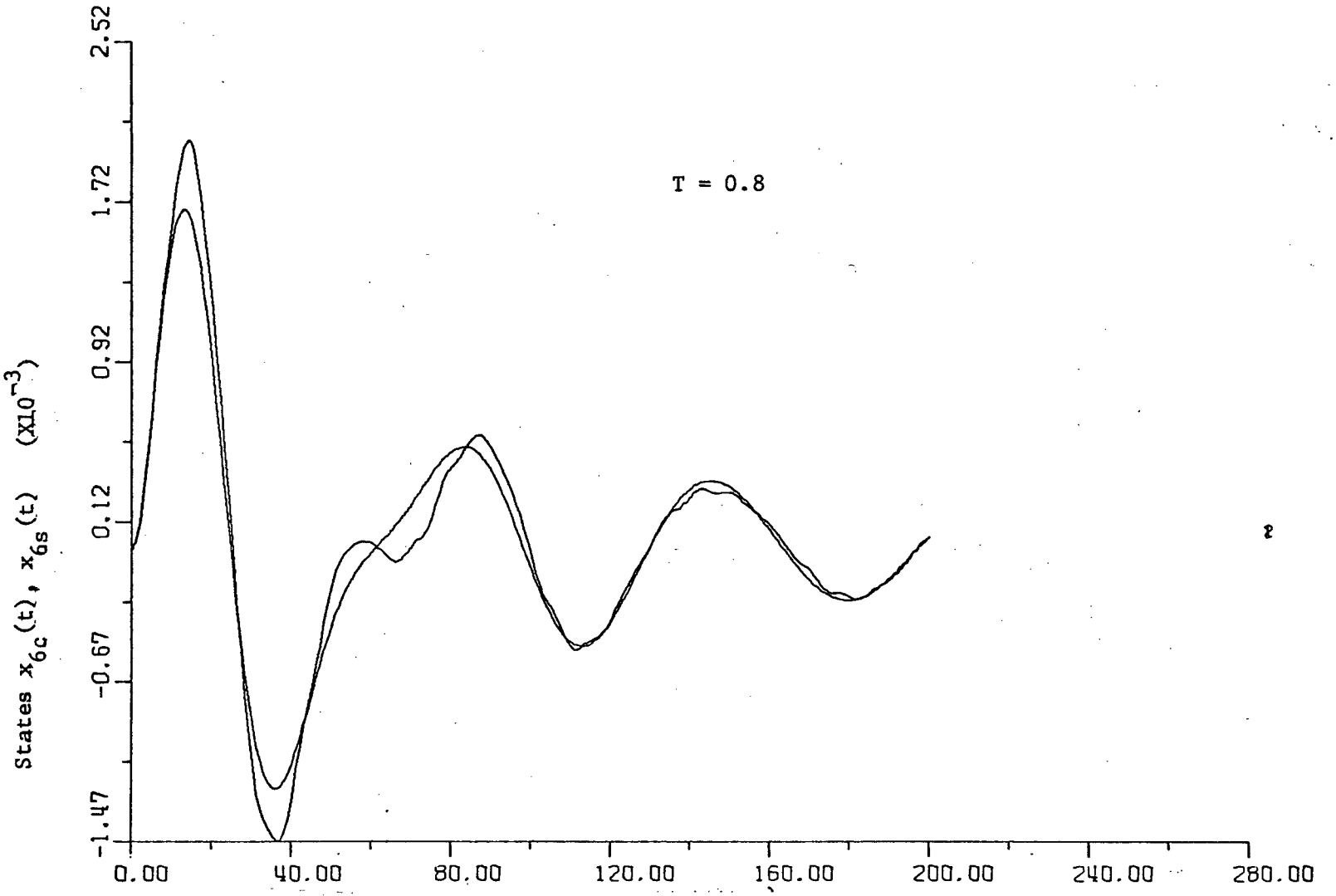

Figure 6-20 State trajectories $x_{6c}(t)$ and $x_{6s}(t)$ for the 12th order model of the Spinning Skylab Satellite. Digital Redesign by the point by point method of partial matching.

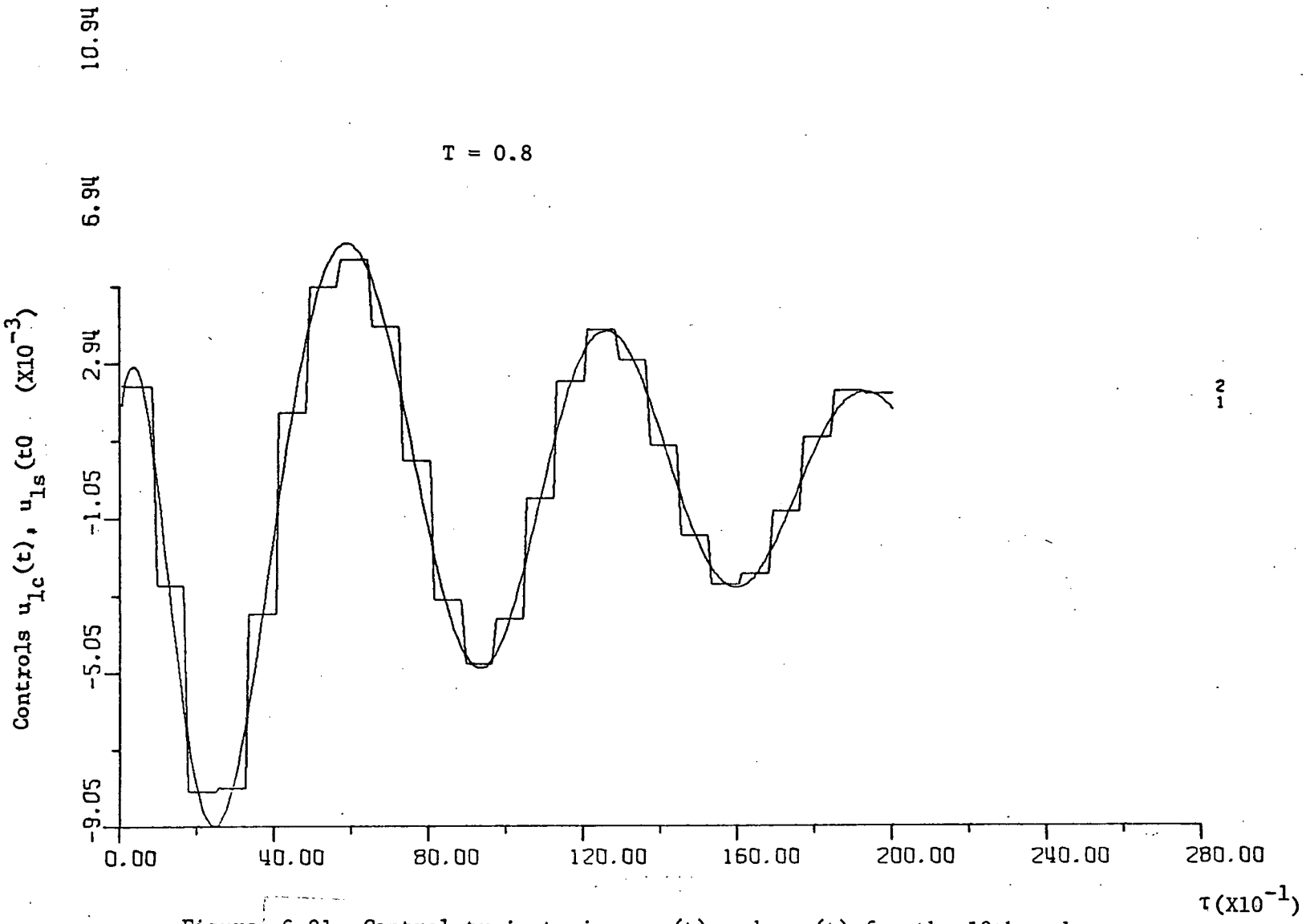

Figure 6-21 Control trajectories $u_{1c}(t)$ and $u_{1s}(t)$ for the 12th order model of the Spinning Skylab Satellite. Digital Redesign by the point by point method of partial matching.

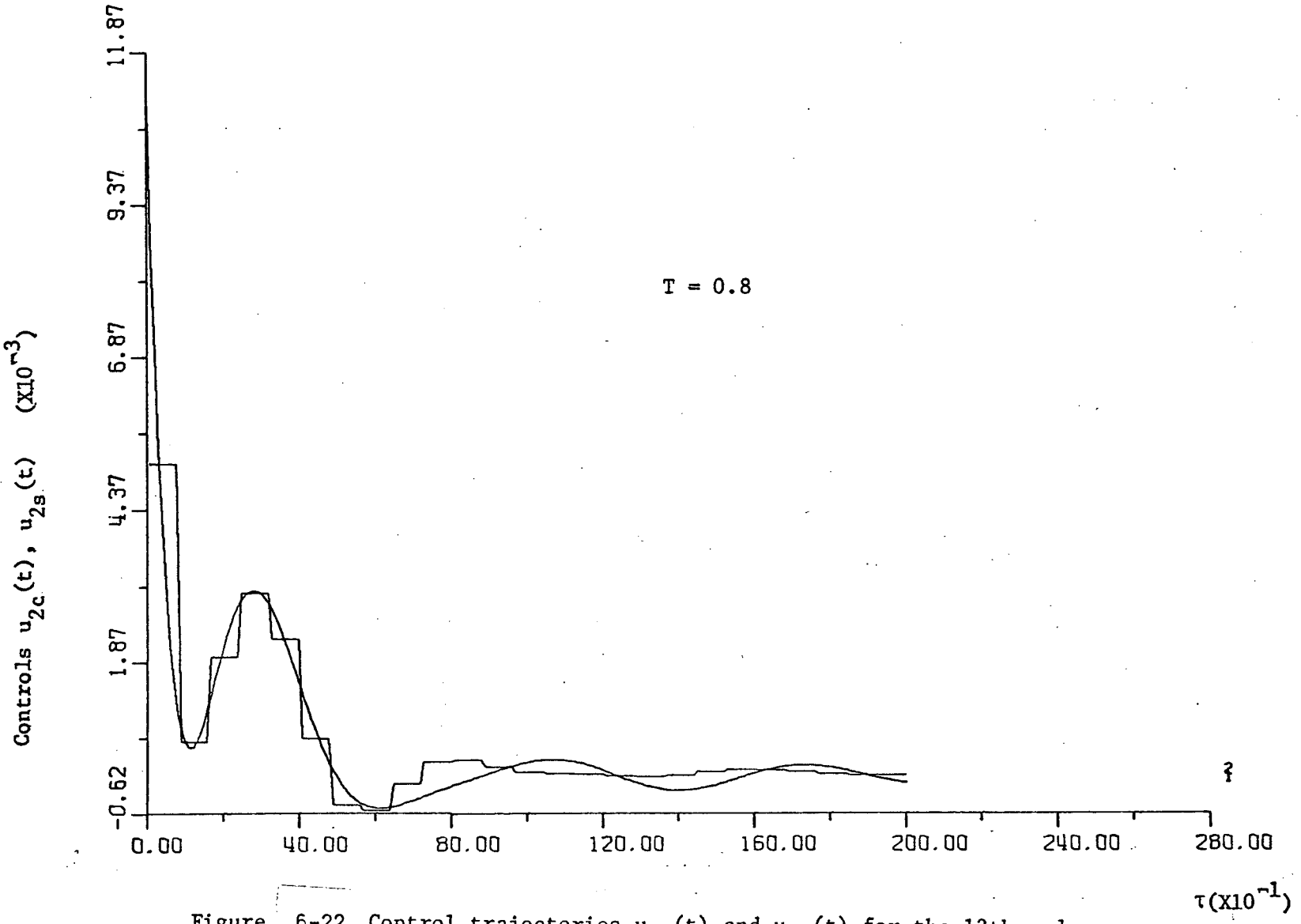

Figure 6-22 Control trajectories $u_{2c}(t)$ and $u_{2s}(t)$ for the 12th order model of the Spinning Skylab Satellite. Digital Redesign by the point by point method of partial matching.

7. ANALYSIS OF THE ATTITUDE DYNAMICS OF A LARGE SPACE TELESCOPE (LST) MODEL

7.1 Introduction

The problem considered in this report is the determination of the condition of limit cycle in the Large Space Telescope (LST) using Control Moment Gyros (CMG's). Due to the on-board digital control system, the dynamics of the LST are represented by the sampled-data system of Figure 7-1.

A suitable model of the CMG is considered to be a combination of a nonlinear element and a linear element [6]. The simplified input-output relationship of the nonlinear element is shown in Figure 7-2.

One established method of predicting limit cycles in nonlinear sampled-data systems is the discrete describing function method [7]. The stability study of the LST system with k = 0 for the nonlinearity in Figure 7-2 can be readily predicted [12]. This report is concerned with the derivation of the discrete describing function when $k \neq 0$ in Figure 7-2.

Specific system models have been considered by NASA, and these are listed below:

Case I. (First-order CMG, perfect attitude rate sensor)

$H(s) = 1$ - perfect attitude rate sensor

$$G(s) = \frac{\omega_c}{s+\omega_c} \quad \text{first-order CMG} \tag{7-1}$$

Case II. (Second-order CMG, perfect attitude rate sensor)

$H(s) = 1$ perfect attitude rate sensor

$$G(s) = \frac{K_G}{s^2+g_1 s+g_0} \tag{7-2}$$

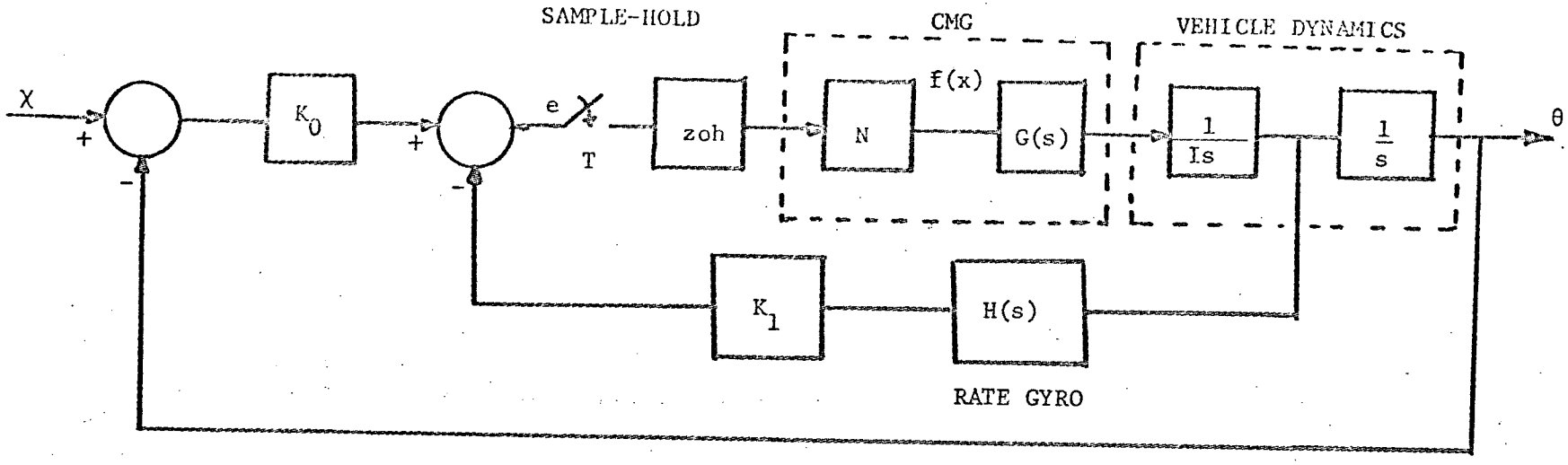

Figure 7-1

I = Vehicle moment of inertia about the chosen axis

K_0 = control gain for θ

K_1 = control gain for $\dot{\theta}$

H(s) = transfer function of attitude rate sensor, rate gyro

G(s) = linear transfer function of CMG

N = nonlinear portion of CMG

χ = command

θ = actual vehicle attitudes

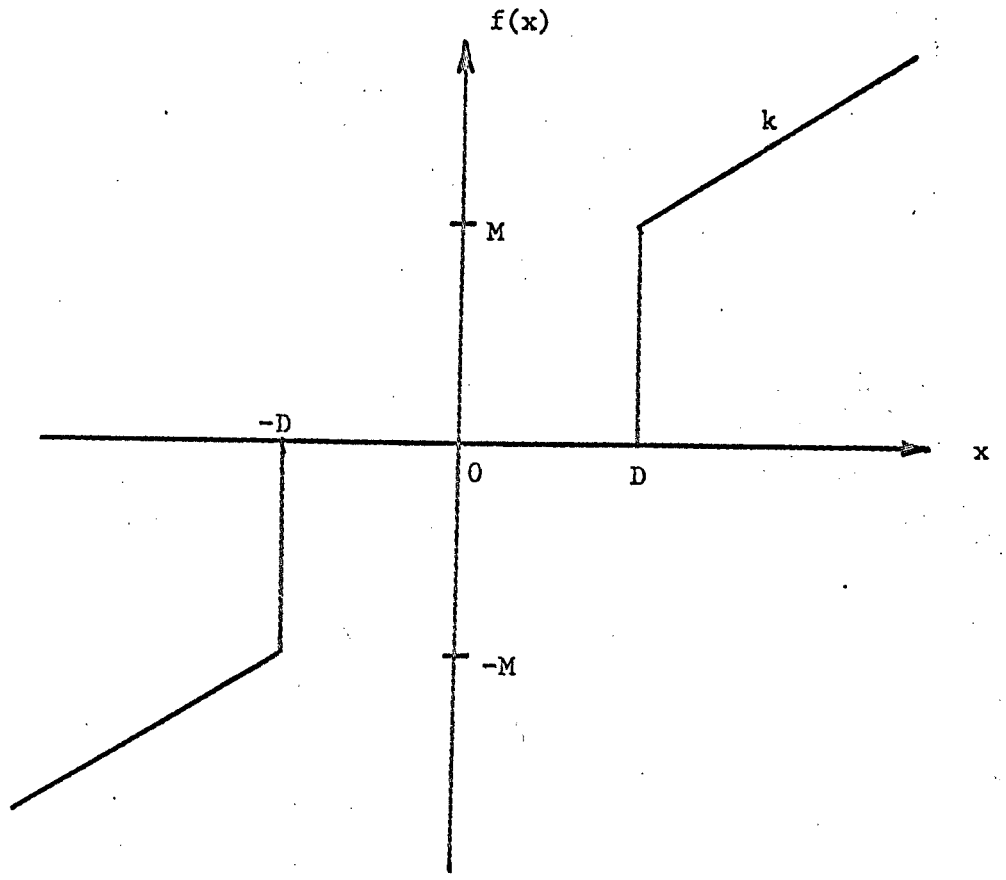

Figure 7-2

Case III. (First-order CMG, first-order attitude rate gyro)

$$H(s) = \frac{\omega_g}{s+\omega_g} \quad \text{imperfect attitude rate sensor} \tag{7-3}$$

$$G(s) = \frac{\omega_c}{s+\omega_c} \tag{7-4}$$

Case IV. (Second-order CMG, first-order rate gyro)

$$H(s) = \frac{\omega_g}{s+\omega_g} \tag{7-5}$$

$$G(s) = \frac{K_G}{s^2+g_1 s+g_0} \tag{7-6}$$

List of System Parameters

$I = 1.356 \times 10^5$ Nms

$K_0 = 4.6843 \times 10^6$ Nm

$K_1 = 1.1153 \times 10^6$ Nms

$g_0 = K_G = 10^4$ $(\text{rad/s})^2$

$g_1 = 141.4$ rad/s

$\omega_c = 70.7$ rad/s

$\omega_g = 30$ rad/s

For the purpose of stability analysis, the system shown in Figure 7-1 can be represented by the equivalent system of Figure 7-3. The two systems are equivalent in the sense that the characteristic equations are identical. The equivalent transfer function of the system shown in Figure 7-3 is given by

$$G_e(s) = \frac{K_0+K_1 H(s)s}{Is^2} G(s) \tag{7-7}$$

Thus, for the four cases listed previously,

$$\text{Case I.} \quad G_e(s) = \frac{(K_1 s+K_0)\omega_c}{Is^2(s+\omega_c)} \tag{7-8}$$

$$\text{Case II.} \quad G_e(s) = \frac{(K_1 s+K_0)K_G}{Is^2(s^2+g_1 s+g_0)} \tag{7-9}$$

$$\text{Case III.} \quad G_e(s) = \frac{K_0 s+K_0\omega_g+K_1\omega_g s}{Is^2(s+\omega_c)(s+\omega_g)}\omega_c \tag{7-10}$$

$$\text{Case IV.} \quad G_e(s) = \frac{K_0 s+K_0\omega_g+K_1\omega_g s}{Is^2(s^2+g_1 s+g_0)(s+\omega_g)}K_G \tag{7-11}$$

7.2 The Discrete Describing Function (DDF)

The discrete describing function may be used to determine the condition of sustained oscillation in a nonlinear sampled-data system of Figure 7-3 It is assumed that the reference input $\chi(t)$ is zero, and the actuating signal e(t) is sinusoidal with period $T_c = nT$, where n = 2, 3, 4, ..., and T is the sampling period in seconds. This assumption is justified, since, in practice, $G_e(s)$ has the characteristics of a low-pass filter.

From the analytical standpoint, an equivalent system of Figure 7-4 is used to replace the block diagram of Figure 7-3 In Figure 7-4 the zero-order hold (zoh) and the nonlinearity are transposed. This does not affect the system behavior if the nonlinear element is amplitude dependent only. However, the nonlinearity must be redefined to act on the strength of impulses.

The closed-loop transfer function of the system of Figure 7-4 is

$$\frac{\theta(z)}{\chi(z)} = \frac{N(z)G(z)}{1+N(z)G(z)} \tag{7-12}$$

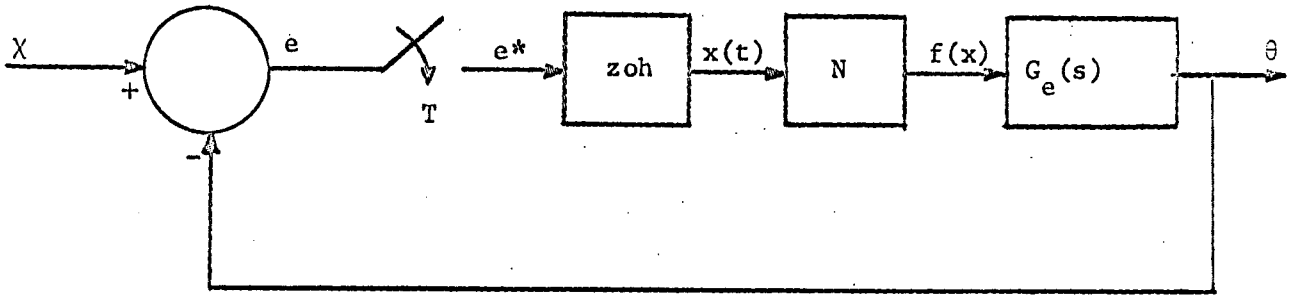

Figure 7-3

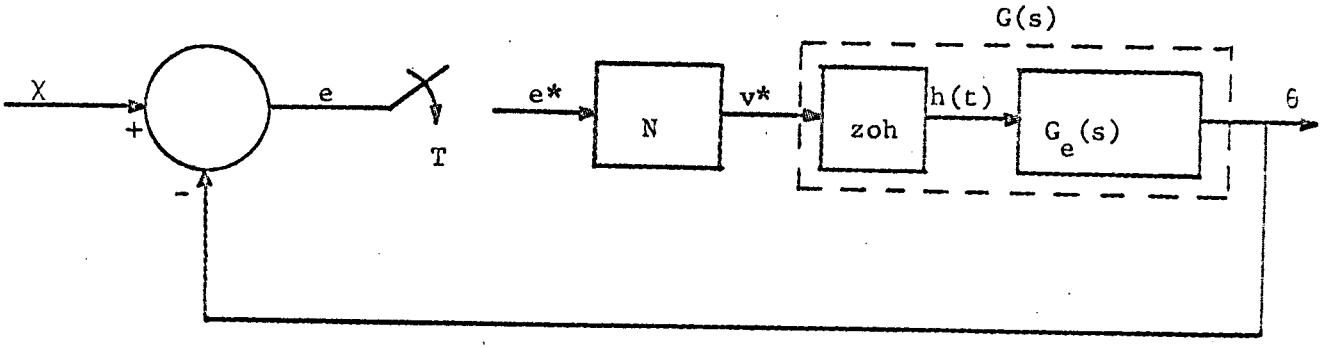

Figure 7-4

where

$$G(z) = z\left[\frac{1-e^{-Ts}}{s} G_e(s)\right]$$

$$= (1 - z^{-1})z[G_e(s)/s] \qquad (7\text{-}13)$$

and N(z) is defined as the DDF; i.e.,

$$N(z) = V(z)/E(z) \qquad (7\text{-}14)$$

As in the conventional describing function technique, self-sustained oscillation occurs in the system when the following equation is satisfied:

$$1 + N(z)G(z) = 0 \qquad (7\text{-}15)$$

or

$$G(z) = -1/N(z) \qquad (7\text{-}16)$$

The derivation of the DDF of a nonlinear element is based on the assumption that the input to N is a sinusoidally amplitude-modulated impulse train. The output of N is also a train of impulses, but with the strengths of the impulses determined by the nonlinear characteristics.

Let the input to the sampler be

$$e(t) = E \cos (\omega_c t + \phi) \qquad (7\text{-}17)$$

The z-transform of the last equation is

$$E(z) = \frac{Ez[(z - \cos \omega_c T) \cos \phi - \sin \omega_c T \sin \phi]}{z^2 - 2z \cos \omega_c T + 1} \qquad (7\text{-}18)$$

The period of the self-sustained oscillations is designated by T_c, where

$$T_c = 2\pi/\omega_c = NT \qquad (7\text{-}19)$$

and N = 2, 3, 4, ... In addition to the characterization of the oscillations by T_c, we need to classify the response with respect to the waveform of h(t)

which is the output of the zoh. Since e(t) is a sinusoid, it can be shown that for all $T_c = NT$, N = even integers, the number of positive relay corrections is equal to that of the negative relay corrections during one period T_c. This number of correction is designated by $\Delta = (i, j)$, where i is the number of positive relay corrections, and j is the number of negative relay corrections, during each period T_c. For $T_c = 2T$, it is apparent that Δ can only be (1,1). For $T_c = 4T$, $\Delta = (1,1)$, or (2,2). For N = odd integers, the number of positive and negative relay corrections may differ by one. Therefore, in the representation for Δ, i and j may not be equal.

For a given period T_c, the loci of $-\frac{1}{N(z)}$ form regions in the magnitude versus phase domain, each for one possible Δ or Δ_{ij}. These regions are defined as the critical regions for the specific nonlinearity, T_c, and Δ. The symbols, $-\frac{1}{N}\Big|_{max}$ and $-\frac{1}{N}\Big|_{min}$ are used to indicate the boundaries of the critical region. The condition of self-sustained oscillation in the system of Figure 7-4 is determined with the graphical procedure described as follows:

1. Plot G(z) in the gain-phase (db-degrees) coordinates for $T_c = 2T, 3T, 4T, \ldots$ using T as a parameter on the loci.
2. Superpose on the G(z) plot the family of critical regions of $-\frac{1}{N(z)}$ for $T_c = 2T, 3T, 4T, \ldots$.
3. If the portion of the G(z) locus for some T_c falls within the critical region of the same T_c, then there exists a set of E, ϕ, Δ, such that Eq. (7-16) is satisfied. Consequently, self-sustained oscillations characterized by the Δ, E, ϕ, and T_c will occur for the range of T which corresponds to the portion of G(z) found inside the critical region.

4. The sampling periods T along the portion of G(z) locus outside the critical region of the same T_c and some Δ correspond to operations which will not give rise to self-sustained oscillations of the prescribed mode.

The typical procedure of deriving the critical region for the nonlinearity of Figure 7-2 for $k \neq 0$ is described in the following section for $T_c = 3T$, or $N = 3$, for all possible combinations of Δ. The procedure for generating the gain-phase plots of G(z) is described in a later section.

7.3 Derivation of the Critical Regions

In this section, the sample derivation of the critical regions for the nonlinearity of Figure 7-2 for $k \neq 0$ and for $N = 3$ is described. All the possible Δ values $\Delta_r = (1,0), (1,1), (1,2)$ are considered.

The input to the sampler, e(t), is assumed to be a sinusoid as described by Eq. 7-17 , and is repeated here,

$$e(t) = E \cos (\omega_c t + \phi) \tag{7-20}$$

The z-transform of e(t) is

$$E(z) = \frac{Ez[(z - \cos \omega_c T) \cos \phi - \sin \omega_c T \sin \phi]}{z^2 - 2z \cos \omega_c T + 1} \tag{7-21}$$

The period of self-sustained oscillations, T_c is given by

$$T_c = \frac{2\pi}{\omega_c} = NT \tag{7-22}$$

For $N = 3$, $T_c = 3T$ and $\omega_c = \frac{2\pi}{3T}$.

Then $$z = e^{j\omega_c T} = e^{j2\pi/3} = -0.5 + j0.866 \tag{7-23}$$

and Eq. (7-21) becomes

$$E(z) = \frac{Ez[(z+.5)\cos\phi - .866\sin\phi]}{z^2 + z + 1} \qquad (7\text{-}24)$$

The waveform for e(t) is shown in Figure 7-5 for $\phi = 0$. Figure 7.6 shows the corresponding waveforms of v*(t) for $\Delta = (1, 0)$, $(1, 1)$ and $(1, 2)$.

For $\Delta = (1, 0)$:

The z-transform of v*(t) is

$$V(z) = [M + k(E\cos\phi - D)][1 + z^{-3} + z^{-6} + \ldots]$$

$$= [M + k(E\cos\phi - D)]\left(\frac{z^3}{z^3-1}\right) \qquad (7\text{-}25)$$

The restrictions on E for this mode to exist are

$$\begin{aligned} -30 < \phi \leq 0° \qquad & E\cos\phi > D \\ & E\cos(60+\phi) < D \\ 0 \leq \phi < 30° \qquad & E\cos\phi > D \\ & E\cos(60-\phi) < D \end{aligned} \qquad (7\text{-}26)$$

which lead to the following upper and lower bounds on E

$$-30° < \phi \leq 0 \qquad E_{min} = \frac{D}{\cos\phi}, \qquad E_{max} = \frac{D}{\cos(60+\phi)}$$

$$0 \leq \phi < 30° \qquad E_{min} = \frac{D}{\cos\phi}, \qquad E_{max} = \frac{D}{\cos(60-\phi)} \qquad (7\text{-}27)$$

For $\Delta = (1,1)$:

The z transform of v*(t) is

$$V(z) = [M + k(E\cos\phi - D)]\left[\frac{z^3}{z^3-1}\right]$$

$$- [M + k(E\cos(60+\phi) - D)]\left[\frac{z}{z^3-1}\right] \qquad (7\text{-}28)$$

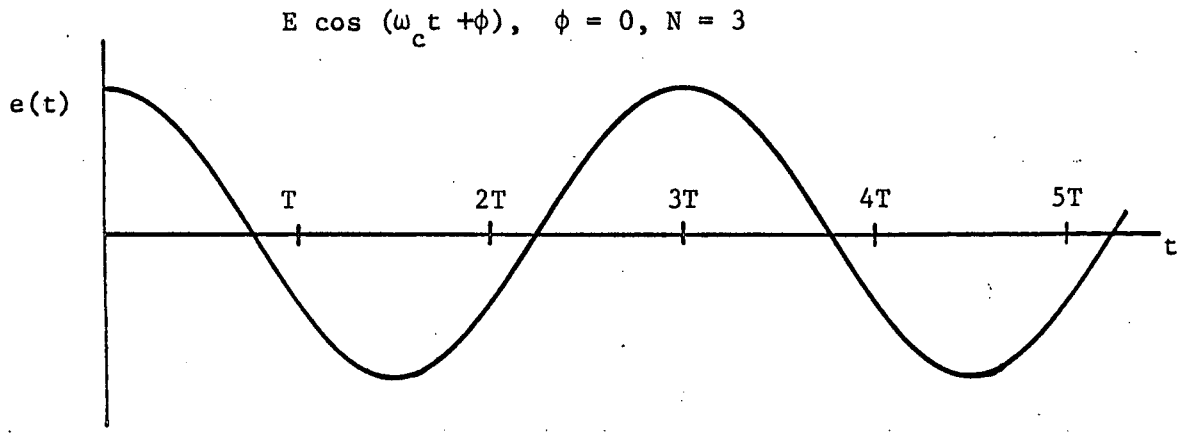

Figure 7-5

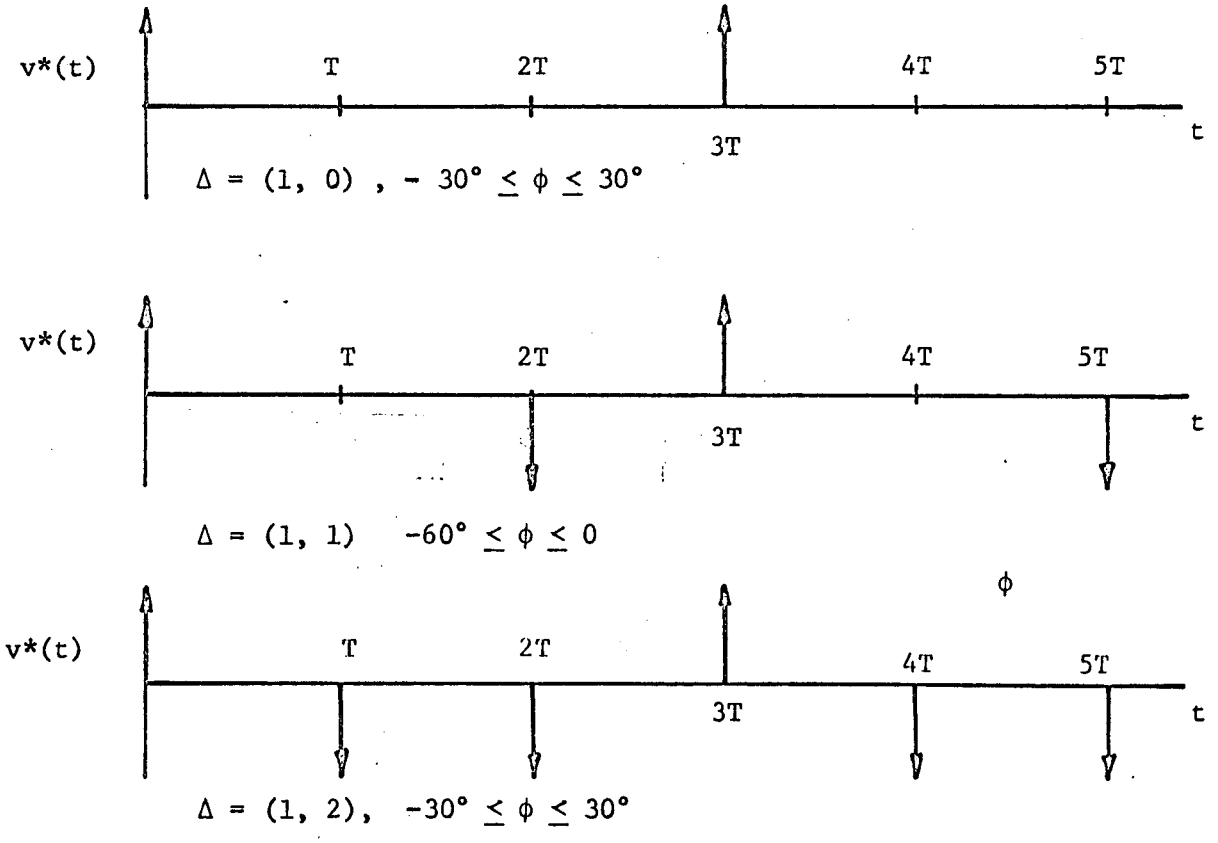

Figure 7-6

with the following restrictions on E:

$$\begin{aligned} -30° < \phi \leq 0 \qquad & E \cos (60 + \phi) > D \\ & E \cos (60 - \phi) < D \\ -60° < \phi \leq -30° \qquad & E \cos \phi > D \\ & E \cos (120 + \phi) < D \end{aligned} \tag{7-29}$$

The corresponding bounds on E are

$$\begin{aligned} -30° < \phi \leq 0 \qquad & E_{min} = \frac{D}{\cos(60+ \phi)} \\ & E_{max} = \frac{D}{\cos(60-\phi)} \\ -60° < \phi \leq -30° \qquad & E_{min} = \frac{D}{\cos \phi} \\ & E_{max} = \frac{D}{\cos(120+\phi)} \end{aligned} \tag{7-30}$$

For $\Delta = (1,2)$:

The z-transform of v*(t) is

$$\begin{aligned} V(z) = [M + k (E \cos \phi - D)] \left[\frac{z^3}{z^3-1}\right] \\ - [M + k (E \cos (60 - \phi) - D)] \left[\frac{z^2}{z^3-1}\right] \\ - [M + k (E \cos (60 + \phi) - D)] \left[\frac{z}{z^3-1}\right] \end{aligned} \tag{7-31}$$

with the restrictions on E being

$$\begin{aligned} -30° < \phi \leq 0 \qquad & E \cos(60 - \phi) > D \\ 0 \leq \phi < 30° \qquad & E \cos(60 + \phi) > D \end{aligned} \tag{7-32}$$

and the corresponding bounds on E being

$$\begin{aligned} -30° < \phi \leq 0 \qquad & E_{min} = \frac{D}{\cos(60-\phi)} \\ & E_{max} = \infty \\ 0 \leq \phi < 30° \qquad & E_{min} = \frac{D}{\cos(60+\phi)} \\ & E_{max} = \infty \end{aligned} \tag{7-33}$$

Using E(z) from Eq. (7-24) and V(z) from Eqs. (7-25),(7-28) and (7-31) the expressions for $-\frac{1}{N(z)}$ are as follows:

For $\Delta = (1,0)$,

$$-\frac{1}{N(z)} = -\frac{E(z)}{V(z)} = \frac{-E(z-1)((z+.5)\cos\phi - .866 \sin\phi)}{z^2[M + k(E\cos\phi - D)]} \tag{7-34}$$

For $\Delta = (1,1)$,

$$-\frac{1}{N(z)} = \frac{-E(z-1)((z+.5)\cos\phi - .866 \sin\phi)}{z^2[M+k(E\cos\phi - D)] - [M+k(E\cos(60+\phi) - D)]} \tag{7-35}$$

For $\Delta = (1,2)$,

$$-\frac{1}{N(z)} = \frac{-E(z-1)((z+.5)\cos\phi - .866 \sin\phi)}{z^2[M+k(E\cos\phi - D)] - z[M+k(E\cos(60-\phi) - D)] - [M+k(E\cos(60+\phi) - D)]} \tag{7-36}$$

With $z = -0.5 + j0.866$, Eqs.(7-34),(7-35) and (7-36) can be written as

$$-\frac{1}{N(z)} = \frac{1.5E \angle -120+\phi}{(bm + cE) + j(dm + fE)} \qquad (7\text{-}37)$$

where $m = M - kD$, and the coefficients b, c, d, f are defined in the following table.

Table 7-1

Δ	1, 0	1, 1	1, 2
b	0.5	1.5	0
c	$0.5k\cos\phi$	$k(0.5\cos\phi + \cos(60+\phi))$	$k(0.5\cos\phi - 0.5\cos(60-\phi) + \cos(60+\phi))$
d	0.866	.866	0.
f	$0.866k\cos\phi$	$0.866k\cos\phi$	$0.866k(\cos\phi + \cos(60-\phi))$

The critical region for each Δ is the area enclosed by the $-\frac{1}{N(z)}$ locus in the gain-phase plane, as E and ϕ are varied over their admissible ranges (defined by Eqs. (7-27),(7-30) or (7-33) for that Δ).

The procedure used to generate a critical region is as follows:

1. Choose a value of ϕ in the admissible range.
2. Using this ϕ in Eq. (7-37) determine the extremums of the magnitude and phase of $-\frac{1}{N}(z)$ as a function of E, with E restricted to its admissible range.
3. Plot these extremums in the gain-phase plane and repeat the procedure for all possible ϕ's. The region generated by this plot will be the critical ϕ region. Figures 7-14,7-15 and 7-16 show the critical regions for N = 3, Δ = (1, 0), (1, 1) and (1, 2), respectively, for several values of M, k, and D.

It should be noted that the extremums necessary in step 2 above can in fact be easily obtained by use of the upper and lower bounds of E [Eqs. (7-27),(7-30) and (7-33)]. Also, the extreme magnitude and extreme phase occur simultaneously. This result is now proved by use of the expression in Eq. (7-37).

The magnitude of $-\frac{1}{N}$, as it is defined in Eq. (7-37) is

$$\left|-\frac{1}{N}\right| = \left(\frac{2.25E^2}{(bm+cE)^2 + (dm+fE)^2}\right)^{\frac{1}{2}} \qquad (7\text{-}38)$$

Since it is easier to work with $\left|-\frac{1}{N}\right|^2$, the extremums of $\left|-\frac{1}{N}\right|^2$ (which are also the extremums of $\left|-\frac{1}{N}\right|$) will be determined.

$$\text{Let} \quad F = \left|-\frac{1}{N}\right|^2 = \frac{2.25\ E^2}{(bm + cE)^2+(dm + fE)^2} \qquad (7\text{-}39)$$

If F has any extremums, they must satisfy the following necessary condition:

$$\frac{\partial F}{\partial E} = 0 = \frac{4.5mE[(b^2+d^2)m + (bc+df)E]}{[(bm+cE)^2 + (dm+fE)^2]^2} \qquad (7\text{-}40)$$

which gives

$$E = 0$$

or

$$E = -\frac{(b^2+d^2)m}{bc+df} \qquad (7\text{-}41)$$

In the above results, E = 0 represents a minimum, while $E = -(b^2+d^2)m/(bc+df)$ represents a maximum. Let this latter value of E be denoted as E_x.

With $E = E_x$, the value of $F = \left|-\frac{1}{N}\right|^2$ is

$$F_x = \frac{2.25(b^2+d^2)}{(cd-bf)^2} \qquad (7\text{-}42)$$

For the admissible ranges of ϕ, it is seen that the following properties of the coefficients are true for all three values of Δ:

$$b \geq 0$$

$$c > 0$$

$$d \geq 0$$

$$f > 0 \qquad (7\text{-}43)$$

Using Eq. (7-41),

$$E_x < 0 \quad \text{if} \quad m > 0 \ (M > kD)$$

$$E_x > 0 \quad \text{if} \quad m < 0 \ (M < kD) \qquad (7\text{-}44)$$

By physical considerations, the upper and lower bounds of E, which also define the admissible ranges of E, are always positive. Thus $E_x < 0$ is only one of academic importance.

Figures 7-7 and 7-8 show the typical behavior of F, with positive and negative values of m, respectively. The asymptotic values of F, as $E \to \pm \infty$, are described by

$$F_\infty = \frac{2.25}{c^2+f^2} \qquad (7\text{-}45)$$

Also, it can be shown that $F_x \geq F_\infty$ for all values of b, c, d, f.

With N = 3 and any Δ, it can be shown that E_x is less than the upper and lower bounds of E. Thus, for the admissible ranges of ϕ, F, and, consequently, $\left|-\frac{1}{N}\right|$, are always monotonic in E. The maximum and minimum values of $\left|-\frac{1}{N}\right|$ are, therefore, obtained by use of (i) the allowable maximum and minimum values of E, respectively, if $m < 0$, or (ii) the allowable minimum and maximum values of E, respectively, if $m > 0$.

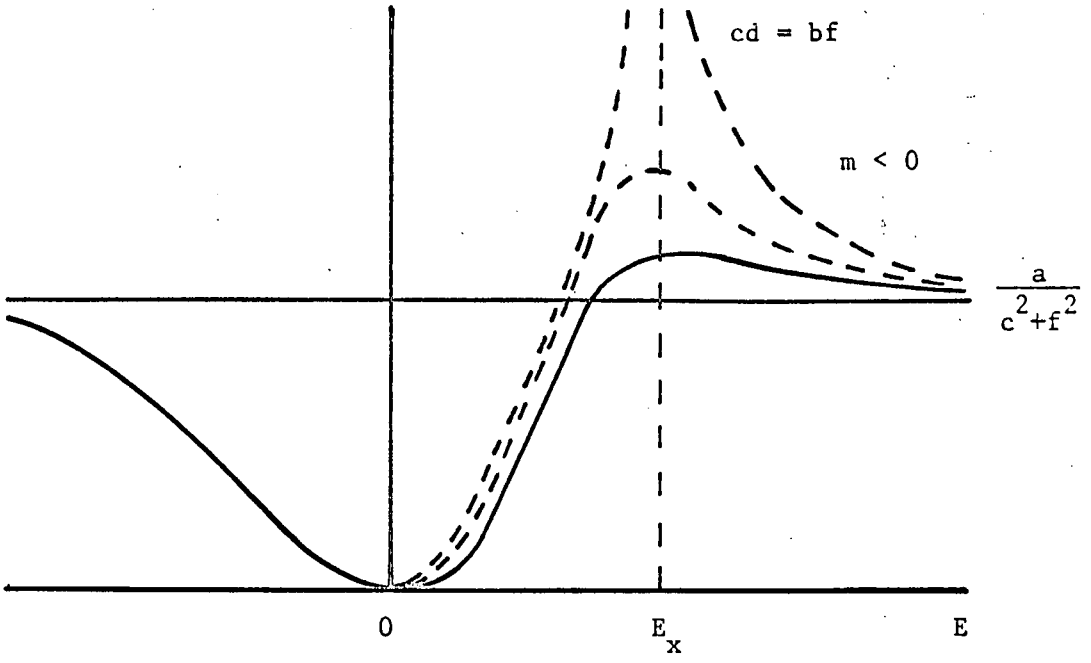

Figure 7-7

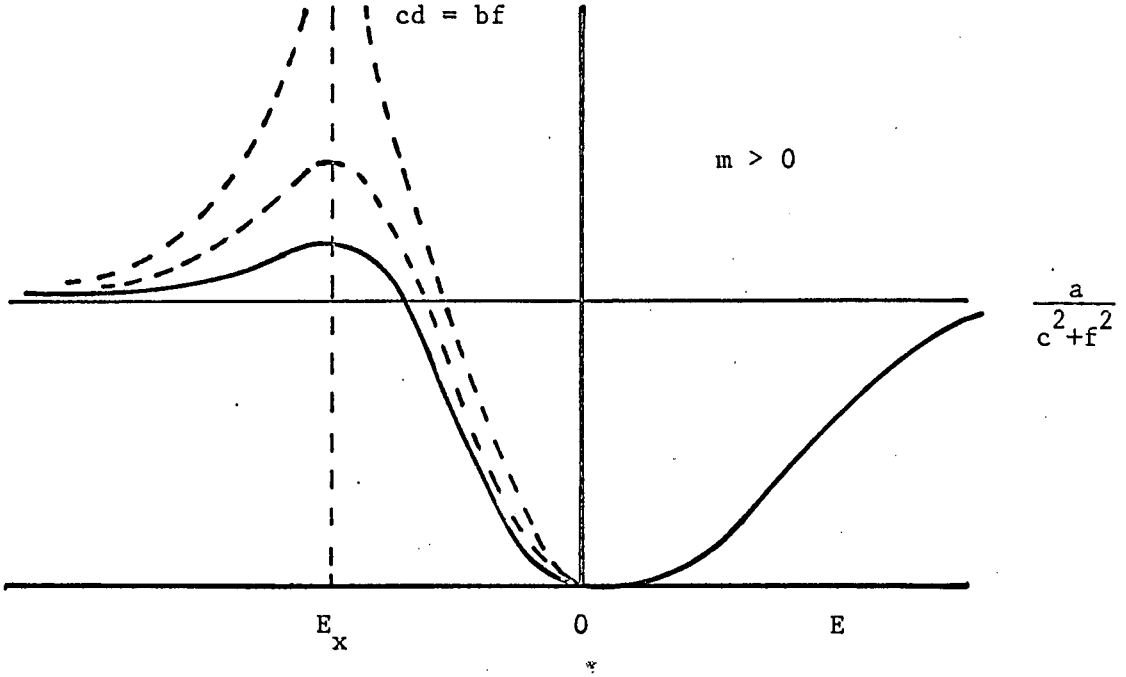

Figure 7-8

The phase of $-\frac{1}{N}$ from Eq. (7-37) is

$$\theta = \left| -\frac{1}{N} \right. = -120° + \phi - \tan^{-1}\left(\frac{dm+fE}{bm+cE}\right) \qquad (7\text{-}46)$$

Let $g = \frac{dm+fE}{bm+cE}$ and $\psi = \tan^{-1} g$, then, at constant ϕ, the maximum and minimum of the phase of $-\frac{1}{N}$ or θ is determined by the minimum and maximum, respectively, of ψ. For ψ in the range $\pm 90°$, this is determined by minimum and maximum of g.

Thus, θ has only one extremum, and this is when

$$E = E_y = -\frac{bm}{c} \qquad (7\text{-}47)$$

Figures 7-9 through 7-12 show several typical plots of g with $m > 0$ and $m < 0$. With $N = 3$ and any Δ, it can be shown that E_y is less than the upper and lower bounds of E. Thus, for the admissible ranges of ϕ, θ is monotonic in E. The maximum and minimum values of the phase of $-\frac{1}{N}$ are, therefore, also obtained by use of the maximum and minimum values of E. The roles of maximum and minimum can be reversed, depending on the sign of m and the sign of $(\frac{d}{b} - \frac{f}{c})$.

The above results can be extended to all the cases for $N > 3$, if the corresponding expressions are appropriately modified. The number of modes and the ranges of ϕ will of course be different for different N.

The expressions for $-1/N(z)$ for $N = 2$ through $N = 8$ have been derived and are tabulated in Tables 7-2 through 7-8.

The critical regions for $N = 2$ through $N = 8$ are drawn in Figures 7-13 through 7-37, for several combinations of k, M, and D.

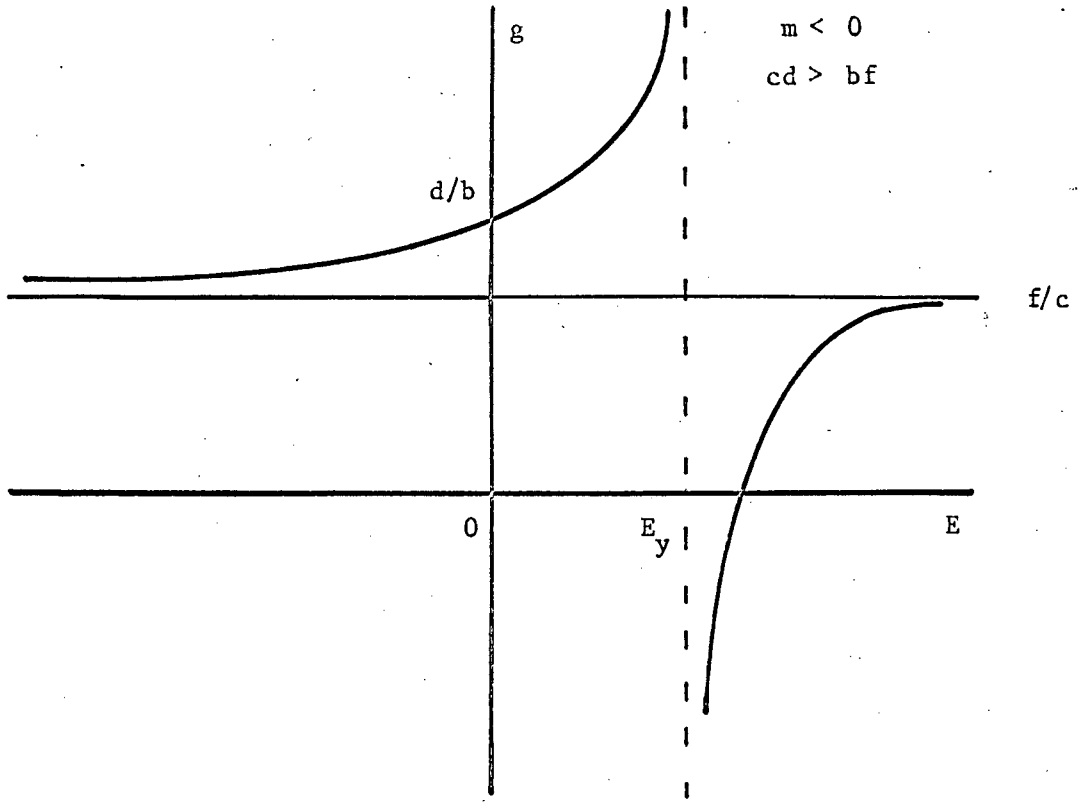

Figure 7-9

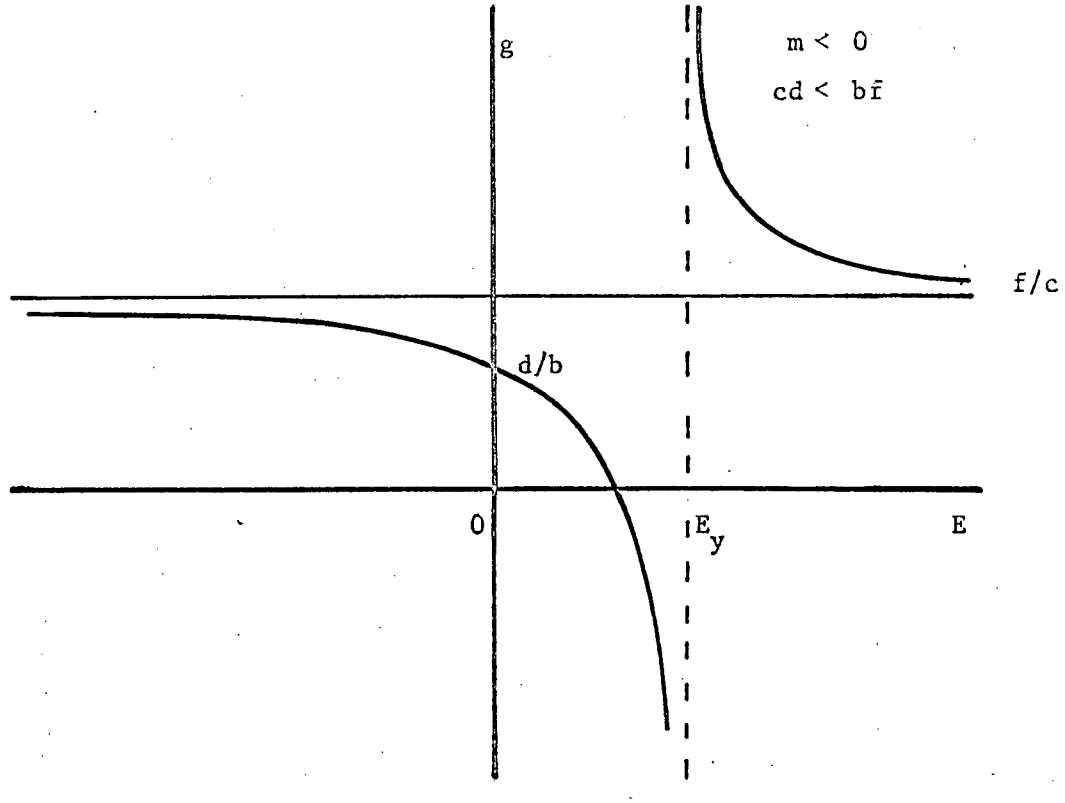

Figure 7-10

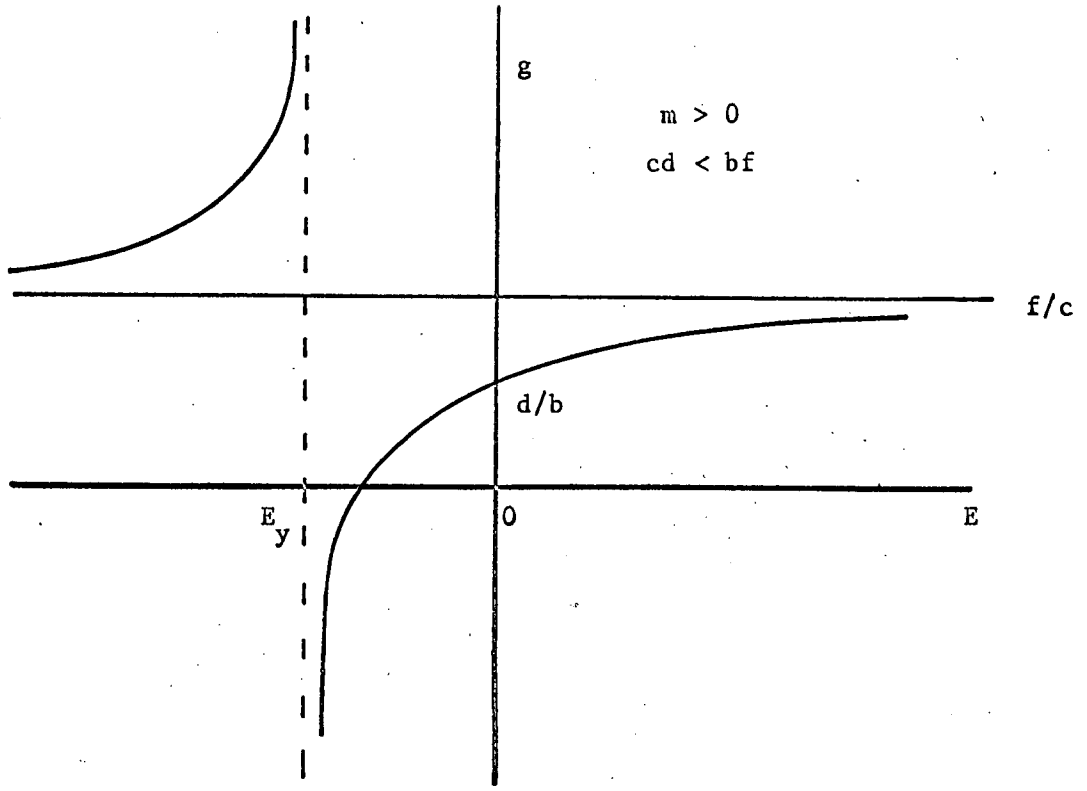

Figure 7-11

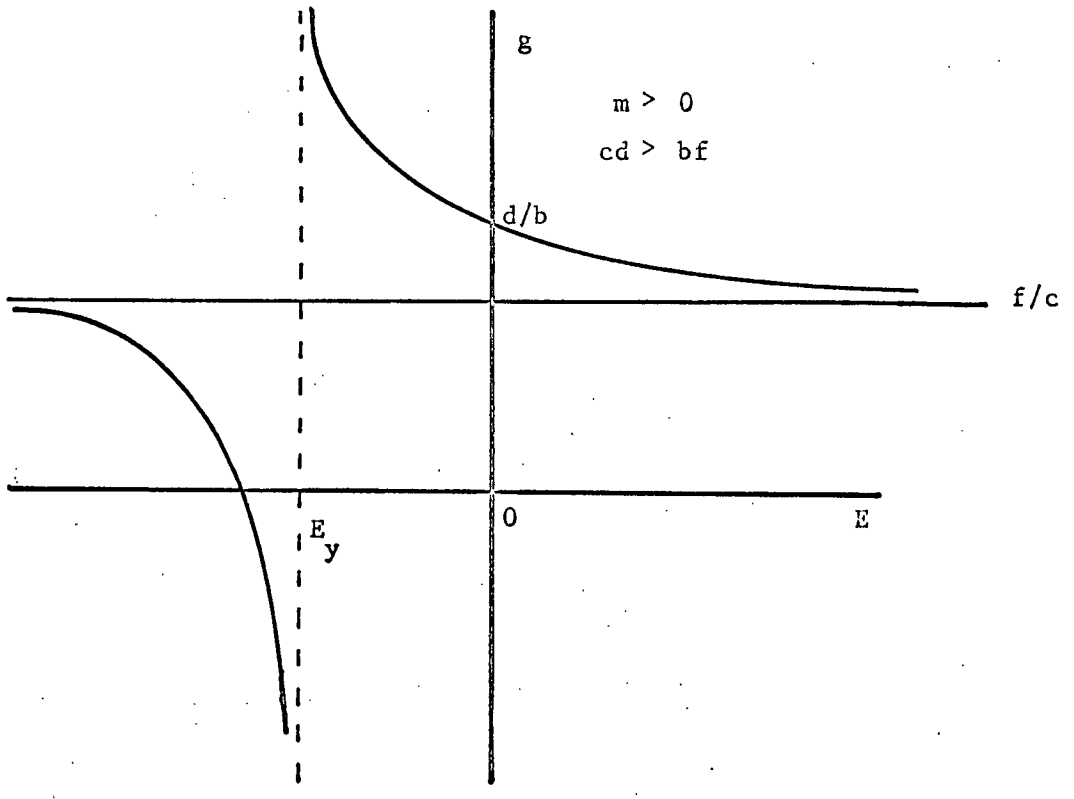

Figure 7-12

Examination of these critical regions leads to the following conclusions:

(1) Unlike the critical regions for relay with dead zone (k=0), the critical regions for the nonlinearity in Figure 7-2 cannot be normalized in amplitude with respect to D/M.

(2) The critical regions bounded by the loci of $-\left.\frac{1}{N}\right|_{min}$ and $-\left.\frac{1}{N}\right|_{max}$ are symmetrical about the -180-degree axis. The maximum span of the horizontal width of these regions is given by $2\pi T/T_c = 2\pi/N$ for N = all even integers ≥ 4, and $\pi T/T_c = \pi/N$, for N = odd integers ≥ 3. When N increases the critical regions become narrower, and finally approach to a straight line along the -180-degree axis when $N = \infty$.

(3) Since the objective of a great majority of system design problems is to arrive at a stable system, for a given system whose transfer function G(z) is plotted in the magnitude versus phase plot, it is necessary and sufficient that for a given sampling period T none of the G(z) points coincides with the corresponding critical regions.

In general, for a quick check on stability, rectangular regions bounded by the widths given in item (2) may be used as a necessary condition for stability. However, it should be noted that the nonlinear system with $k \neq 0$ has less chance of going into self-sustained oscillations than the case when $k = 0$.

The loci for G(z) for the four cases of the LST system model are plotted in Figures 7-38 through 7-47 for N = 2 through 8. The transfer functions for these models are tabulated below. In all these cases, the expressions for $G_e(s)$ are given. Then $G(s) = G_{h0}(s)G_e(s)$ is expanded by partial fraction expansion into the following form:

$$G(s) = (1 - e^{-Ts})\left(\frac{a_3}{s^3} + \frac{a_2}{s^2} + \frac{a_1}{s} + \frac{b_1}{s+b} + \frac{c_1}{s+c} + \frac{d_1}{s+d} \right) \tag{7-48}$$

where

$$G_{h0}(s) = \frac{1-e^{-Ts}}{s} \tag{7-49}$$

The z-transform of G(s) is written

$$G(z) = z[G(s)] = (1-z^{-1})\ z\left[\frac{a_3}{s^2} + \frac{a_2}{s^2} + \frac{a_1}{s} + \frac{b_1}{s+b} + \frac{c_1}{s+c} + \frac{d_1}{s+d}\right]$$

$$= (z-1)\left[\frac{a_3T^2(z+1)}{2(z-1)^3} + \frac{a_2T}{(z-1)^2} + \frac{a_1}{z-1} + \frac{b_1}{z-e^{-bT}} + \frac{c_1}{z-e^{-cT}} + \frac{d_1}{z-e^{-dT}}\right] \tag{7-50}$$

Case I.

$$G_e(s) = \frac{(K_1s+ K_0)\omega_c}{Is^2(s+\omega_c)} = \frac{581.5023\ (s+4.2)}{s^2(s + 70.7)} \tag{7-51}$$

Case II.

$$G_e(s) = \frac{(K_1s + K_0)K_G}{Is^2(s^2+g_1s+g_0)} = \frac{82249(s+4.2)}{s^2(s^2+141.4s+10^4)} \tag{7-52}$$

Case III.

$$G_e(s) = \frac{(K_0 + K_1\omega_g)s + K_0\omega_g}{Is^2(s+\omega_c)(s+\omega_g)}\ \omega_c$$

$$= \frac{19887.4(s+3.6842)}{s^2(s^2+100.7s+2121)} \tag{7-53}$$

Case IV.

$$G_e(s) = \frac{(K_0 + K_1\omega_g)s + K_0\omega_g}{Is^2(s^2+g_1s+g_0)(s+\omega_g)}\ K_G$$

$$= \frac{281.2928 \times 10^4(s+3.6842)}{s^2(s^3+171.4s^2+14242s+3 \times 10^5)} \tag{7-54}$$

CASE	a_3	a_2	a_1	b_1	c_1	d_1	b	c	d
I	34.544678	7.7363138	-0.10942453	0.10942453	0	0	+70.7	0	0
II	34.544586	7.7364483	-0.11284781	0.0564239 -j0.0017102	0.0564239 +j0.0017102	0	+70.7 -j70.7	+70.7 +j70.7	0
III	34.544632	7.7363682	-0.3835905	0.47625273	-0.0926622	0	+30	+70.7	0
IV	34.544629	7.736475	-0.38701315	0.41178255	-0.0123846 -j0.0202611	-0.01238466 +j0.0202611	+30	+70.7 -j70.7	+70.7 +j70.7

Table 7-2

$$N = 2$$

$$-\frac{1}{N(z)} = \frac{E\cos\phi}{M + k(E\cos\phi - D)}$$

$$E_{min} = \frac{D}{|\cos\phi|} \qquad E_{max} = \infty$$

Table 7-3

$$N = 3$$

$$-\frac{1}{N(z)} = \frac{-E(z-1)[(z+0.5)\cos\phi - 0.866\sin\phi]}{az^2(M - kD + kE\cos\phi) + bz(M - kD + kE\cos(60-\phi)) + c(M - kD + kE\cos(60+\phi))}$$

Δ	a	b	c	ϕ	E_{min}	E_{max}
(1,0)	1	0	0	$-30^\circ \le \phi \le 0$	$D/\cos\phi$	$D/\cos(60+\phi)$
				$0 \le \phi \le 30^\circ$	$D/\cos\phi$	$D/\cos(60-\phi)$
(1,1)	1	0	-1	$-30^\circ \le \phi \le 0$	$D/\cos(60+\phi)$	$D/\cos(60-\phi)$
				$-60^\circ \le \phi \le -30^\circ$	$D/\cos\phi$	$D/\cos(120+\phi)$
(1,2)	1	-1	-1	$-30^\circ \le \phi \le 0$	$D/\cos(60-\phi)$	∞
				$0 \le \phi \le 30^\circ$	$D/\cos(60+\phi)$	∞

Table 7-4

$N = 4$

$$-\frac{1}{N(z)} = \frac{-E(z\cos\phi - \sin\phi)}{a(M - kD + kE\cos\phi) + b(M - kD - kE\sin\phi)}$$

Δ	a	b	ϕ	E_{min}	E_{max}
(1,1)	1	0	$-45° \leq \phi \leq 0$	$D/\cos\phi$	$D/-\sin\phi$
			$0 \leq \phi \leq 45°$	$D/\cos\phi$	$D/\sin\phi$
(2,2)	1	1	$-45° \leq \phi \leq 0$	$D/-\sin\phi$	∞
			$-90° \leq \phi \leq -45°$	$D/\cos\phi$	∞

Table 7-5

$N = 5$

$$-\frac{1}{N(z)} = \frac{-E(z-1)(z^2 - 2z\cos 4\pi/5 + 1)[(z - \cos 2\pi/5)\cos\phi - \sin 2\pi/5 \sin\phi]}{a z^4 (M - kD + kE\cos\phi) + b z^3 (M - kD + kE\cos(\phi + 2\pi/5))}$$
$$+ c z^2 (M - kD + kE\cos(\phi - \pi/5))$$
$$+ d z (M - kD + kE\cos(\phi + \pi/5))$$
$$+ e (M - kD + kE\cos(\phi - 2\pi/5))$$

Δ	a	b	c	d	e	ϕ	E_{min}	E_{max}
(1,0)	1	0	0	0	0	$-\frac{\pi}{10} \le \phi \le 0$	$D/\cos\phi$	$D/\cos(\phi + \pi/10)$
						$0 \le \phi \le \frac{\pi}{10}$	$D/\cos\phi$	$D/\cos(\phi - \pi/10)$
(1,1)	1	0	0	-1	0	$-\frac{\pi}{10} \le \phi \le 0$	$D/\cos(\phi + \pi/10)$	$D/\cos(\phi - \pi/10)$
						$-\frac{\pi}{5} \le \phi \le -\frac{\pi}{10}$	$D/\cos\phi$	$D/\cos(\phi + 2\pi/5)$
(1,2)	1	0	-1	-1	0	$-\frac{\pi}{10} \le \phi \le 0$	$D/\cos(\phi - \pi/5)$	$D/\cos(\phi + 2\pi/5)$
						$0 \le \phi \le \frac{\pi}{10}$	$D/\cos(\phi + \pi/5)$	$D/\cos(\phi - 2\pi/5)$
(2,2)	1	1	-1	-1	0	$-\frac{\pi}{10} \le \phi \le 0$	$D/\cos(\phi + 2\pi/5)$	$D/\cos(\phi - 2\pi/5)$
						$-\frac{\pi}{5} \le \phi \le -\frac{\pi}{10}$	$D/\cos(\phi - \pi/5)$	$D/\cos(\phi + 3\pi/5)$
(3,2)	1	1	-1	-1	1	$-\frac{\pi}{10} \le \phi \le 0$	$D/\cos(\phi - 2\pi/5)$	∞
						$0 \le \phi \le \frac{\pi}{10}$	$D/\cos(\phi + 2\pi/5)$	∞

Table 7-6

$N = 6$

$$-\frac{1}{N(z)} = \frac{-E\left[(z-0.5)\cos\phi - 0.866\sin\phi\right](z+1)}{a(M-kD+kE\cos\phi)z^2 + b(M-kD+kE\cos(60+\phi))z + c(M-kD+kE\cos(60-\phi))}$$

Δ	a	b	c	ϕ	E_{min}	E_{max}
(1,1)	1	0	0	$-30^\circ \le \phi \le 0$	$D/\cos\phi$	$D/\cos(\phi+60)$
				$0 \le \phi \le 30^\circ$	$D/\cos\phi$	$D/\cos(\phi-60)$
(2,2)	1	1	0	$-30^\circ \le \phi \le 0$	$D/\cos(\phi+60)$	$D/\cos(\phi-60)$
				$-60^\circ \le \phi \le -30^\circ$	$D/\cos\phi$	$D/\cos(\phi+120)$
(3,3)	1	1	-1	$-30^\circ \le \phi \le 0$	$D/\cos(\phi-60)$	∞
				$0 \le \phi \le 30^\circ$	$D/\cos(\phi+60)$	∞

Table 7-7

$N = 7$

$$-\frac{1}{N} = \frac{-E\left[(z-\cos\frac{2\pi}{7})\cos\phi - \sin\frac{2\pi}{7}\sin\phi\right](z^2-2z\cos\frac{6\pi}{7}+1)(z-1)(z^2-2z\cos\frac{4\pi}{7}+1)}{\begin{array}{l} az^6(M-kD+kE\cos\phi)+bz^5(M-kD+kE\cos(\phi+\frac{2\pi}{7}))+cz^4(M-kD+kE\cos(\phi-\frac{3\pi}{7})) \\ +dz^3(M-kD+kE\cos(\phi-\frac{\pi}{7}))+ez^2(M-kD+kE\cos(\phi+\frac{\pi}{7})) \\ +fz(M-kD+kE\cos(\phi+\frac{3\pi}{2}))+g(M-kD+kE\cos(\phi-\frac{2\pi}{7})) \end{array}}$$

Δ	a	b	c	d	e	f	g	ϕ	E_{min}	E_{max}
(1,0)	1	0	0	0	0	0	0	$-\frac{\pi}{14} \le \phi \le 0$	$\frac{D}{\cos\phi}$	$\frac{D}{\cos(\phi+\frac{\pi}{7})}$
								$0 \le \phi \le \frac{\pi}{14}$	$\frac{D}{\cos\phi}$	$\frac{D}{\cos(\phi-\frac{\pi}{7})}$
(1,1)	1	0	0	0	-1	0	0	$-\frac{\pi}{14} \le \phi \le 0$	$\frac{D}{\cos(\phi+\frac{\pi}{7})}$	$\frac{D}{\cos(\phi-\frac{\pi}{7})}$
								$-\frac{\pi}{7} \le \phi \le -\frac{\pi}{14}$	$\frac{D}{\cos\phi}$	$\frac{D}{\cos(\phi+\frac{2\pi}{7})}$
(1,2)	1	0	0	-1	-1	0	0	$-\frac{\pi}{14} \le \phi \le 0$	$\frac{D}{\cos(\phi-\frac{\pi}{7})}$	$\frac{D}{\cos(\phi+\frac{2\pi}{7})}$
								$0 \le \phi \le \frac{\pi}{14}$	$\frac{D}{\cos(\phi+\frac{\pi}{7})}$	$\frac{D}{\cos(\phi-\frac{2\pi}{7})}$
(2,2)	1	1	0	-1	-1	0	0	$-\frac{\pi}{14} \le \phi \le 0$	$\frac{D}{\cos(\phi+\frac{2\pi}{7})}$	$\frac{D}{\cos(\phi-\frac{2\pi}{7})}$
								$-\frac{\pi}{7} \le \phi \le -\frac{\pi}{14}$	$\frac{D}{\cos(\phi-\frac{\pi}{7})}$	$\frac{D}{\cos(\phi+\frac{3\pi}{7})}$
(3,2)	1	1	0	-1	-1	0	1	$-\frac{\pi}{14} \le \phi \le 0$	$\frac{D}{\cos(\phi-\frac{2\pi}{7})}$	$\frac{D}{\cos(\phi+\frac{3\pi}{7})}$
								$0 \le \phi \le \frac{\pi}{14}$	$\frac{D}{\cos(\phi+\frac{2\pi}{7})}$	$\frac{D}{\cos(\phi-\frac{3\pi}{7})}$
(3,3)	1	1	0	-1	-1	-1	1	$-\frac{\pi}{14} \le \phi \le 0$	$\frac{D}{\cos(\phi+\frac{3\pi}{7})}$	$\frac{D}{\cos(\phi-\frac{3\pi}{7})}$
								$-\frac{\pi}{7} \le \phi \le -\frac{\pi}{14}$	$\frac{D}{\cos(\phi-\frac{3\pi}{7})}$	$\frac{D}{\cos(\phi+\frac{4\pi}{7})}$
(3,4)	1	1	-1	-1	-1	-1	1	$-\frac{\pi}{14} \le \phi \le 0$	$\frac{D}{\cos(\phi-\frac{3\pi}{7})}$	∞
								$0 \le \phi \le \frac{\pi}{14}$	$\frac{D}{\cos(\phi+\frac{3\pi}{7})}$	∞

Table 7-8

$N = 8$

$$-\frac{1}{N} = \frac{-E\left[(z-0.707)\cos\phi - 0.707\sin\phi\right](z^2+\sqrt{2}z+1)}{a\left[M-kD+kE\cos\phi\right]z^3 + b\left[M-kD+kE\cos(\phi+\frac{\pi}{4})\right]z^2}$$

$$\frac{}{+c\left[M-kD+kE\cos(\phi+\frac{\pi}{2})\right]z + d\left[M-kD+kE\cos(\phi-\frac{\pi}{4})\right]}$$

Δ	a	b	c	d	ϕ	E_{min}	E_{max}
(1,1)	1	0	0	0	$-\frac{\pi}{8} \le \phi \le 0$	$\frac{D}{\cos\phi}$	$\frac{D}{\cos(\phi+\frac{\pi}{4})}$
					$0 \le \phi \le \frac{\pi}{8}$	$\frac{D}{\cos\phi}$	$\frac{D}{\cos(\frac{\pi}{4}-\phi)}$
(2,2)	1	1	0	0	$-\frac{\pi}{8} \le \phi \le 0$	$\frac{D}{\cos(\phi+\frac{\pi}{4})}$	$\frac{D}{\cos(\frac{\pi}{2}-\phi)}$
					$-\frac{\pi}{4} \le \phi \le -\frac{\pi}{8}$	$\frac{D}{\cos\phi}$	$\frac{D}{\cos(\phi+\frac{\pi}{2})}$
(3.3)	1	1	0	-1	$-\frac{\pi}{8} \le \phi \le 0$	$\frac{D}{\cos(\frac{\pi}{4}-\phi)}$	$\frac{D}{\cos(\phi+\frac{\pi}{2})}$
					$0 \le \phi \le \frac{\pi}{8}$	$\frac{D}{\cos(\frac{\pi}{4}+\phi)}$	$\frac{D}{\cos(\frac{\pi}{2}-\phi)}$
(4.4)	1	1	1	-1	$-\frac{\pi}{8} \le \phi \le 0$	$\frac{D}{\cos(\frac{\pi}{2}+\phi)}$	∞
					$0 \le \phi \le \frac{\pi}{8}$	$\frac{D}{\cos(\frac{\pi}{4}-\phi)}$	∞

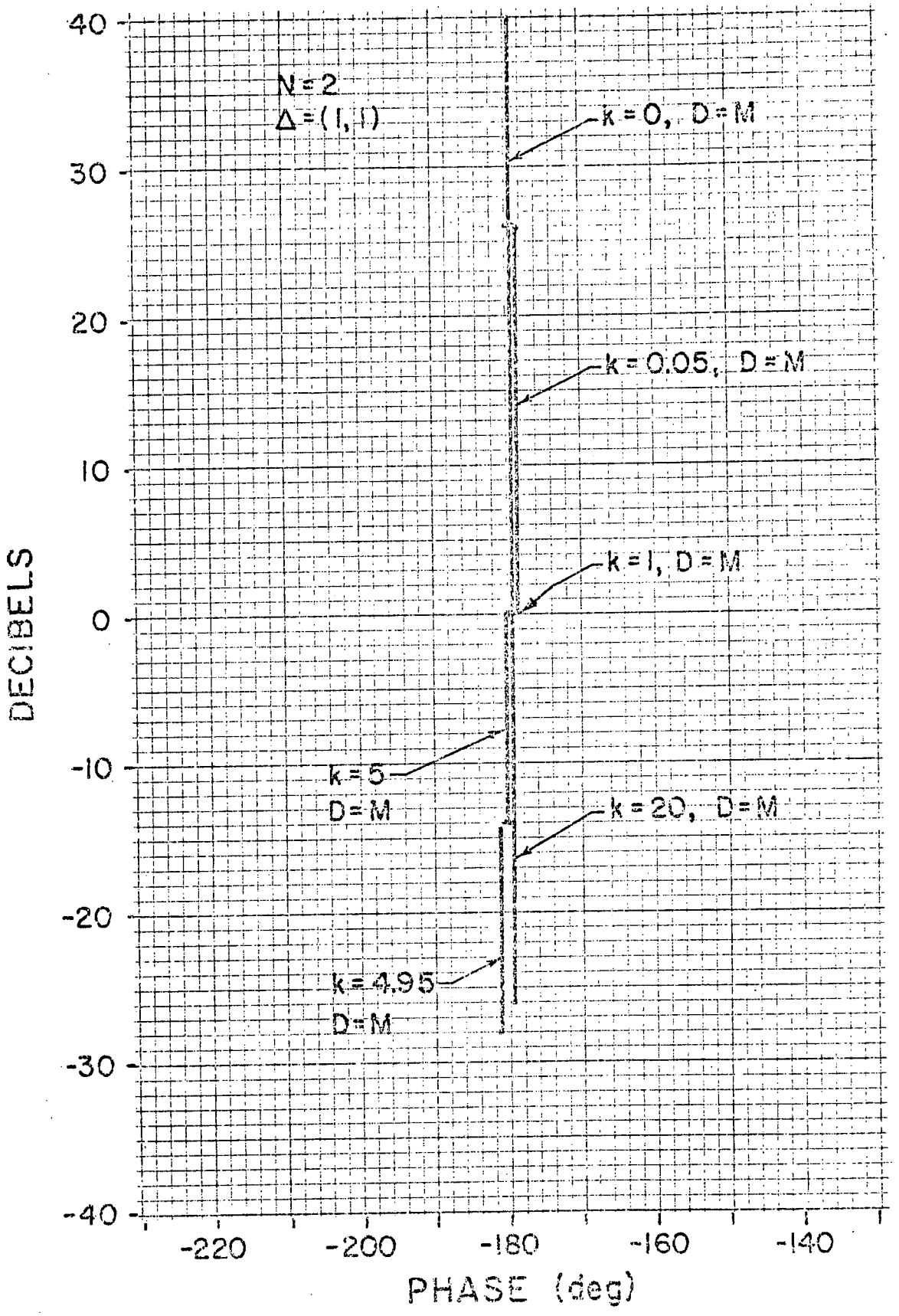
N=2
Δ=(1,1)
k=0, D=M
k=0.05, D=M
k=1, D=M
k=5
D=M
k=20, D=M
k=4.95
D=M
DECIBELS
PHASE (deg)
40
30
20
10
0
-10
-20
-30
-40
-220
-200
-180
-160
-140

Figure 7-13

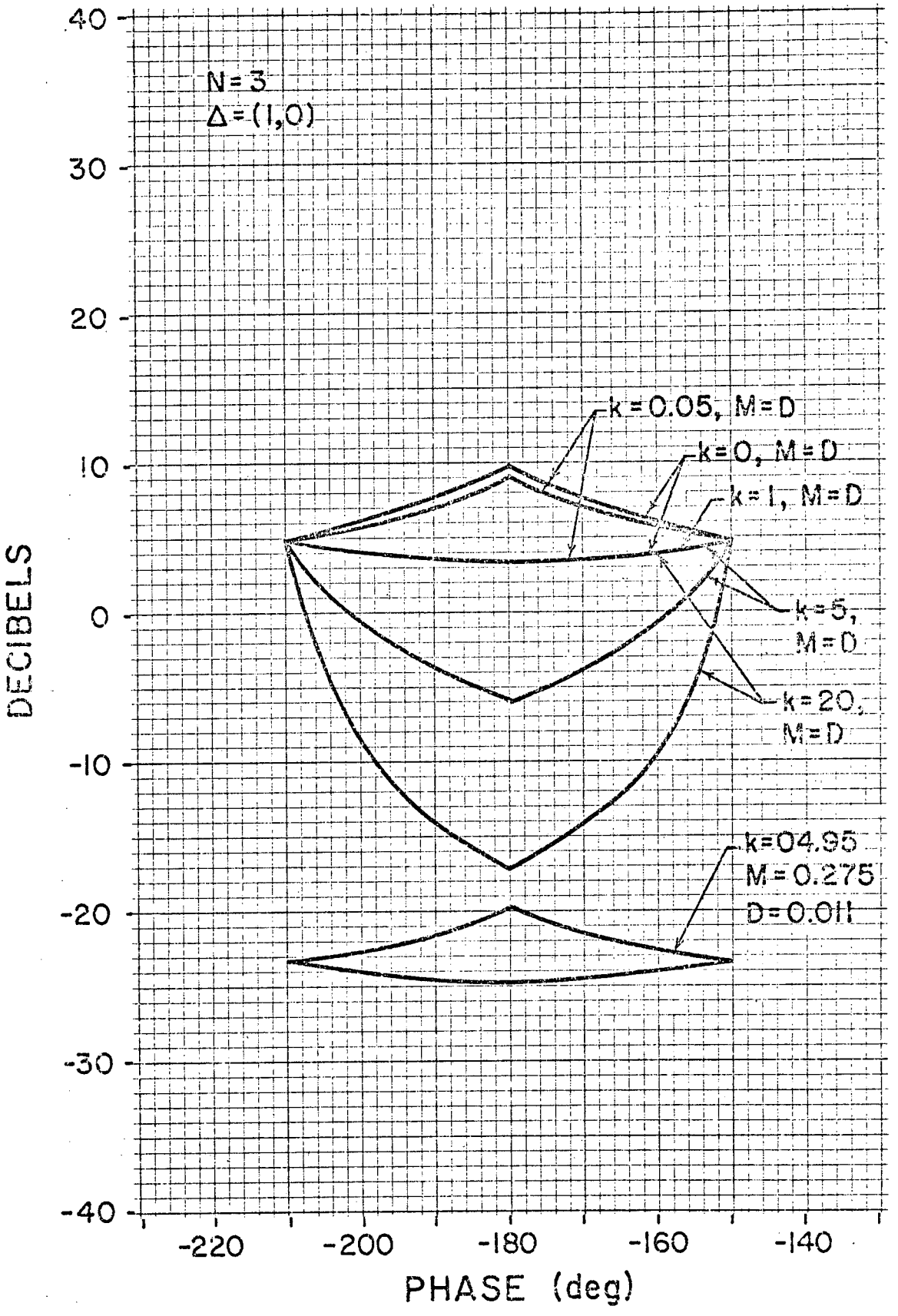
N=3
Δ=(1,0)
k=0.05, M=D
k=0, M=D
k=1, M=D
k=5, M=D
k=20, M=D
k=04.95
M=0.275
D=0.011
DECIBELS
PHASE (deg)
40
30
20
10
0
-10
-20
-30
-40
-220
-200
-180
-160
-140

Figure 7-14

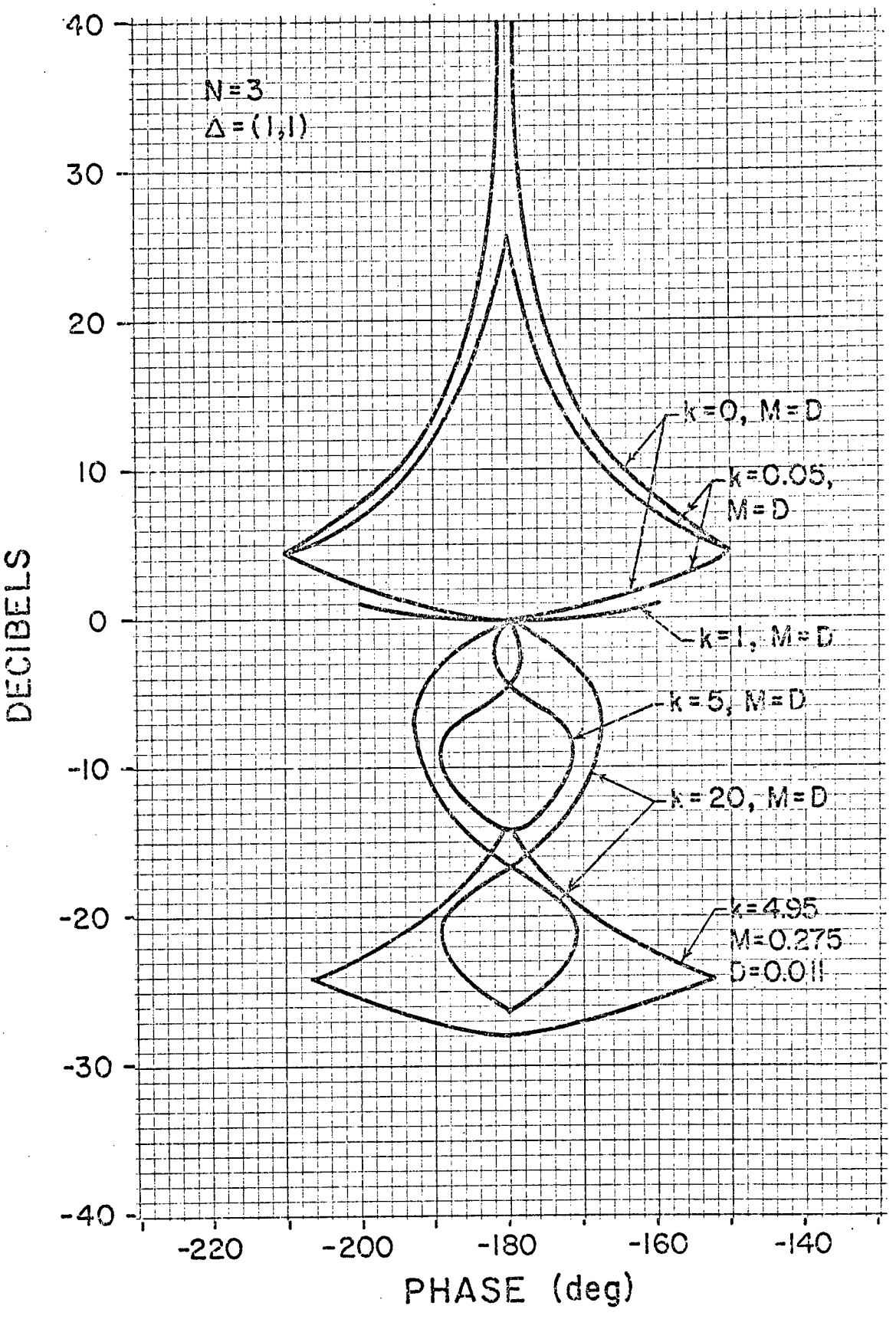
N=3
Δ=(1,1)
k=0, M=D
k=0.05, M=D
k=1, M=D
k=5, M=D
k=20, M=D
k=4.95
M=0.275
D=0.011
DECIBELS
PHASE (deg)
40
30
20
10
0
-10
-20
-30
-40
-220
-200
-180
-160
-140

Figure 7-15

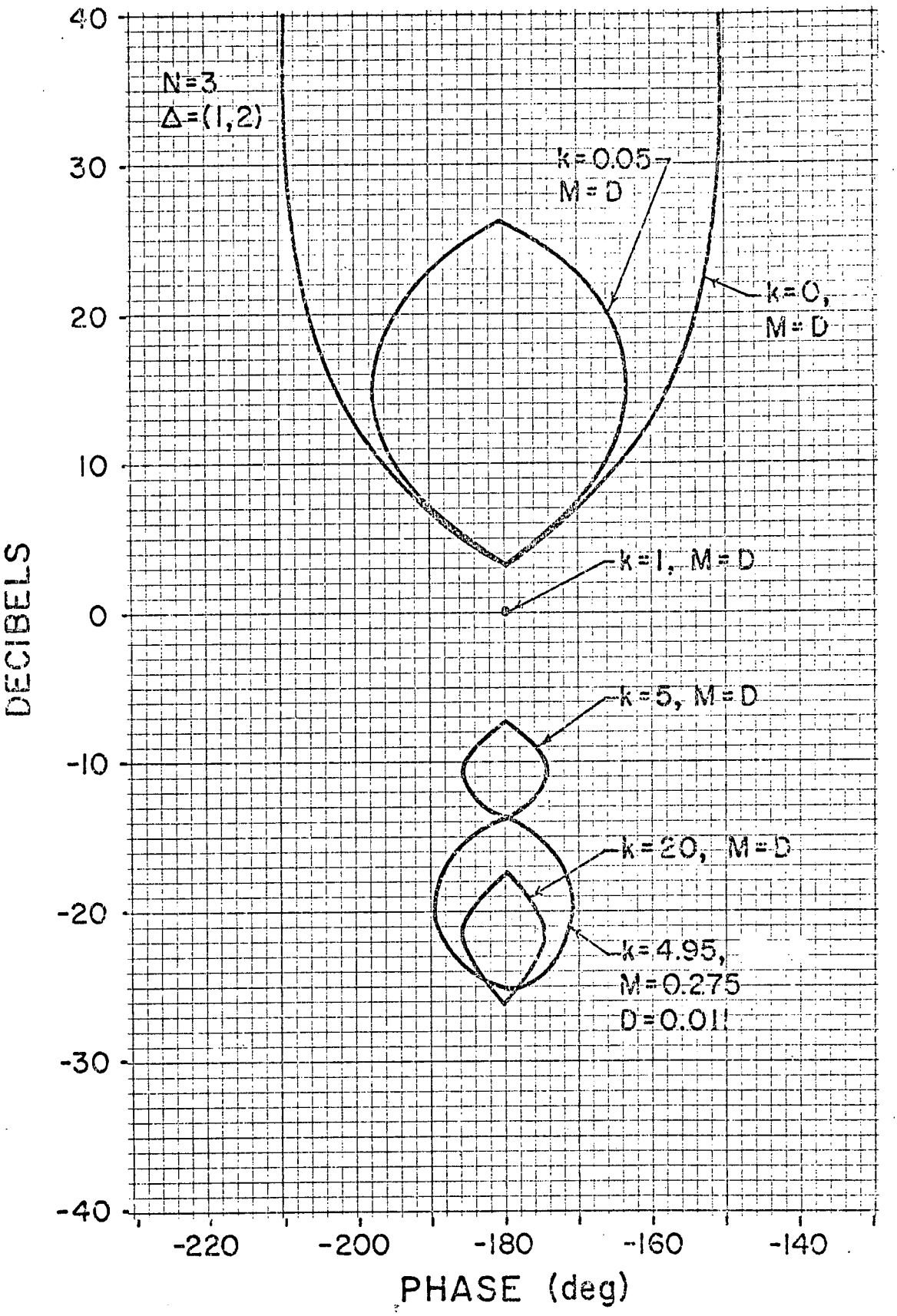
N=3
Δ=(1,2)
k=0.05
M=D
k=0,
M=D
k=1, M=D
k=5, M=D
k=20, M=D
k=4.95,
M=0.275
D=0.01
40
30
20
10
0
-10
-20
-30
-40
-220
-200
-180
-160
-140
DECIBELS
PHASE (deg)

Figure 7-16

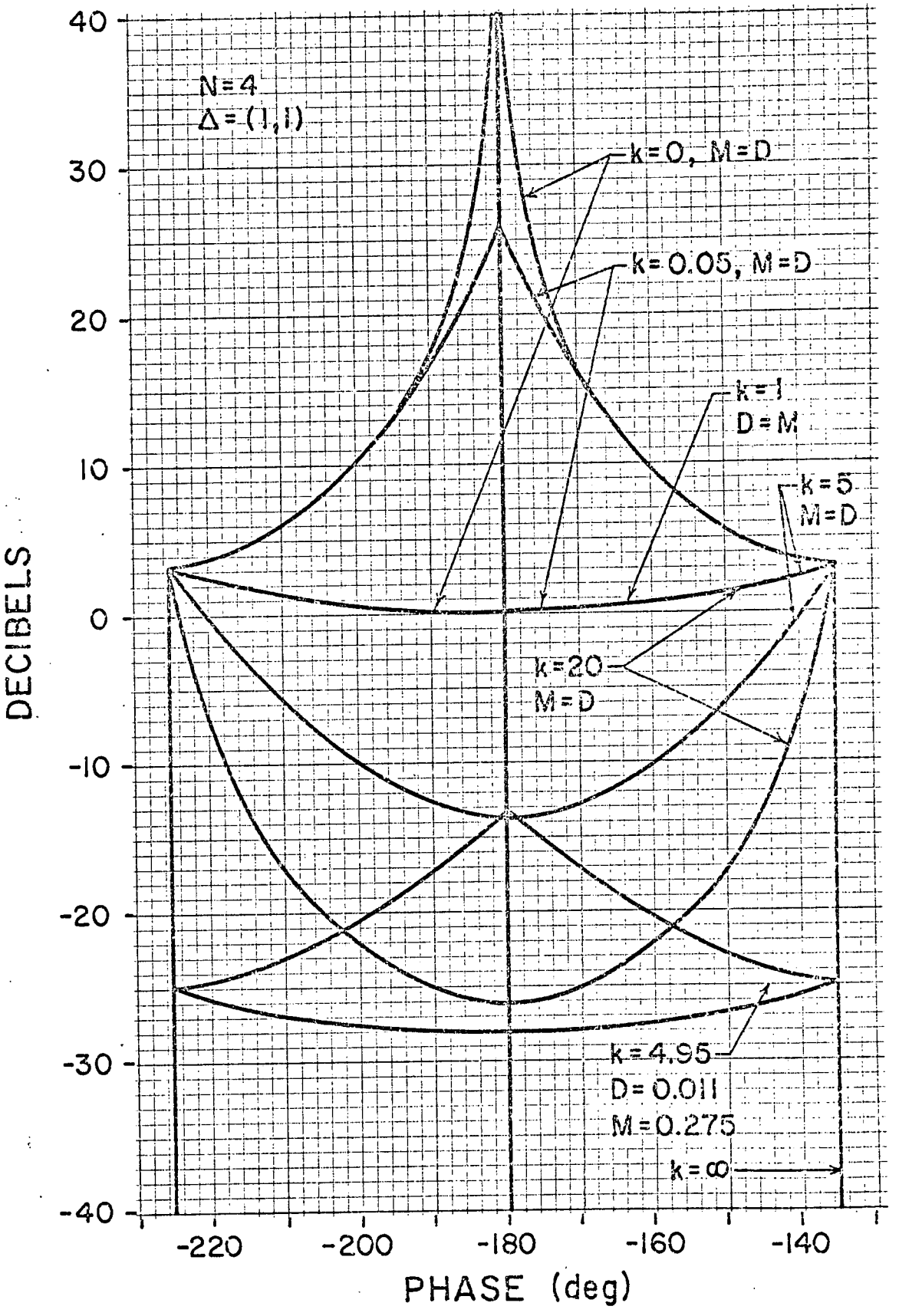
N=4
Δ=(1,1)
k=0, M=D
k=0.05, M=D
k=1
D=M
k=5
M=D
k=20
M=D
k=4.95
D=0.011
M=0.275
k=∞
DECIBELS
PHASE (deg)
40
30
20
10
0
-10
-20
-30
-40
-220
-200
-180
-160
-140

Figure 7-17

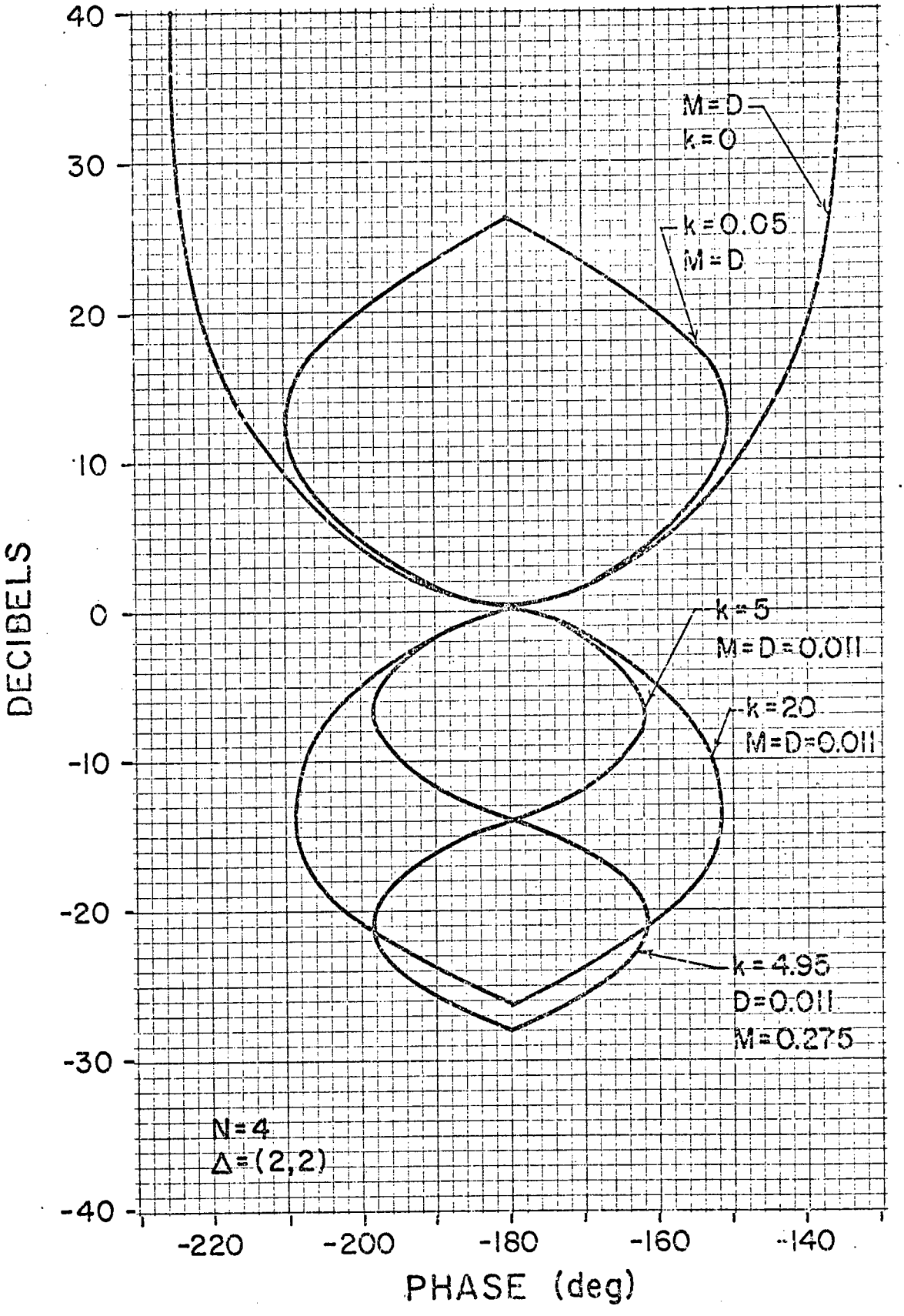
40
30
20
10
0
-10
-20
-30
-40
DECIBELS
-220
-200
-180
-160
-140
PHASE (deg)
M=D
k=0
k=0.05
M=D
k=5
M=D=0.011
k=20
M=D=0.011
k=4.95
D=0.011
M=0.275
N=4
Δ=(2,2)

Figure 7-18

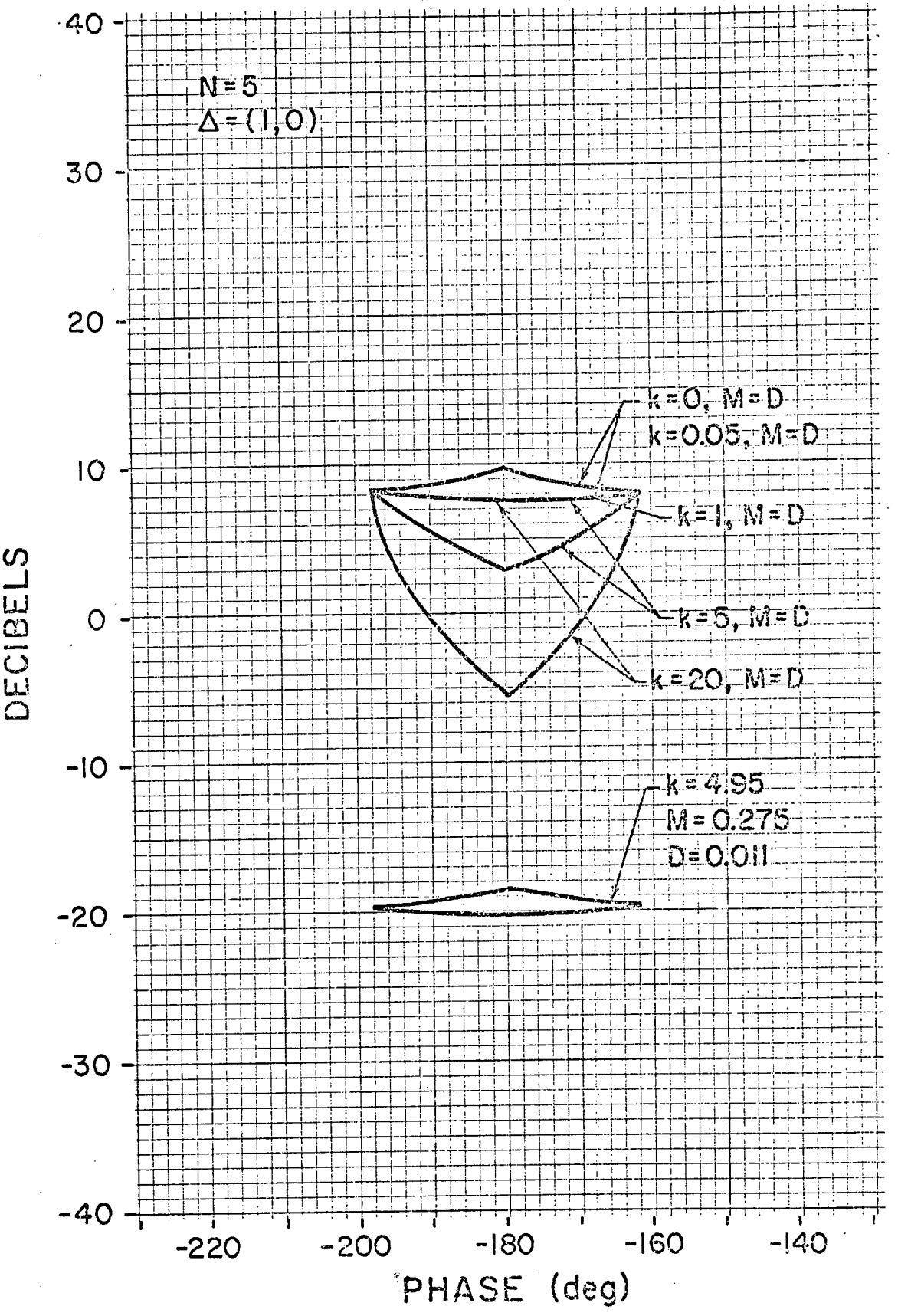
N=5
Δ=(1,0)
k=0, M=D
k=0.05, M=D
k=1, M=D
k=5, M=D
k=20, M=D
k=4.95
M=0.275
D=0.011
DECIBELS
PHASE (deg)
40
30
20
10
0
-10
-20
-30
-40
-220
-200
-180
-160
-140

Figure 7-19

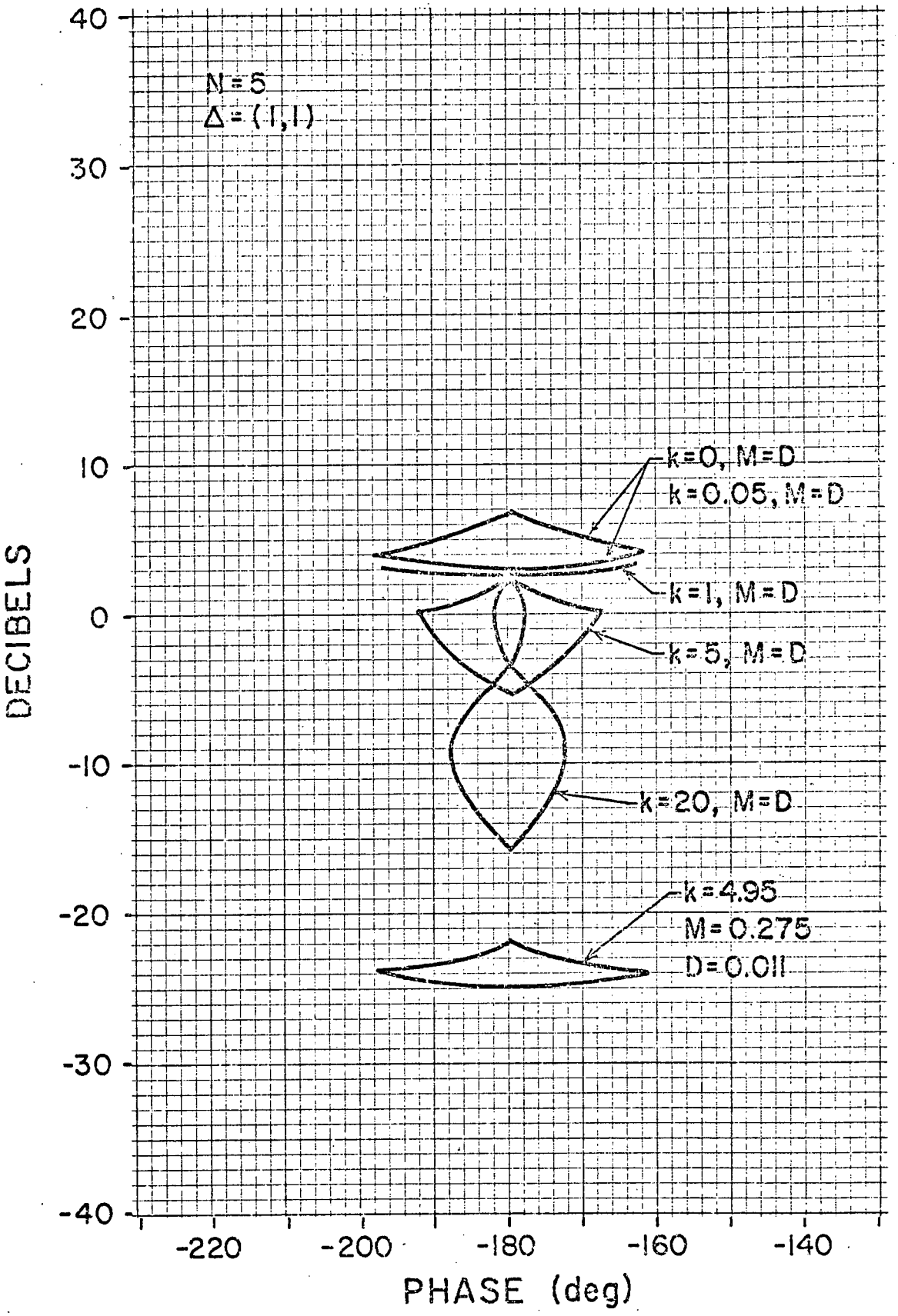
N=5
Δ=(1,1)
k=0, M=D
k=0.05, M=D
k=1, M=D
k=5, M=D
k=20, M=D
k=4.95
M=0.275
D=0.011
DECIBELS
PHASE (deg)
40
30
20
10
0
-10
-20
-30
-40
-220
-200
-180
-160
-140

Figure 7-20

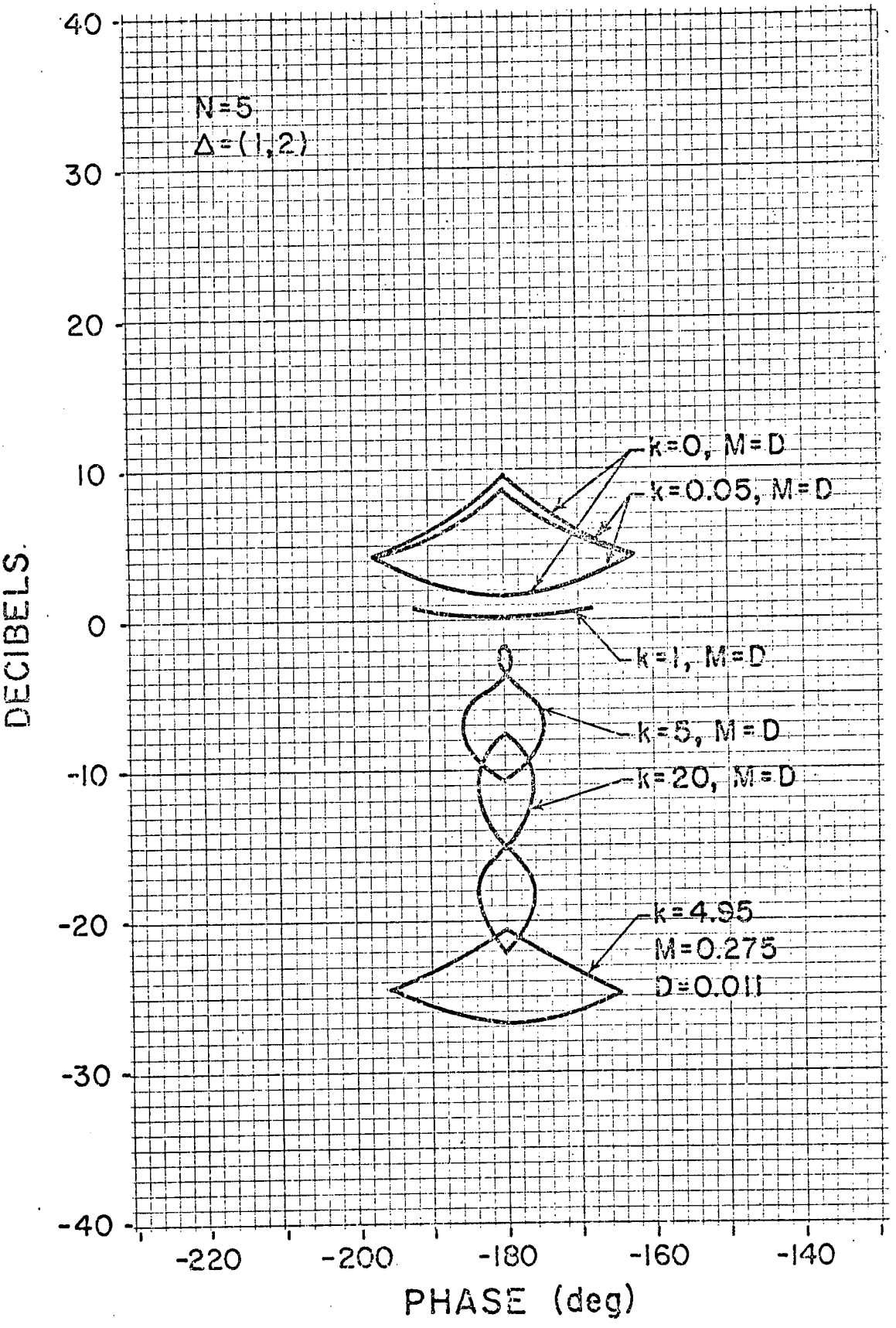
N=5
Δ=(1,2)
k=0, M=D
k=0.05, M=D
k=1, M=D
k=5, M=D
k=20, M=D
k=4.95
M=0.275
D=0.011
DECIBELS
PHASE (deg)
40
30
20
10
0
-10
-20
-30
-40
-220
-200
-180
-160
-140

Figure 7-21

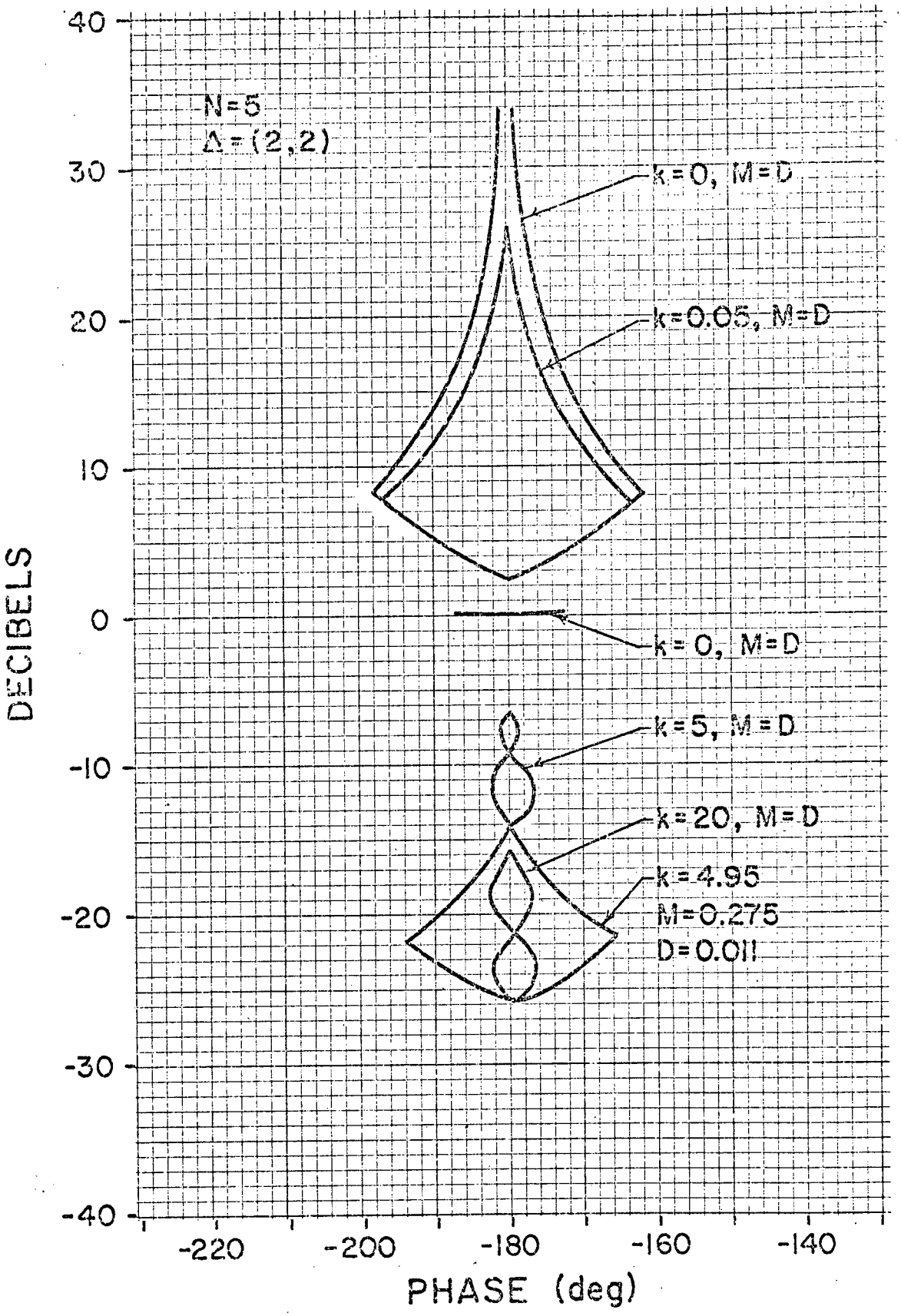
N=5
Δ=(2,2)
k=0, M=D
k=0.05, M=D
k=0, M=D
k=5, M=D
k=20, M=D
k=4.95
M=0.275
D=0.011
DECIBELS
PHASE (deg)
40
30
20
10
0
-10
-20
-30
-40
-220
-200
-180
-160
-140

Figure 7-22

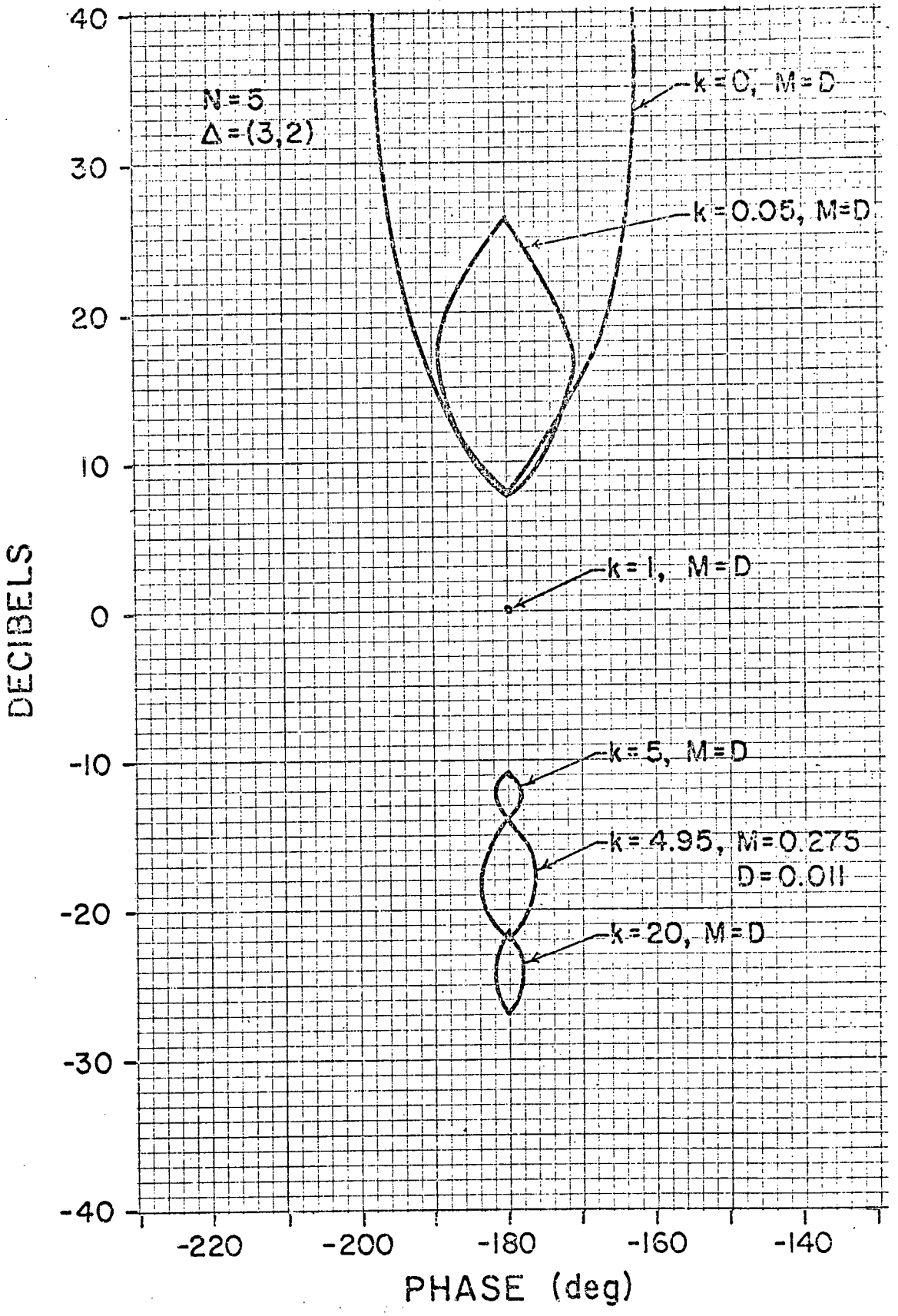
N=5
Δ=(3,2)
k=0, M=D
k=0.05, M=D
k=1, M=D
k=5, M=D
k=4.95, M=0.275
D=0.011
k=20, M=D
DECIBELS
PHASE (deg)
40
30
20
10
0
-10
-20
-30
-40
-220
-200
-180
-160
-140

Figure 7-23

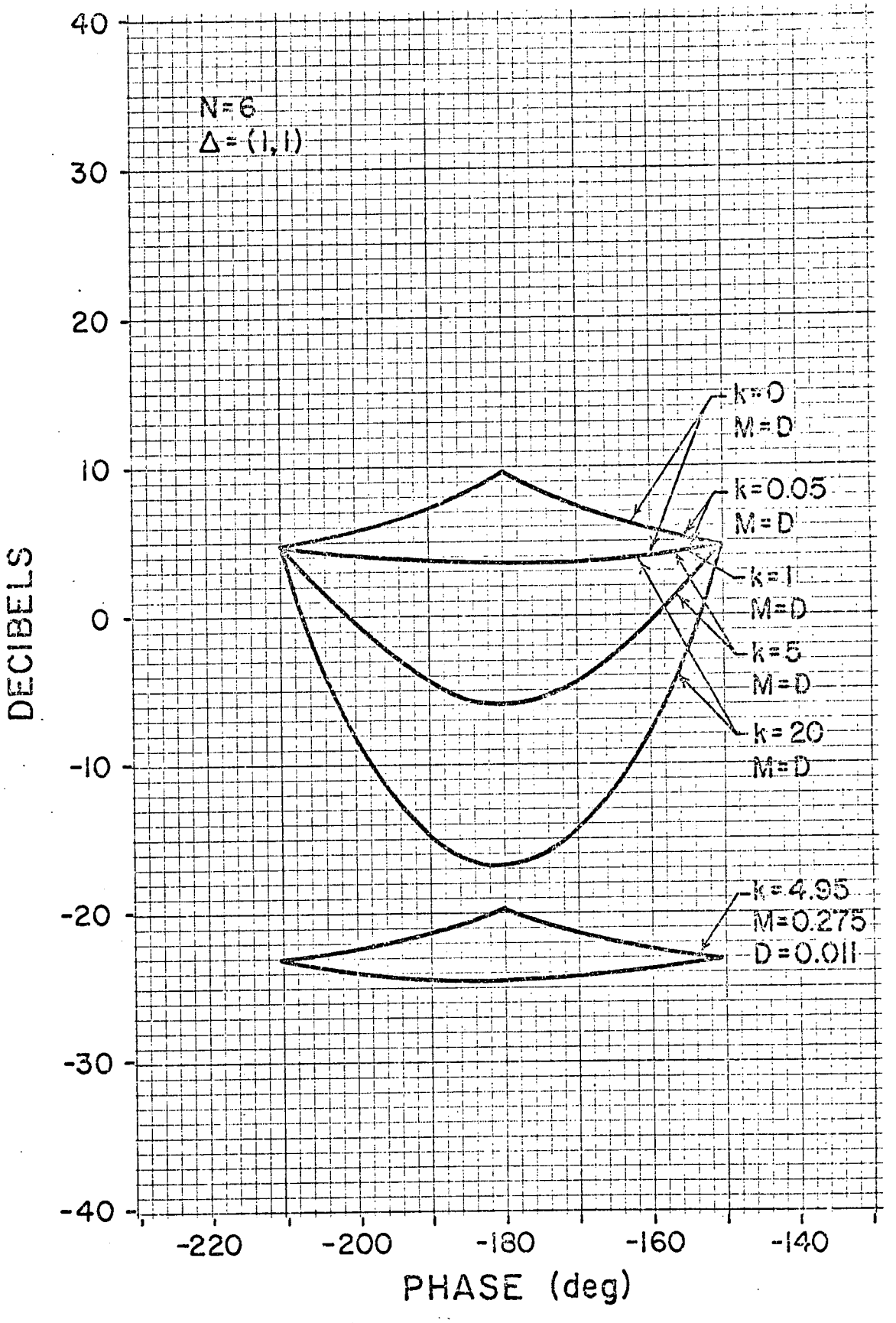
N=6
Δ=(1,1)
k=0
M=D
k=0.05
M=D
k=1
M=D
k=5
M=D
k=20
M=D
k=4.95
M=0.275
D=0.011
DECIBELS
PHASE (deg)
40
30
20
10
0
-10
-20
-30
-40
-220
-200
-180
-160
-140

Figure 7-24

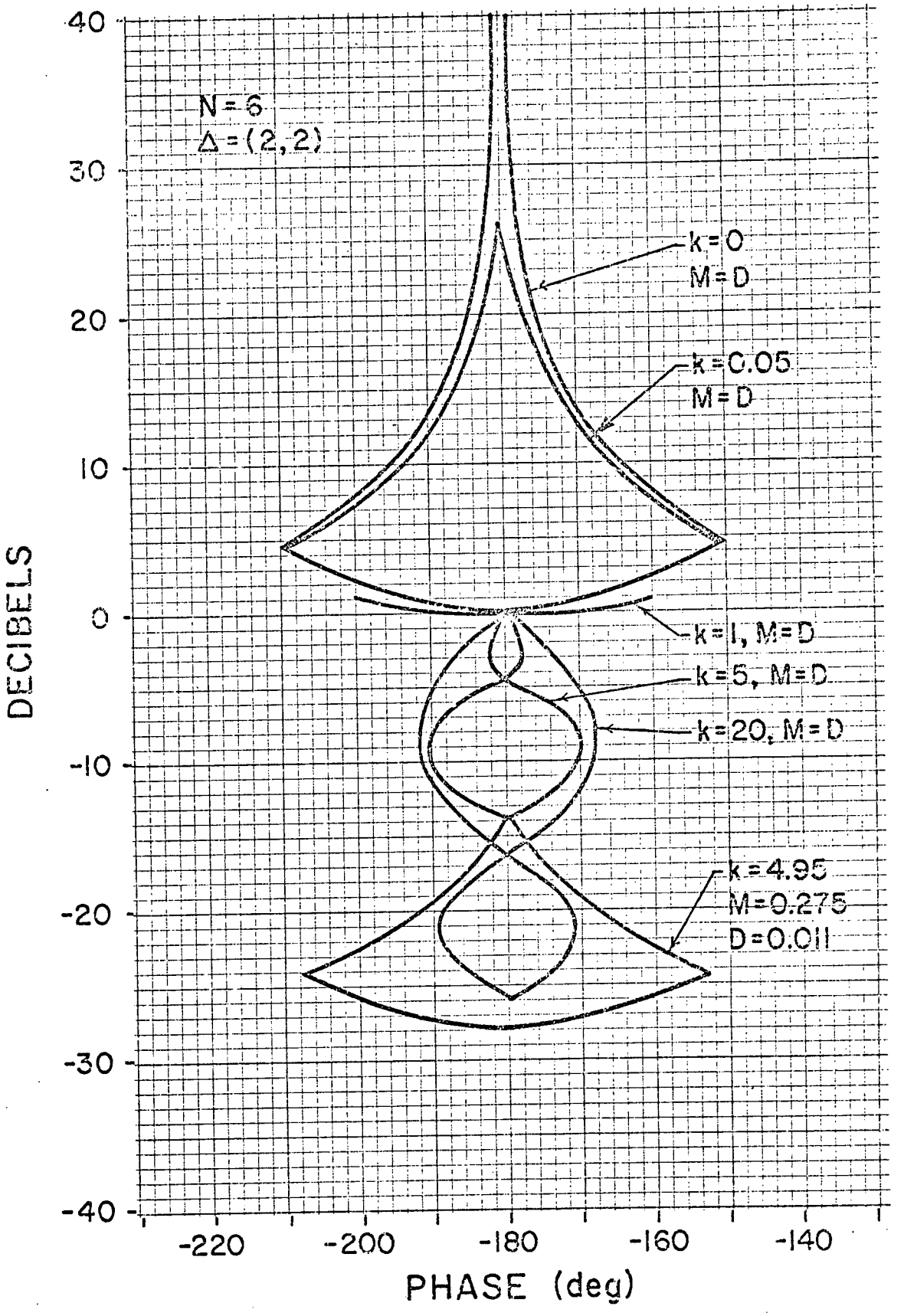
N=6
Δ=(2,2)
k=0
M=D
k=0.05
M=D
k=1, M=D
k=5, M=D
k=20, M=D
k=4.95
M=0.275
D=0.011
DECIBELS
PHASE (deg)
40
30
20
10
0
-10
-20
-30
-40
-220
-200
-180
-160
-140

Figure 7-25

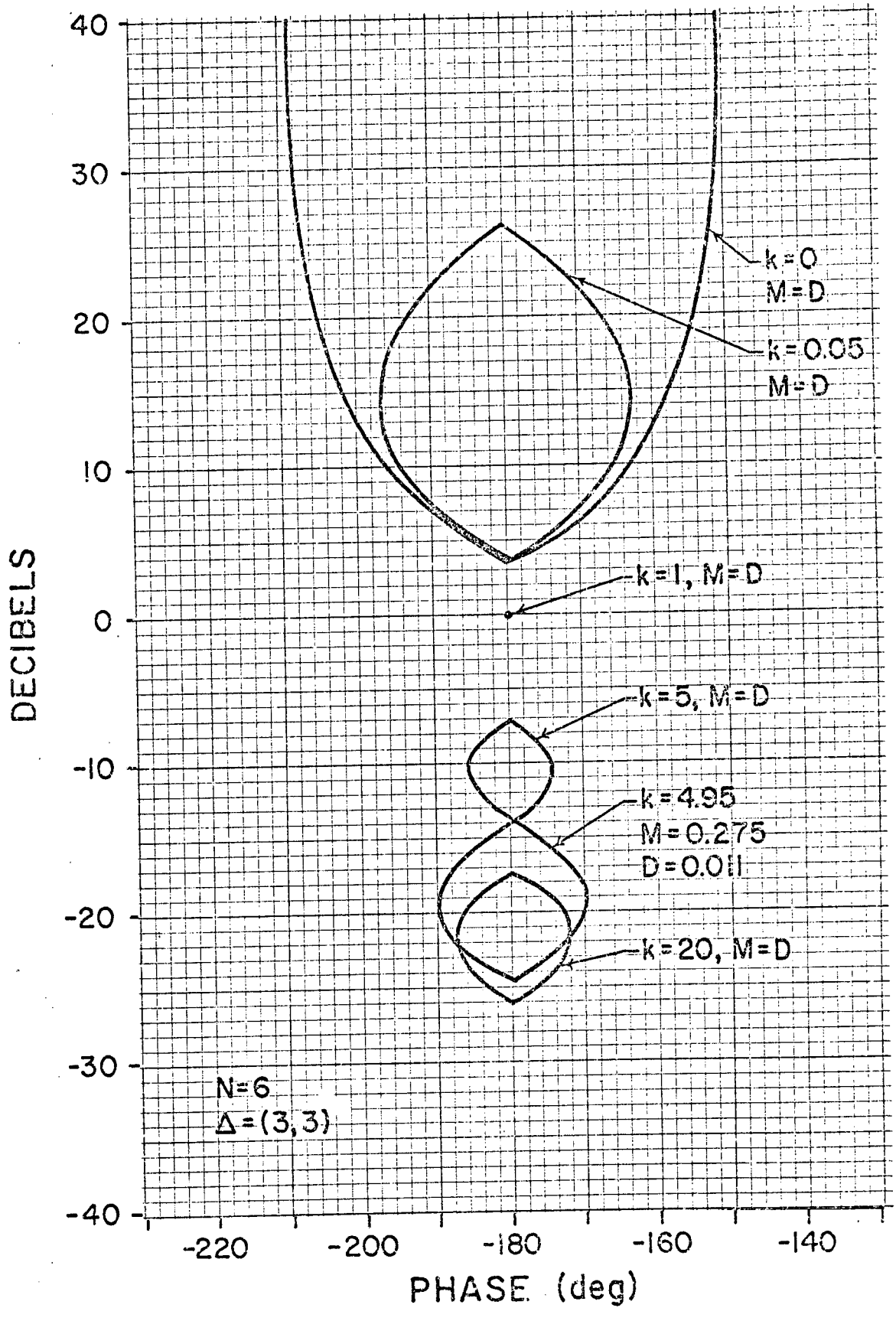
40
30
20
10
0
-10
-20
-30
-40
DECIBELS
-220
-200
-180
-160
-140
PHASE (deg)
k=0
M=D
k=0.05
M=D
k=1, M=D
k=5, M=D
k=4.95
M=0.275
D=0.011
k=20, M=D
N=6
Δ=(3,3)

Figure 7-26

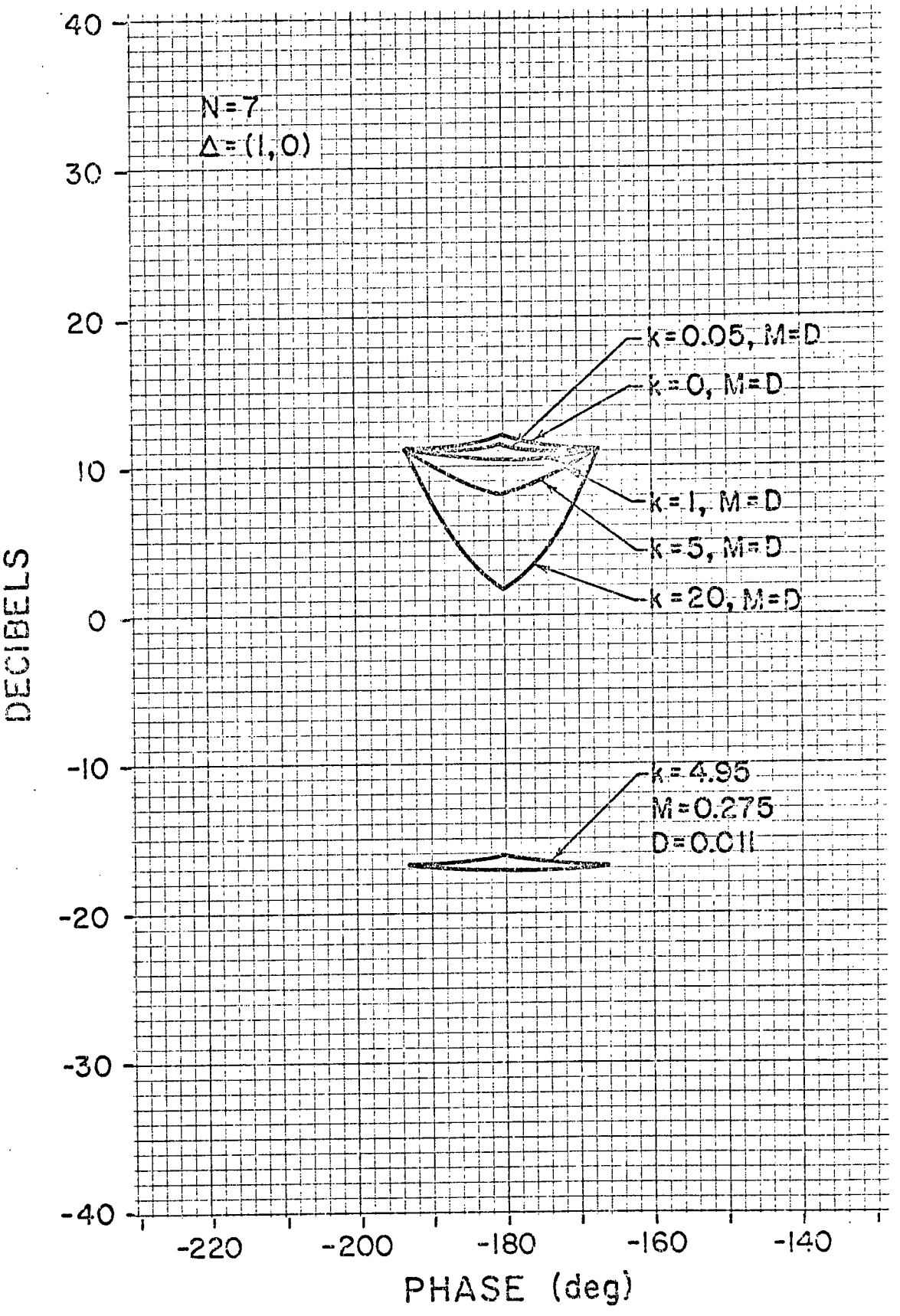
N=7
Δ=(1,0)
k=0.05, M=D
k=0, M=D
k=1, M=D
k=5, M=D
k=20, M=D
k=4.95
M=0.275
D=0.011
DECIBELS
PHASE (deg)
40
30
20
10
0
-10
-20
-30
-40
-220
-200
-180
-160
-140

Figure 7-27

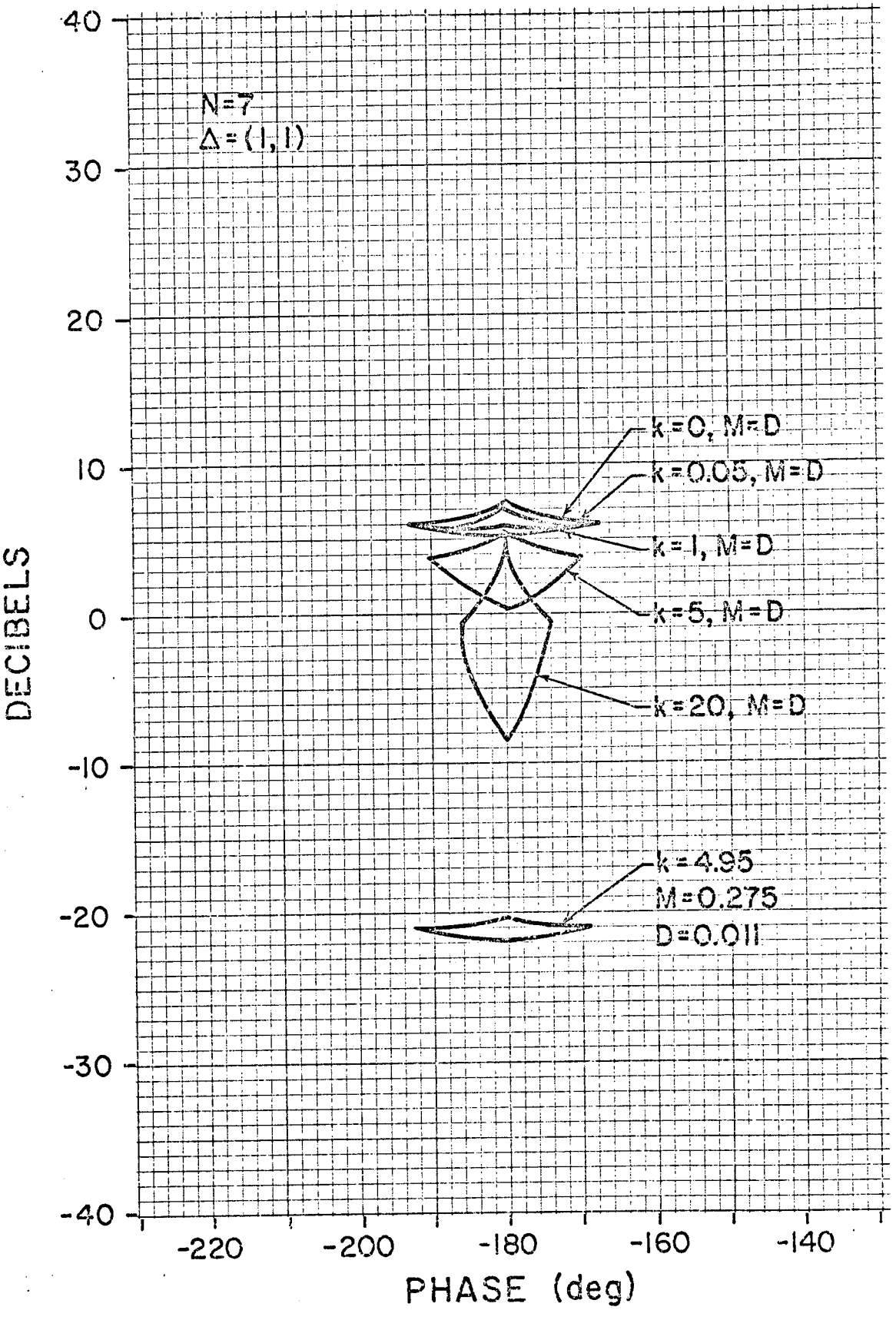
N=7
Δ=(1,1)
k=0, M=D
k=0.05, M=D
k=1, M=D
k=5, M=D
k=20, M=D
k=4.95
M=0.275
D=0.011
DECIBELS
PHASE (deg)
40
30
20
10
0
-10
-20
-30
-40
-220
-200
-180
-160
-140

Figure 7-28

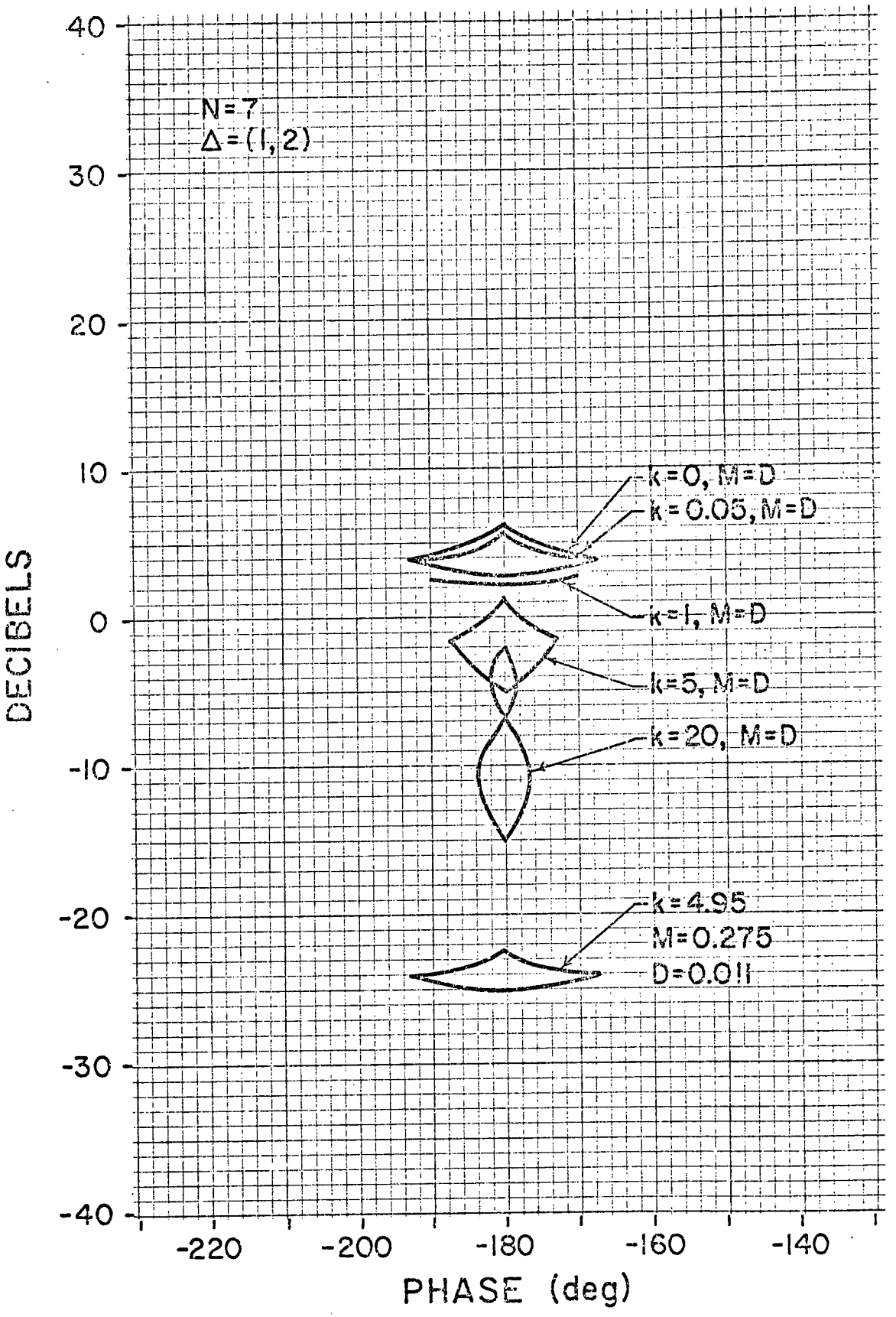
N=7
Δ=(1,2)
k=0, M=D
k=0.05, M=D
k=1, M=D
k=5, M=D
k=20, M=D
k=4.95
M=0.275
D=0.011
DECIBELS
PHASE (deg)
40
30
20
10
0
-10
-20
-30
-40
-220
-200
-180
-160
-140

Figure 7-29

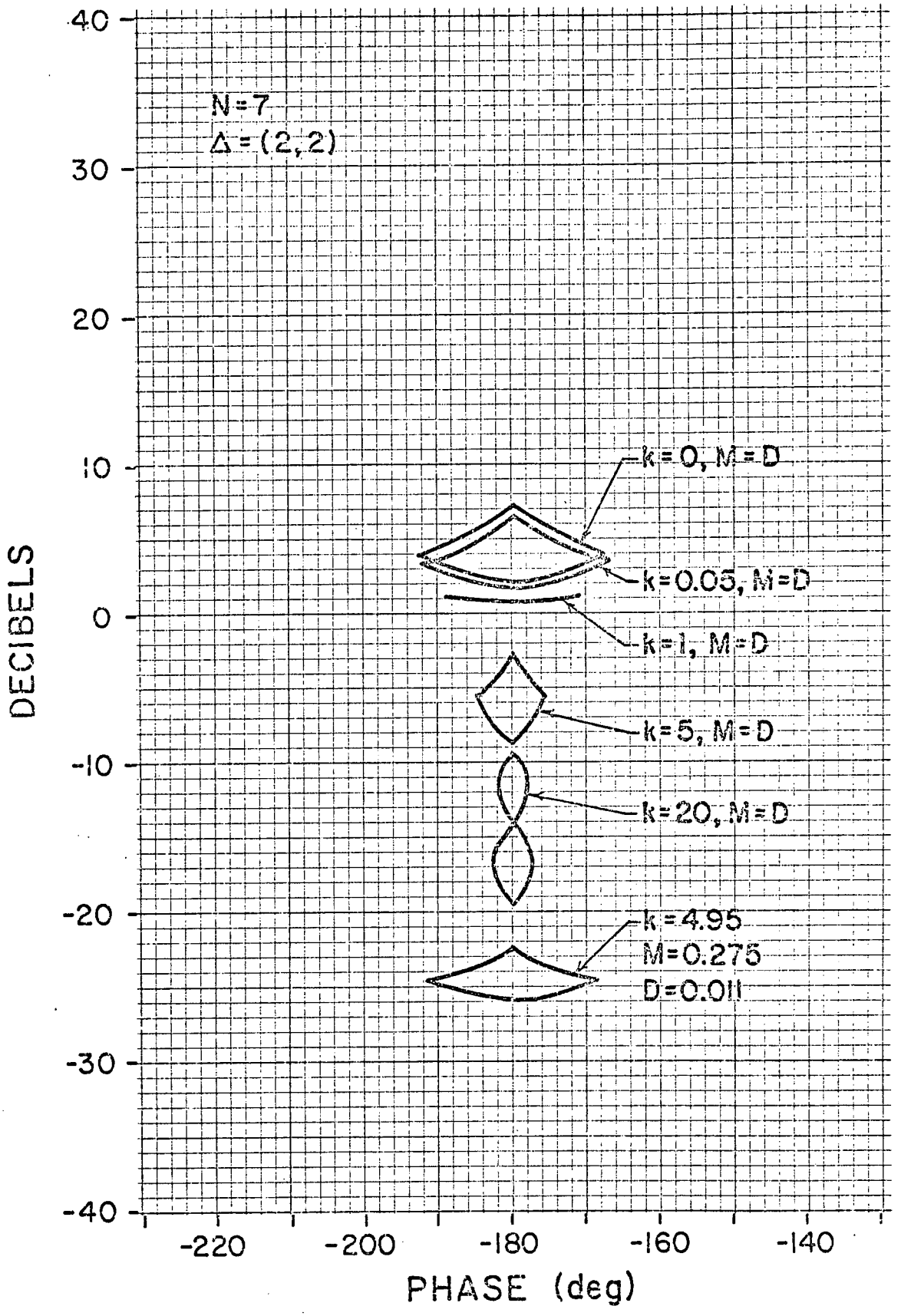
N=7
Δ=(2,2)
k=0, M=D
k=0.05, M=D
k=1, M=D
k=5, M=D
k=20, M=D
k=4.95
M=0.275
D=0.011
DECIBELS
PHASE (deg)
40
30
20
10
0
-10
-20
-30
-40
-220
-200
-180
-160
-140

Figure 7-30

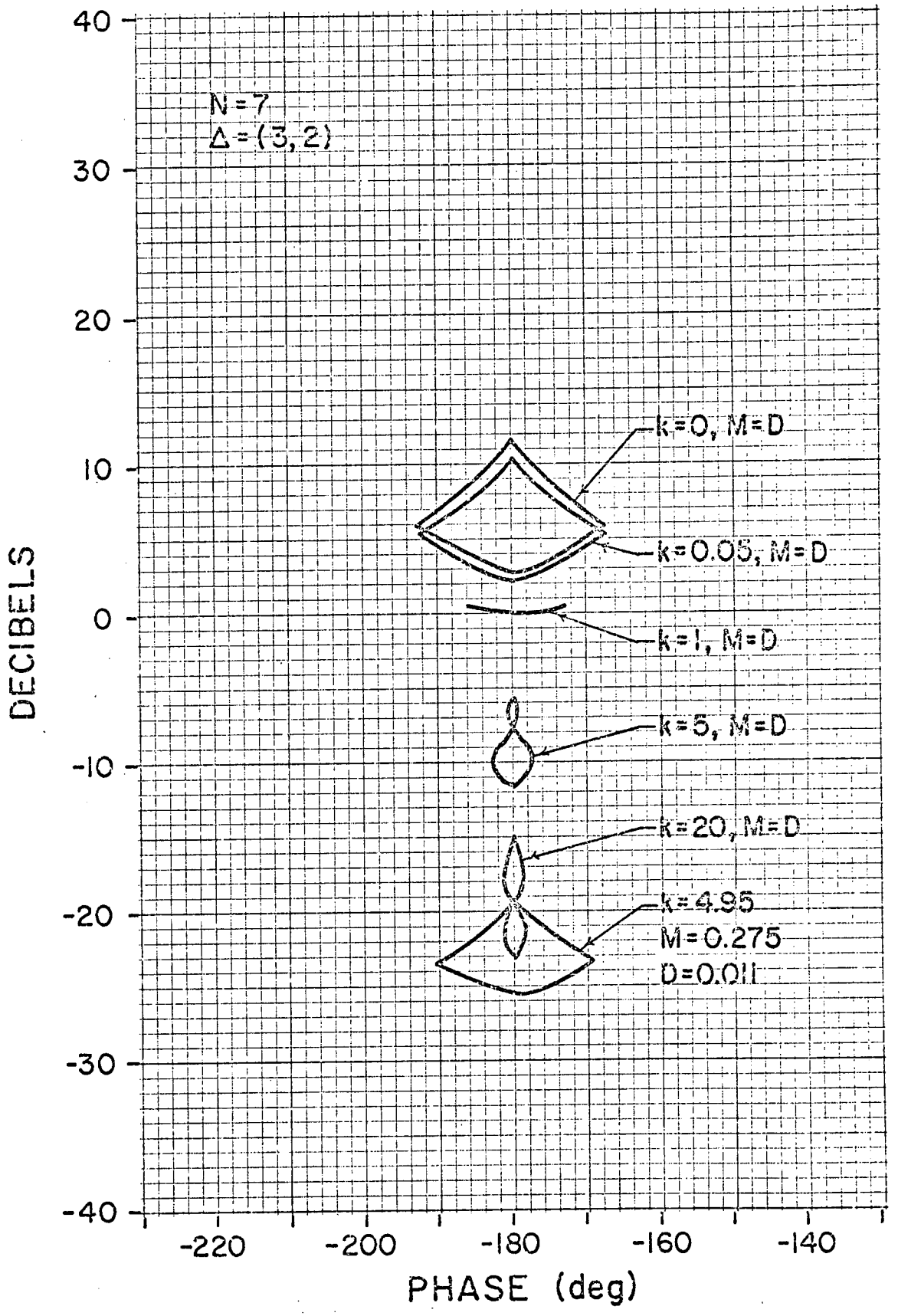
N=7
Δ=(3,2)
k=0, M=D
k=0.05, M=D
k=1, M=D
k=5, M=D
k=20, M=D
k=4.95
M=0.275
D=0.011
DECIBELS
PHASE (deg)
40
30
20
10
0
-10
-20
-30
-40
-220
-200
-180
-160
-140

Figure 7-31

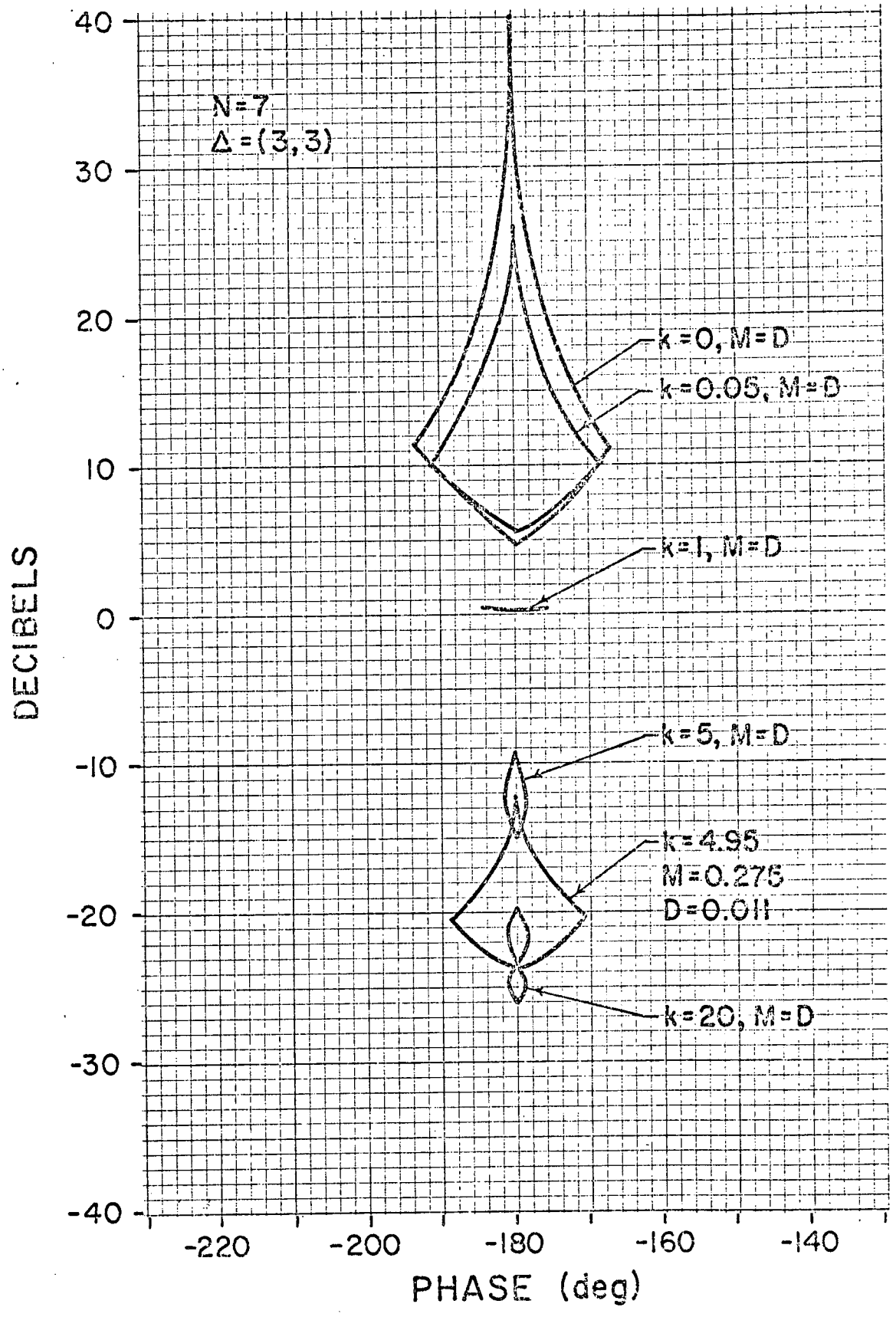
N=7
Δ=(3,3)
k=0, M=D
k=0.05, M=D
k=1, M=D
k=5, M=D
k=4.95
M=0.275
D=0.011
k=20, M=D
DECIBELS
PHASE (deg)
40
30
20
10
0
-10
-20
-30
-40
-220
-200
-180
-160
-140

Figure 7-32

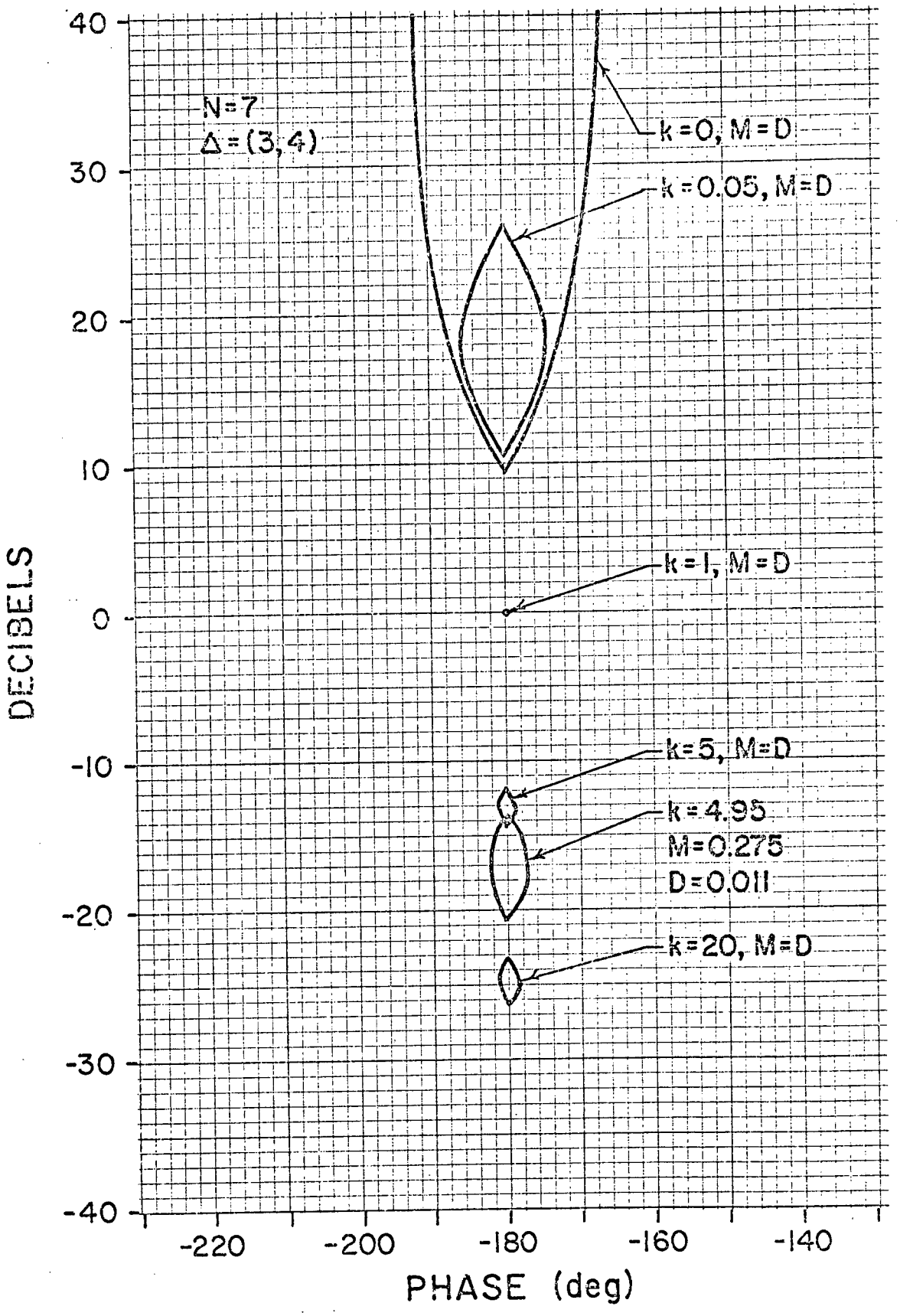
N=7
Δ=(3,4)
k=0, M=D
k=0.05, M=D
k=1, M=D
k=5, M=D
k=4.95
M=0.275
D=0.011
k=20, M=D
DECIBELS
PHASE (deg)
40
30
20
10
0
-10
-20
-30
-40
-220
-200
-180
-160
-140

Figure 7-33

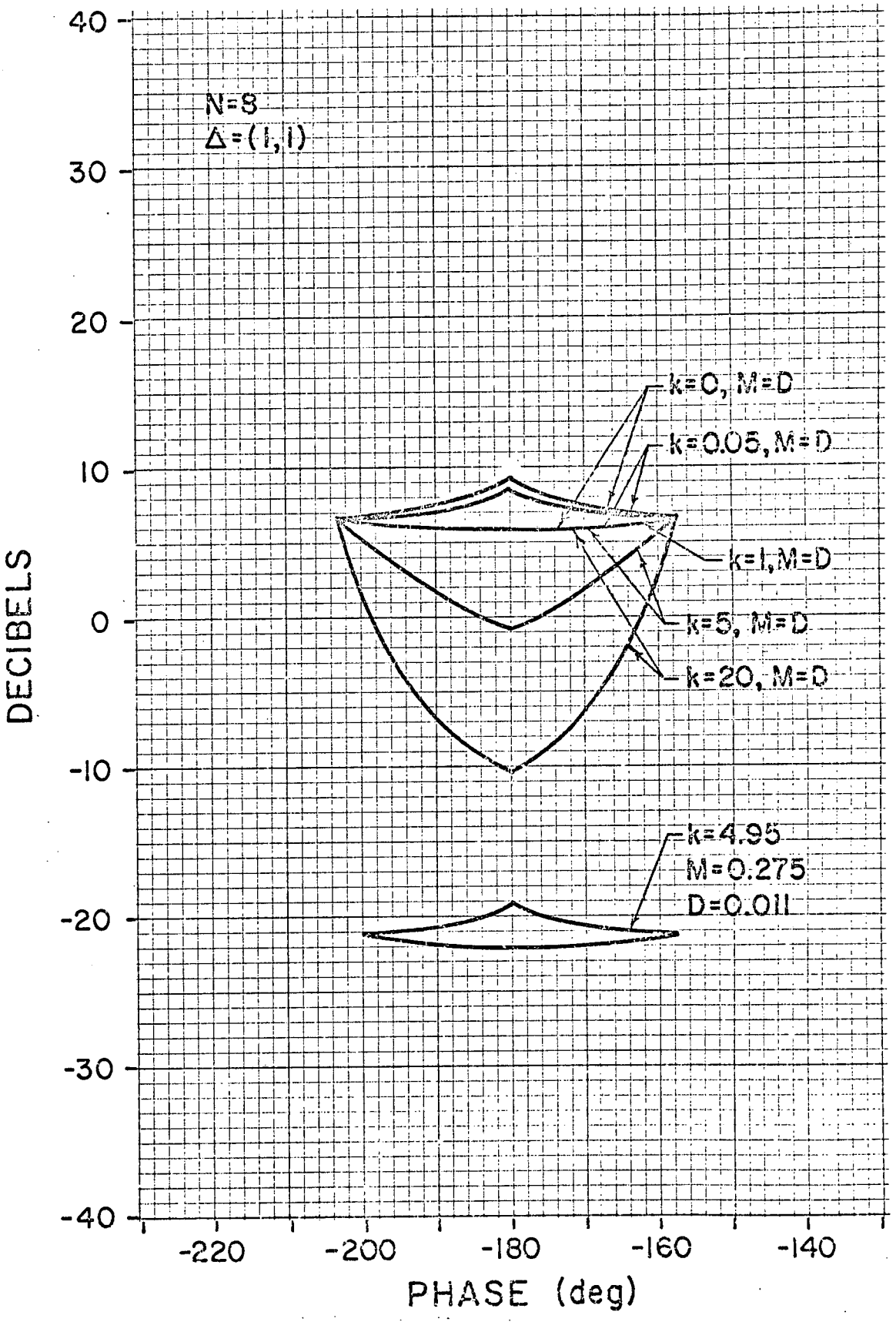
N=8
Δ=(1,1)
k=0, M=D
k=0.05, M=D
k=1, M=D
k=5, M=D
k=20, M=D
k=4.95
M=0.275
D=0.011
DECIBELS
PHASE (deg)
40
30
20
10
0
-10
-20
-30
-40
-220
-200
-180
-160
-140

Figure 7-34

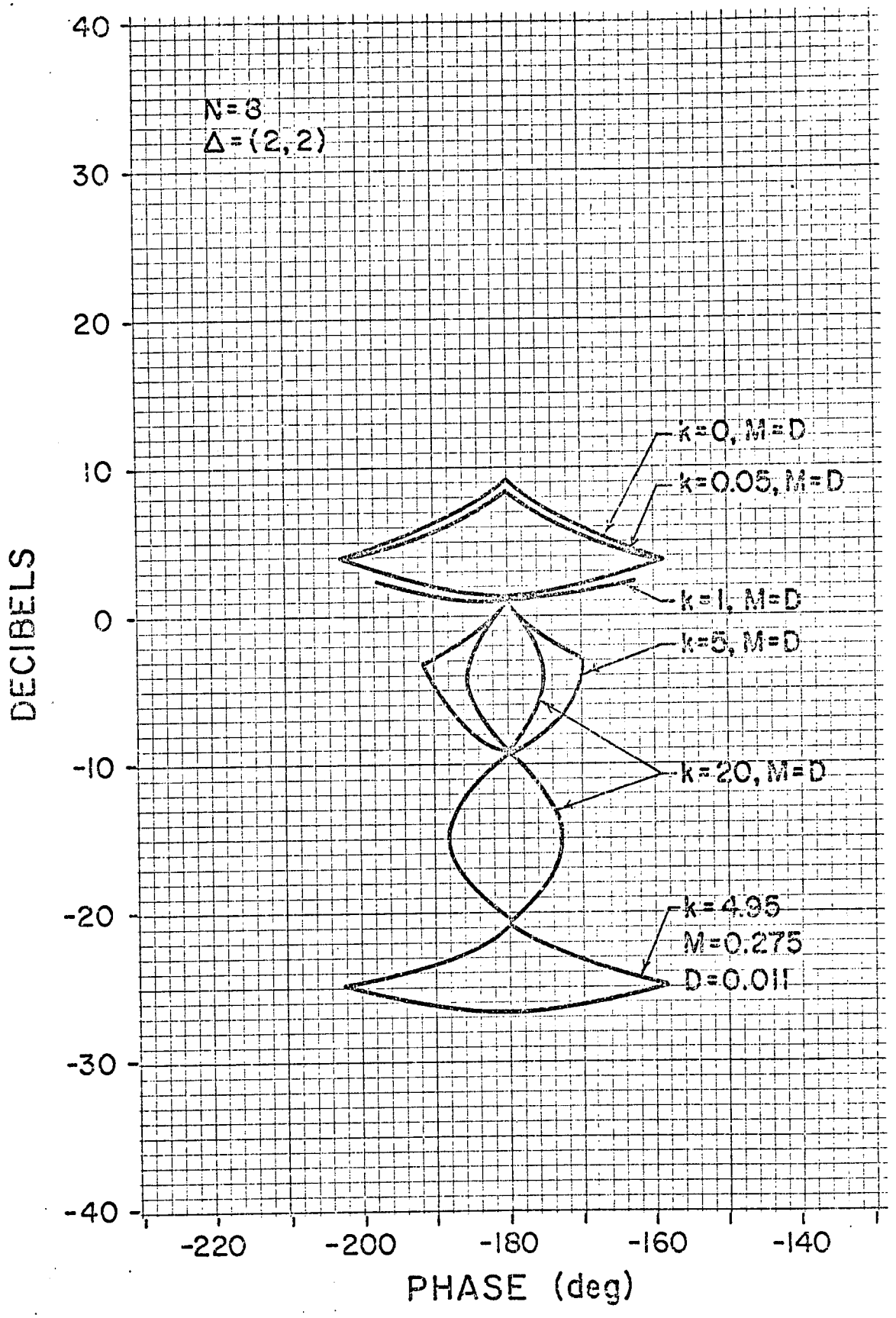
N=3
Δ=(2,2)
k=0, M=D
k=0.05, M=D
k=1, M=D
k=5, M=D
k=20, M=D
k=4.95
M=0.275
D=0.011
DECIBELS
PHASE (deg)
40
30
20
10
0
-10
-20
-30
-40
-220
-200
-180
-160
-140

Figure 7-35

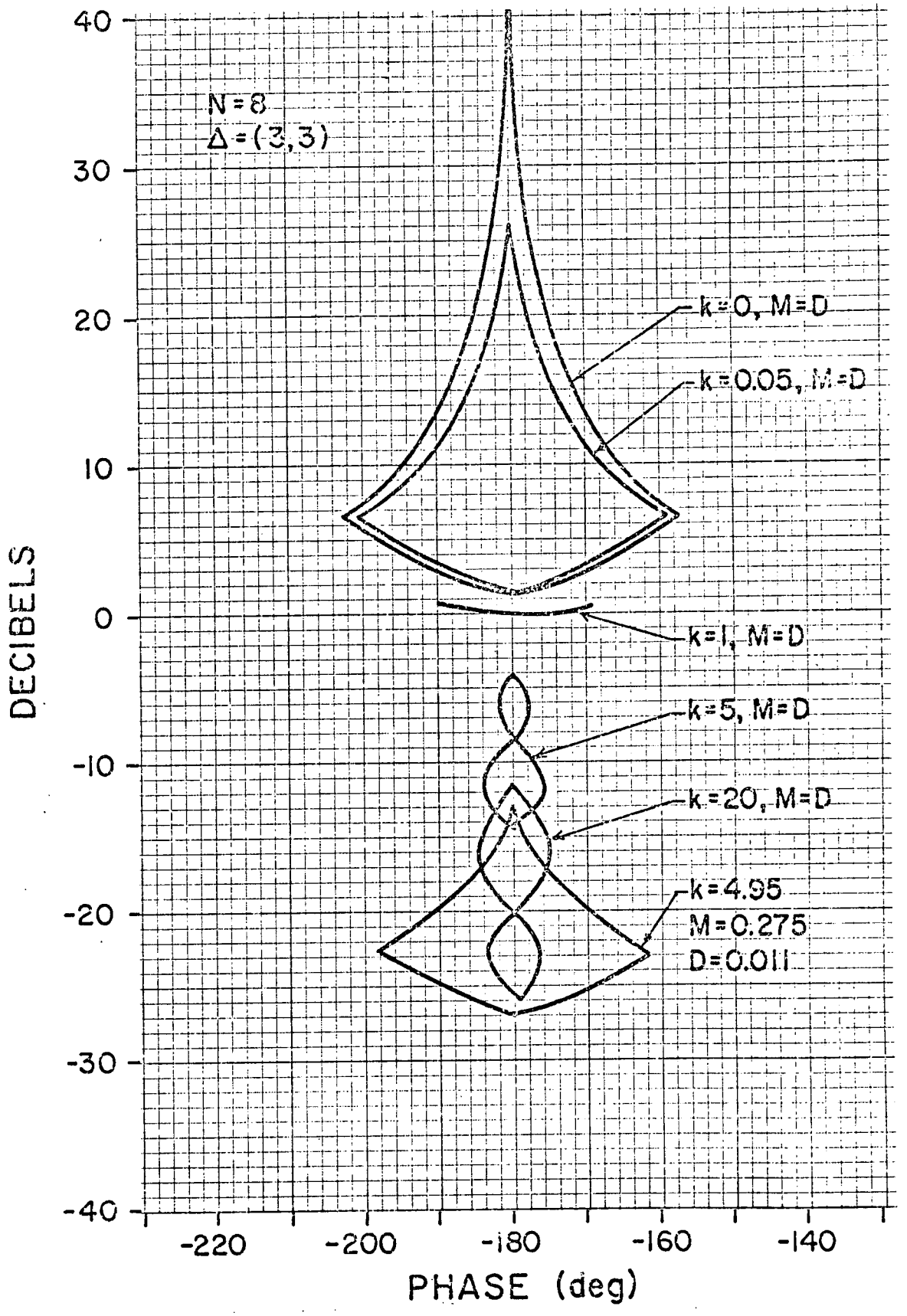
N=8
Δ=(3,3)
k=0, M=D
k=0.05, M=D
k=1, M=D
k=5, M=D
k=20, M=D
k=4.95
M=0.275
D=0.011
DECIBELS
PHASE (deg)
40
30
20
10
0
-10
-20
-30
-40
-220
-200
-180
-160
-140

Figure 7-36

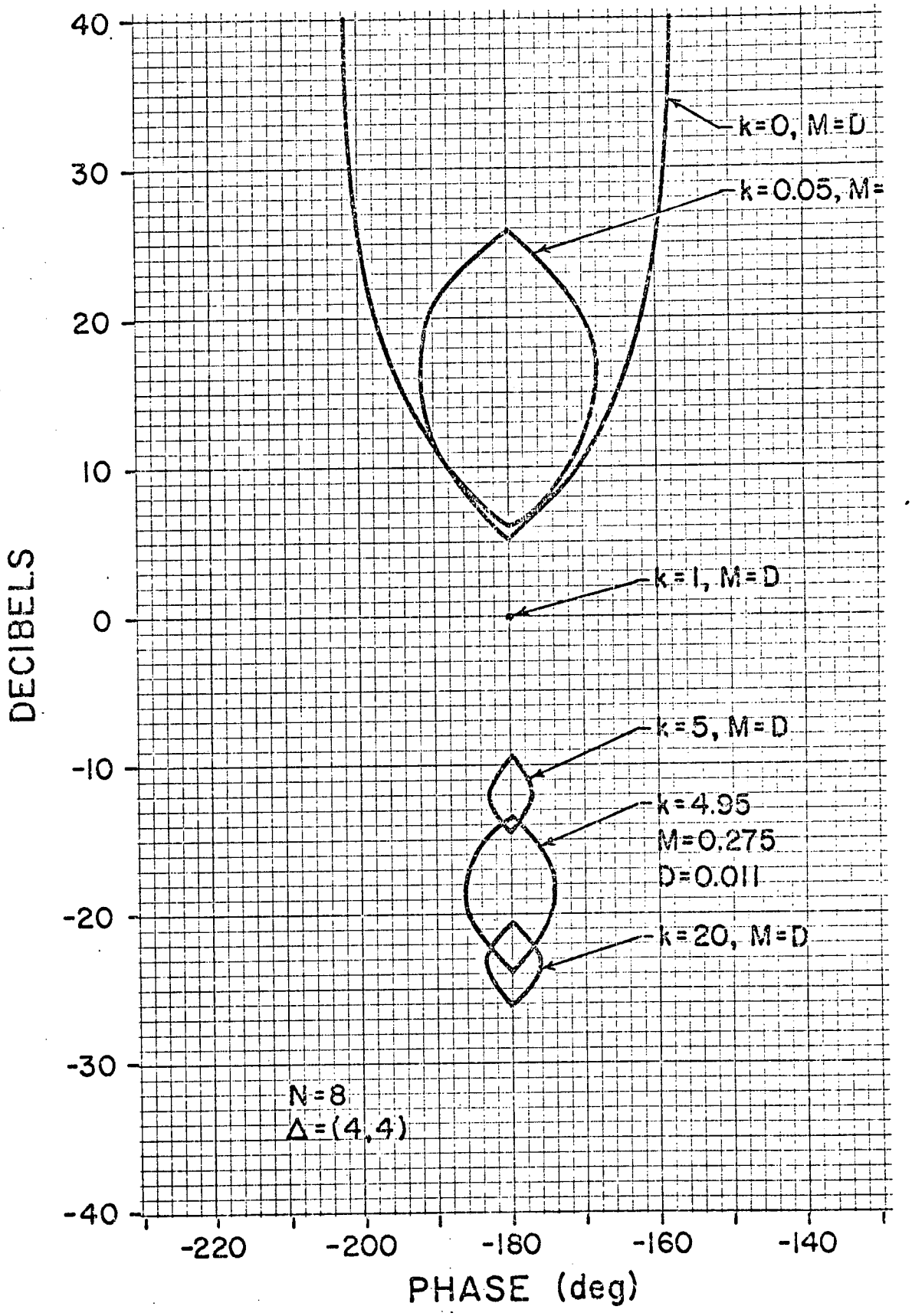
40
30
20
10
0
-10
-20
-30
-40
DECIBELS
-220
-200
-180
-160
-140
PHASE (deg)
k=0, M=D
k=0.05, M=
k=1, M=D
k=5, M=D
k=4.95
M=0.275
D=0.011
k=20, M=D
N=8
Δ=(4,4)

Figure 7-37

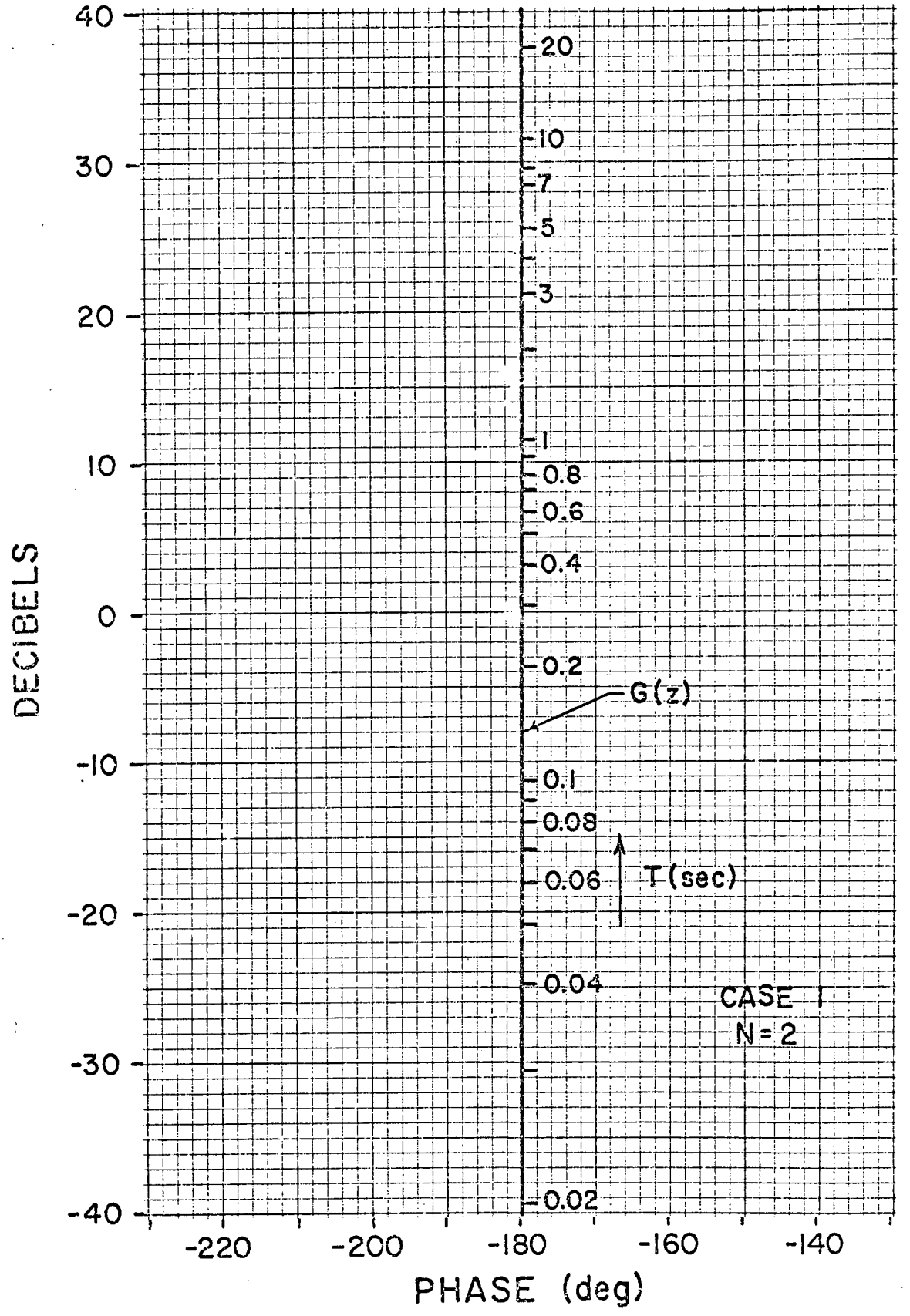
40
30
20
10
0
-10
-20
-30
-40
DECIBELS
20
10
7
5
3
1
0.8
0.6
0.4
0.2
G(z)
0.1
0.08
0.06
T(sec)
0.04
0.02
CASE I
N=2
-220
-200
-180
-160
-140
PHASE (deg)

Figure 7-38

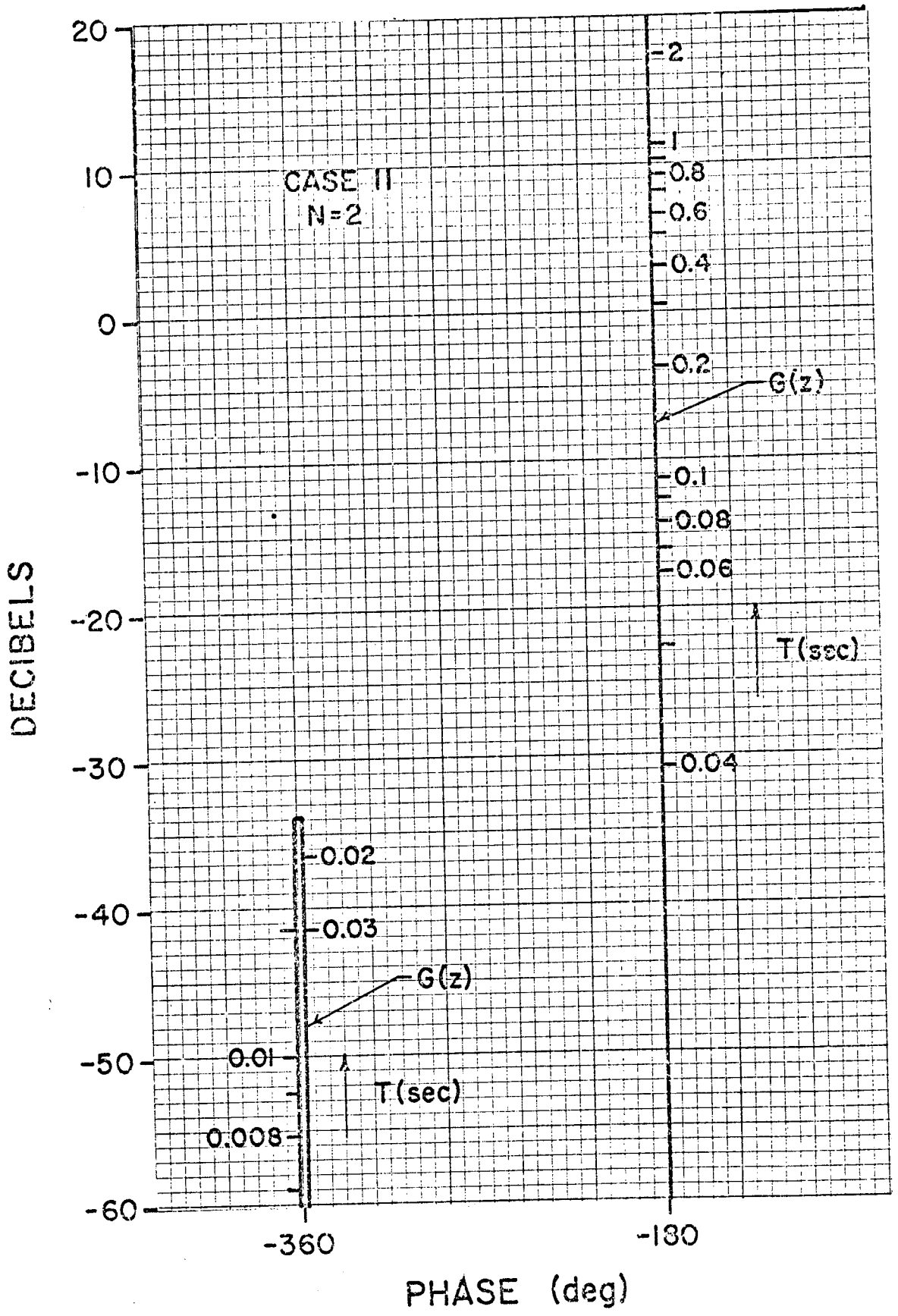
CASE II
N=2
DECIBELS
PHASE (deg)
20
10
0
-10
-20
-30
-40
-50
-60
-360
-180
-2
1
0.8
0.6
0.4
0.2
0.1
0.08
0.06
0.04
0.02
0.03
0.01
0.008
G(z)
T(sec)
G(z)
T(sec)

Figure 7-39

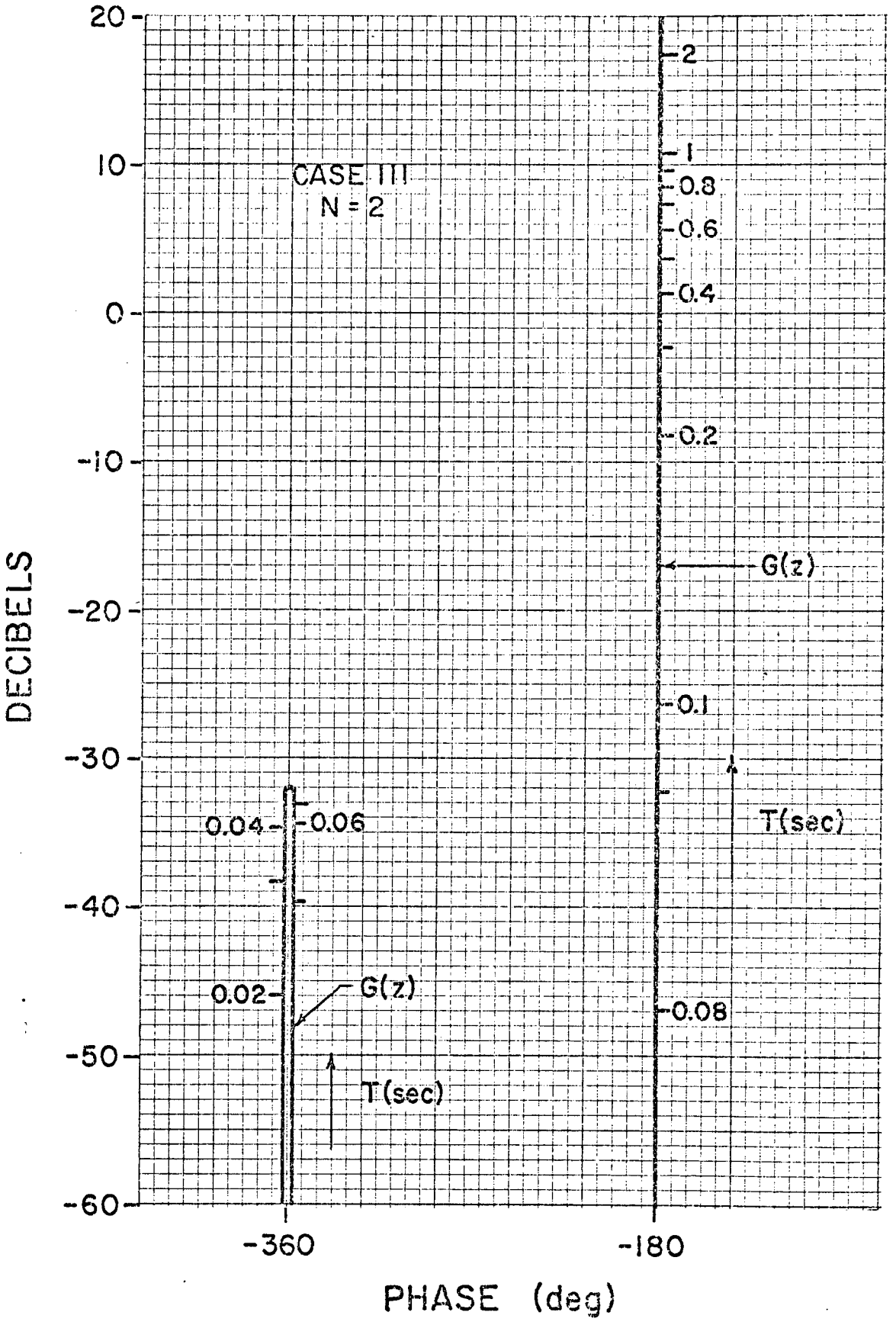
20
10
0
-10
-20
-30
-40
-50
-60
DECIBELS
CASE III
N = 2
2
1
0.8
0.6
0.4
0.2
0.1
0.08
G(z)
T(sec)
0.04
0.06
0.02
G(z)
T(sec)
-360
-180
PHASE (deg)

Figure 7-40

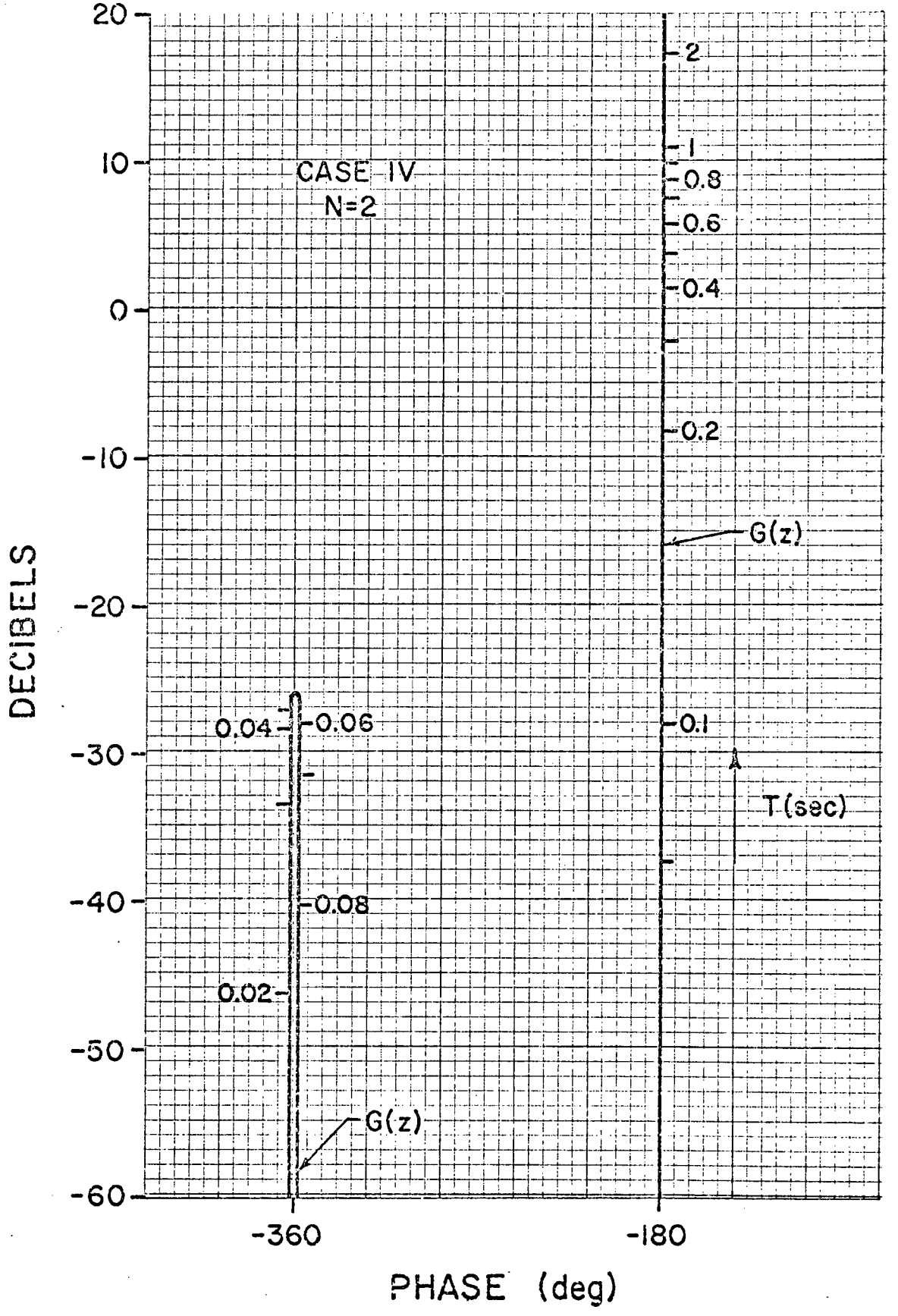
20
10
0
-10
-20
-30
-40
-50
-60
DECIBELS
CASE IV
N=2
2
1
0.8
0.6
0.4
0.2
0.1
G(z)
T(sec)
0.04
0.06
0.08
0.02
G(z)
-360
-180
PHASE (deg)

Figure 7-41

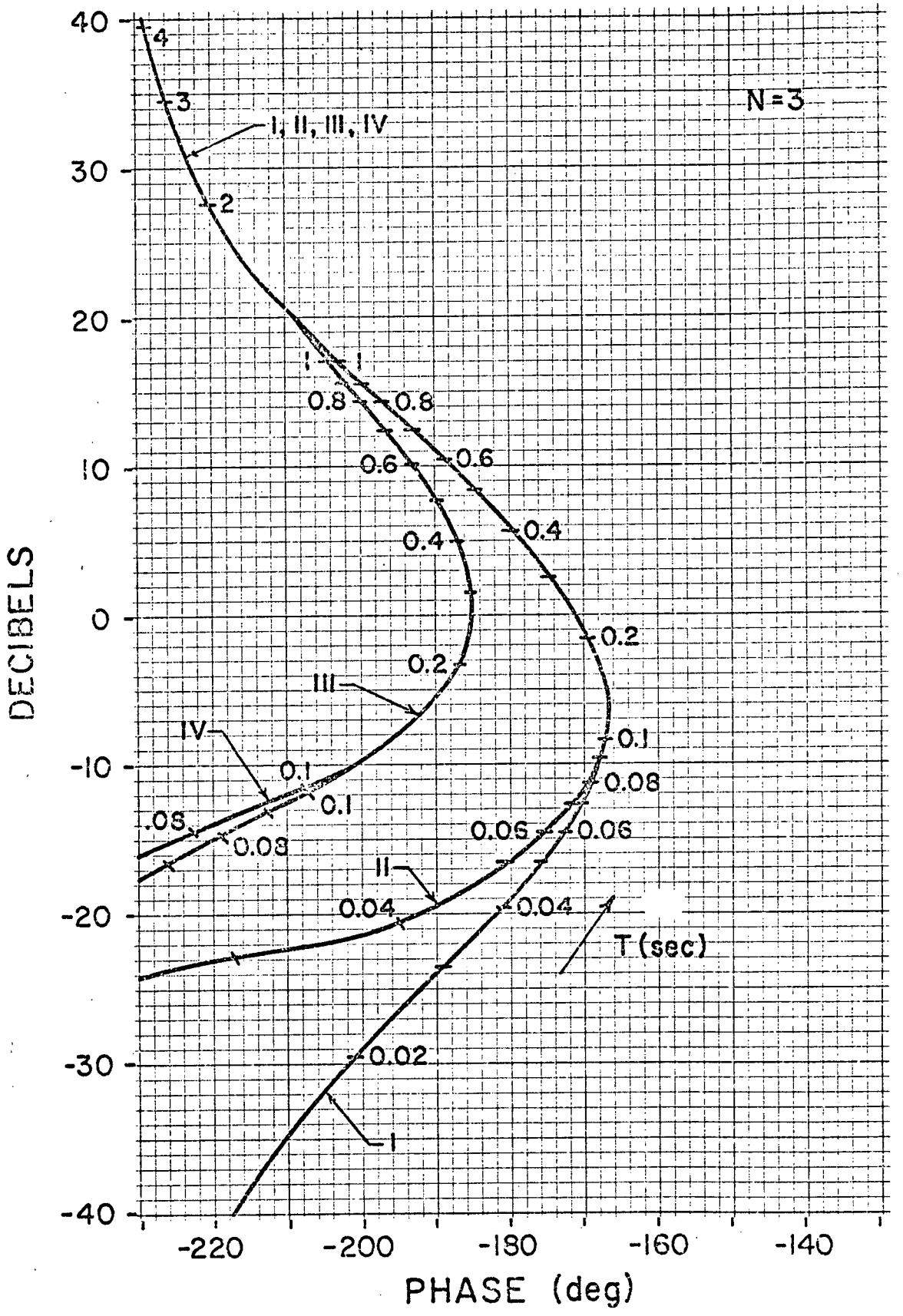
N=3
I, II, III, IV
DECIBELS
PHASE (deg)
T (sec)
40
30
20
10
0
-10
-20
-30
-40
-220
-200
-180
-160
-140
4
3
2
1
0.8
0.6
0.4
0.2
0.1
0.08
0.06
0.04
0.02
0.05
III
IV
II
I

Figure 7-42

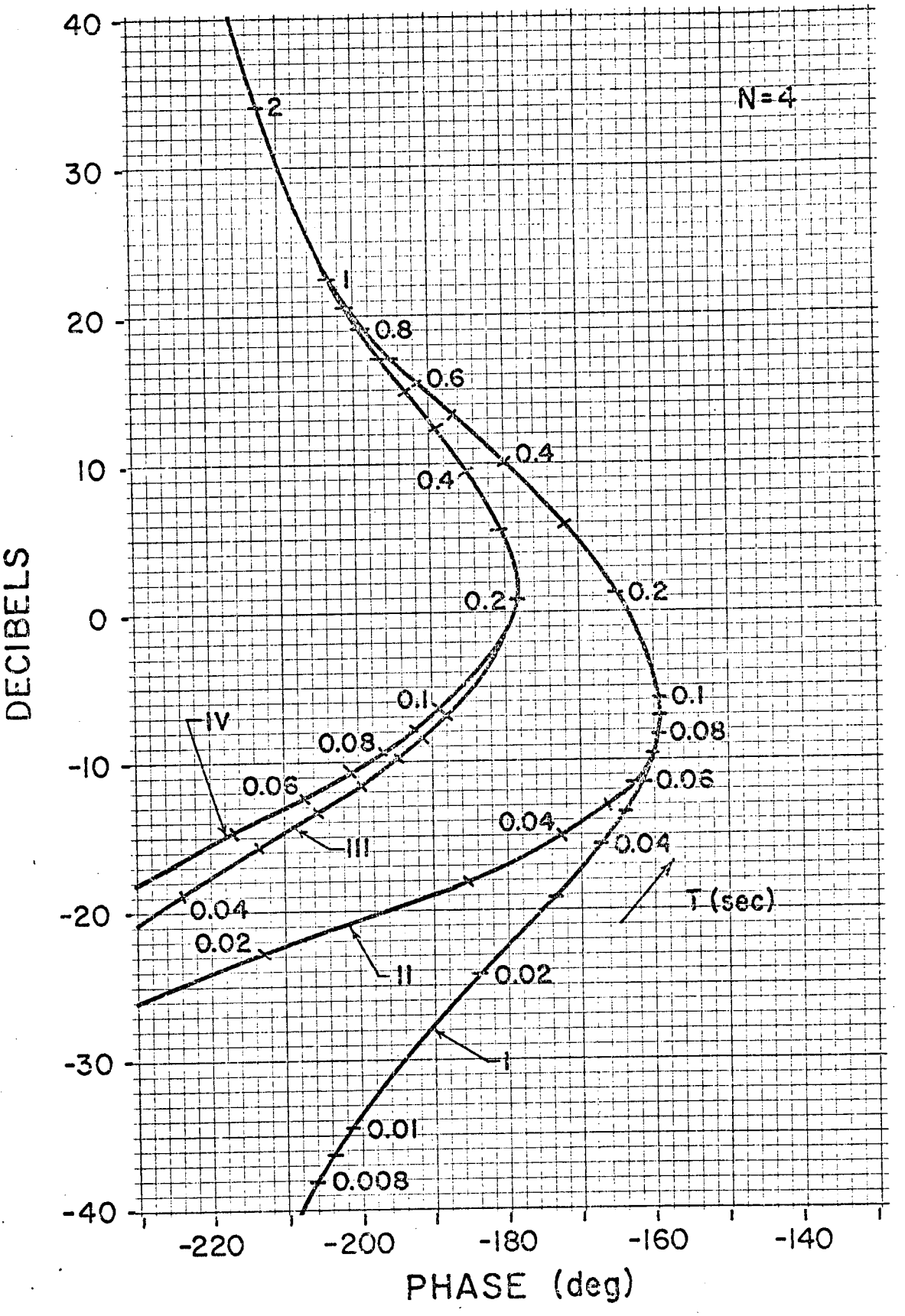
N=4
DECIBELS
PHASE (deg)
T (sec)
40
30
20
10
0
-10
-20
-30
-40
-220
-200
-180
-160
-140
2
1
0.8
0.6
0.4
0.4
0.2
0.2
0.1
0.1
0.08
0.08
0.06
0.06
0.04
0.04
0.02
0.02
0.01
0.008
IV
III
II
I

Figure 7-43

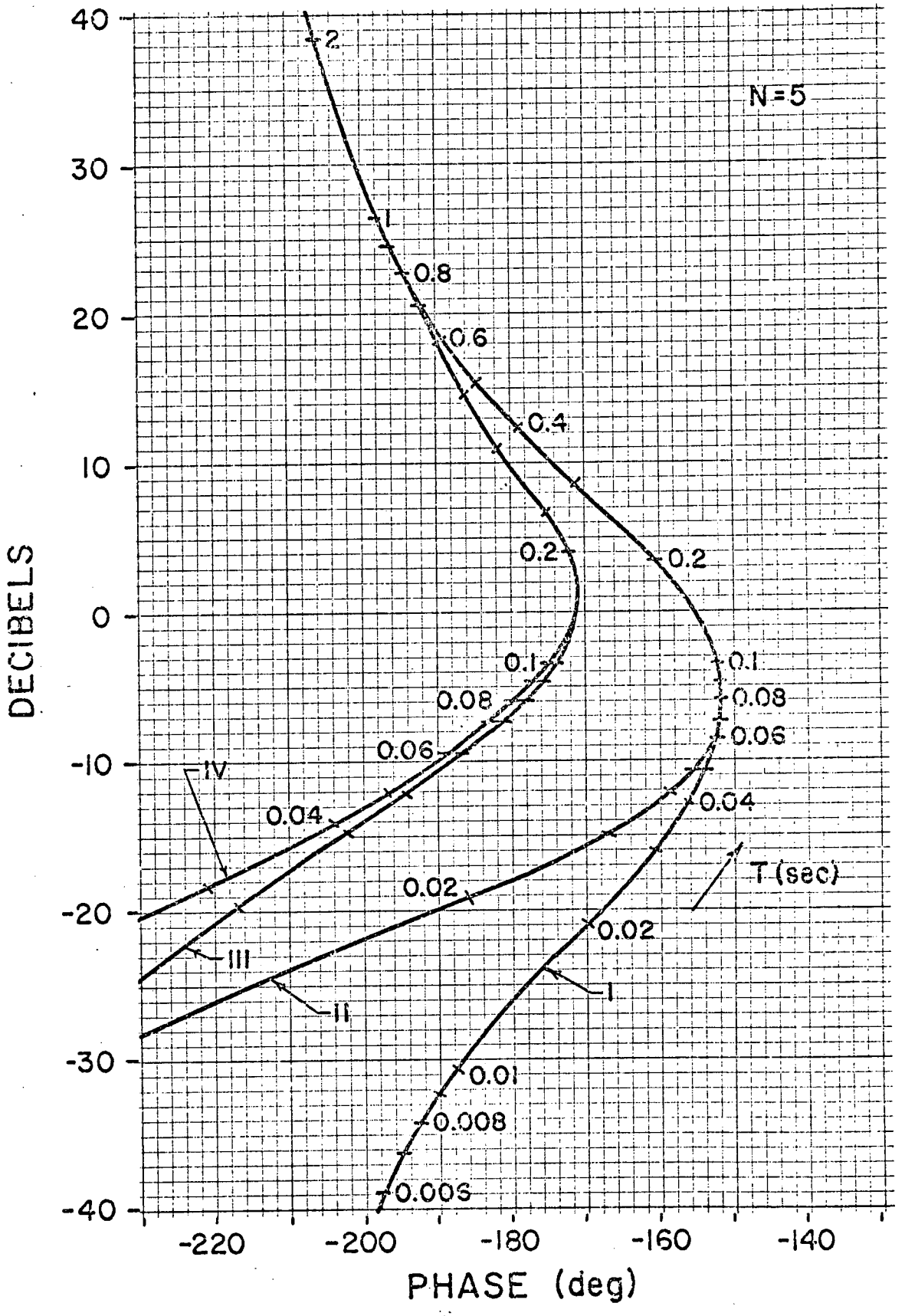
N=5
DECIBELS
PHASE (deg)
T (sec)
40
30
20
10
0
-10
-20
-30
-40
-220
-200
-180
-160
-140
2
1
0.8
0.6
0.4
0.2
0.2
0.1
0.08
0.06
0.04
0.02
0.1
0.08
0.06
0.04
0.02
0.01
0.008
0.006
I
II
III
IV

Figure 7-44

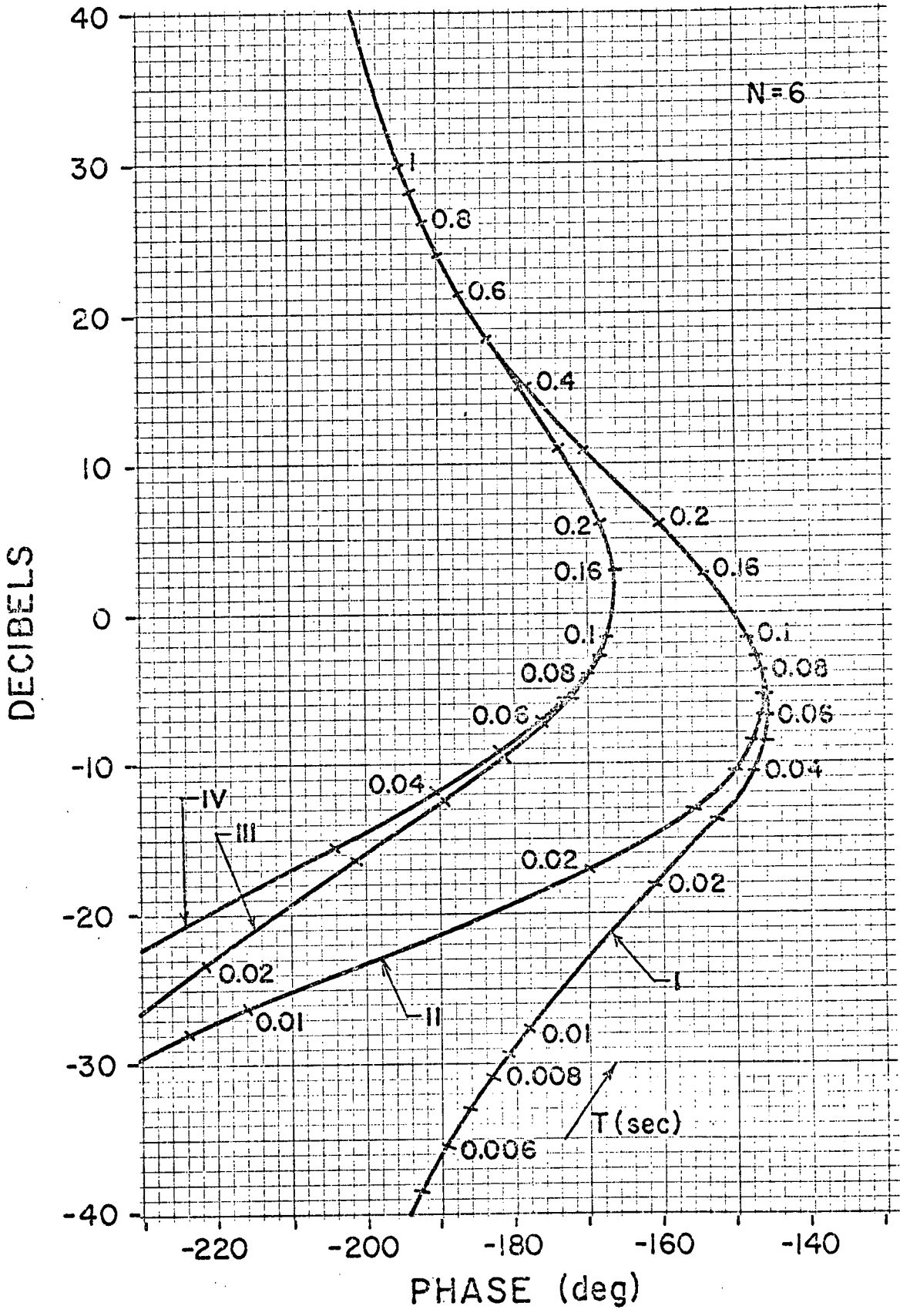
N=6
DECIBELS
PHASE (deg)
T(sec)
40
30
20
10
0
-10
-20
-30
-40
-220
-200
-180
-160
-140
I
0.8
0.6
0.4
0.2
0.16
0.1
0.08
0.06
0.04
0.02
0.01
0.008
0.006
IV
III
II
I

Figure 7-45

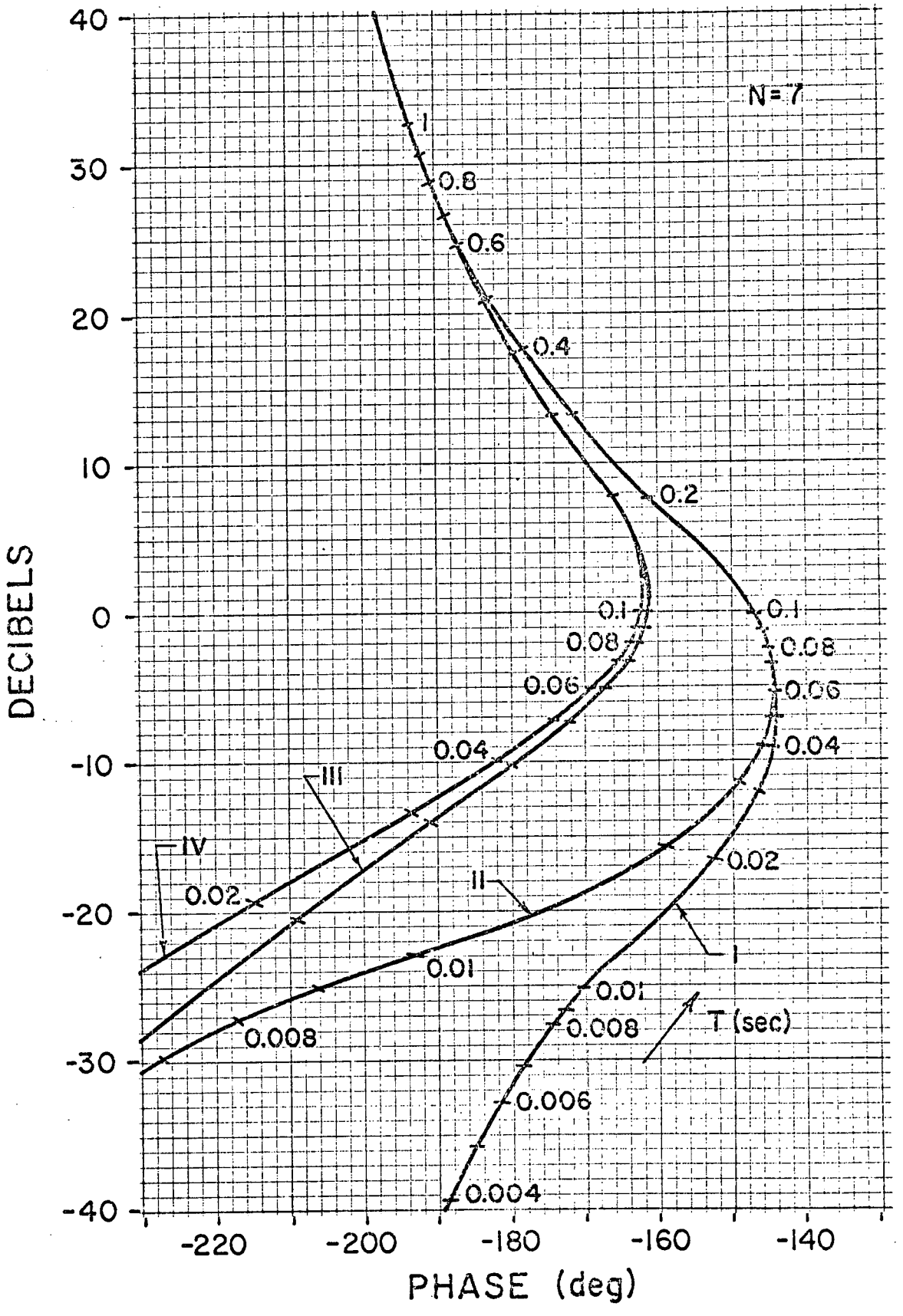
N=7
DECIBELS
PHASE (deg)
T (sec)
40
30
20
10
0
-10
-20
-30
-40
-220
-200
-180
-160
-140
I
0.8
0.6
0.4
0.2
0.1
0.08
0.06
0.04
0.02
0.01
0.008
0.006
0.004
III
IV
II
I

Figure 7-46

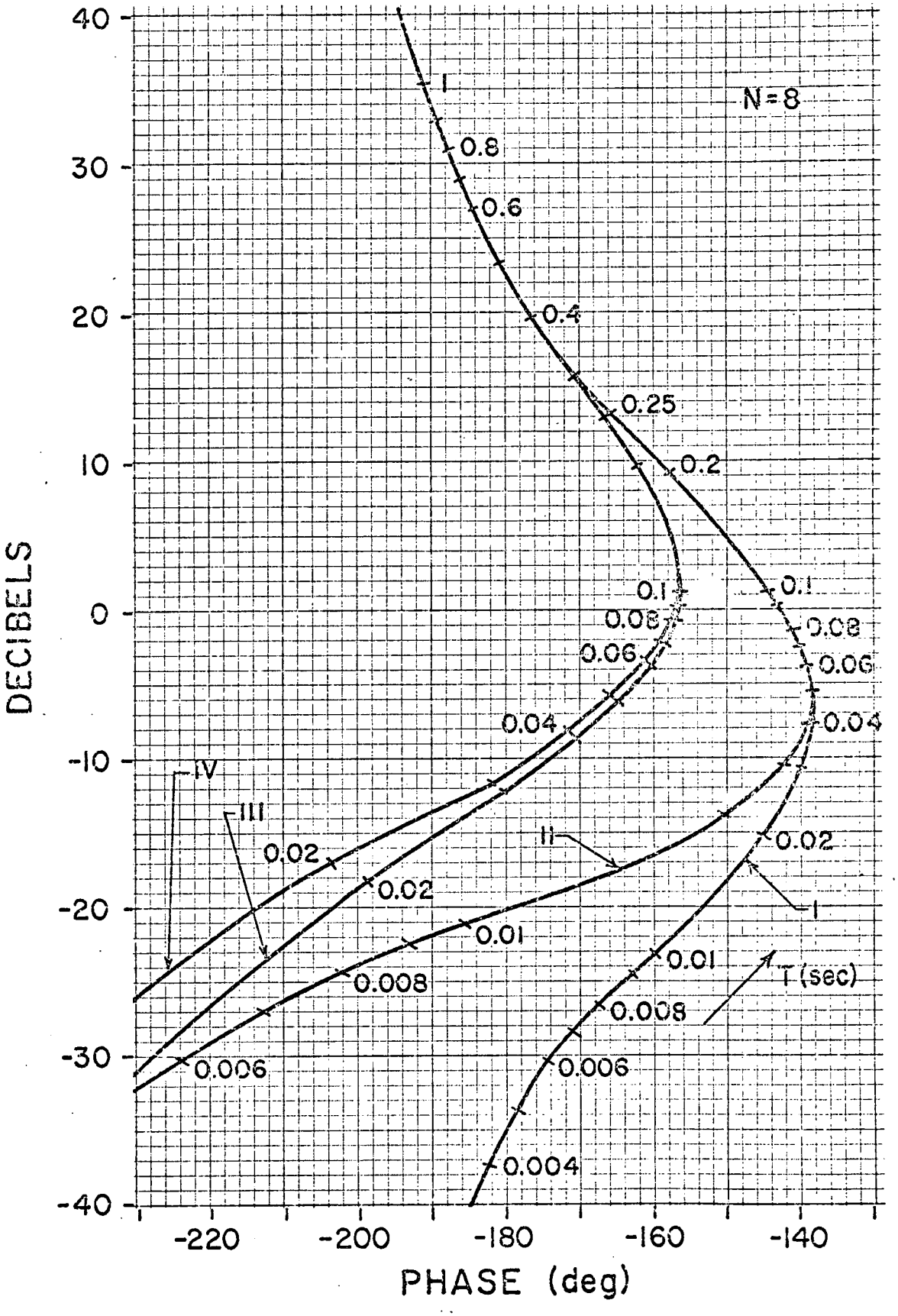
N=8
DECIBELS
PHASE (deg)
T (sec)
40
30
20
10
0
-10
-20
-30
-40
-220
-200
-180
-160
-140
I
0.8
0.6
0.4
0.25
0.2
0.1
0.08
0.06
0.04
0.02
0.01
0.008
0.006
0.004
IV
III
II
I

Figure 7-47

References

[1] Liou, M. L., "A Noval Method of Evaluating Transient Response," Proceedings IEEE vol. 54, No. 1, January 1966, pp. 20-23.

[2] Everling, W., "On the Evaluation of e^{AT} by Power Series," Proceedings IEEE (letters), Vol. 55, March 1967, pp. 413.

[3] Seltzer, S. M., Patel, J. S., Justice, D. W., and Schweitzer, G., "Stabilizing a Spinning Skylab", NASA Technical Memorandum NASA TM X - 64635, George C. Marshall Space Flight Center, January 1972.

[4] Seltzer, S. M., "Passive Stability of a Spinning Skylab", NASA Technical Memorandum NASA TM X - 64646, George C. Marshall Space Flight Center, Alabama, February 1972.

[5] Potter, James A., "Matrix Quadratic Solutions" J. Siam Appl Math., Vol. 14, No. 3, May 1966, pp. 496-501.

[6] Seltzer, S. M., An Analysis of the Effect of Assumed Nonlinear Model of A Control Moment Gyro (CMG) on The Attitude Dynamics of A Large Space Telescope (LST)Model, NASA Report, 1972.

[7] Kuo, B. C., Analysis and Synthesis of Sampled-Data Control Systems, Prentice-Hall, Inc., Englewood Cliffs, New Jersey, 1963.

[8] Rybak, S. C., High Accuracy Stabilization and Control, Technical Report, MT=2383, Bendix Corporation, Denver Facility, December 14, 1971.

[9] Rybak, S. C., Research and Applications Module (RAM) Phase B Study: Free Flyer GN&C Trade Study Report, RAM-B-GNC-407, Bendix Corporation, Denver Facility, October 29, 1971.

[10] Frieder, M., A Note on CMG Characteristics and Spacecraft Limit Cycling. Engineering File MT-15, Bendix Corporation, Teterboro, New Jersey, April 19, 1972.

References

[11] Whitley, G. W., LST Fine Pointing Control System Design. MSFC S & E ASTR-SD-78-72 Letter, October 3, 1972.

[12] Kuo, B. C., Singh, G., Yackel, R. A., Analysis of the Attitude Dynamics of A Large Space Telescope (LST) Model, Monthly Report, January, 1973, Systems Research Laboratory, Champaign, Illinois.